Ultrasound in the Critically Ill

A Practical Guide

Andrew Walden
Andrew Campbell
Ashley Miller
Matthew Wise
Editors

Springer

Ultrasound in the Critically Ill

Andrew Walden · Andrew Campbell ·
Ashley Miller · Matthew Wise
Editors

Ultrasound in the Critically Ill

A Practical Guide

Springer

Editors
Andrew Walden
Intensive Care Unit
Royal Berkshire Hospital
Reading, Berkshire, UK

Andrew Campbell
Department of Critical Care Medicine
Wrexham Maelor Hospital
Wrexham, UK

Ashley Miller
Department of Anaesthetics
Shrewsbury and Telford
Hospital NHS Trust
Shrewsbury, UK

Matthew Wise
Adult Critical Care
University Hospital of Wales
Cardiff, UK

ISBN 978-3-030-71740-7 ISBN 978-3-030-71742-1 (eBook)
https://doi.org/10.1007/978-3-030-71742-1

This Springer imprint is published by the registered company Springer Nature Switzerland AG
The registered company address is: Gewerbestrasse 11, 6330 Cham, Switzerland

Preface

Historically, ultrasound has been delivered as a department-based diagnostic intervention within the radiology, cardiology and obstetric departments. As machines were often large and cumbersome, patients had to attend those departments for the examination to be performed. Rigorous training and governance structures developed to ensure a thorough and consistent approach among radiographers, obstetric sonographers and cardiac technicians. This system is very good for ambulatory patients in which a comprehensive assessment is required; however, for acutely unwell patients who may require intensive monitoring, oxygen therapy or organ support, this is not such a practical approach.

With the increased portability and usability of ultrasound machines, a new approach has developed where the machine comes to the patient rather than the other way round. This Point of Care approach to ultrasound has led to whole new areas of ultrasound examination and clinical decision-making. The time constraint on a clinician caring for a sick patient means that the comprehensive departmental use of ultrasound is replaced by a more abbreviated technique designed to answer specific questions, often in a dichotomous way and as an extension of clinical assessment and examination. Ruling in or ruling out certain pathologies can be invaluable in the deciding of patient triage, further investigations and the need for intervention or surgery.

Another advantage of point of care ultrasound over departmental ultrasound is the ability to look at dynamic changes in physiology following interventions. For instance, the effect of a fluid bolus on cardiac output or how a recruitment maneuver in a mechanically ventilated patient leads to improved lung aeration.

The use of point of care ultrasound has undoubtedly led to reduced morbidity around interventional procedures such as paracentesis, central venous cannulation and thoracocentesis.

One counterpoint to this flourishing of point of care ultrasound is the issue of training and competence. Sonographers and radiographers have to spend a long time training to ensure they see the range of pathology to be able to safely diagnose certain pathologies. Cognisant of this, clinicians have developed training curriculums with theoretical and practical modules to allow accreditation in a particular

area of point of care ultrasound. Notably, within the United Kingdom, the Royal College of Radiologists has developed guidelines for non-radiology specialties (https://www.rcr.ac.uk/system/files/publication/field_publication_files/bfcr173_ultrasound_training_med_surg.pdf). In addition, several professional bodies have also developed similar guidelines and curriculums, e.g. Focused Acute Medicine Ultrasound (http://famus.org.uk/) and

Focused Ultrasound in Intensive Care (https://www.ics.ac.uk/ICS/FUSIC/ICS/FUSIC/FUSIC_Accreditation.aspx?hkey=c88fa5cd-5c3f-4c22-b007-53e01a523ce8).

This book is aimed at all frontline staff who are looking to use ultrasound in their clinical practice to try to improve the care of acutely and critically ill patients. The book is laid out in two sections. The first section attempts to take a comprehensive approach to specific systems of examination taking an organ-focused approach. The second part of the book attempts to pull those chapters together by looking at specific clinical scenarios.

We hope the reader of this book ends up with the same degree of enthusiasm that each of the editors has with respect to point of care ultrasound and how it improves the care of our patients.

Reading, UK — Andrew Walden
andrew.walden@nhs.net
Wrexham, UK — Andrew Campbell
Shrewsbury, UK — Ashley Miller
Cardiff, UK — Matthew Wise

Contents

Contributors

Karim Fouad Alber Royal Berkshire Hospital, Reading, UK

Andrew Bodenham Department of Anaesthesia, Leeds Teaching Hospitals NHS Trust, Leeds, West Yorkshire, UK

Enrico Boero Anesthesiology and Intensive Care, School of Medicine, University of Torino, Torino, Italy

Jane Brenchley Department of Emergency Medicine, Royal Berkshire Hospital, Reading, Berkshire, England

James H. Briggs Royal Berkshire Hospital, Reading, Berkshire, UK

Andrew Campbell Department of Critical Care Medicine, Wrexham Maelor Hospital, Wrexham, UK

Manik Chandra Department of Anaesthesia, Leeds Teaching Hospitals NHS Trust, Leeds, West Yorkshire, UK

Thomas Clark Department of Critical Care, Torbay and South Devon NHS Foundation Trust, Torquay, UK

Martin R. Dachsel Acute Medicine, East Surrey Hospital, Redhill, Surrey, UK

Sonya Daniel University Hospital of Wales, Cardiff, UK

Luna Gargani Cardiologist, Senior Researcher of the Institute of Clinical Physiology - National Research Council, Pisa, Italy

Maria-Magdalena Gurzun Department of Anaesthesia, Swansea, West Glamorgan, UK

Tom Holmes University Hospital of Wales, Cardiff, UK

Farhan T. Husain Department of Anaesthesia, Swansea, West Glamorgan, UK

Hefin Jones Consultant in Radiology, University Hospitals of North Midlands, Stoke-on-Trent, Staffordshire, UK

Liza Keating Intensive Care Unit, Royal Berkshire Hospital, Reading, UK

Michael S. Kristensen Rigshospitalet, Copenhagen Ø, Denmark

Ashley Miller Department of Anaesthetics, Shrewsbury and Telford Hospitals NHS Trust, Shrewsbury, UK

Kausik Mukherjee Department of Radiology, University Hospital of Wales, Wales, UK

Pawan Patel Locum Consultant, Consultant Radiologist, St George's University Hospitals NHS Foundation Trust, Tooting, London, UK

James M. Pilcher Consultant Radiologist, St George's University Hospitals NHS Foundation Trust, Tooting, London, UK

Susanna Price Cardiologist & Intensivist, Royal Brompton Hospital, London, UK;
National Heart & Lung Institute, Imperial College, London, UK

Annia Schreiber Respiratory Intensive Care Unit, Salvatore Maugeri Foundation, Pavia, Italy

Poonam Mohan Shenoy Department of Radiology, Wrexham Maelor Hospital, Wrexham, UK

Claire Shevlin Intensive Care Unit, Craigavon Area Hospital, Portadown, Northern Ireland, UK

Eugene Tabiowo Royal Glamorgan Hospital, Ynysmaerdy, Llantrisant, Wales, UK

Wendy H. Teoh Private Anaesthesia Practice, Wendy Teoh Pte. Ltd., Singapore, Singapore

Giovanni Volpicelli Department of Emergency Medicine, San Luigi Gonzaga University Hospital, Torino, Italy

Andrew Walden Royal Berkshire Hospital, Reading, UK

Chapter 1
Physics of Ultrasound

Martin R. Dachsel

Keywords Physics · Doppler · Point of care ultrasound

1.1 Introduction

Studying the physics of ultrasound allows for a greater understanding of how images are acquired and artefacts generated. A basic primer in physics is essential in any ultrasound based training program and this chapter sets out to give an overview and introduces common artefacts and imaging modes.

1.2 The Ultrasound Wave

Ultrasound waves are sound waves with similar characteristics. They have an amplitude, which represents the strength (peak pressure) and a period, which represents the length of time to complete 1 cycle (Fig. 1.1). The distance of a complete cycle is called wavelength (Fig. 1.2).

The frequency of a wave is the number of cycles over time:

$$\text{Frequency} = \text{n cycles/time}$$
$$1\,\text{Hertz (Hz)} = 1\,\text{cycle per second}$$

Ultrasound is sound of any frequency above the standard human pitch (>20 kHz). Diagnostic ultrasound uses frequencies from 1 to 20 MHz (Fig. 1.3).

Sound waves propagate through tissue with a Velocity, which is equal to wavelength (λ) times frequency (f):

M. R. Dachsel (✉)
Acute Medicine, East Surrey Hospital, Canada Avenue, Redhill, Surrey RH15RH, UK
e-mail: rdachsel@nhs.net

A. Walden et al. (eds.), *Ultrasound in the Critically Ill*,
https://doi.org/10.1007/978-3-030-71742-1_1

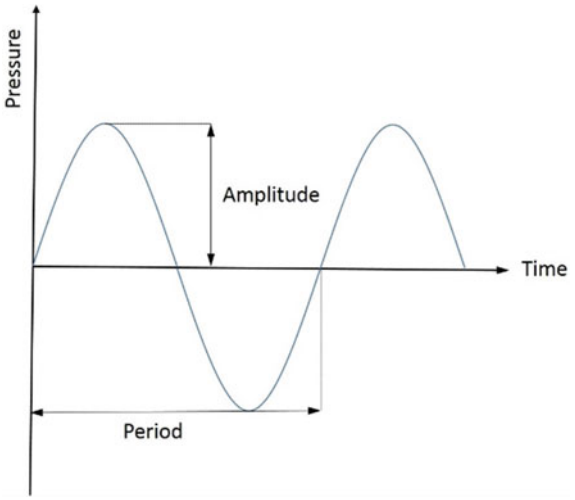

Fig. 1.1 Amplitude and period

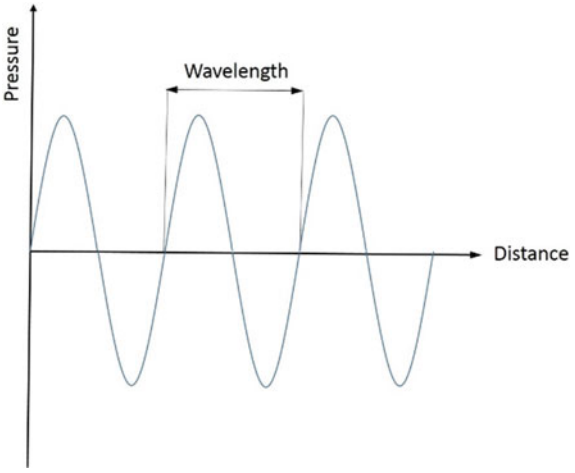

Fig. 1.2 Wavelength

$$V = \lambda \times f$$

The velocity is constant in a given medium and will be determined by the density and stiffness of the medium (Fig. 1.4). The ultrasound device uses a velocity of 1540 m/s for its calculations.

The velocity of ultrasound is very similar in fluids and solid organs. In contrast the velocity is much lower in air and much higher in bone (Table 1.1).

Given the constant velocity in a tissue, a higher frequency will decrease the wavelength, which will result in a better resolution. However, the higher the

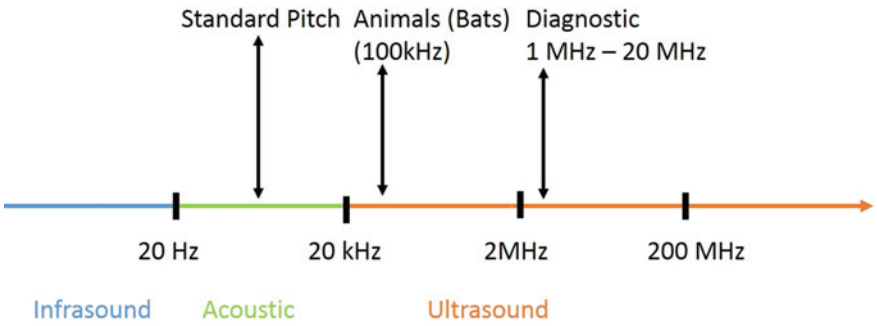

Fig. 1.3 Standard pitch and ultrasound frequency range

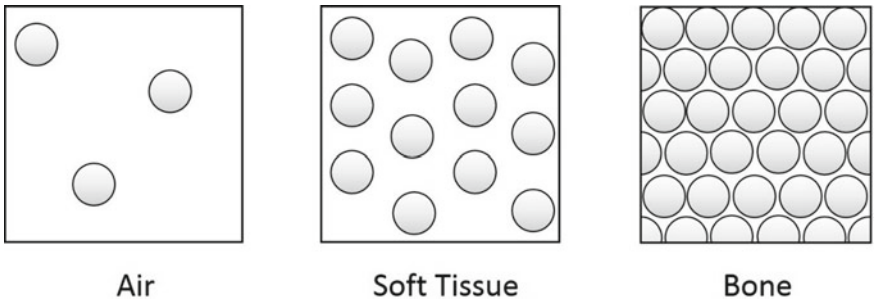

Fig. 1.4 Density of different body organs

Table 1.1 Velocity of ultrasound in different tissues

Tissue	Air	Fat	Water	Kidney	Spleen	Muscle	Liver	Bone
V (m/s)	331	1470	1490	1560	1565	1575	1570	3360

frequency the larger the attenuation of the ultrasound wave, which will result in a lower depth:

↑ Frequency → ↓ Wavelength → ↑ Resolution

↑ Frequency → ↑ Attenuation → ↓ Depth of Field

Figure 1.5 shows the ultrasound absorption rising in all media with rising frequencies. Please note that while bone will absorb most of the ultrasound even at low frequencies, fluid filled structures will absorb almost nothing and so are ideal for use as ultrasound windows to visualise deeper areas (i.e. for pelvic ultrasound your patient should always have a full bladder (Fig. 1.6)).

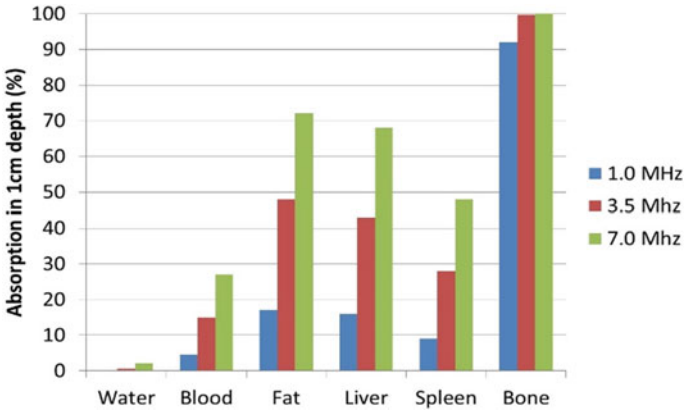

Fig. 1.5 Ultrasound absorption in 1 cm depth for different tissues and frequencies

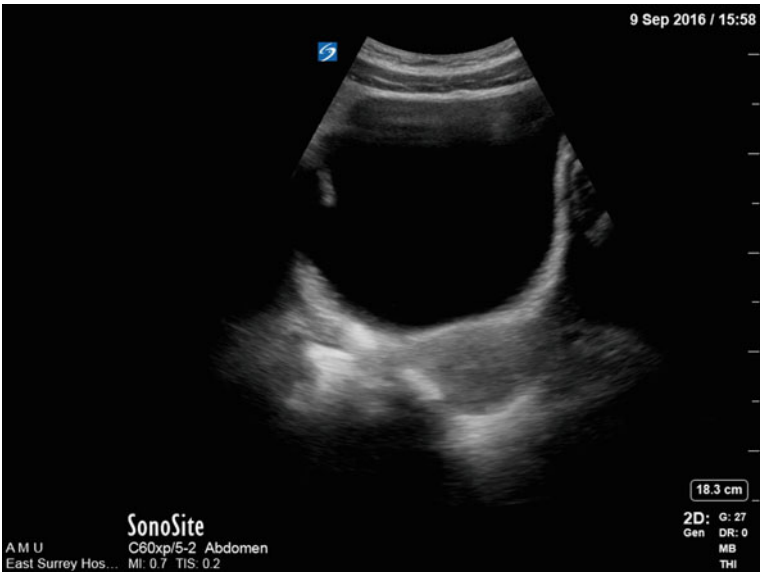

Fig. 1.6 Use fluid filled organs (bladder) as windows to visualise deeper structures

1.3 The Origin of the Ultrasound Image

Ultrasound machines use the piezoelectric principle to transform electrical energy into vibrations and hence ultrasound waves. It then receives ultrasound waves and transforms these waves into electrical energy.

The piezoelectric crystals and with that the ultrasound probes are the most expensive parts of the machines and should be treated with caution. Cleaning the transducers after use is mandatory, dried ultrasound gel on transducers will distort the pictures for the next user.

The ultrasound device sends an ultrasound signal out and measures the time and strength of the returning signals. The device assumes that the velocity of ultrasound in human tissue is constant (1540 m/s). It uses the time until the signal returns to calculate the depth of the structure (Fig. 1.7). The higher the intensity of the returning echo, the brighter the speckle will be on B-mode (for Brightness, also called 2d on some devices).

The intensity of the returning echo is dependent on the impedance difference of the interface between two tissues (Fig. 1.8).

Homogenous substances (e.g. fluids) will not produce any echoes. In Fig. 1.9 the ultrasound picture of an Oil/Water mix is shown. On the left hand side, the fluids are not mixed, resulting in only one interface between oil and water, and thus a bright line. On the right hand side there are millions of small interfaces, resulting in a picture with millions of interfaces (Fig. 1.9).

The laws of optics are valid for ultrasound waves. Ultrasound waves can be reflected, refracted, dispersed, absorbed and diverged. The most important attenuation processes for practising ultrasound are reflection and absorption (Fig. 1.10).

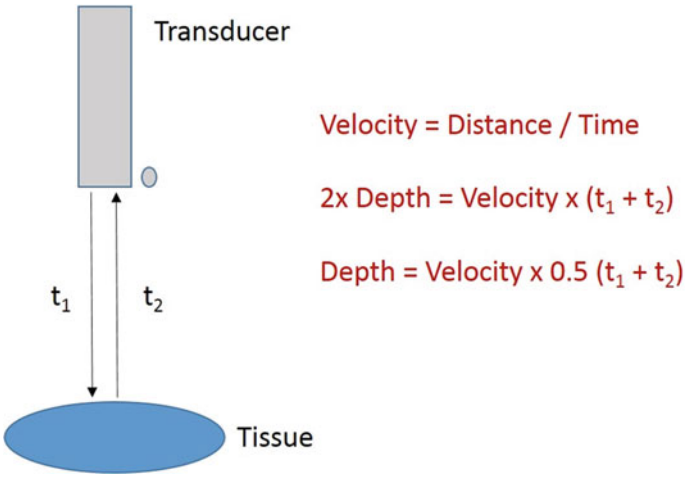

Fig. 1.7 Depth and time

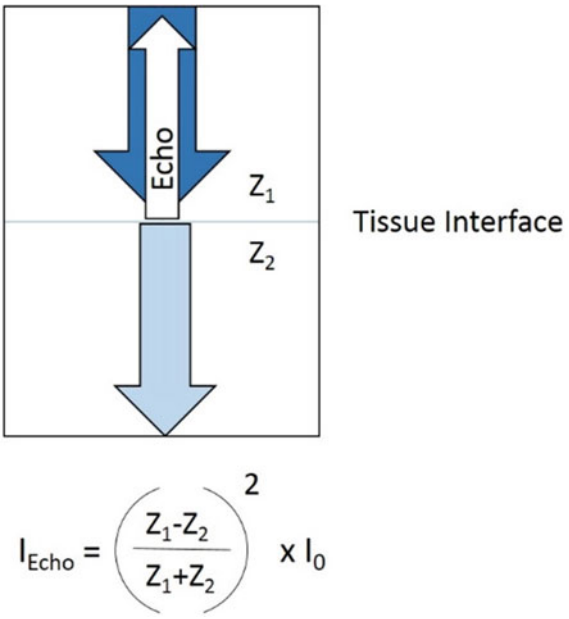

Fig. 1.8 Impedance difference and Echo intensity

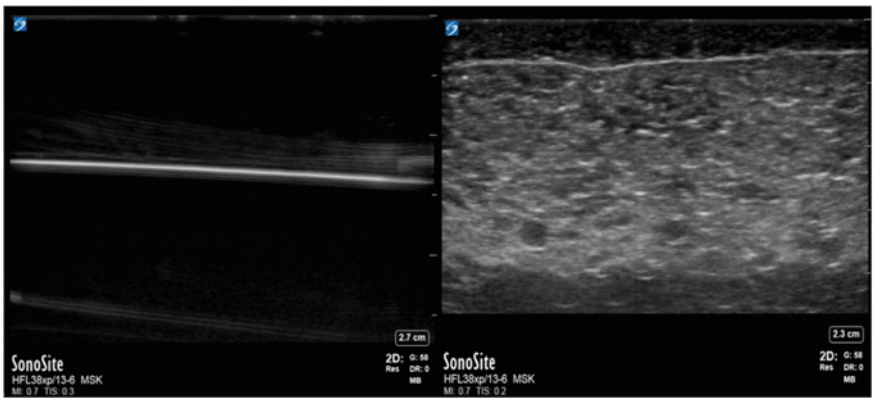

Fig. 1.9 Ultrasound of oil/water solution (unmixed and mixed)

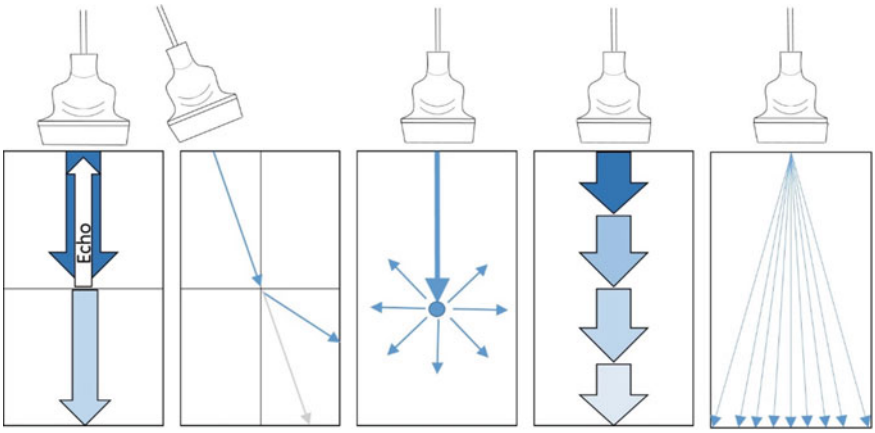

Fig. 1.10 Attenuation of ultrasound waves

1.4 Ultrasound Modes

1.4.1 A—Mode

(not used much in today's medical practice)

For Amplitude. In the early years of ultrasound before easy access to CT scanners ultrasound was used to monitor midline shifts in traumatic brain injuries. Amplitudes over time were used to show structural shifts over time. A-Mode scanning is still in use in Ophthalmology for measuring the axial length of the eye.

1.4.2 B—Mode

Brightness mode also called 2D mode. Ultrasound signals are send out over whole ultrasound transducer and returning signals are plotted against time delays. The result is a 2-dimensional picture showing impedance differences at different depths (Fig. 1.11).

1.4.3 M—Mode

M—Mode (motion) showing the change over time on one line of ultrasound waves. This enables the device to show an area of interest with high temporal resolution. Used for assessment of cardiac muscle, valve assessment and IVC measurements (Fig. 1.12).

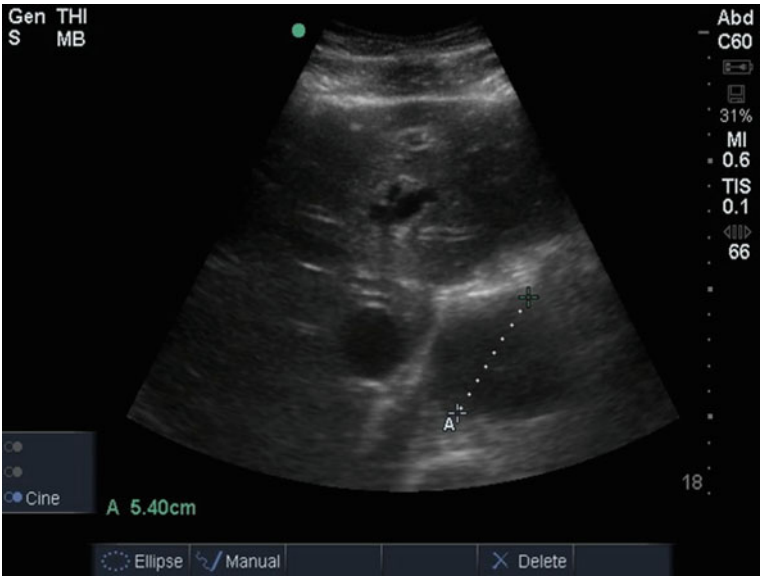

Fig. 1.11 B—mode showing 2d picture

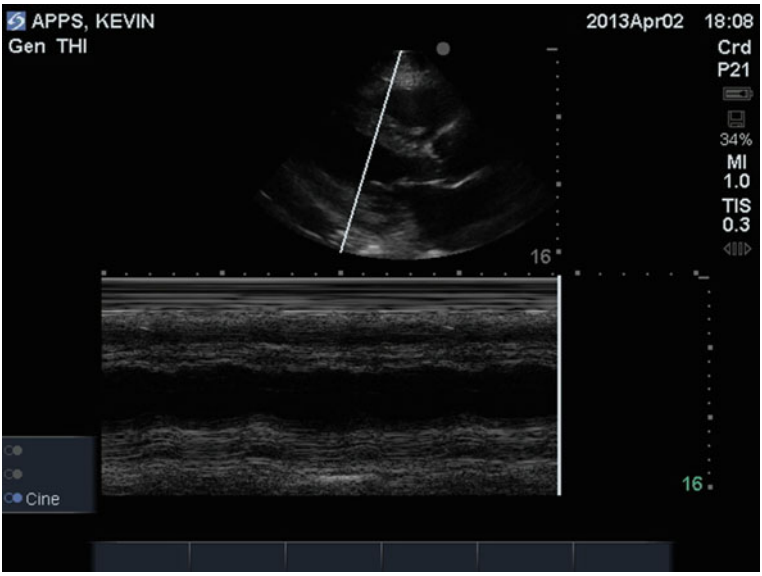

Fig. 1.12 M-mode, showing the change over time across a single plane of Ultrasound

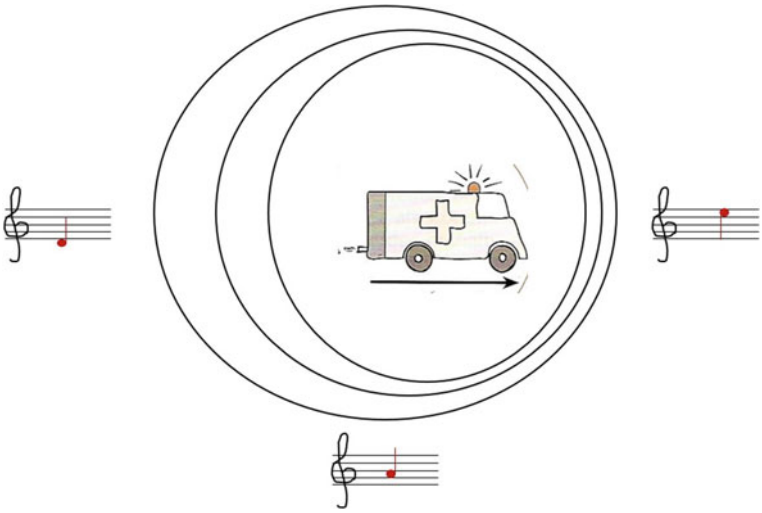

Fig. 1.13 Doppler effect—change of frequency depending on direction of sound waves

1.4.4 Doppler

The Doppler Effect describes a change in frequency of sound waves depending on the direction. As an example, in Fig. 1.13 the pitch (and with that the frequency) changes depending on the relative movement of the ambulance towards a listening person. If the ambulance travels towards a person the pitch is relatively high, gets lower once the ambulance is passing and even lower once the ambulance is moving away.

The ultrasound angle for Doppler measurements should be different from 90°, otherwise no flow can be observed (particularly in veins, where velocities are low). The amplitude and direction of the Doppler signal will change depending on the angle of the ultrasound transducer towards the flow through a blood vessel or heart valve (Fig. 1.14).

1.5 Ultrasound Transducers

For point of care ultrasound (POCUS), the most used probes are curvilinear, linear and phased array transducers. Other more specialised probes are cavity (gynaecology), hockey stick and TOE (both cardiology) transducers.

The Linear probe (Fig. 1.15) is a high frequency transducer (>7 MHz, small wavelength), which has excellent superficial resolution. However, secondary to the high frequencies the absorption of ultrasound is large, resulting in a small (usual less than 9 cm) depth. It is used for the visualisation of superficial structures (i.e.

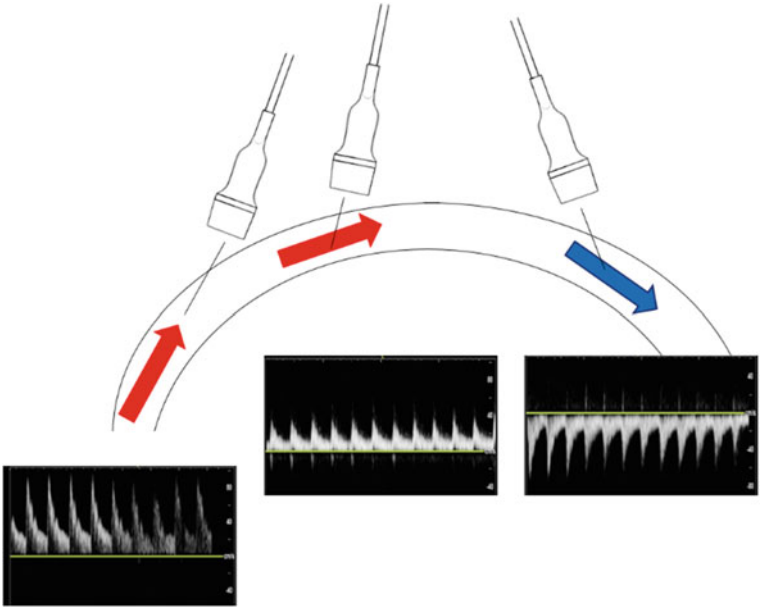

Fig. 1.14 Ultrasound angle and doppler signal

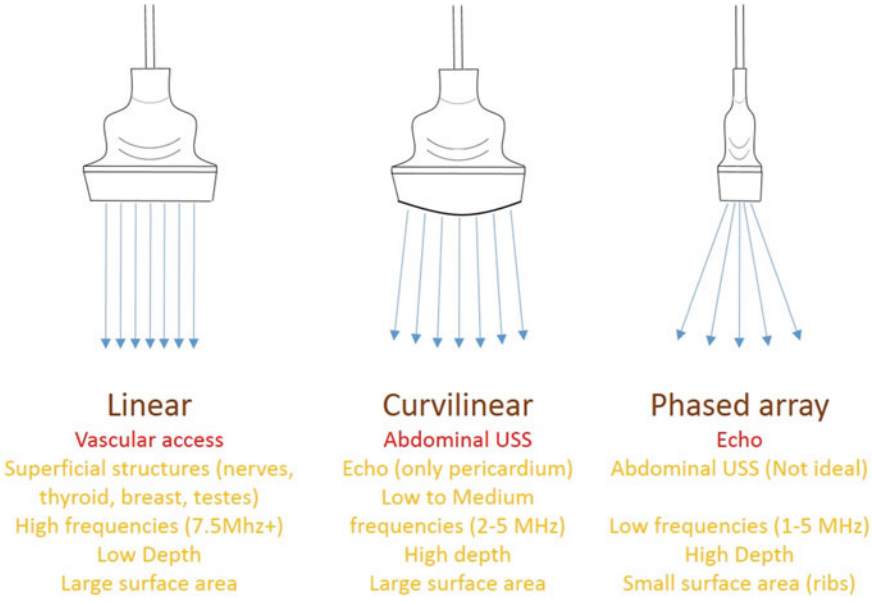

Fig. 1.15 Ultrasound transducer

nerves, muscles, arteries, veins, thyroid, breast and testes) and needle guidance for biopsies, nerve blocks and vascular access.

The curvilinear probe (Fig. 1.15) is a low frequency transducer with a relatively preserved superficial resolution and a great depth (up to 30 cm). It is used for thoracic and abdominal ultrasound and can be used for purposes of the linear probe if greater depth is required (e.g. patients with higher BMI). It has a relatively large footprint.

The phased array probe (Fig. 1.15) is a low frequency transducer with a small footprint. Superficial resolution is extremely poor. It is ideal for Echocardiography with great depth (up to 30 cm), and the right pulse repetition to assess muscle and valvular movement.

1.6 Ultrasound Terminology

Echogenic: ability to produce echoes

Isoechoic: similar echogenicity to a neighbouring structure

Anechoic: no echoes, appears black on ultrasound (fluid, Fig. 1.16)

Hyperechoic: highly reflective, bright when compared with neighbouring structures

Hypoechoic: less reflective, less bright when compared with neighbouring structures (see Fig. 1.17).

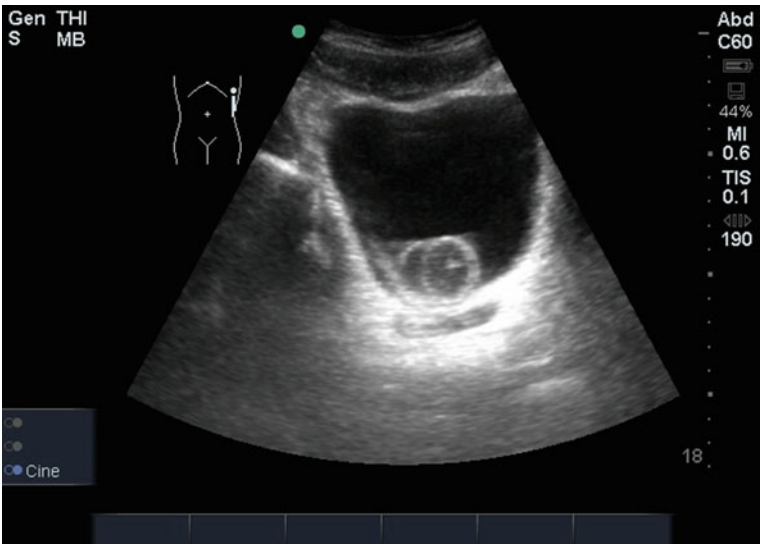

Fig. 1.16 The urine in the bladder is anechoic, the balloon of the catheter is hyperechoic compared to surrounding fluid: Note the posterior enhancement behind the fluid filled bladder

1.7 Artefacts

Ultrasound images may show structures which are not there or changes which are not anatomical. These phenomena are called artefacts. Some artefacts are avoidable while others are used for diagnostic purposes. The following elaboration introduces some general artefacts. Organ specific artefacts will be presented in their respective chapters.

1.7.1 Dorsal Acoustic Shadow

If there is a large difference of impedance between tissues, as in soft tissue to bone, almost all of the ultrasound energy will be reflected, resulting in a very bright echo. Additionally, in the case of bone or calcium (stones) the little non reflected ultrasound will be absorbed, leaving an echo free (shadow) area behind the reflexion.

1.7.2 Posterior Enhancement

The word enhancement is not quite correct. A fluid filled area will absorb less ultrasound than the surrounding areas. Having gained deeper areas more than superficial areas (TGC), the structures behind a fluid filled space will appear brighter than the surrounding tissue. This is one of the diagnostic criteria for fluid filled spaces (e.g. cysts) see Fig. 1.16.

1.7.3 Lateral Wall Sign

If ultrasound hits a round structure tangentially, it will be deflected. No ultrasound waves will be found just behind the lateral wall resulting in a narrow shadow.

1.7.4 Mirror Artefact (Figs. 1.18 and 1.19)

If the ultrasound hits a strong reflector at around 45° angle (e.g. the hemi-diaphragm), a second mirrored structure will appear on the screen on the other side of the reflector, caused by the longer travelling time for the reflected ultrasound wave (the ultrasound device does not know that reflection happened and so will show the structure at the measured depth according to the time taken). The mirror artefact can be used as a diagnostic aid. A mirrored liver above the hemi-diaphragm excludes a pleural effusion at the scanned level.

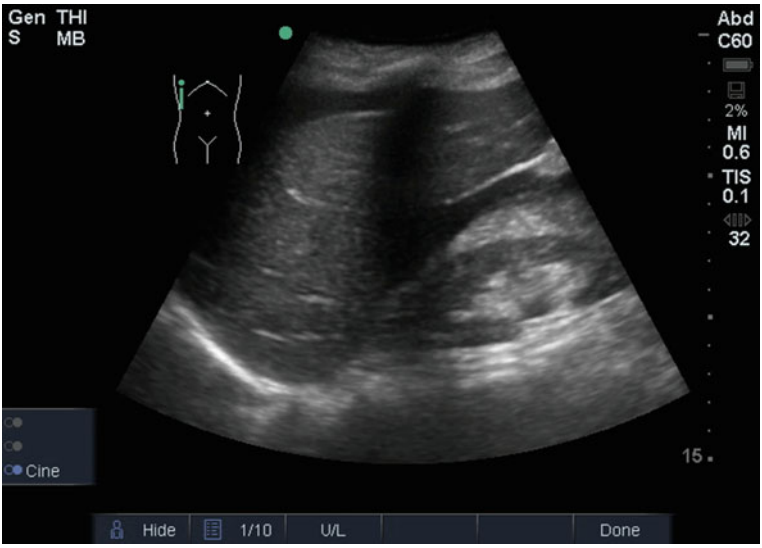

Fig. 1.17 Liver and kidney tissues are isoechoic, the surrounding ascites is anechoic

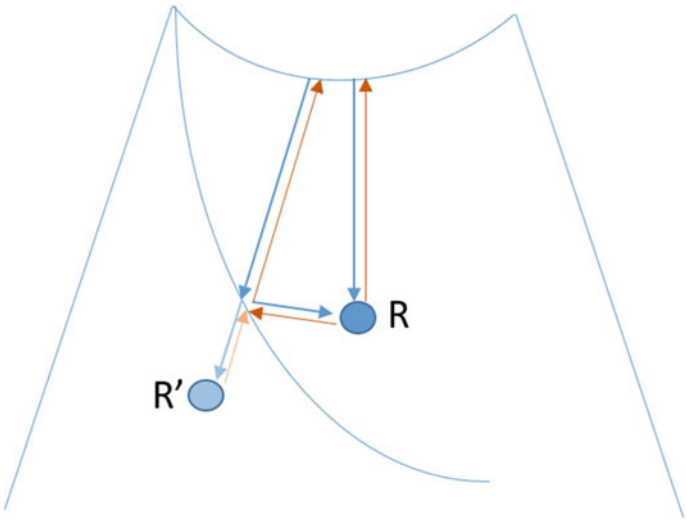

Fig. 1.18 A structure R will be shown as R' behind a strong reflector, caused by reflection of ultrasound

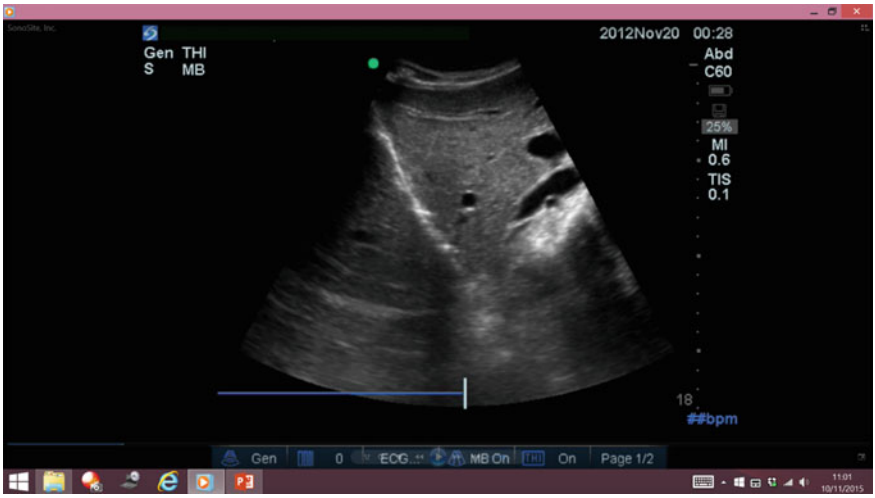

Fig. 1.19 The diaphragm will act as a strong reflector if there is no pleural effusion and so the mirrored liver tissue can be used as a diagnostic marker to exclude a pleural effusion

1.8 Conclusion

An understanding of the physics of ultrasound is vital as it allows the point of care ultrasound operator to understand the genesis of artefacts, how to avoid them and also how to use them diagnostically.

See also Chap. 2.

Chapter 2
Preparation and Image Optimisation

Martin R. Dachsel

Keywords Physics · Doppler · Point of care ultrasound

2.1 Introduction

There are many customs which have developed for ultrasound examination of different body systems and within different areas of ultrasound. The principles of preparation and image optimisation remain much the same regardless of which part of the body is being examined. This chapter elaborates on how to orientate and optimise ultrasound images.

2.2 Preparation

In abdominal ultrasound and lung ultrasound, the marker dot should be on the left hand side of the screen. The corresponding marker on the ultrasound transducer should aim towards the patient's head or the patient's right hand side.

For vascular access the marker should always be on the left hand side of the operator (particularly important if used from the head end to insert central lines!). In echocardiography the marker dot should be on the right hand side of the screen with different probe positions for different windows.

If the picture quality is suboptimal, there are some important manoeuvres to attempt. A left lateral position is useful for echocardiography (minimising lung between chest wall and heart) and abdominal ultrasound (displacing bowel).

Deep inspiration will move the liver inferiorly and will enable the liver to be used as a window to assess deeper structures.

M. R. Dachsel (✉)
Acute Medicine, East Surrey Hospital, Canada Avenue, Redhill, Surrey R1 5RH, England
e-mail: rdachsel@nhs.net

A. Walden et al. (eds.), *Ultrasound in the Critically Ill*,
https://doi.org/10.1007/978-3-030-71742-1_2

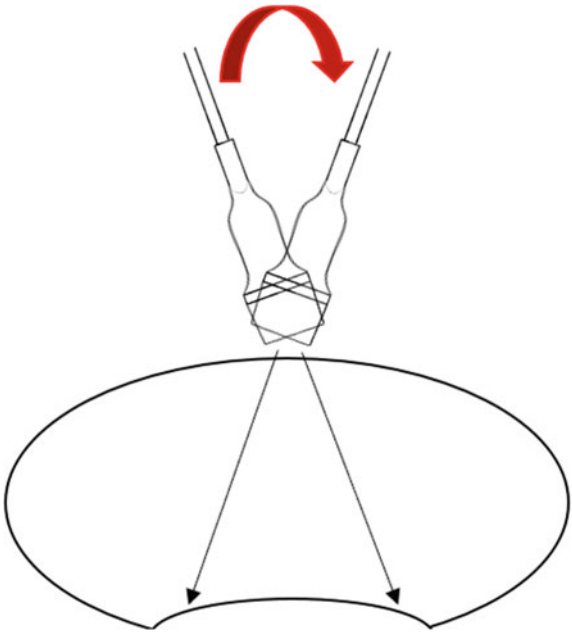

Fig. 2.1 Tilting (short axis of curvilinear probe shown)

The use of pressure (after warning your patient) can be also useful in displacing air from stomach or bowel.

Once an organ has been found, the whole organ should be imaged. It is best to move to a position where the organ has just disappeared and then to image through the whole organ. The next step is to change to a different axis and repeat the process. The following transducer movements are possible (Figs. 2.1, 2.2 and 2.3).

2.3 Image Optimisation

2.3.1 Depth (Fig. 2.4)

The depth of the ultrasound field is important for imaging. It is always worthwhile to start with an extended depth and once satisfied that there is no pathology behind the structures of interest, the depth can be decreased (particularly important when imaging the heart to assess for pericardial/pleural fluid). When decreasing the depth remember that in most point of care ultrasound systems, the focus zone cannot be changed and is in the middle of the screen (the focus zone is the area with the narrowest beam and hence the best resolution).

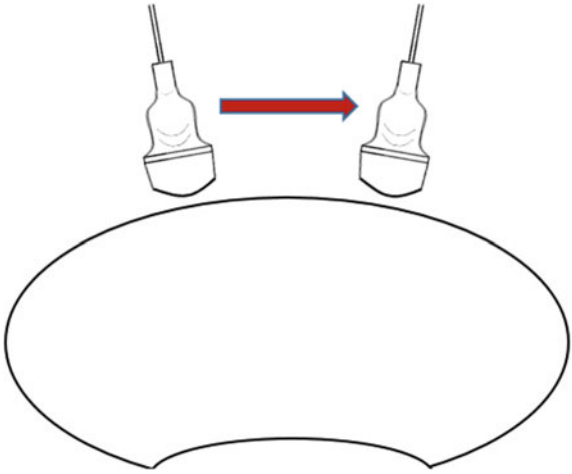

Fig. 2.2 Sliding

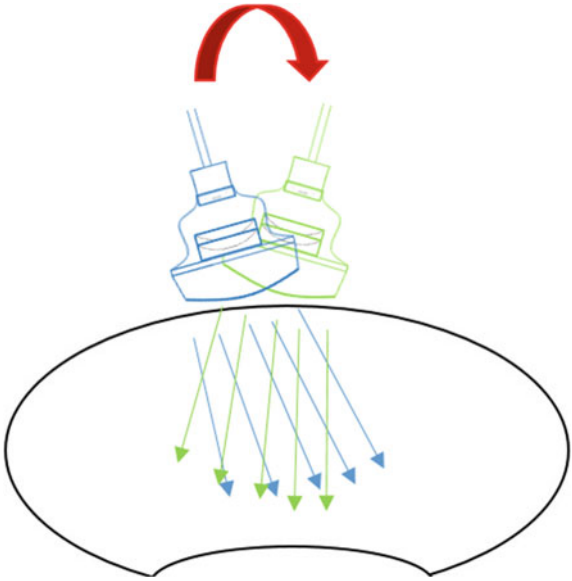

Fig. 2.3 Rocking (long axis of curvilinear probe shown)

2.3.2 Gain (Fig. 2.5)

Gain is adjusting the overall brightness of the image. Ideally the image should have good contrast without being too dark or bright. Increasing the gain will also increase the noise in the image. Most current point of care ultrasound devices will have an Autogain button.

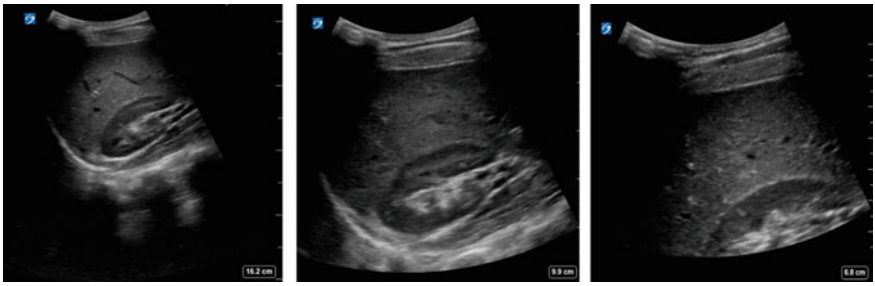

Fig. 2.4 B-mode image of right upper quadrant with extended, ideal and insufficient depth

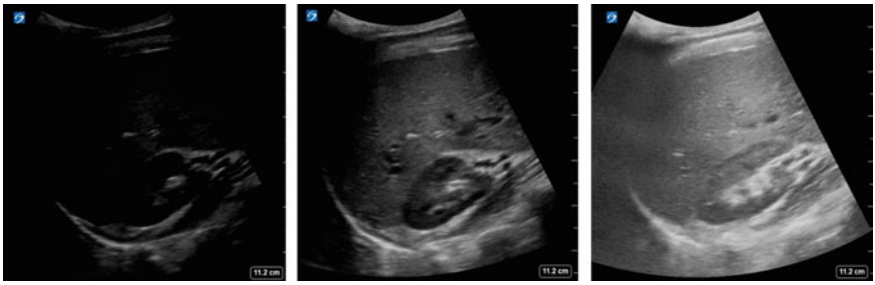

Fig. 2.5 B-mode image of right upper quadrant with too little, optimal and too much gain

2.3.3 Time Gain Compensation (TGC, Fig. 2.6)

Ultrasound waves will be attenuated while passing through tissue. Signals from deeper areas (more time) therefore need to be more gained than superficial areas (less time). Point of care ultrasound devices usual have a near field and a far field knob, while departmental devices have 6 to 8 different sliders to change TGC.

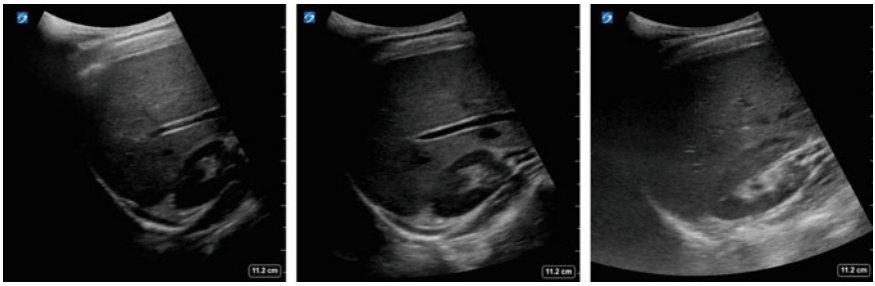

Fig. 2.6 B-mode image of right upper quadrant with different settings for TGC: left: superficial area too much gained, middle: optimal, right: deeper areas too much gained

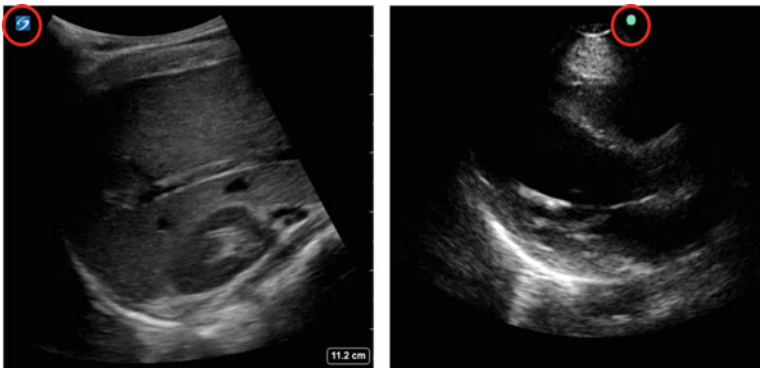

Fig. 2.7 Orientation of marker dot in abdominal/chest ultrasound (left picture) and echocardiography (right picture)

On the left hand side of Fig. 2.6 the superficial areas were gained too much, while on the right hand side the deeper structures were gained too much. The middle image shows optimal TGC.

2.3.4 Orientation (Fig. 2.7)

In abdominal and chest ultrasound, the marker dot should always be on the left hand side of the screen (Fig. 2.7, left picture). In echocardiography however, the marker dot should be on the right hand side of the screen (Fig. 2.7, right picture). Newer ultrasound systems will change the orientation of the screen according to the ultrasound program. In older devices however it is important to check to avoid difficulties in interpreting the ultrasound image.

2.4 Conclusion

Adequate preparation and image optimisation are especially important in point of care ultrasound where patient positioning and access may be difficult. Mastering these skills will enhance the diagnostic performance of point of care ultrasound.

See also Chap. 1 Physics of Ultrasound.

Chapter 3
Clinical Governance

Sonya Daniel and Tom Holmes

Keywords Governance · Point of Care Ultrasound

3.1 Introduction

'Clinical Governance is the system through which NHS organisations are accountable for continuously improving the quality of their services and safeguarding high standards of care, by creating an environment in which clinical excellence can flourish', DoH 1998.

Responsibility for ultrasound clinical governance exists at an organisational, departmental and individual level. The exact structure and process may vary between organisations. However, the general purpose is always to ensure a service delivers high quality patient care that continuously improves. The Institute for Healthcare Improvement has developed a list of attributes that define high quality healthcare including: safety, effectiveness, patient-centredness, timeliness, efficiency and equity.

The two unique responsibilities specific to ultrasound governance are: to ensure the service has well trained, high performing ultrasound practitioners; and that equipment has appropriate specification and adequate maintenance. This chapter will outline the governance of these two specific areas in the context of a hierarchy of governance responsibility.

S. Daniel (✉) · T. Holmes
University Hospital of Wales, Heath Park Way, Heath Park, Cardiff C14 4XW, UK
e-mail: Thomas.Holmes2@wales.nhs.uk

A. Walden et al. (eds.), *Ultrasound in the Critically Ill*,
https://doi.org/10.1007/978-3-030-71742-1_3

3.2 Organisational Ultrasound Governance Board

At an organisational level, the forum through which ultrasound clinical governance is often delivered is an ultrasound governance board. Members may include the director of governance, lead ultrasound radiologist, lead ultra-sonographer, clinical lead for each specialist department using ultrasound, a medical physics representative, procurement representative and a finance department representative.

The board are responsible for the following aspects of ultrasound governance:

1. Maintaining a register of trained ultrasound operators including names, grades and qualifications to practice. If an operator has no formal qualifications, a description of the process of training and assessment the operator has undertaken is recorded.
2. Maintaining a register of all ultrasound machines in use within the organisation, which purposes they are used for, how frequently the machines are used, records of the maintenance contracts, picture archiving and communication system (PACS) connectivity or alternative archiving method of each machine.
3. Ensuring ongoing supervision for practitioners in training and those who are already qualified. This includes development of a policy outlining structures for the support of appraisal/professional development review (PDR), continuous professional development (CPD) and expected audit activity of studies to be carried out.
4. Creating standards for providing information to patients regarding their ultrasound examination such as patient information leaflets and the process of informed consent.
5. Compliance with information governance standards and must ensure policies on data security, standards for image recording, study documentation and communication of results are adhered to.
6. Patient safety due to the potential bio-effects of ultrasound. This should be highlighted through policy and development of strategies to minimise these risks.
7. Promoting occupational safety by devising a policy to protect practitioners from work related musculoskeletal disorders.
8. Policies and procedures for infection control relevant to ultrasound equipment.

3.3 Departmental Ultrasound Governance Group

At a departmental level, an ultrasound governance group may include: the clinical lead for ultrasound, the department's registered ultrasound practitioners and equipment technicians. A good collaborative working relationship with the organisation's radiology department is essential, therefore a nominated ultrasound lead from radiology is often part of many departmental governance groups. Regular

meetings to review and reflect upon a sample of studies, audit results and prioritise improvement projects is the traditional forum through which departmental governance is coordinated.

In addition to maintaining practitioner and equipment specific data for the ultrasound board, the group is also responsible for delivering the following:

1. Training and assessment of the department's ultrasound practitioners. This should adhere to standards defined by the relevant college e.g. Intensive Care Society Focused Intensive Care Ultrasound (FUSIC) competencies. Where training and assessment for a specific scope of practice is not covered by colleges the Royal College of Radiologists document 'Ultrasound Training Recommendation for Medical and Surgical Specialties—2nd edition" (2012) can be followed.
2. Support of trained practitioners to develop their ultrasound practice through regular appraisal/PDR process and CPD activities.
3. Ensuring equipment have service contracts through which they are regularly quality assured and maintained.
4. Specific policy regarding equipment hygiene practice for the machine within that department should be in place.

Much of the departmental policy development should use the organisation's policies as a foundation and then expanded to specific detail relevant for their service. Importantly, however, each department will need to write a policy document that explicitly defines and describes the scope, indications and extent of ultrasound studies it will be accountable for delivering.

3.4 Individual Practitioner Governance

Each practitioner has a responsibility for self governance. Specifically, this will include fulfilling requirements of training and assessment prior to independent practice, demonstration of maintenance of their skills through keeping a logbook/record of practice, engagement and contribution to departmental governance process and demonstration of regular commitment to CPD and appraisal.

3.5 Conclusion

In this chapter we have described the structure, process and specific components of clinical governance in an ultrasound service. We have emphasised the importance of having this structure to bring clarity of responsibility and accountability, processes needed to deliver the requirements of governance and outlined on the main components relevant to ultrasound. Bringing all of these elements together requires

commitment, diligence and a culture of strong leadership, supportive team work and good communication.

There are many customs which have developed for ultrasound examination of different body systems and within different areas of ultrasound. The principles of preparation and image optimisation remain much the same regardless of which part of the body is being examined. This chapter elaborates on how the ultrasound image should be orientated and optimised.

Chapter 4
Airway Ultrasound

Michael S. Kristensen and Wendy H. Teoh

Keywords Ultrasonography · Airway management · Cricothyroid membrane · Emergency airway access · Intubation

4.1 Introduction

Airway ultrasonography as both a diagnostic and interventional modality, is now an essential and integrated part of point of care sonography.

In this chapter we will describe the equipment needed, typical features and appearances from the tip of the tongue to the pleura. We will also demonstrate the application of published clinical applications. This chapter should be read in conjunction with the Lung Ultrasound chapter.

4.2 Equipment Needed for Airway Sonography

The linear, medium to high frequency (5–14 MHz) transducer is suitable for imaging superficial airway structures (within 0–5 cm beneath the skin surface). The curved low-frequency transducer (~4.0 MHz) is most suitable for obtaining sagittal and parasagittal views of the tongue and structures in the submandibular and supraglottic regions, mainly because of its wider field of view. Linear transducers which are used for assessment of the upper airways provides excellent images of superficial structures such as ribs and the pleura, but deeper structures can be difficult to assess. A microconvex transducer (~8.0 MHz) is a good all-round transducer for focused ultrasonographic examination of the lungs, since most

M. S. Kristensen (✉)
Rigshospitalet, Section 3071, Blegdamsvej 9, 2100 Copenhagen Ø, Denmark
e-mail: Michael.seltz.kristensen@regionh.dk

W. H. Teoh
Private Anaesthesia Practice, Wendy Teoh Pte. Ltd., Singapore, Singapore

A. Walden et al. (eds.), *Ultrasound in the Critically Ill*,
https://doi.org/10.1007/978-3-030-71742-1_4

microconvex transducers have an acceptable image quality of both superficial (pleura) and deeper structures (e.g. lung consolidation, atelectasis). Furthermore, microconvex transducers are often small, which makes is easier to access the posterior thoracic wall, when the patient can only be examined in the supine position. An alternative to the microconvex transducer for examination of the lungs is the curved low-frequency transducer ($\sim$4.0 MHz), which also has an acceptable image quality of both superficial and deeper structures Since visualisation of superficial and deep structures is needed, it is important to continuously optimise transducer frequency in order to obtain the best possible images. The presence or absence of artefacts such as B-lines are an important part of lung-ultrasonography hence one should be mindful to deactivate any image optimisation software that is inherently built-into newer ultrasound machines, as this would remove or diminish the presence of these useful artefacts when performing lung-ultrasonography.

4.3 Typical Features of Airway Sonography and the Tissue/Air Border

From a historical radiological point of view, air and bony structures have been considered enemies of ultrasonography. Air from bowel gas is a well-known challenge in ultrasonography e.g. the air reduces the diagnostic view to underlying abdominal parenchyma. Several studies have, however, established that the air artefacts can often be used in clinical practice, rather than being an annoyance to the physician performing sonography. By understanding the generated air artefacts seen with ultrasonography, the information can serve as an important diagnostic tool. The technical explanation of air artefacts and how to understand the information gleaned from them are explained below. As soon as the ultrasound (US) beam reaches air a strong echo (=a strong white line) will arise, this is the tissue-air-border and everything beyond that line is only artefact (Fig. 4.1). This means that we can depict the tissue from the skin and until the anterior part of the airway as for example the posterior surface of the tongue, the mucosal lining of the anterior trachea and the pleura. Intraluminal air will thus prevent visualization of structures such as the posterior pharynx, posterior commissure, and posterior wall of the trachea.

Due to differences in velocity and acoustic impedance of ultrasound between normal tissue and air filled parenchyma (lung, trachea, etc.), a total reflection of ultrasound occurs. Air has a high attenuation coefficient for the transmission of ultrasound. Therefore normal lung parenchyma appears as a homogenous grey picture on B-mode and often, special reverberation artefact creates multiple parallel white lines on the screen. Furthermore the presence of characteristic artefacts can be used as an indirect marker of lung disease. The most useful of these artefacts are the B-line artefacts, which are believed to occur when the density of the lung is increased, for example in interstitial oedema or pulmonary fibrosis. The ultrasonic

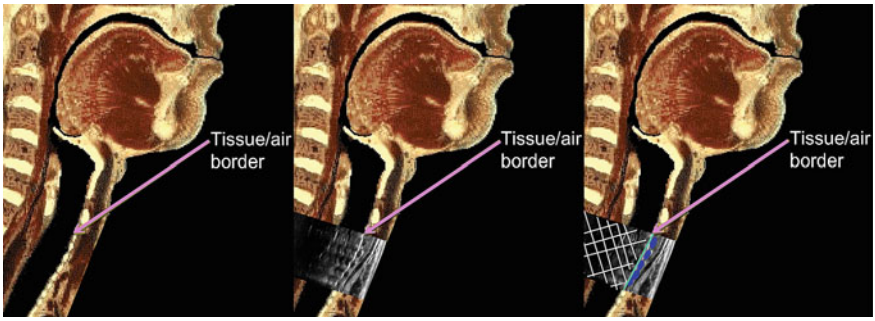

Fig. 4.1 The tissue/air border. Left: A cadaveric slice of the upper airway. The arrow indicates the tissue/air border. Middle: The ultrasonographic image. Right: Explanation of the ultrasonographic image: Blue rings indicate the anterior part of the tracheal rings, The green line is the tissue/air border between the mucosal lining of the anterior trachea and air. The image area covered by the white grid is entirely made up of artifacts (Courtesy The Scandinavian Airway Management Course, Airwaymanagement.dk)

waves are believed to cause resonance in the lung interstitium with increased density: this continuing echo-signal appears on the screen as a strong hyper echoic, laser-like, vertical line from the pleura and extends to the bottom of the field of view, moving synchronously with lung sliding.

4.4 Normal Airway from the Tongue to the Pleura Is Depicted (Figs. 4.2, 4.3, 4.4, 4.5, 4.6 and 4.7)

Figures 4.2, 4.3, 4.4, 4.5, 4.6 and 4.7 demonstrate the normal pattern of ultrasound seen moving in a caudal direction from the tongue to the apex of the lung. The correct orientation of the probe with major structures are shown.

4.5 Clinical Application of Airway Ultrasound

Whilst there are lots of applications of airway ultrasound, the following are most relevant to emergency and critical care.

The equally useful airway-procedures: The ruling-out of an intraoperative pneumothorax and the evaluation of lung-pathology are described in the lung ultrasound chapter.

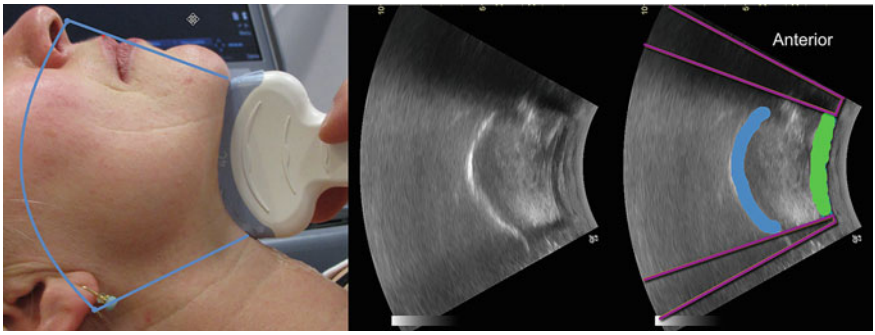

Fig. 4.2 Mouth and tongue. Left: The curved, low frequency transducer and the area covered by the scanning (light blue). Middle: The resulting ultrasound image. Right: The dorsal surface of the tongue (blue), muscles in the floor of the mouth (light green). The shadows (purple) from the mentum of the mandible anteriorly and from the hyoid bone posteriorly (Courtesy The Scandinavian Airway Management Course, Airwaymanagement.dk)

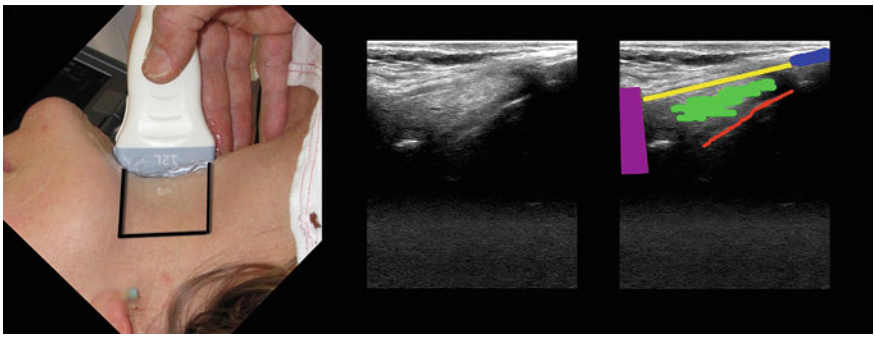

Fig. 4.3 Midline sagittal scan from the hyoid bone to the proximal part of the thyroid cartilage. Left: The black outline shows the area covered by the scanning. Middle: The scanning image. Right: The shadow from the hyoid bone (purple). The thyro-hyoid membrane (yellow). Posterior surface of part of epiglottis (red). Pre-epiglottic fat (green). Thyroid cartilage (blue) (Courtesy The Scandinavian Airway Management Course, Airwaymanagement.dk)

4.5.1 Qualifying and Quantifying Airway Pathology and Deviations from Normal Anatomy that Are Relevant to Airway Management

If the history or physical findings give rise to suspicion of airway pathology and deviations from normal anatomy that are relevant to airway management, then a brief ultrasonography examination of the relevant part of the airway can help in identifying deviations from the midline, (Fig. 4.8) hypertrophy, tumours (Fig. 4.9a, b), cysts, papillomas, haemangiomas, stenosis, or blood vessels overlaying the

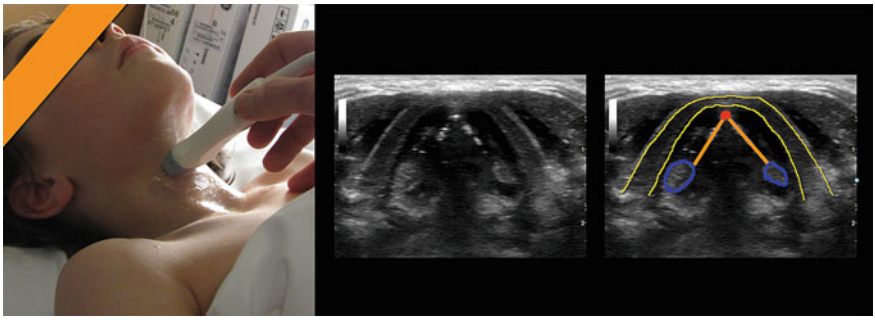

Fig. 4.4 Larynx and vocal cords. Left: Transverse midline scan over the thyroid cartilage (in an 8 year old boy). Vocal cords (orange). Anterior commissure (red). Arytenoid cartilages (blue). Thyroid cartilage (yellow) (Courtesy The Scandinavian Airway Management Course, Airwaymanagement.dk)

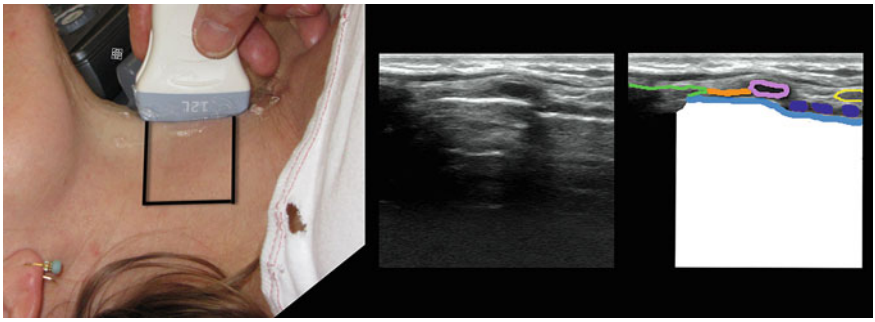

Fig. 4.5 Cricothyroid Membrane. Left: The linear high frequency transducer placed in the mid-sagittal plane, the scanning area is marked with a black line. Right: The cricothyroid membrane (orange). The thyroid cartilage (green). The cricoid cartilage (purple). Anterior part of tracheal rings (dark blue). The tissue/air border (light blue). The isthmus of the thyroid gland (yellow). Below the orange line only artifacts are seen (white) (Courtesy The Scandinavian Airway Management Course, Airwaymanagement.dk)

airway structures. An oesophageal ("Zenker's") diverticulum can be identified and might cause increased risk of aspiration. In addition to the observation of relevant pathology there are screening methods for prediction of difficult airway management with ultrasonography. These screening methods focus on the sonographic appearance of different structures; Measuring the thickness of the tissue in front of the airway, the hyo-mental distance in the neutral and the extended position and the distance from the skin to the epiglottis in the thyro-hyoid region can identify patients with a higher risk of having a difficult direct laryngoscopy. However the benefit of these screening methods have so far only been show in small series of selected patients and we can thus not recommend these techniques for routine wide spread screening yet.

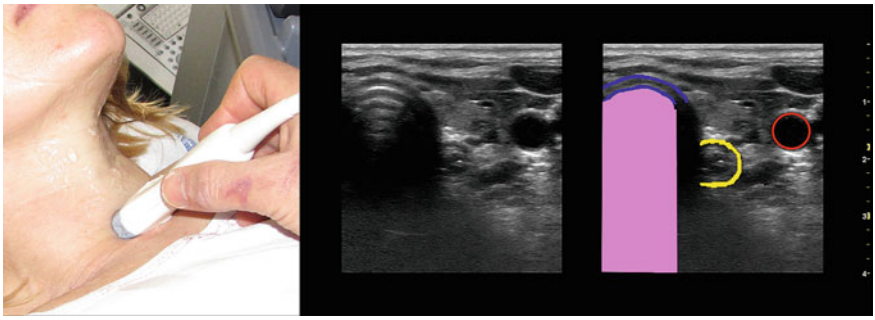

Fig. 4.6 Oesophagus and trachea. Transverse scan just cranial to the suprasternal notch and to. Anterior part of tracheal cartilage (dark blue). Oesophagus (yellow) is seen on the left side of the patient's trachea. Carotid artery (red). Below the tissue/air border in trachea only artefacts are seen (purple) (Courtesy The Scandinavian Airway Management Course, Airwaymanagement.dk)

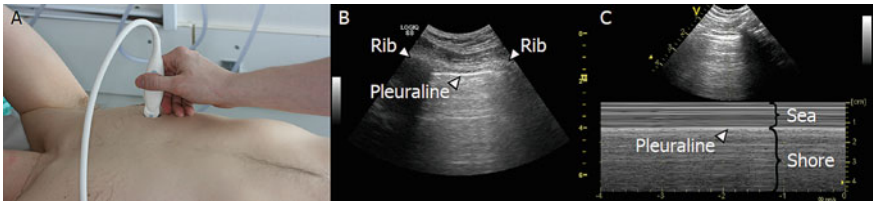

Fig. 4.7 Normal lung ultrasonography findings: **a** The transducer is placed in a longitudinal axis over an intercostal space at the anterior surface of the chest. **b** In the corresponding B-mode image, two ribs are visible aligning the intercostal space, as two hyper-echoic lines with an underlying shadow. Lying deeper between the two ribs, a hyper-echoic horizontal line is seen representing the visceral and parietal pleura. Using B-mode the movement of the pleural line is called "lung sliding". **c** If M-mode scanning is applied, a characteristic pattern called "seashore sign" is visible. The pleural line appears as a hyper-echoic line, with the more superficially placed structures appearing as horizontal lines similar to the sea and the part of the picture below the pleural line is grittier looking, mimicking the sand on a seashore (Courtesy The Scandinavian Airway Management Course, Airwaymanagement.dk)

4.5.2 Identification of the Trachea and the Cricothyroid Membrane

The cricothyroid membrane should be identified in all patients before induction of anaesthesia and in all other patients with airway compromise, if time allows. In a significant fraction of patients, especially the obese, the cricothyroid membrane cannot be identified with inspection and palpation [7].

In these cases ultrasonographic identification should be performed. We describe two approaches that have each been show to achieve a ninety per cent success rate in the morbidly obese after a short training for the practitioner. The cricothyroid

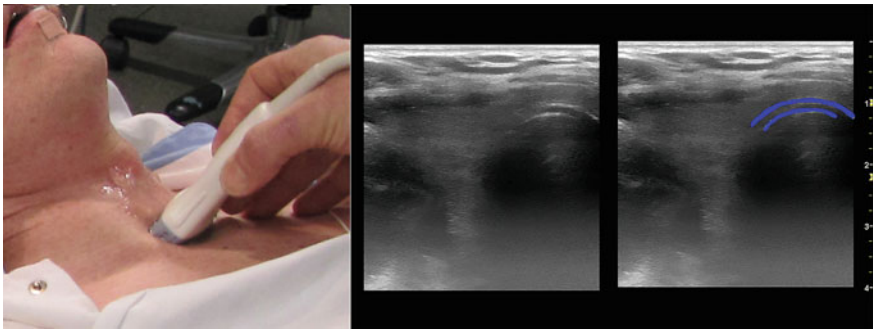

Fig. 4.8 Tracheal deviation. Patient with lateral deviation of the trachea after surgery and radiation therapy. The transducer is placed transversely in the midline over the suprasternal notch. Middle: The scanning image. Right: The cartilage of the tracheal ring (blue) is deviated to the patient's left side (Courtesy The Scandinavian Airway Management Course, Airwaymanagement.dk)

membrane could be identified in all cases with at least one of the techniques suggesting that the clinician should be proficient in both techniques [4].

The Transverse technique (the "TACA"-technique, ("Thyroid cartilage, Airline, Cricoid cartilage, Airline") [4]:

(1) Place the transducer transversely on the anterior neck at the estimated level of the thyroid cartilage and move the transducer until the thyroid cartilage is identified as a hyper-echoic triangular structure (Fig. 4.10).
(2) Move the transducer caudally until the cricothyroid membrane is identified: this is recognizable as a hyper-echoic white line resulting from the echo of the air-tissue border of the mucosal lining on the inside of the cricothyroid membrane, often with parallel white lines (reverberation artefacts) below.
(3) Move the transducer further caudally until the cricoid cartilage is identified (a "black lying-"C" with a white lining).
(4) Finally move the transducer slightly back cephalad until the centre of the cricothyroid membrane is identified.
(5) The location of the cricothyroid membrane can be marked both transversely and sagittal on the skin with a pen. By identifying both the highly characteristic shapes of the thyroid and the cricoid cartilages, both the cephalad and caudal borders of the cricothyroid membrane can been identified.
The technique is demonstrated in this video: http://airwaymanagement.dk/taca.

The Longitudinal technique (the "String of Pearls"-technique) [4]:

(1) Palpate the sternal bone and place the ultrasound transducer transversely on the patient's anterior neck cephalad to the suprasternal notch to visualize the trachea (horseshoe-shaped dark structure with a posterior white line) (Fig. 4.11).
(2) Slide the transducer towards the patient's right side (towards the operator), so that the right border of the transducer is positioned midline of the trachea, and

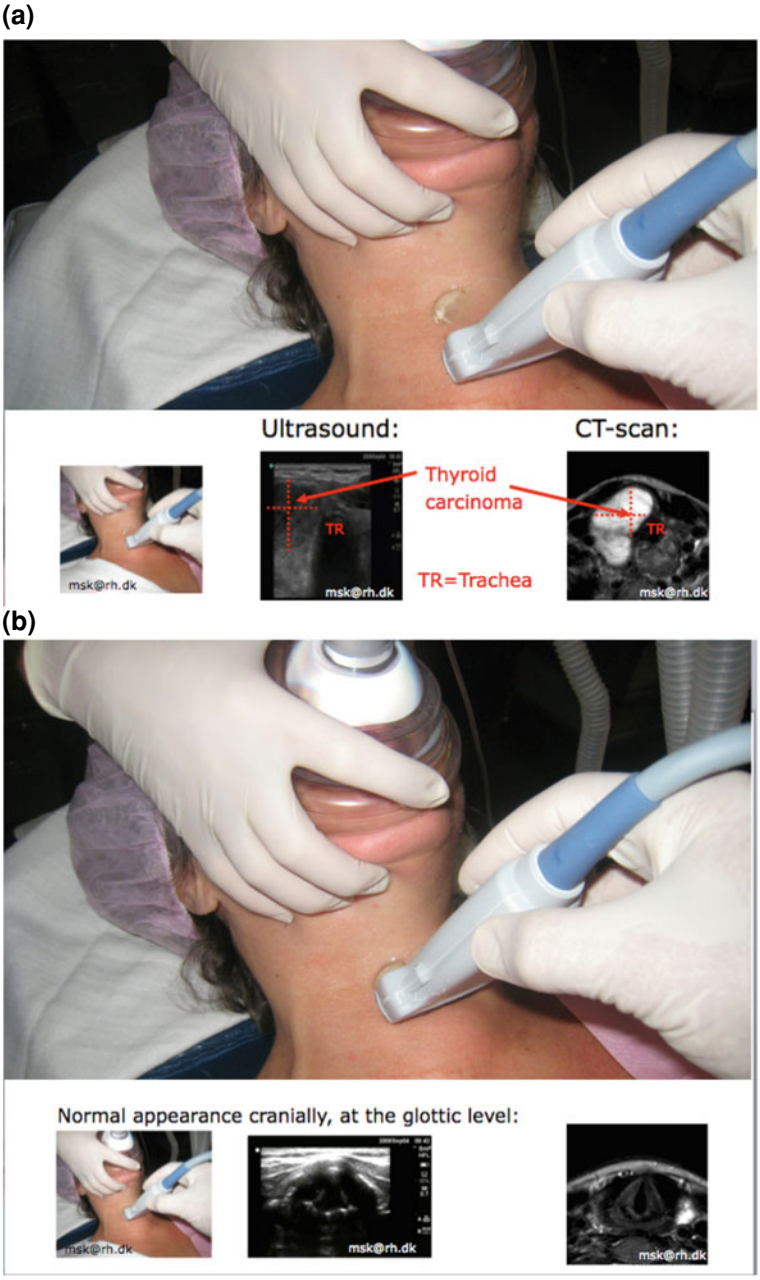

Fig. 4.9 **a** A mass on the neck. The ultrasound scanning at the level of the thyroid gland reveals a thyroid tumour and gives the same information as the ct-scan. **b** A mass on the neck, continued. The ultrasound probe is place more cranial than in Fig. 9a and reveals a glottic opening in the midline, without pathology (Courtesy The Scandinavian Airway Management Course, Airwaymanagement.dk)

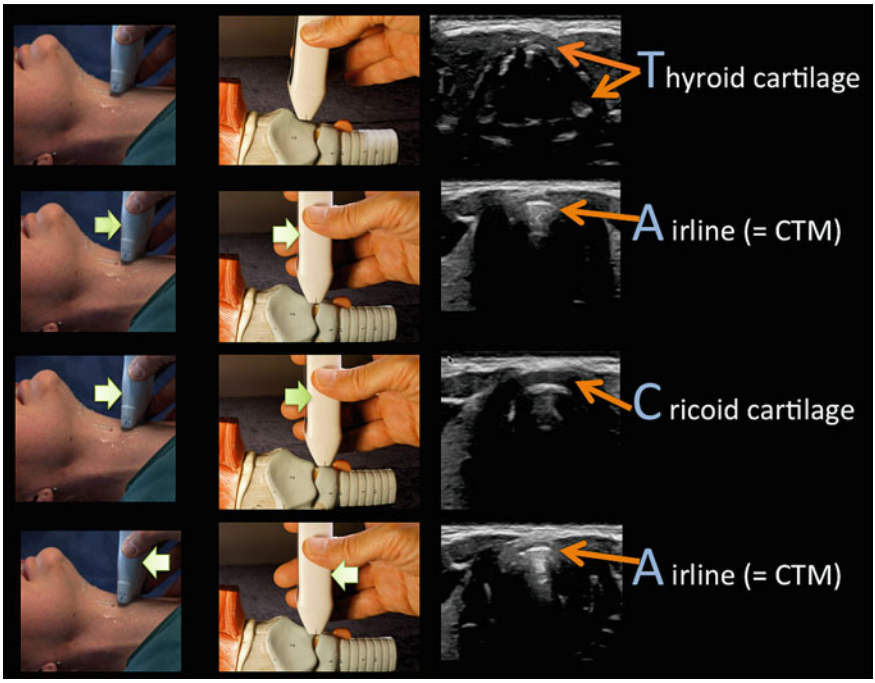

Fig. 4.10 Transverse. The Transverse ("Thyroid-Airline-Cricoid-Airline = TACA") method for identification of the cricothyroid membrane. First row: The transducer is placed transversely on the neck where the thyroid cartilage is thought to be until the triangular shape of the thyroid cartilage (The "T") is identified. Second Row: The transducer is moved caudally until the "Airline" (=the "A") is seen; this is the hyper-echoic (=white) line from the tissue/air border on the luminal side of the cricothyroid membrane. The white line has similar echo–lines deep to it, those are reverberation artefacts. Third Row: The transducer is moved further caudally until the cricoid cartilage (=the "C") is seen as a black lying "C" with a posterior white lining. The white lining represents the tissue/air border on the luminal side of the anterior part of the cricoid cartilage. Forth Row: Subsequently the transducer is moved a few millimetres back in cephalad direction and the approximate centre of the "Airline", (=the "A"), =the cricothyroid membrane, is thus identified and can be marked with a pen

the ultrasound image of the tracheal ring is thus truncated into half on the screen

(3) Keep the right end of the transducer in the midline of the trachea, whilst the left end of the transducer is rotated 90° into the sagittal plane resulting in a longitudinal scan of the midline of the trachea. A number of dark (hypo-echoic) rings will be seen anterior to the white hyper-echoic line (air-tissue border), akin to a "string-of-pearls". The dark hypo echoic "pearls" are the anterior part of the tracheal rings.

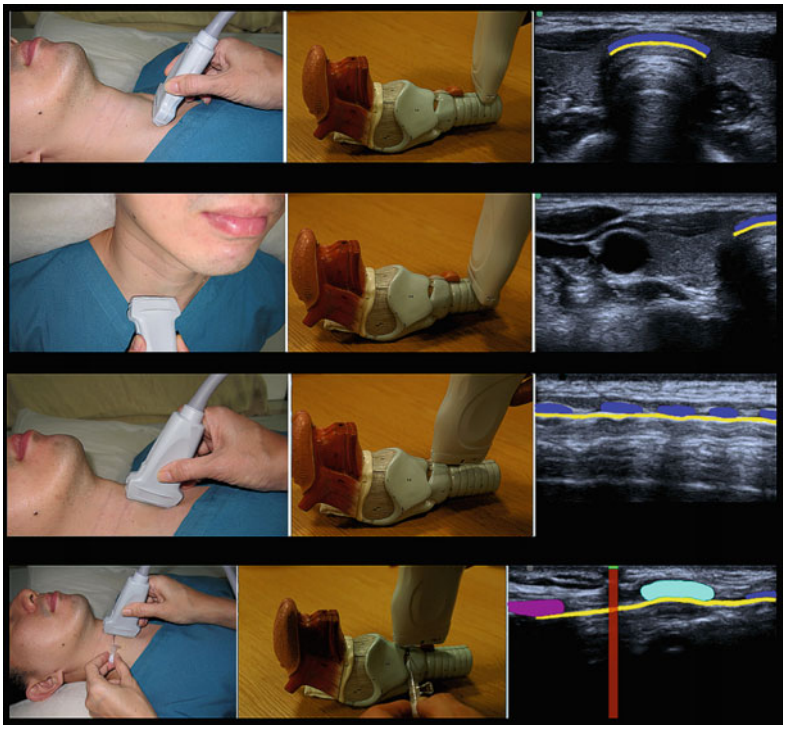

Fig. 4.11 Longitudinal. Upper row: Step One; The patient is lying supine and the operator stands on the patient's right side facing the patient. The sternal bone and the suprasternal notch are palpated, which can be done in even the morbidly obese patient. The linear high frequency transducer is placed transversely over the neck just cranial to the suprasternal notch and the trachea is seen in the midline. The middle and the right photo show the ultrasound image and the relevant structures are highlighted on the photo to the right. Blue is the anterior part of a tracheal ring. Yellow indicates the tissue-air boundary inside the trachea. Everything below the tissue-air boundary is artefact. Second row: Step two; The transducer is slid laterally towards the patient's right side, until the midline of the trachea is at the right border of the transducer, and the corresponding ultrasound image of the trachea (in the right photo) is truncated into half. Blue is the anterior part of a tracheal ring. Yellows indicate the tissue-air boundary inside the trachea. Third row: Step three; Staying midline with the right edge of the transducer, the left edge of the transducer is rotated into the sagittal plane to obtain a longitudinal image of the trachea. The anterior part of the tracheal rings are appearing as black hypo-echoic round structures (like pearls) lying on a strong hyper-echoic white line which is the tissue-air boundary (that looks like a string). Hence, the image is akin to a "string of pearls". The blue markings represent the anterior parts of the tracheal rings. Yellow indicates the tissue-air boundary inside the trachea. Fourth row: Step four; The transducer is slid cephalad and the anterior part of the cricoid cartilage (turquoise) is seen as a slightly elongated structure that is significantly larger and more anterior than the tracheal rings (blue). Yellow indicates the tissue-air boundary inside the trachea. Immediately cephalad to the cricoid cartilage is the distal part of the cricothyroid membrane. The distal part of the thyroid cartilage (purple) is seen. Step five; the cricothyroid membrane can be pointed out by sliding a needle (used only as a marker) underneath the ultrasonography transducer from the cranial end until it casts a shadow (red line) just cranial to the cricoid cartilage (turquoise). The green spot represents the reflection from the needle. Care is taken not to touch the patient with the sharp tip of the needle. After this the transducer is removed, step six, and the needle indicates the level of the distal part of the cricothyroid membrane. This spot can be marked with a pen so that it remains easily located should it be needed for subsequent difficult airway management

(4) Maintain the transducer longitudinally in the midline and slide it cephalad until the cricoid cartilage comes into view (seen as a larger, more elongated and anteriorly-placed dark "pearl" compared to the other tracheal rings). Further cephalad, the distal part of the thyroid cartilage can be seen as well.
(5) Keep holding the ultrasound transducer with the right hand and use the left hand to slide a needle (as a marker that cast a shadow in the ultrasound image) between the transducer and the patient's skin until the needle's shadow is seen midway between the caudal border of the thyroid cartilage and the cephalad border of the cricoid cartilage.
(6) Remove the transducer. Now the needle indicates the centre of the cricothyroid membrane in the transverse plane and this can be marked on the skin with a pen.
The technique is demonstrated on this video: http://airwaymanagement.dk/pearls.

Each of these two techniques has its own advantages For example some patients have too little space in the neck to accommodate the ultrasound transducer in a longitudinal mid-sagittal position e.g. short necks, severe neck flexion deformity. Here, the transverse technique will be useful, and is the faster of the two techniques. The longitudinal technique on the other hand, reveal additional information compared to the transverse technique, i.e. the localisation of the cricoid-tracheal interspace and of the tracheal interspaces. Apart from the ability to identify overlying blood vessels and direct the clinician to choose another tracheal interspace for elective tracheostomy or retrograde intubation, the longitudinal technique is useful in airway rescue-situations where emergency access via the trachea would be needed instead of access via the cricothyroid membrane (e.g. in smaller children, in patients with tumours overlying the cricothyroid membrane and in case of subglottic obstruction). We recommend that clinicians learn and become proficient in both techniques because each ultrasound technique can address the other's shortcomings, and supplement each other synergistically when used in tandem to be a powerful bedside point-of-care tool.

4.5.3 Distinguishing Between Oesophageal, Tracheal, and Main-Stem Intubation

During tracheal intubation, visualization of the tracheal tube passing the vocal cords and the detection of end-tidal CO_2 are considered the gold standards of verification. These standards may not always be possible to meet—for example, in the difficult laryngoscopy patient or the low cardiac output state, respectively.

Ultrasonography (US) is able to provide a new monitor to determine the success of tracheal intubation and has the added facility to detect bronchial intubation. During attempts at tracheal intubation, Confirmation of the tracheal tube position within the trachea can be verified by US in two major ways—US scans of the

anterior neck during or immediately after intubation (direct detection), or by detecting ventilation at the pleural or diaphragmatic level.

Direct US scans of the anterior neck can be performed in three distinct areas: transversely, high on the neck at the level of the vocal cords where the dynamic, real time tissue movement due to the tracheal tube can be detected; transversely, lower on the neck at the level of the suprasternal notch where both dynamic and static scanning are effective; and longitudinal scanning covering the visible length of trachea.

We recommend placing a linear, high-frequency transducer transversely on the neck immediately cranial to the suprasternal notch in the midline (Fig. 4.6). The trachea is identified as a horseshoe-shaped dark structure with a strong white line "tissue–air-border" artefact and a "comet-tail" artefact immediately posterior. The oesophagus is seen postero-lateral to the trachea on the patient's left side and has a "bulls eye" appearance due to its concentric layers. Asking the patient to swallow will make the oesophagus compress and expand and aid in its identification. Intubation should then be performed. If the tracheal tube enters trachea, a brief "snowstorm" artefact may be seen as the tracheal tube touches the anterior tracheal wall. No artefact may be seen if a layer of air separates the tracheal tube from the mucosa, precluding conduction of the US beam to the tracheal tube. If the tube enters oesophagus, it will create a "tissue–air border" in the otherwise collapsed oesophagus. This will appear as a strong white horizontal line that may repeat itself several times (like a flutter) due to "comet tail"—like artefact. The oesophagus will assume a shape similar to the trachea, but smaller, and a "double-trachea" sign (Fig. 4.12) will arise. This test has a sensitivity of 86–100% for detecting oesophageal intubation in emergency and cardiac arrest patients.

If the tracheal tube is seen passing into the oesophagus, it should be removed without initiating positive-pressure ventilation. Tracheal intubation may be reattempted as indicated. Successful intubation may or may not create an echo from trachea, so ventilation can be initiated as long as the tube is not appreciated in the oesophagus.

Subsequently, the transducer is moved to the mid-axillary line on either side of the patient's chest. The pleural line is identified, posterior to the rib. During positive-pressure ventilation, a "lung-slide" sign should be visualized bilaterally (Fig. 4.7). Lung sliding appears as a to-and-fro movement synchronous with ventilation. The movement is striking because the surrounding tissue is motionless. The detection of lung sliding can be enhanced by applying M-mode scanning which highlights a clear distinction between a wave-like pattern located above the pleural line and a sand-like pattern below. This is referred to as the "seashore" or the "sandy beach" sign. Detecting unilateral lung sliding confirms the intra-airway location of the tracheal tube, but does not rule out main-stem bronchus intubation. In this situation, a contralateral lung-pulse sign can be sought. The lung pulse arises from the beating heart pushing the lung and the pleura with each heartbeat (Fig. 4.13). If there is one-sided lung sliding and a contralateral lung pulse, then a main-stem intubation is likely, and the tracheal tube should be withdrawn gradually until bilateral lung sliding is present. If lung sliding cannot be detected on either

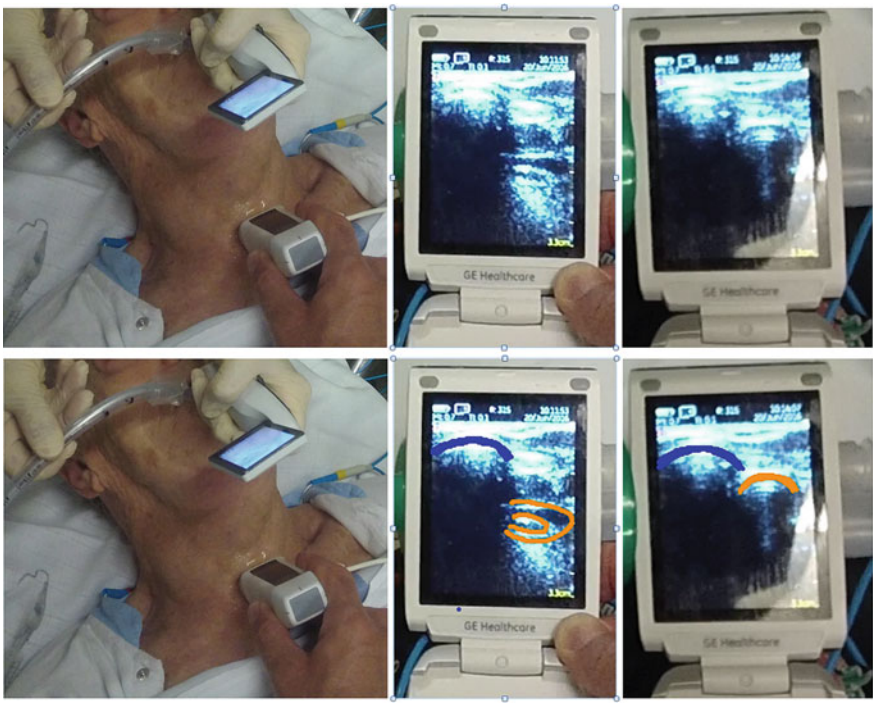

Fig. 4.12 Double trachea sign. Before intubation the linear transducer is placed transversely on the neck just cephalad to the jugular notch (left image in both rows). The anterior part of a tracheal cartilage as well as the oesophagus is depicted (upper row middle picture). The patient is intubated and the tube has entered the oesophagus, which results in the "double trachea sign" where the oesophagus resembles a smaller and more posterior second trachea (rightmost picture). The pictures in the lower row are identical with those in the upper row with the added color-coding of the tracheal cartilage (blue) and of the oesophagus (orange) (Courtesy The Scandinavian Airway Management Course, Airwaymanagement.dk)

side, but a bilateral lung pulse is present, the presence of oesophageal intubation should be reconsidered, and appropriate remedies should be taken. If there is neither lung pulse nor lung sliding, then a pneumothorax should be suspected.

The sensitivity for US distinction between tracheal and main-stem bronchus intubation is less (69–78%) than that for oesophageal and tracheal intubation when the differentiation is based on presence/absence of lung sliding/lung pulse alone. When evaluation of pleural lung sliding is combined with direct ultrasound guided observation of tracheal dilation via cuff inflation with air the accuracy is increased, the combination has a sensitivity of 93% and specificity of 96% compared to 66 and 59% obtained with auscultation. [5] Furthermore: In accidental main-stem bronchus scanning of the diaphragm will show no motion, or even paradoxical motion of the diaphragm, opposite to the side in which a main-stem intubation has occurred.

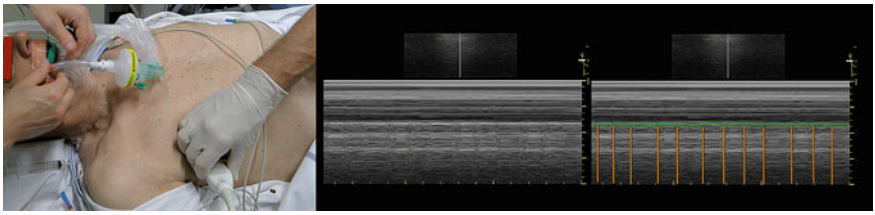

Fig. 4.13 Lung Pulse. Left: The ultrasound probe is placed transversely in an inter-space between two ribs during normal ventilation. Middle: The scanning image, upper: B-mode scan, lower: M-(Motion-)mode. Right: In the non-ventilated, but inflated, lung the heart will make the two pleural layers (green) move a bit with every heartbeat, creating the artefact known as "lung pulse" (orange) (Courtesy The Scandinavian Airway Management Course, Airwaymanagement.dk)

In children one can deliberately perform a right mainn-stem intubation, fill the cuff with saline and withdraw the tube until the saline-filled cuff is seen on ultrasonography with the linear transducer placed in the suprasternal notch. This technique showed a very high sensitivity (99%) and specificity (96%) [8].

4.5.4 Ultrasound Guided Surgical or Percutaneous Dilatational Tracheostomy

Ultrasonography allows real-time localization of the trachea, visualization of the anterior tracheal wall and pre-tracheal tissue including blood vessels, and selection of the optimal inter-cartilaginous space for placement of the tracheostomy tube. Ultrasound guided percutaneous dilatational tracheostomy results in a significantly lower rate of cranial misplacement of the tracheostomy tube than "blind" placement. The distance from the skin surface to the tracheal lumen can be measured in order to predetermine the length of the puncture cannula that is needed to reach the tracheal lumen without perforating the posterior wall. The distance can also be used to determine the optimal length of the tracheostomy cannula. Successful Ultrasound guided percutaneous dilatational tracheostomy has been utilised in cases when bronchoscope-guided techniques were abandoned. Bronchoscope guided percutaneous dilatational tracheostomy also often results in considerable hypercapnia whereas ultrasound Doppler guided percutaneous dilatational tracheostomy does not. Autopsy reports of cases of fatal bleeding following percutaneous dilatational tracheostomy have revealed erosion of the innominate vein and the arch of the aorta, where the tracheostomy level turned out to be much more caudal then intended. It is likely that pre-procedure ultrasonographic determination of the optimal percutaneous dilatational tracheostomy level could diminish this risk by allowing us to avoid major blood vessels.

In a prospective series of percutaneous dilatational tracheostomies, the combination of ultrasonography and bronchoscopy was applied. All subjects had their pre-tracheal space examined with ultrasonography pre-procedurally, leading to a change in the planned puncture site in a quarter of cases and to a change of the procedure to a surgical tracheostomy in one case where a goitre with extensive subcutaneous vessels was discovered on ultrasound examination. In a different approach, when a small curved transducer was used in the transverse plane to localise the trachea in the midline, then turned longitudinally to allow in-plane needle puncture, this enabled the needle course to be followed from the skin surface to the trachea. After guide-wire insertion, CT-scans that were performed showed that although all punctures successfully entered the trachea in first (89%) or second (11%) attempt. An alternative approach using real-time ultrasonic guidance with a linear high frequency transducer placed transversely over the trachea often results in visualization of the needle path und satisfactory guide wire placement.

Ultrasound guidance results in less deviation from the midline and in a higher first-pass success rate than palpation [6]. When ultrasound guidance was compared with bronchoscopy guidance there were no differences in outcome- or complications-parameters.

When ultrasound guidance alone is used there is still a risk of penetrating the endotracheal tube or te posterior tracheal wall with the needle, so the ideal approach is to use ultrasound guidance for identification of the optimal tracheal-ring-interspace and subsequently observe the rest of the procedure with a slim bronchoscope placed in the endotracheal tube.

When determining the ideal puncture site for a percutaneous dilatational tracheostomy one can employ the same “pearls on a string” approach (Fig. 4.11) as described for identification of the cricothyroid membrane, but in this case the needle is used to delineate the selected interspace between two tracheal rings.

4.6 Conclusion

Airways ultrasound in the point of care setting is invaluable both in terms of diagnosis and also in the facilitation of safe procedures on and off the intensive care unit and the anaesthetic room.

See also:

Chapter 5 Basic Lung Ultrasound.
Chapter 6 Advanced Lung Ultrasound.

References

1. Kristensen MS, Teoh WH. Ultrasound identification of the cricothyroid membrane: the new standard in preparing for front-of-neck airway access. Br J Anaesth. 2021 Jan;126(1):22–27.
2. Kristensen MS. Ultrasonography in the management of the airway. Acta Anaesthesiol Scand. 2011;55:1155–73.
3. Kristensen MS, Teoh WH, Graumann O, et al. Ultrasonography for clinical decision-making and intervention in airway management: from the mouth to the lungs and pleurae. Insights Imaging. 2014;5:253–79.
4. Kristensen MS, Teoh WH, Rudolph SS, et al. A randomised cross-over comparison of the transverse and longitudinal techniques for ultrasound-guided identification of the cricothyroid membrane in morbidly obese subjects. Anaesthesia. 2016;71:675–83.
5. Ramsingh D, Frank E, Haughton R, et al. Auscultation versus point-of-care ultrasound to determine endotracheal versus bronchial intubation: a diagnostic accuracy study. Anesthesiology. 2016;124:1012–20.
6. Rudas M, Seppelt I, Herkes R, et al. Traditional landmark versus ultrasound guided tracheal puncture during percutaneous dilatational tracheostomy in adult intensive care patients: a randomised controlled trial. Crit Care. 2014;18:514.
7. Teoh WH, Kristensen MS. Ultrasonographic identification of the cricothyroid membrane. Anaesthesia. 2014;69:649–50.
8. Tessaro MO, Salant EP, Arroyo AC et al. Tracheal rapid ultrasound saline test (T.R.U.S.T.) for confirming correct endotracheal tube depth in children. Resuscitation. 2015;89:8–12.

Chapter 5
Basic Lung Ultrasound

Luna Gargani

Keywords Lung ultrasound · B-lines · Ultrasound lung comets · Sliding sign · Pneumothorax · Consolidations

5.1 Introduction

Until only a few years ago, sonography was considered unhelpful in the assessment of the lung. Air has long been a renowned foe of the ultrasonographer as its physical properties do not allow penetration of the beam [1]. The evaluation of pleural effusions was the only "accepted" application of ultrasound on the chest. In more recent years, evidence has shown that ultrasound can provide useful clinical information not only about pleural effusions but also pneumothorax, interstitial disease (oedema and fibrosis), consolidations and collapse.

5.2 Basic Semiotics of Lung Ultrasound

Understanding the basic semiotics is the most important step in lung ultrasound (LUS) training. Ultrasound is very well suited to detect pulmonary de-aeration and should be considered as a "densitometer" of the lung parenchyma. When the lung is normally aerated, LUS can depict only the pleural line. As the lung loses its air content, the physical properties of the pulmonary parenchyma change, and part of the ultrasound beam can penetrate the lung, resulting in sonographic images. These images are artifactual when a certain percentage of air is still present in the parenchyma, and become real when the air is greatly reduced or has completely disappeared [2, 3] (Fig. 5.1).

L. Gargani (✉)
Cardiologist, Senior Researcher of the Institute of Clinical Physiology - National Research Council, Via Moruzzi 1, 56124 Pisa, Italy
e-mail: gargani@ifc.cnr.it

A. Walden et al. (eds.), *Ultrasound in the Critically Ill*,
https://doi.org/10.1007/978-3-030-71742-1_5

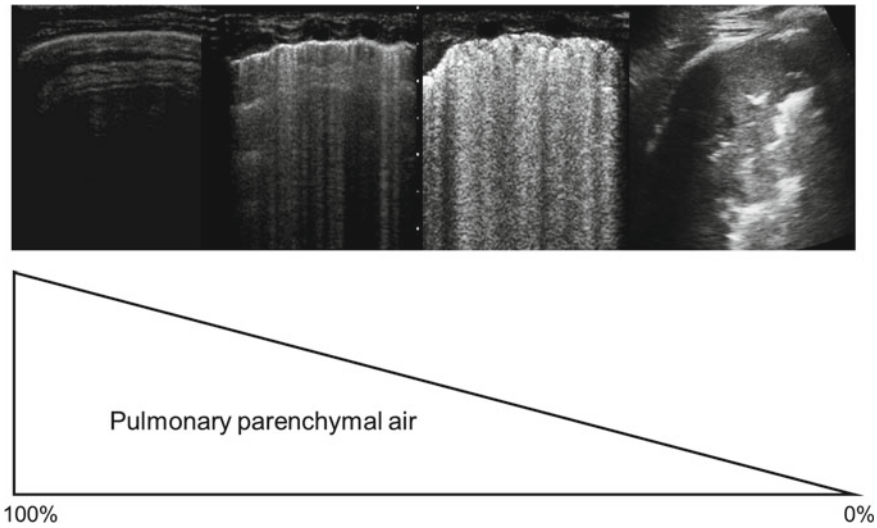

Fig. 5.1 Relation of ultrasound images to pulmonary air content

Lung ultrasound can be performed with most common ultrasound probes. A high frequency linear probe (such as is used for vascular access) gives high resolution images of the superficial pleura and allows lung sliding to be easily appreciated. Such probes are less useful for the lung bases due to their poor depth penetration. Phased array probes (used for echocardiography) have an ideal footprint for the intercostal spaces and can demonstrate all the sonographic information needed for LUS, although superficial resolution can be suboptimal. Curvilinear probes (usually used for abdominal scanning) allow a good balance between resolution of superficial and deep structures and are arguably the best single probes to use.

5.3 Normal Pattern

When the lung is normally aerated we can appreciate a horizontal hyperechoic line, the *pleural line*, which is the sonographic representation of the parietal and visceral pleura. The pleural line moves synchronously with respiration and this movement is called *lung sliding* [4, 5]. This can be demonstrated with M-mode with the cursor perpendicular to the pleural line when the so-called *seashore sign* can be appreciated [6].

Horizontal reverberation artefacts of the pleural line, the so-called *A-lines,* can be seen. A-lines are regularly spaced, and the distance between each A-line reproduces the distance between the pleura and the probe surface. A-lines can be more or less evident, depending on the probe, setting of the machine and the angle at which the beam hits the pleura (being most visible when the beam hits the pleura

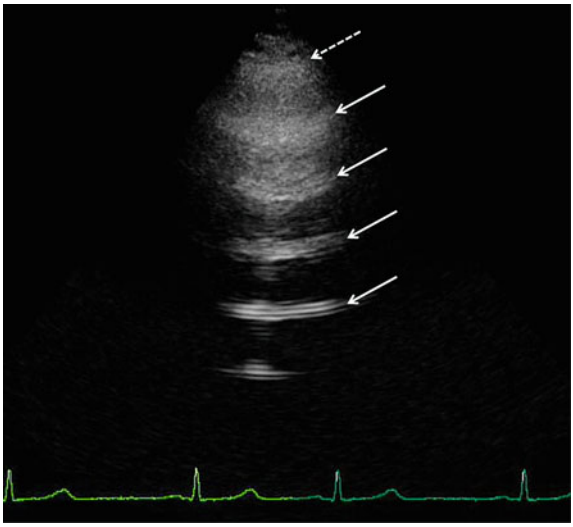

Fig. 5.2 Normal B-mode lung sonographic pattern. The dotted arrow indicates the pleural line; the continuous arrows indicate the A-lines

perpendicularly). They signify there is air below the pleural line and are therefore demonstrated in normal lung and pneumothoraces (Fig. 5.2).

For the above-mentioned physical reasons, ultrasound is not able to detect hyperinflation of the lung, whose imaging is similar to that of a normally aerated lung (Fig. 5.3).

5.4 Absence of Lung Sliding

To start a LUS examination, we should always search for the pleural line and lung sliding as reference points. When the pleural line is visible but there is no clear lung sliding, we should at first ensure that the hyperechoic horizontal line we are observing is the real pleural line; sometimes other horizontal lines, often generated by muscular sheaths, can be confused with the pleural line. Subcutaneous emphysema can be similarly confusing. The pleural line is identified as being around 0.5 cm below the rib line. If we are visualising the pleural line, but no lung sliding is present, different possible aetiologies should be considered (Table 5.1).

Pneumothorax (PTX) is one of the main causes of absence of lung sliding. In PTX, the image is completely still (other than soft tissue movement) and only artefacts below the parietal pleura can be seen. If we apply the M-mode to this pattern, we do not see the seashore sign anymore, but the so-called *stratosphere sign* [6] (Fig. 5.4).

Absence of lung sliding is quite sensitive but not specific for PTX, because, as you can see in Table 5.1, other situations can lead to very reduced or absent lung sliding [5]. The most specific sign for PTX is the *lung point*: it is the physical

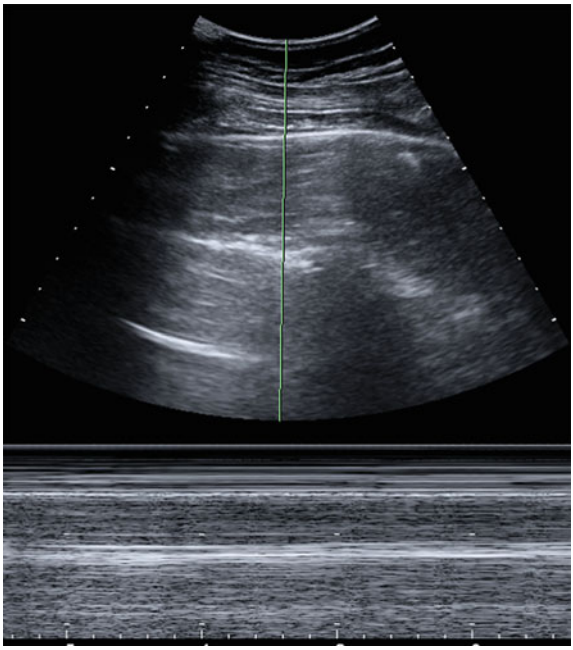

Fig. 5.3 M-mode pattern of the lung sliding: the *seashore sign*

Table 5.1 Main causes of absence of lung sliding

• Pneumothorax
• Mainstem intubation
• High-frequency ventilation
• Massive atelectasis
• Pleural adherences
• Severe fibrosis
• Cardiopulmonary arrest

location where abolished lung sliding transitions into an area of sliding, which represents the physical limit of PTX as mapped on the chest wall [7]. The LUS algorithm for the detection of PTX is summarised in Fig. 5.5. The *lung pulse* is another sign that should be taken into account in the diagnosis/exclusion of PTX. It refers to the subtle rhythmic movement of the visceral upon the parietal pleura with cardiac oscillations [5, 8]. To visualise the lung pulse, we need the apposition of visceral and parietal pleural (i.e. no PTX); moreover, absent or very reduced ventilation is also needed (i.e. no/reduced lung sliding). The lung pulse can be useful for the diagnosis of a non-ventilated lung, and its presence excludes a PTX.

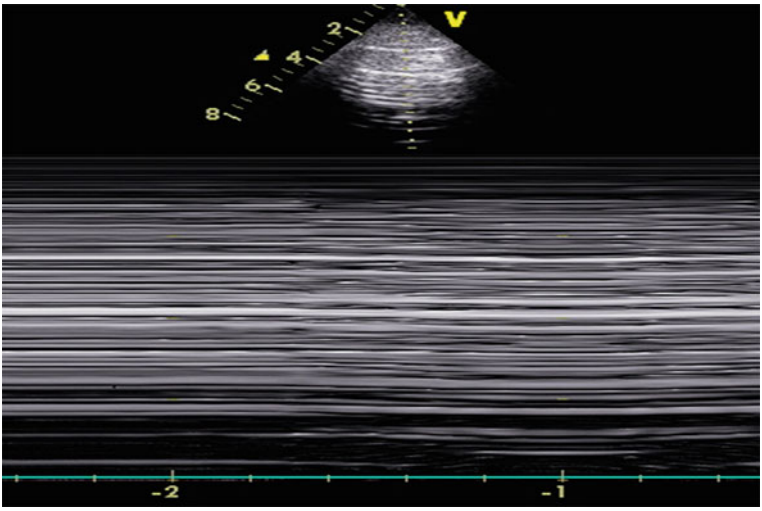

Fig. 5.4 M-mode pattern of absence of lung sliding: the *stratosphere sign*

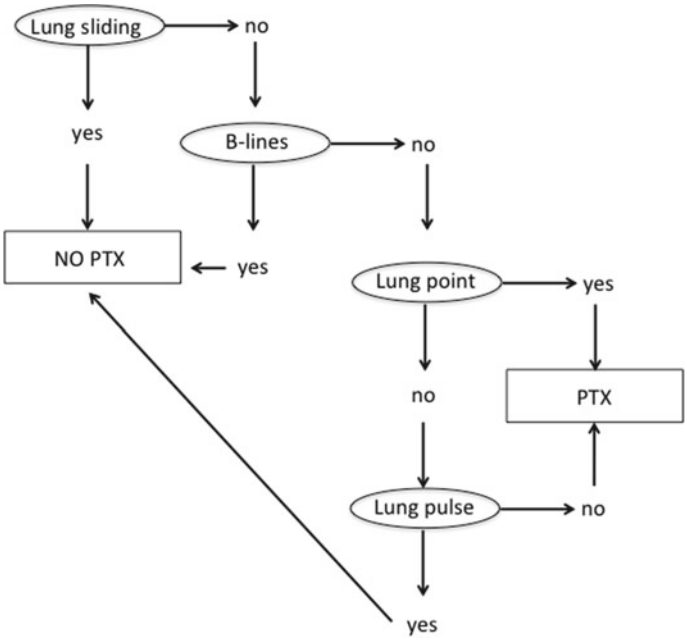

Fig. 5.5 Flow-chart for the diagnosis of pneumothorax

5.5 B-Lines

When the pulmonary air content is reduced, the physical properties of the lung change, and the ultrasound beam can partially penetrate the parenchyma. This partial penetration leads to the appearance of vertical hyperechoic artefacts, called *B-lines*, whose number is inversely proportional to the pulmonary air content (see Fig. 5.1). They look like comet tails, arise from the pleural line, continue to the depths of the image and move with lung sliding.

B-lines are typically present in patients with reduced aeration, but when the parenchyma is not yet completely consolidated. B-lines have been described in patients with cardiogenic [9] and non-cardiogenic pulmonary oedema [10], diffuse parenchymal lung disease [11] and interstitial pneumonia [12]. Although a differential diagnosis can be reached only by integrating the images with clinical, biochemical and other instrumental findings, some features can help distinguishing these various conditions [3, 9, 10].

In cardiogenic pulmonary oedema B-lines are typically bilateral and more abundant in the dependent areas [9, 13]. Presence of B-lines in non-dependent areas, such as the antero-superior chest is usually a sign of a more severe degree of cardiogenic pulmonary congestion [14]. The pleural line is usually similar to that of a normal lung, and doesn't show specific alterations (see Fig. 5.6a).

In non-cardiogenic pulmonary oedema, such as in acute lung injury (ALI) and acute respiratory distress syndrome (ARDS), B-lines do not follow the dependent areas and are patchily distributed over the lung. It is even possible to visualise single scans where an area of normal sonographic lung appearance and an area with many B-lines are simultaneously present, the so-called *spared areas* referring to parenchymal portions which are spared from alterations, in close continuity with diseased areas [10]. This behaviour is typical of ALI/ARDS and can be also appreciated on CT scans. Lung consolidations of different size are generally present in ALI/ARDS. Small sub-pleural consolidations are visualised by ultrasound as

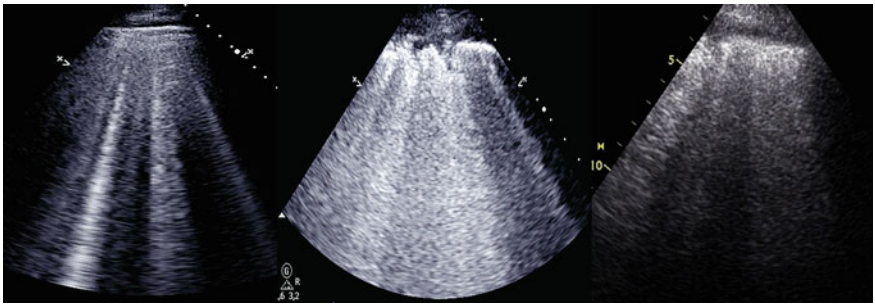

Fig. 5.6 **a** B-lines in cardiogenic pulmonary oedema; **b** B-lines in ARDS; **c** B-lines in pulmonary fibrosis. Note the different appearance of the pleural line

alterations of the pleural line (see Fig. 5.6b), a feature that may help in the differentiation between cardiogenic and non-cardiogenic pulmonary oedema [10].

In patients with diffuse parenchymal lung disease, such as interstitial pulmonary fibrosis, B-lines are also visible and their number correlates with the severity of disease [11, 15]. The distribution follows the characteristics of the specific interstitial disease (in most cases beginning at posterior lung bases). In more advanced cases, the pleural line appears frankly abnormal as it is thickened and distorted (see Fig. 5.6c) [3].

In the differential diagnosis it is important to distinguish diffuse bilateral B-lines from unilateral focal B-lines. Focal B-lines may be present in many conditions and usually represent the peri-lesional interstitial oedema around a parenchymal consolidation, such as in pulmonary embolism, pneumonia, contusion and neoplasia [5]. Sometimes focal B-lines are visible a few hours or even days before the consolidation itself.

5.6 Lung Consolidations

Lung consolidations appear either as a hypoechoic region or region with a tissue-like echotexture (see Fig. 5.1, right panel). To be evident by ultrasound, lung consolidations should reach the pleura, otherwise the air between the probe and the consolidation will prevent the penetration of the ultrasound beam and the visualisation of any abnormality. Lung consolidations may have many different aetiologies, including infection, pulmonary embolism, primary or secondary lung cancer, compression and obstructive atelectasis, and lung contusion [5]. Just as with B-lines, differentiating these diagnoses may need additional sonographic signs to help to determine the cause. An example of this is the presence or absence of dynamic air bronchograms within a consolidated lung segment. Lung ultrasound can also be used for the follow-up of consolidations, i.e. in pneumonia [16]. In patients with radio-opacity on chest X-ray, LUS can be useful to clearly differentiate a consolidation from pleural effusion.

5.7 Pleural Effusion

Lung ultrasound has been used for many years for bedside detection of pleural effusion. Sensitivity of LUS in this setting is higher than chest X-ray, especially in very small effusions [17]. Moreover, LUS can provide some information about the nature of a pleural effusion, although the final diagnosis can be established only by thoracocentesis. In particular, we can exclude the effusion as a transudate if fibrin strands or septa are present, whereas their absence does not rule out an exudate [18, 19]. Lung ultrasound can be employed to quantify pleural effusion, although there is not one single universally accepted method to establish the liquid volume, and a

very precise assessment is not possible given the complex tridimensional shape of the chest. Lung ultrasound can be very useful to guide interventional procedures, and in expert hands it significantly reduces the risk of iatrogenic PTX and bleeding complications.

5.8 Conclusion

Unlike previously thought, lung ultrasound is extremely useful for assessing pleural, interstitial and parenchymal diseases and the degree of aeration of the lung with higher sensitivity and specificity than radiography. Normal lung demonstrates lung sliding and A-lines. Abnormal signs such as absent sliding, B-lines, consolidation and effusion signify disease and all are easily detected with ultrasound. Lung ultrasound is easy to learn and quick to perform making it the ideal as a point-of-care test.

See also:

Chapter 4 Airway Ultrasound
Chapter 6 Advanced Lung Ultrasound
Chapter 21 The Acutely Dyspnoeic Patient
Chapter 22 The Patient Difficult to Wean from Mechanical Ventilation.

References

1. Kasper D, Fauci A, Longo D, Hauser S, Jameson J L. Harrison's principles of internal medicine, 19th ed. McGraw-Hill; 2015. 1663–1664 p.
2. Soldati G, Copetti R, Sher S. Sonographic interstitial syndrome: the sound of lung water. J Ultrasound Med [Internet]. 2009 Feb;28(2):163–74. http://www.ncbi.nlm.nih.gov/pubmed/19168766.
3. Gargani L, Volpicelli G. How I do it: Lung ultrasound. Cardiovasc Ultrasound [Internet]. 2014 [cited 2014 Aug 9];12(1):1–10. http://www.cardiovascularultrasound.com/content/12/1/25/abstract.
4. Lichtenstein D a. A bedside ultrasound sign ruling out pneumothorax in the critically III. CHEST J [Internet]. 1995 Nov 1 [cited 2013 Oct 22];108(5):1345. http://journal.publications.chestnet.org/article.aspx?doi=10.1378/chest.108.5.1345.
5. Volpicelli G, Elbarbary M, Blaivas M, Lichtenstein DA, Mathis G, Kirkpatrick AW, et al. International Liaison Committee on Lung Ultrasound (ILC-LUS) for International Consensus Conference on Lung Ultrasound (ICC-LUS). International evidence-based recommendations for point-of-care lung ultrasound. Intensive Care Med. 2012;38(4):577–91.
6. Lichtenstein D a. Ultrasound in the management of thoracic disease. Crit Care Med [Internet]. 2007 May [cited 2013 Oct 22];35(5 Suppl):S250–61. http://www.ncbi.nlm.nih.gov/pubmed/17446785.

7. Lichtenstein D, Mezière G, Biderman P, Gepner A. The “lung point”: an ultrasound sign specific to pneumothorax. Intensive Care Med [Internet]. 2000 Oct 17 [cited 2013 Oct 22];26 (10):1434–40. http://link.springer.com/10.1007/s001340000627.
8. Lichtenstein D a, Lascols N, Prin S, Mezière G. The “lung pulse”: an early ultrasound sign of complete atelectasis. Intensive Care Med [Internet]. 2003 Dec [cited 2013 Oct 22];29(12): 2187–92. http://www.ncbi.nlm.nih.gov/pubmed/14557855.
9. Gargani L. Lung ultrasound: a new tool for the cardiologist. Cardiovasc Ultrasound. 2011;9:6.
10. Copetti R, Soldati G, Copetti P. Chest sonography: a useful tool to differentiate acute cardiogenic pulmonary edema from acute respiratory distress syndrome. Cardiovasc Ultrasound [Internet]. 2008 Jan [cited 2013 Oct 19];6:16. http://www.pubmedcentral.nih.gov/articlerender.fcgi?artid=2386861&tool=pmcentrez&rendertype=abstract.
11. Gargani L, Doveri M, D’Errico L, Frassi F, Bazzichi ML, Delle Sedie A, et al. Ultrasound lung comets in systemic sclerosis: a chest sonography hallmark of pulmonary interstitial fibrosis. Rheumatology [Internet]. Br Soc Rheumatol. 2009 Nov [cited 2013 Oct 17];48 (11):1382–7. http://www.ncbi.nlm.nih.gov/pubmed/19717549.
12. Lichtenstein D, Mézière G, Biderman P, Gepner a, Barré O. The comet-tail artifact. An ultrasound sign of alveolar-interstitial syndrome. Am J Respir Crit Care Med [Internet]. 1997 Nov;156(5):1640–6. http://www.ncbi.nlm.nih.gov/pubmed/9372688.
13. Miglioranza MH, Gargani L, Sant’anna RT, Rover MM, Martins VM, Mantovani A, et al. Lung ultrasound for the tvaluation of pulmonary congestion in outpatients: a comparison with clinical assessment, natriuretic peptides, and rchocardiography. JACC Cardiovasc Imaging [Internet]. 2013 Sep 26 [cited 2013 Oct 18]. http://www.ncbi.nlm.nih.gov/pubmed/24094830.
14. Volpicelli G, Noble VE, Liteplo A, Cardinale L. Decreased sensitivity of lung ultrasound limited to the anterior chest in emergency department diagnosis of cardiogenic pulmonary edema: a retrospective analysis. Crit Ultrasound J [Internet]. 2010 Jul 2 [cited 2013 Oct 22];2 (2):47–52. http://link.springer.com/10.1007/s13089-010-0037-0.
15. Barskova T, Gargani L, Guiducci S, Randone SB, Bruni C, Carnesecchi G, et al. Lung ultrasound for the screening of interstitial lung disease in very early systemic sclerosis. Ann Rheum Dis. BMJ Publishing Group Ltd and European League Against Rheumatism; 2013;72 (3):390–5.
16. Reissig A, Copetti R, Mathis G, Mempel C. Lung ultrasound in the diagnosis and follow-up of community-acquired pneumonia: a prospective, multicenter, diagnostic accuracy study. Chest [Internet]. 2012 Oct [cited 2014 Aug 20];142(4):965–72. http://europepmc.org/abstract/MED/22700780.
17. Roch A, Bojan M, Michelet P, Romain F, Bregeon F, Papazian L, et al. Usefulness of ultrasonography in predicting pleural effusions > 500 mL in patients receiving mechanical ventilation. Chest [Internet]. 2005 Jan [cited 2013 Oct 22];127(1):224–32. http://www.ncbi.nlm.nih.gov/pubmed/15653988.
18. Sajadieh H, Afzali F, Sajadieh V, Sajadieh A. Ultrasound as an alternative to aspiration for determining the nature of pleural effusion, especially in older people. Ann N Y Acad Sci. 2004;1019:585–92.
19. Chen H-J, Tu C-Y, Ling S-J, Chen W, Chiu K-L, Hsia T-C, et al. Sonographic appearances in transudative pleural effusions: not always an anechoic pattern. Ultrasound Med Biol [Internet]. 2008 Mar [cited 2013 Oct 22];34(3):362–9. http://www.ncbi.nlm.nih.gov/pubmed/17996356.

Chapter 6
Advanced Lung Ultrasound

Giovanni Volpicelli, Annia Schreiber, and Enrico Boero

Keywords Lung ultrasound · Critically ill patients · Intensive care unit · Acute respiratory failure · Monitoring · Multiorgan ultrasound

6.1 Introduction

Lung ultrasound may be considered a simple imaging technique because it is based on a limited number of signs and straightforward pattern recognition. Yet, despite its simplicity, there is a number of advanced clinical applications at the patient bedside, including the possibility of monitoring the haemodynamic condition or the change in pulmonary aeration during recruitment manoeuvres. This is mainly based on the inherent nature of the interaction between the ultrasound beam and different balances between air and fluid in the lung that may change during the time course of pulmonary diseases and differentiate pulmonary conditions [1]. Lung ultrasound is also a non-invasive surface imaging technique, which makes application easy even in complex situations, like those encountered in extreme emergency and in critically ill patients in the intensive care unit (ICU). The performance of lung ultrasound is also improved by the combination with some other point-of-care ultrasound techniques, like cardiac, abdominal and venous ultrasound, thus allowing a multi-organ evaluation [2, 3]. This chapter deals with some advanced applications of lung ultrasound in critically ill patients, which include ultrasound monitoring of critical diseases and multi-organ protocols.

G. Volpicelli (✉)
Department of Emergency Medicine, San Luigi Gonzaga University Hospital, Torino, Italy
e-mail: gio.volpicelli@tin.it

A. Schreiber
Respiratory Intensive Care Unit, Salvatore Maugeri Foundation, Pavia, Italy
e-mail: annia.schreiber@icloud.com

E. Boero
Anesthesiology and Intensive Care, School of Medicine, University of Torino, Torino, Italy
e-mail: enrico.boero@hotmail.com

A. Walden et al. (eds.), *Ultrasound in the Critically Ill*,
https://doi.org/10.1007/978-3-030-71742-1_6

6.2 Monitoring

Lung ultrasound is sensitive to changes in lung aeration and density, giving the clinician crucial information. These changes may be a result of increased lung water, deflation or a combination of the two. The diagnostic potential of lung ultrasound is thus limited to conditions with loss of air, whereas all the diseases characterised by abnormal increase of the air content cannot be studied by sonography. Moreover, the ultrasound study only gives information about the lung surface or pathology which reaches the surface. Having in mind these two important limitations, lung ultrasound is still useful to monitor many pulmonary conditions. The recognition and analysis of three fundamental lung ultrasound patterns allow the possibility of monitoring change over time of the degree of pulmonary aeration and density [4]. The first pattern is the A-pattern, observed when the balance between air and fluid is normal or air is increased (pulmonary emphysema): a visible regular pleural line with lung sliding and without significant B-lines. The second pattern is the B-pattern, observed when fluids are increased while air is partially lost: a visible pleural line regular or irregular, with multiple vertical echoic lines (the B-lines). B-lines may vary in number and density, thus giving a measure of the severity of loss of aeration, from the less severe condition showing few regularly spaced B-lines to the higher degree of loss of air imaged by shining and merged B-lines (the white lung). The third pattern is the consolidated lung, observed when air is totally lost and the lung is deflated or alveoli are filled with fluid: absence of a visible pleural line or interrupted pleural line and a sub-pleural anechoic or a tissue-like image, with or without lung sliding [5].

These three patterns indicate variation of air content in the lung parenchyma, but a fourth sign indicates presence of air into the pleural space: the lung point. It is used to diagnose and monitor a specific condition of the lung, pneumothorax [6]. The lung point indicates the projection on the chest wall of the boundary of the intra-pleural air [7].

The observation of these simple four signs and their change in time, allow the clinician to monitor pulmonary congestion, pulmonary aeration, the hemodynamic state and pneumothorax size at the bedside, particularly in the critically ill.

Monitoring pulmonary congestion. There is a tight relationship between the number of B-lines detected by lung ultrasound and pulmonary congestion. This has been demonstrated in selected patients with acute decompensated heart failure and in critically ill patients, both in post cardiac surgery or admitted to a mixed ICU [8–10]. Based on these observations, it was intuitive to predict the useful role of lung ultrasound in monitoring pulmonary congestion in the cardiology setting [11, 12]. Quantification of pulmonary congestion may be obtained by dividing the anterior-lateral chest wall into eight or eleven areas, and giving to each area a score of one if multiple B-lines (at least three) are detected, and then comparing any change in time [10] (Fig. 6.1). In the setting of outpatients with chronic cardiac diseases, a more complex but still very accurate technique may be used. The chest wall is divided into 28 intercostal spaces and a score of 0, 5 or 10 is given to each

scan depending on the absence of significant B-lines, detection of multiple B-lines but only visible in a part of the screen image, or detection of multiple B-lines on most or the whole image [9, 11] (Fig. 6.2). This technique allows a semi-quantification of B-lines that correlate well with extravascular lung water (EVLW) in patients with cardiac diseases [8, 9]. Again, the score obtained by summing all the 28 areas can be used to monitor change over time, to observe the efficacy of treatment and aid its titration [13]. Finally, the pulmonary congestion in chronic haemodialysis patients can be assessed by lung ultrasound by using the same techniques applied to study and monitor patients with heart failure [14, 15]. However, whether lung ultrasound may be used to guide the timing and intensity of the treatment remains to be studied [4].

Monitoring pulmonary aeration. A decrease of pulmonary aeration may be due not only to congestion. It may also happen when infection, or other conditions that cause loss of aeration of the alveolar spaces, affect the organ. Thus, the problem of diagnosing and monitoring aeration of the lung should include the analysis of consolidations and not only B-lines. Moreover, the ultrasound study should include dorsal scans, because very often in critically ill patients the consolidations are posterior and these areas should be observed to verify the success in re-aeration during recruitment manoeuvres (Fig. 6.3). The technique is performed on twelve chest areas, two anterior, two lateral and two dorsal per side [16]. A score from 0 to 3 is given to each scan, depending on the detection of a normal A-pattern (score 0), multiple separated B-lines (score 1), multiple coalescent B-lines (score 2), or consolidation (score 3) (Table 6.1) [16, 17]. The ultrasound aeration score is

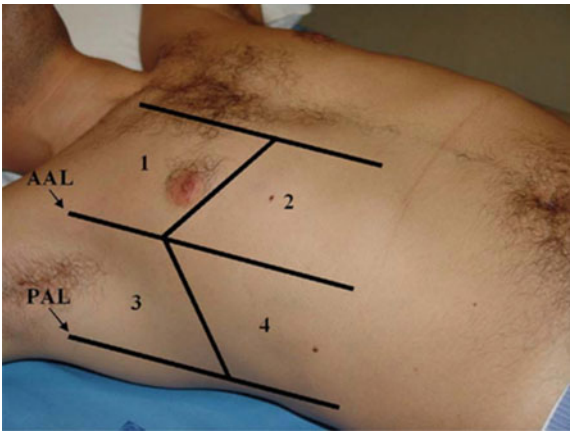

Fig. 6.1 Eight-zone scanning scheme of the anterior-lateral chest (modified from Am J Emerg Med, 24(6), Volpicelli G, Mussa A, Garofalo G, Cardinale L, Casoli G, Perotto F, Fava C, Frascisco M, Bedside lung ultrasound in the assessment of alveolar-interstitial syndrome, 689–96, Copyright 2006, with permission of Elsevier). Areas 1 and 2: upper anterior and lower anterior; areas 3 and 4: upper lateral and basal lateral. Each area was the same on right and left side. AAL, anterior axillary line; PAL, posterior axillary line

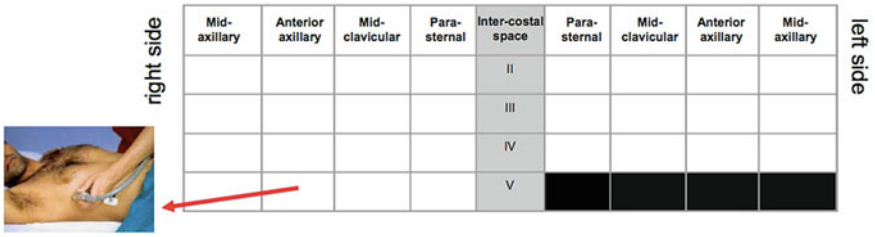

Fig. 6.2 Twenty-eight scanning sites scheme of the anterior-lateral chest (from Gargani, Luna. "Lung Ultrasound: A New Tool for the Cardiologist." Cardiovascular Ultrasound 9 (2011): 6. PMC. Web. 4 Aug. 2016)

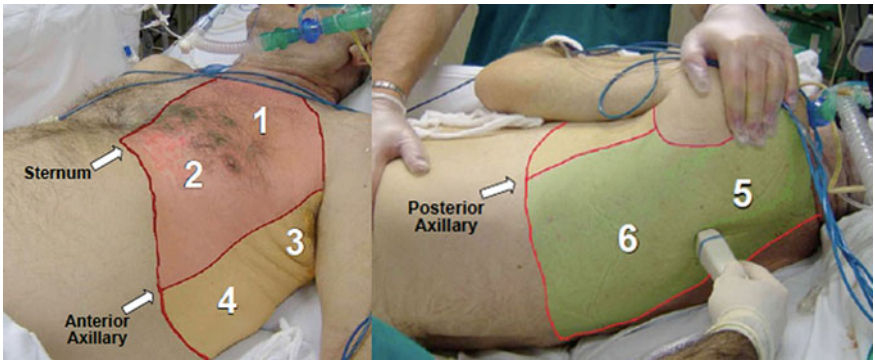

Fig. 6.3 Twelve-zone scanning scheme (six per side) of the anterior-lateral-posterior chest, used to assess and monitor pulmonary aeration in critically ill patients by bedside lung ultrasound

obtained by summing all the 12 areas, thus giving a score ranging from 0 to 36. To monitor changes in time, a validated method is to assign a dynamic score by assigning 1, 3 or 5 points respectively in case of a slight, moderate or substantial increase in lung aeration, or subtracting the same points in case of aeration loss (Fig. 6.4) [17, 18].

Monitoring the haemodynamic state. The haemodynamic state of critically ill patients may be predicted and monitored by assessing B-lines [19]. There is evidence in literature that absence of B-lines is a good predictor of low EVLW [8]. This application of lung ultrasound may be particularly useful in the emergency setting, before invasive and more advanced monitoring tools can be applied. Indeed, lung ultrasound may be used to assess the lung tolerance to fluid administration, when the physicians face critically ill patients in haemodynamic shock [19, 20]. Absence of B-lines indicates tolerance to a fluid challenge (as far as pulmonary oedema is concerned), whereas new appearance of B-lines mandates the suspension of fluid administration. The relationship between B-lines and another common haemodynamic measure, the pulmonary artery occlusion pressure (PAOP), is more controversial. Previous data showing a good correlation between

Table 6.1 Lung ultrasound score and corresponding ultrasound patterns

Points	Degree of lung aeration	Pattern	Image
0 point	Normal aeration	Horizontal ***A-lines*** (or no more than two B-lines)	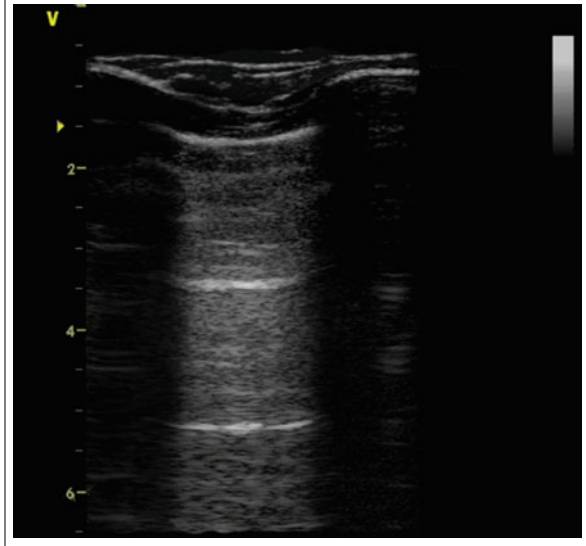

(continued)

Table 6.1 (continued)

Points	Degree of lung aeration	Pattern	Image
1 point	Moderate loss of aeration	***Multiple B-lines***, either regularly spaced (7 mm apart), or irregularly spaced and even coalescent but only visible in a limited area of the intercostal space	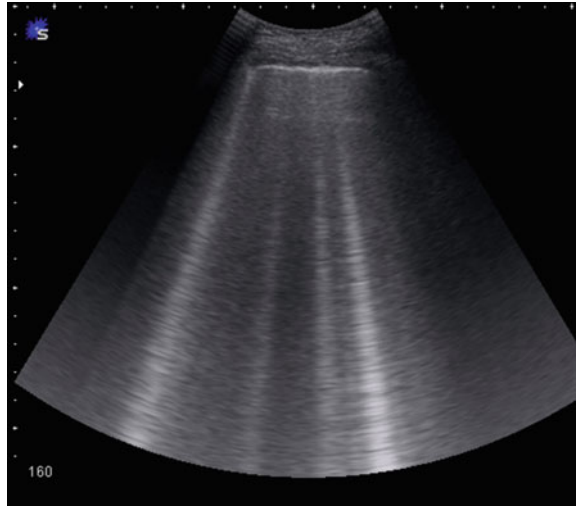

(continued)

Table 6.1 (continued)

Points	Degree of lung aeration	Pattern	Image
2 points	Severe loss of aeration	***Multiple coalescent B-lines***, in prevalent areas of the intercostal spaces and observed in one or several intercostal spaces	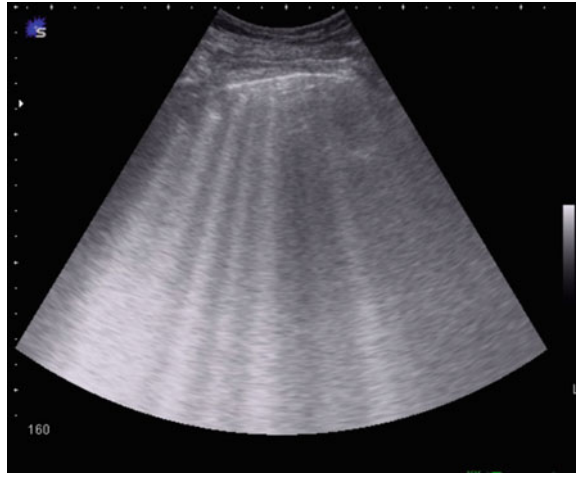

(continued)

Table 6.1 (continued)

Points	Degree of lung aeration	Pattern	Image
3 points	Complete loss of aeration	***Lung consolidation***, with or without air bronchograms	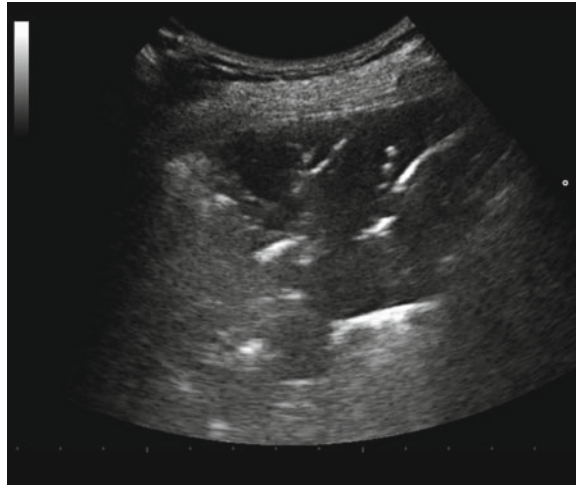

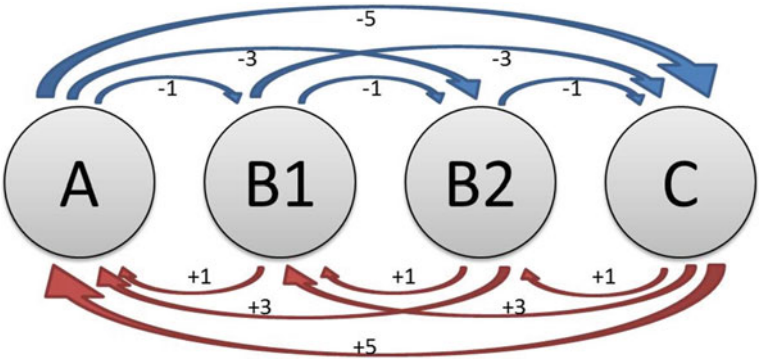

Fig. 6.4 Lung ultrasound score for aeration changes in time. A = Normal pattern; B1 = Well defined and irregular spacing B lines; B2 = Coalescent B lines; C = Alveolar consolidation. The red arrows indicate the scores assigned to improvement in aeration, whereas the blue arrows indicate the loss of aeration

absence of B-lines and low PAOP [21], have been recently disputed by opposite results [22]. This is in agreement with the consideration that high EVLW and high PAOP indicate two different sources of congestion [23]. There may be conditions where, despite high levels of PAOP (hemodynamic congestion), the patient does not show pulmonary congestion. These conditions may be encountered when a capillary resistance to fluid leakage is induced by chronic diseases. Thus the the evaluation of B-lines is useful to assess the haemodynamic condition of critically ill patients and can be coupled with more invasive techniques in the ICU.

Monitoring pneumothorax size. The projection of the lung point on the chest wall is a sign of the distribution of the air in pneumothorax. The laterality of this point is a measure of the superficial extension of a pneumothorax that, of course, does not directly indicate the volume of pneumothorax. Indeed, similar extensions may be observed in different pneumothorax volumes, depending on the distance between the collapsed lung and the chest wall (Fig. 6.5). This distance, and consequently the exact volume, cannot be measured by lung ultrasound. However, there is good evidence in literature that the position of the lung point allows a sufficient semiquantification of the pneumothorax volume both in animal models [24] and in patients [25]. The prediction of the real pneumothorax volume by lung ultrasound is much superior to the potential of chest radiography reading when compared to volumetric CT [25, 26]. A lung point anterior to the mid axillary line is a good predictor of a volume less than 15% [25]. Moreover, lung ultrasound seems to be a consistent tool to evaluate residual presence of air in pneumothoraces treated by drainage [27]. These observations indicate the potential of lung ultrasound in monitoring pneumothorax in many settings. For instance, monitoring pneumothorax at the bedside is useful in the evaluation of successful treatment, but also to allow more conservative treatment in trauma patients who require mechanical ventilation [28].

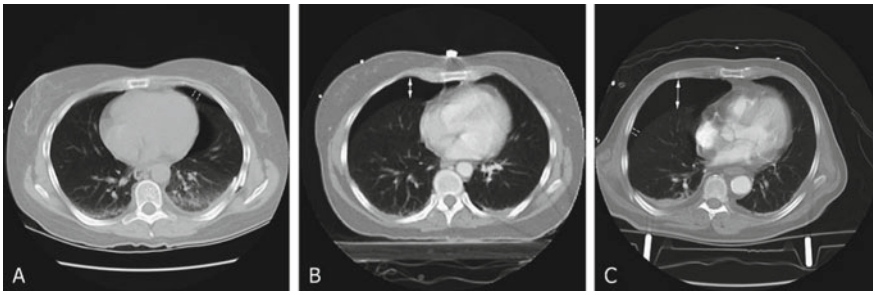

Fig. 6.5 The progression of lateral edge of intrapleural air is shown on these CT scan images, demonstrating the greater the pneumothorax, the more lateral is the lung point. However, in large pneumothorax, the laterality of the lung point may fail in indicating the progression of pneumothorax volume (from Michael Blaivas, Matthew Lyon, Sandeep Duggal, Prospective Comparison of Supine Chest Radiography and Bedside Ultrasound for the Diagnosis of Traumatic Pneumothorax, Acad Emerg Med. 2005 Sep;12(9):844–9)

6.3 Multiorgan Ultrasound

In some critical situations, a combination of the ultrasound study of the lung with other organs, allows a more accurate diagnostic assessment and increases the diagnostic power of lung ultrasound signs. The lack of sufficient sensitivity and especially specificity of some lung ultrasound patterns, may be corrected by combining ultrasound findings obtained by the study of the heart, vessels and abdomen. This has been experienced in the evaluation of major trauma, undifferentiated hypotension, cardiac arrest and acute respiratory failure.

Multiorgan ultrasound in Trauma. In severe trauma patients, the use of ultrasound in the primary survey is already recommended in societal guidelines to detect possible abdominal, pericardial and pleural haemorrhage, by applying a basic technique. The FAST examination has been employed since 1999 as the result of the first consensus conference of ultrasound in trauma [29]. Later, in 2004, the FAST examination was extended to the early detection of pneumothorax, as this is the most urgent pulmonary condition to be excluded in severe thoracic trauma [30]. This extended FAST (eFAST), is a combination of cardiac, abdominal and pulmonary ultrasound and is used to rule out pneumothorax in addition to pleural, pericardial or abdominal blood collections, during the bedside early management of a severe trauma patient. However, lung ultrasound is not only useful to detect pneumothorax and haemothorax, but also pulmonary contusions with higher sensitivity than chest radiography [31–33]. There is also evidence that the severity of pulmonary contusions significantly affect the possibility of evolution to ARDS, thus influencing the prognosis of trauma patients [34]. Thus, the early evaluation of pulmonary contusions should be performed routinely and its results should

influence the following treatment, ventilator strategy and monitoring [34]. It is now debated whether this early detection of contusions should be included in the primary survey of severe trauma.

Multiorgan ultrasound in undifferentiated hypotension. Evaluation of shock and undifferentiated hypotension is a challenge in the emergency setting. A pathophysiologic classification of the main causes of shock—cardiogenic, obstructive, distributive and hypovolemic—allows the physician to concentrate the differential diagnosis on few conditions to orientate the early treatment in emergency [35]. Point-of-care multi-organ ultrasound, (cardiac, venous, abdominal, pulmonary) is useful for the early diagnosis of hypotensive states [2]. In particular, ultrasound evaluation of the lung may add some crucial information in hypotensive states. Indeed, lung ultrasound may indicate not only the haemodynamic effects of the condition on the pulmonary circulation, such as pulmonary oedema from cardiogenic shock, but also the presence of primary pulmonary diseases causing haemodynamic instability, such as pneumonia in sepsis and distributive shock (Table 6.2).

Multiorgan ultrasound in cardiac arrest. In cardiac arrest, a multiorgan ultrasound approach may aid in the early diagnosis of the condition. Particularly in pulseless electric activity, the ultrasound evaluation performed during resuscitation manoeuvres may allow the early diagnosis of 4 main causes, hypovolemia, pneumothorax, tamponade and pulmonary embolism, or it may allow the recognition of a true standstill heart [36–39]. Of course, the lung evaluation is a crucial integration to cardiac, abdominal and inferior vena cava assessment. Particularly, the pattern recognition for pneumothorax, haemothorax and the interstitial syndrome with lung ultrasound is used to finalise the diagnosis and lifesaving treatment [37, 40].

Multiorgan ultrasound in acute respiratory failure. In acute respiratory failure bedside lung ultrasound allows a rapid and direct insight into the respiratory organ. Used as the clinicians usually apply the stethoscope, a very early first look into the lung may help orientate the differential diagnosis with higher accuracy than other bedside methods. A basic technique, the BLUE protocol, showed high accuracy in the early diagnosis of the underlying condition in critically ill patients [41]. The protocol is mainly based on a lung ultrasound study, eventually adding the evaluation of peripheral veins to confirm thrombosis by the compression technique. The lung study consists in the evaluation of very basic ultrasound signs, namely the sliding sign, B-lines, anterior consolidations and posterior-lateral consolidations with or without effusion and the lung point. The BLUE protocol, applied to the early evaluation of acute severe respiratory failure, allows the diagnosis of cardiogenic pulmonary oedema, pneumonia, COPD exacerbation or asthma, pulmonary embolism and pneumothorax with good accuracy. However, important limitations of the protocol include the possibility of pulmonary embolism without venous thrombosis in the periphery, the occurrence of pulmonary embolism showing anterior consolidations due to infarctions and the frequent condition of basal effusion with compressive consolidations not due to pneumonia. Moreover, the BLUE protocol does not consider the low specificity of B-lines for cardiogenic pulmonary oedema and does not differentiate a B pattern caused by ARDS, interstitial pneumonia or chronic preexisting diseases of the lung. To this purpose and to

Table 6.2 The list of 7 possible ultrasound patterns in patients presenting with shock/undifferentiated hypotension, and corresponding combination of findings detected at multi-organ point-of-care ultrasonography evaluation

Ultrasound pattern	Organ evaluation	Corresponding signs
Hypovolemic	Heart	Hyperkinetic LV
	Inferior Vena Cava	Diam. <2 cm + Resp. collapse >50%
	Lungs	A pattern
	Abdomen	*Free fluids/aortic aneurysm
Distributive	Heart	Hyperkinetic LV
	Inferior Vena Cava	Diam. <2 cm + Resp. collapse >50%
	Lungs	B pattern with consolidation or consolidation with air bronchograms
Hypovolemic/distributive	Heart	Hyperkinetic LV
	Inferior Vena Cava	Diam. <2 cm + Resp. collapse >50%
	Lungs	A/B pattern
	Abdomen	*Free fluids
Obstructive type 1 (cardiac tamponade)	Heart	Pericard. effusion with tamponade
Obstructive type 2 (pulmonary embolism)	Heart	Dilated/hypokinetic RV
	Inferior Vena Cava	Sludge or no respiratory collapse and max diam. >2 cm
	Lungs	A pattern
	Peripheral Veins	*Deep vein thrombosis
Obstructive type 3 (pneumothorax)	Heart	Dilated/hypokinetic RV
	Inferior Vena Cava	Sludge or no respiratory collapse and max diam. >2 cm
	Lungs	No sliding and pulse, no B-lines, no consolidation
Cardiogenic	Heart	Hypokinetic left ventricle
	Lungs	B pattern

In the majority of the diagnoses listed, the role of lung ultrasound is crucial
LV = Left Ventricle; RV = Right Ventricle; A pattern = a visible regular pleural line with lung sliding and without significant B-lines; B pattern = a visible pleural line regular or irregular, with multiple and diffuse (bilateral) vertical echoic lines (the B-lines); A/B pattern = a visible pleural line regular or irregular, with or without sliding, with multiple B-lines focally distributed. *= Not necessarily present
Aadapted from Intensive Care Med, Point-of-care multiorgan ultrasonography for the evaluation of undifferentiated hypotension in the emergency department, 39(7), 2013, 1290–1298, G. Volpicelli, A. Lamorte, M. Tullio, L. Cardinale, M. Giraudo, V. Stefanone, E. Boero, P. Nazerian, R. Pozzi, M. F. Frascisco. With permission of Springer

increase the predictive power of B-lines for acute decompensated heart failure, some multiorgan ultrasound protocols have been proposed in the emergency evaluation of acute respiratory failure [42–44]. These protocols integrate the evaluation for B-lines with a focused cardiac study of the left ventricular function and diameter combined with respiratory excursion of the inferior vena cava. Scientific evidence has affirmed the superiority of the combination of lung, cardiac and venous signs to diagnose acute decompensated heart failure, when compared to the ultrasound evaluation of each organ alone.

6.4 Conclusion

Lung ultrasound is a simple, bedside, non invasive surface imaging technique based on basic signs and simple pattern recognition, applicable almost in any conditions.

Despite its simplicity, there is a number of advanced clinical applications which makes it particularly suitable and useful in critically ill patients on the intensive care unit (ICU).

In particular the recognition, and analysis of, four fundamental lung ultrasound signs and their change in time, allow the clinician to monitor pulmonary congestion, pulmonary aeration, the haemodynamic state and pneumothorax size at the bedside, especially in these types of critically ill patients.

Furthermore, a combination of lung ultrasound with the ultrasonographic study of other organs, mainly heart, vessels and abdomen, allows a more accurate diagnostic assessment in many clinical situations like major trauma, undifferentiated hypotension, cardiac arrest and acute respiratory failure.

References

1. Volpicelli G. Lung sonography. J Ultrasound Med. 2013;32:165–71.
2. Volpicelli G, Lamorte A, Tullio M, et al. Point-of-care multiorgan ultrasonography for the evaluation of undifferentiated hypotension in the emergency department. Intensive Care Med. 2013;39:1290–8.
3. Moore CL, Copel JA. Point-of-care ultrasonography. N Engl J Med. 2011;364:749–57.
4. Volpicelli G, Elbarbary M, Blaivas M, et al. International evidence-based recommendations for point-of-care lung ultrasound. Intensive Care Med. 2012;38:577–91.
5. Lichtenstein DA, Lascols N, Meziere G, et al. Ultrasound diagnosis of alveolar consolidation in the critically ill. Intensive Care Med. 2004;30:276–81.
6. Lichtenstein D, Meziere G, Biderman P, et al. The “lung point”: an ultrasound sign specific to pneumothorax. Intensive Care Med. 2000;26:1434–40.
7. Volpicelli G. Sonographic diagnosis of pneumothorax. Intensive Care Med. 2011;37:224–32.
8. Agricola E, Bove T, Oppizzi M, et al. Ultrasound comet-tail images”: a marker of pulmonary edema: a comparative study with wedge pressure and extravascular lung water. Chest. 2005;127:1690–5.

9. Jambrik Z, Monti S, Coppola V, et al. Usefulness of ultrasound lung comets as a nonradiologic sign of extravascular lung water. Am J Cardiol. 2004;93:1265–70.
10. Volpicelli G, Caramello V, Cardinale L, et al. Bedside ultrasound of the lung for the monitoring of acute decompensated heart failure. Am J Emerg Med. 2008;26:585–91.
11. Gargani L. Lung ultrasound: a new tool for the cardiologist. Cardiovasc Ultrasound. 2011;9:6.
12. Picano E, Frassi F, Agricola E, et al. Ultrasound lung comets: a clinically useful sign of extravascular lung water. J Am Soc Echocardiogr. 2006;19:356–63.
13. Miglioranza MH, Gargani L, Sant'Anna RT, et al. Lung ultrasound for the evaluation of pulmonary congestion in outpatients: a comparison with clinical assessment, natriuretic peptides, and echocardiography. JACC Cardiovasc Imaging. 2013;6:1141–51.
14. Mallamaci F, Benedetto FA, Tripepi R, et al. Detection of pulmonary congestion by chest ultrasound in dialysis patients. JACC Cardiovasc Imaging. 2010;3:586–94.
15. Noble VE, Murray AF, Capp R, et al. Ultrasound assessment for extravascular lung water in patients undergoing hemodialysis. Time Course for Resolution Chest. 2009;135:1433–9.
16. Soummer A, Perbet S, Brisson H, et al. Ultrasound assessment of lung aeration loss during a successful weaning trial predicts postextubation distress*. Crit Care Med. 2012;40:2064–72.
17. Bouhemad B, Liu ZH, Arbelot C, et al. Ultrasound assessment of antibiotic-induced pulmonary reaeration in ventilator-associated pneumonia. Crit Care Med. 2010;38:84–92.
18. Bouhemad B, Brisson H, Le-Guen M, et al. Bedside ultrasound assessment of positive end-expiratory pressure-induced lung recruitment. Am J Respir Crit Care Med. 2011;183:341–7.
19. Lichtenstein DA. BLUE-protocol and FALLS-protocol: two applications of lung ultrasound in the critically ill. Chest. 2015;147:1659–70.
20. Lichtenstein D. Fluid administration limited by lung sonography: the place of lung ultrasound in assessment of acute circulatory failure (the FALLS-protocol). Expert Rev Respir Med. 2012;6:155–62.
21. Lichtenstein DA, Meziere GA, Lagoueyte JF, et al. A-lines and B-lines: lung ultrasound as a bedside tool for predicting pulmonary artery occlusion pressure in the critically ill. Chest. 2009;136:1014–20.
22. Volpicelli G, Skurzak S, Boero E, et al. Lung ultrasound predicts well extravascular lung water but is of limited usefulness in the prediction of wedge pressure. Anesthesiology. 2014;121:320–7.
23. Picano E, Gargani L, Gheorghiade M. Why, when, and how to assess pulmonary congestion in heart failure: pathophysiological, clinical, and methodological implications. Heart Fail Rev. 2010;15:63–72.
24. Oveland NP, Lossius HM, Wemmelund K, et al. Using thoracic ultrasonography to accurately assess pneumothorax progression during positive pressure ventilation: a comparison with CT scanning. Chest. 2013;143:415–22.
25. Volpicelli G, Boero E, Sverzellati N, et al. Semi-quantification of pneumothorax volume by lung ultrasound. Intensive Care Med. 2014;40:1460–7.
26. Kelly AM, Druda D. Comparison of size classification of primary spontaneous pneumothorax by three international guidelines: a case for international consensus? Respir Med. 2008;102:1830–2.
27. Galbois A, Ait-Oufella H, Baudel JL, et al. Pleural ultrasound compared with chest radiographic detection of pneumothorax resolution after drainage. Chest. 2010;138:648–55.
28. Kirkpatrick AW, Rizoli S, Ouellet JF, et al. Occult pneumothoraces in critical care: a prospective multicenter randomized controlled trial of pleural drainage for mechanically ventilated trauma patients with occult pneumothoraces. J Trauma Acute Care Surg. 2013;74:747–54; discussion 745–754.
29. Scalea TM, Rodriguez A, Chiu WC, et al. Focused assessment with sonography for trauma (FAST): results from an international consensus conference. J Trauma. 1999;46:466–72.
30. Kirkpatrick AW, Sirois M, Laupland KB, et al. Hand-held thoracic sonography for detecting post-traumatic pneumothoraces: the extended focused assessment with sonography for trauma (EFAST). J Trauma. 2004;57:288–95.

31. Hosseini M, Ghelichkhani P, Baikpour M, et al. Diagnostic accuracy of ultrasonography and radiography in detection of pulmonary contusion; a systematic review and meta-analysis. Emerg (Tehran). 2015;3:127–36.
32. Soldati G, Testa A, Silva FR, et al. Chest ultrasonography in lung contusion. Chest. 2006;130:533–8.
33. Hyacinthe AC, Broux C, Francony G, et al. Diagnostic accuracy of ultrasonography in the acute assessment of common thoracic lesions after trauma. Chest. 2012;141:1177–83.
34. Leblanc D, Bouvet C, Degiovanni F, et al. Early lung ultrasonography predicts the occurrence of acute respiratory distress syndrome in blunt trauma patients. Intensive Care Med. 2014;40:1468–74.
35. Perera P, Mailhot T, Riley D, et al. The RUSH exam: rapid ultrasound in SHock in the evaluation of the critically lll. Emerg Med Clin North Am. 2010;28:29–56, vii.
36. Hernandez C, Shuler K, Hannan H, et al. C.A.U.S.E.: cardiac arrest ultra-sound exam–a better approach to managing patients in primary non-arrhythmogenic cardiac arrest. Resuscitation. 2008;76:198–206.
37. Volpicelli G. Usefulness of emergency ultrasound in nontraumatic cardiac arrest. Am J Emerg Med. 2011;29:216–23.
38. Blaivas M, Fox JC. Outcome in cardiac arrest patients found to have cardiac standstill on the bedside emergency department echocardiogram. Acad Emerg Med. 2001;8:616–21.
39. Breitkreutz R, Price S, Steiger HV, et al. Focused echocardiographic evaluation in life support and peri-resuscitation of emergency patients: a prospective trial. Resuscitation. 2010;81:1527–33.
40. Lichtenstein DA. How can the use of lung ultrasound in cardiac arrest make ultrasound a holistic discipline. The example of the SESAME-protocol. Med Ultrason. 2014;16:252–5.
41. Lichtenstein DA, Meziere GA. Relevance of lung ultrasound in the diagnosis of acute respiratory failure: the BLUE protocol. Chest. 2008;134:117–25.
42. Anderson KL, Jenq KY, Fields JM, et al. Diagnosing heart failure among acutely dyspneic patients with cardiac, inferior vena cava, and lung ultrasonography. Am J Emerg Med. 2013;31:1208–14.
43. Kajimoto K, Madeen K, Nakayama T, et al. Rapid evaluation by lung-cardiac-inferior vena cava (LCI) integrated ultrasound for differentiating heart failure from pulmonary disease as the cause of acute dyspnea in the emergency setting. Cardiovasc Ultrasound. 2012;10:49.
44. Mantuani D, Frazee BW, Fahimi J, et al. Point-of-care multi-organ ultrasound improves diagnostic accuracy in adults presenting to the emergency department with acute dyspnea. West J Emerg Med. 2016;17:46–53.

Chapter 7
Focused Transthoracic Echocardiography

Thomas Clark

Keywords Echocardiography · Ultrasound · Left ventricle · Right ventricle · Pericardium

7.1 Introduction

Focused echocardiography requires a methodical step-wise ultrasound examination of the heart using an algorithm. The clinician must answer a series of binary 'yes/no' questions that aim to detect major cardiac abnormalities that could be responsible for significant cardiovascular compromise. As an investigation it is quick and accurate. It may be easily incorporated into the clinical examination and complements other forms of focused ultrasound such as lung ultrasound. Not only can it provide answers to the cause of patient deterioration but it can also direct treatment. There are numerous algorithms and training packages worldwide, but the main two within the United Kingdom are FUSIC Heart (Focused Ultrasound in Intensive Care) and FEEL (Focused Echocardiography in Emergency Life-support, sponsored by the Resuscitation Council). All training packages appear similar in that they require the examiner to only detect obvious, significant pathology, that they predominantly rely upon 2D echocardiography and that they are to be used in the critically ill or arrested patient. They are not for diagnosing chronic disease. This chapter will describe how to undertake a focused cardiac ultrasound examination and discuss the major pathologies that can be detected. It should be read in conjunction with Chaps. 8 and 9 on advanced echocardiography and tranoesophageal echocardiography.

T. Clark (✉)
Department of Critical Care, Torbay and South Devon Hospital, Lowes Bridge, Torquay TQ2 7AA, Devon, UK
e-mail: tom_clark@mac.com; thomasclark1@nhs.net

A. Walden et al. (eds.), *Ultrasound in the Critically Ill*,
https://doi.org/10.1007/978-3-030-71742-1_7

7.2 Standard Views

Focused echocardiography requires a step by step examination. Table 7.1 outlines the five key cardiac 'views', the probe sites to obtain these and how the probe marker should be orientated.

For all views the probe marker is pointed towards the left-hand side of the patient except the parasternal long axis where the marker is pointed towards the right shoulder.

The patient is scanned in the order as outlined in Table 7.1. For each view the operator should attempt to answer each question outlined in the algorithm outlined later in this chapter. If this is not possible due to difficulty obtaining adequate images then the operator proceeds to the next view. Many of the questions in the algorithm can be answered with only one view although accuracy will be increased by confirming the presence or absence of pathology in different views. Whilst the exam usually proceeds in the order in Table 7.1, when examining the patient in cardiac arrest, it is usual to start by using the subcostal window.

The anatomy (Figs. 7.1, 7.2, 7.3, 7.4 and 7.5).

Table 7.1 The five standard views required for focused echocardiography

View	Probe position	Probe marker orientation	Why?
Parasternal long axis (PSLx)	Left sternal edge, 2nd-6th intercostal space	Right shoulder	Left ventricle (LV) size and function
Parasternal short axis (PSSx)	As above	Left shoulder	LV size and function, regional wall motion abnormalities (RWMAs)
Apical 4 chamber (A4C)	Over the apex beat (palpate with your hand)	Left flank	LV/right ventricle (RV) size and function
Subcostal 4 chamber (S4C)	Under Xyphisternum, pointed towards left shoulder	Left flank	LV/RV size and function
Subcostal Inferior Vena Cava (SIVC)	As above but directed centrally to bring right atrium into centre of image	Towards the ceiling	IVC diameter

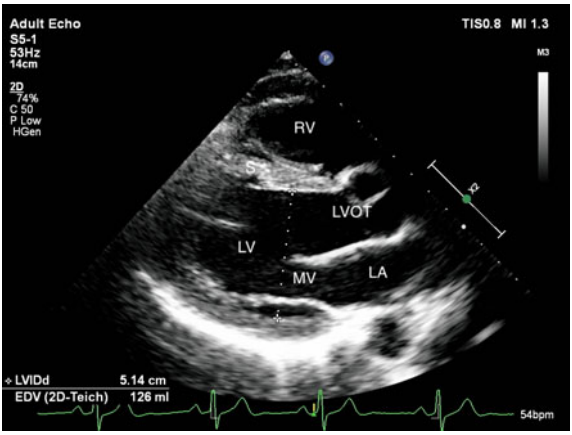

Fig. 7.1 Parasternal long axis view at end-diastole showing right ventricle (RV), septum (S), left ventricle (LV), left atrium (LA), mitral valve (MV) and left ventricular outflow tract (LVOT, including aortic valve)

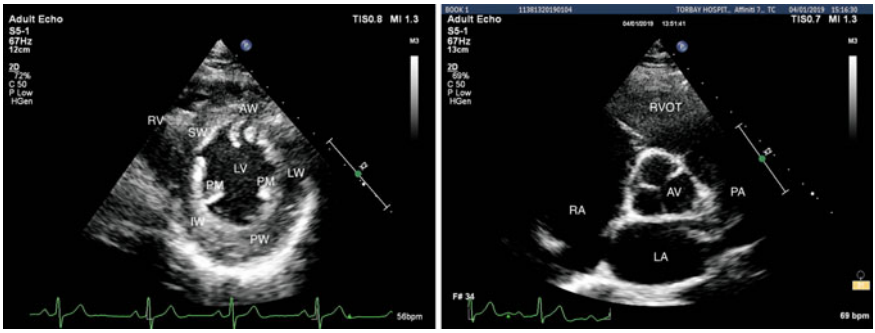

Fig. 7.2 Parasternal short axis view at papillary muscle level (**a**) and aortic valve level (**b**) showing right ventricle (RV), left ventricle (LV), papillary muscles (PM), septal wall (SW), anterior wall (AW), lateral wall (LW), posterior wall (PW) and inferior wall (IW), aortic valve (AV), right atrium (RA), left atrium (LA), right ventricular outflow track (RVOT) and pulmonary artery (PA)

7.3 Scanning Process

Before starting ensure the machine and probe are clean, the correct patient details have been entered and that the ECG leads are attached (although in a time critical situation ECG leads are not necessary). If using a machine for the first time it is always worthwhile to check how the machine works (how to adjust gain, focus and depth) and also how to save images.

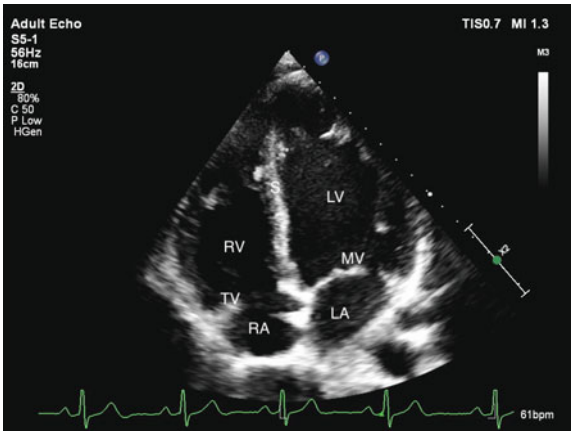

Fig. 7.3 Apical four-chamber at view at end-diastole showing right atrium (RA), tricuspid valve (TV), right ventricle (RV), left atrium (LA), mitral valve (MV), left ventricle (LV) and septum (S)

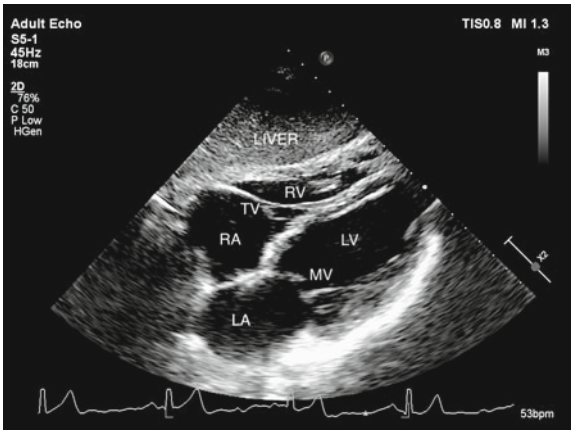

Fig. 7.4 Sub-costal apical four-chamber view showing right atrium (RA), tricuspid valve (TV), right ventricle (RV), left atrium (LA), mitral valve (MV), left ventricle (LV) and septum (S)

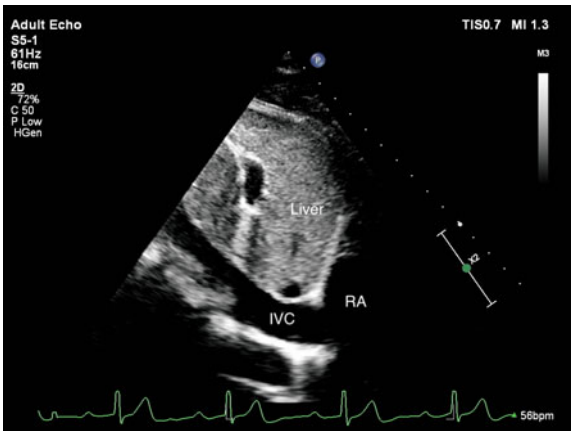

Fig. 7.5 Sub-costal inferior vena cava view showing long-axis of inferior vena cava (IVC) and right atrium (RA)

The first step in diagnosing pathology is in getting a well orientated picture and identifying relevant anatomy. When starting training it is of upmost importance that enough time and care is taken to produce the optimal picture in order to become familiar with what is normal. The power of this test in the ability to spot gross abnormalities, so experience of normal cases first is essential. Small movements make a large difference in obtaining any echo view so the probe should be moved slowly. The skill of echocardiography is seeing an image and knowing which movements to make with the probe to optimise it. There are 10 main probe movements and only one movement should be done at a time. These are angulation up, down, left, right along the x and y axis (4), sliding the probe up, down, left and right along the x and y axis (4) and rotation clockwise and anti-clockwise (2). Angling the probe in its x axis will always cause the image to swing to one side like a pendulum with the near field moving less than the far field. Sliding the probe along the x axis will move the whole image sideways equally from top to bottom. Once the best view is obtained the image should be further optimised by checking depth, gain and focus position (step 2). The image should fill the screen, the gain set so that structures can be seen but are not overly bright (so 'blood' appears black, not grey) and the focus position should be at the depth of the key structure being examined. The final step is image interpretation for which the algorithm below is used.

7.4 Diagnostic Algorithm

Each training competency package has its own algorithm. Focused echocardiography requires the operator to give 'yes/no' answers to a series of questions in each view. Focusing on these questions simplifies echocardiography and avoids the pitfalls of someone operating outside their level of competence.

In general, the main questions to be answered are.

Is there cardiac-activity? (relevant in cardiac arrest—true PEA versus pseudo-PEA has prognostic implications).

1. Is the left ventricle (LV) grossly dilated?
2. Is the LV severely impaired?
3. Are there regional wall motion abnormalities?
4. Is the right ventricle (RV) grossly dilated?
5. Is the RV severely impaired?
6. Is there evidence of severe hypovolaemia?
7. Is there a pericardial effusion?

An answer to each question is sought in each view. Final decision on pathology are reserved until the exam has been completed. The purpose of the scan is to detect gross abnormalities rather than more subtle pathology.

7.5 Common Pathology

It is fairly self explanatory that the above algorithm is aimed at detecting severe LV failure, myocardial infarction, severe RV failure, pulmonary embolism (suggested by the clinical situation alongside evidence of isolated RV failure), cardiac tamponade and severe hypovolaemia as the cause of shock. Confirming the presence or absence of these diagnoses in the acute situation can be invaluable; it may provide a diagnosis that alters the treatment strategy—be it give fluid, give less fluid, start inotropes or re-consider levels of intervention. It is beyond the scope of this chapter to discuss these pathologies in detail, but below are a few key points.

7.5.1 LV Failure

The shape and size of the ventricle is 'eye-balled' in all views. Gross dilatation will appear obvious in comparison to normal. FUSIC Heart uses an end-diastolic diameter of greater than 6 cm in the parasternal long axis as its cut-off for dilatation. Function is assessed by observing how well the walls thicken as well as the systolic change in cavity size (hint—the change in black cavity size during the cardiac cycle is easier to appreciate than the ventricular wall position). Severe impairment will manifest on visual inspection as near a kinesis (minimal/absent wall thickening) of the entire ventricle with little change in cavity area. In the parasternal short-axis the image can be frozen at end-diastole and the internal edge of the cavity (at papillary muscle level) drawn round to produce an end-diastolic area 'benchmark'. Scrolling forward through systole allows comparison of wall thickening/movement to the diastolic area. Each wall is examined in-turn as regional wall abnormalities can be easy to miss. As mentioned above, looking for regional wall abnormalities in the short-axis view is important for detecting myocardial ischemia as all coronary arteries supply this view.

7.5.2 RV Failure

Again, visual inspection is the key to diagnosis. The RV diameter should be less than two-thirds of the left. If it is greater than the LV diameter then this is an indicator of significant dilatation. This is best measured in the apical 4 chamber view but the picture must be correctly orientated before taking this measurement—both tricuspid and mitral valves should be seen, with the septum siting in the centre of the picture running straight downwards from the apex. RV function assessment is made by looking at the extent of tricuspid lateral annulus travel towards the apex during systole—this is a marker of longitudinal function and is called Tricuspid

Annular Plain Systolic Excursion or TAPSE. This can be measured using m-mode. Severe impairment is indicated when TAPSE is less than 10 mm.

7.5.3 Severe Hypovolaemia

This is indicated by a tachycardic LV that shows complete systolic collapse (or 'cavity obliteration'—sometimes described as having 'kissing papillary muscles'). The differential diagnosis for this is severe vasodilatation secondary to anaphylaxis or septic shock. An accompanying feature to severe hypovolaemia is inferior vena cava collapse indicating a low filling pressure (although this could also be caused by severe venodilatation). An IVC of less than 10 mm combined with a small hyperdynamic LV is a strong indicator of low filling pressure.

7.6 Advanced Focused Echocardiography

Some parties recommend learning more advanced Doppler skills that can then be incorporated into a focused exam. These are primarily used to determine stroke volume, fluid responsiveness and adequacy of valve function. However, these additional abilities remain entirely separate to diagnostic level Doppler echocardiography and remain well aligned to the 'focused concept' of detecting severe pathology that is likely to be a cause of shock.

7.6.1 Stroke Volume

By measuring left ventricular outflow tract (LVOT) diameter (to obtain LVOT area —Pi.r2) and multiplying this by the LVOT Velocity Time Integral (obtained by placing a pulsed wave Doppler into the LVOT using the apical 5 chamber view) stroke volume can be quantified. This is useful in declaring a low cardiac output state—a low ejection fraction does not necessarily equate to this. One can also use this in the assessment of fluid responsiveness, either alongside a straight leg raise, rapid mini-fluid challenge or 10mls/kg mandatory ventilator breath in the intubated patient.

7.6.2 Valve Function

Using basic Doppler techniques to assess valve function can be very useful. Acute severe valve regurgitation (typically aortic or mitral) are important causes of

cardiogenic shock with flash pulmonary oedema. Another benefit is the ability to utilise a jet of tricuspid regurgitation to estimate pulmonary artery systolic pressure —echo is the replacement for the Swan Ganz catheter.

7.7 Conclusion

A focussed echo examination is based on 5 views of the heart in which the presence of cardiac activity, LV size and function, RV size and function, volaemic status and any pericardial fluid are simply assessed. It is quick and accurate test to look for major causes of cardiac compromise and when incorporated into the clinical examination and integrated with other tests it becomes an integral part of a complete patient assessment. It is also an excellent starting point for progressing to more advanced cardiac ultrasound. As such, a focussed echo should be mandatory for any patient with cardiovascular compromise.

See also:

Chapter 8 Advanced Transthoracic Echocardiography.

Chapter 9 Transoesophageal Echocardiography.

Chapter 19 The Haemodynamically Unstable Patient.

Chapter 22 The Patient Difficult to Wean from Mechanical Ventilation.

Chapter 8
Advanced Transthoracic Echocardiography

Susanna Price

Keywords Focused ultrasound · Targeted echocardiography · Comprehensive echocardiography

8.1 Introduction

The use of echocardiography in the assessment and management of the critically ill patient has extended greatly over the previous two decades. Previously considered the remit of the outpatient cardiologist/cardiac physiologist, its unique position as a portable diagnostic and monitoring tool has resulted in it being widely used throughout the whole acute patient pathway, by cardiologists and non-cardiologists alike. Echocardiography is now recommended in guidelines for assessment of the shocked patient, comprises a component of the universal definition of myocardial infarction, is included in guidelines on cardiac arrest, and recommendations for the use of echocardiography in acute cardiovascular care (including cardiac intensive care) have also been published [1–4].

Although many critical care practitioners will not use echocardiography beyond its most basic application, its full potential remains unrivalled. Echocardiography is not only a diagnostic imaging technique, but is also increasingly valuable in improving our understanding of cardiovascular pathophysiology in the critically ill, as well as monitoring the response to interventions—both beneficial and detrimental. Unfortunately, a number of challenges exist in its application and interpretation in the critical care setting (Table 8.1) and therefore it is important that both the scope and limitations of the techniques used are understood, not only by

S. Price (✉)
Cardiologist & Intensivist, Royal Brompton Hospital, Sydney Street, London SW36NP, UK
e-mail: s.price@rbht.nhs.uk

S. Price
National Heart & Lung Institute, Imperial College, London, UK

A. Walden et al. (eds.), *Ultrasound in the Critically Ill*,
https://doi.org/10.1007/978-3-030-71742-1_8

Table 8.1 Considerations that influence echocardiography interpretation in critically ill patients

Variable
Filling status
Effects and type of ventilation
Degree of inotropic/inodilator support
Metabolic milieu
Sedative drugs
Mechanical circulatory support
Respiratory circulatory support
Evaluation of right versus left heart and interactions
Most critically ill patients unrepresented in RCTs

those who perform the studies, but also the treating clinician, who is fundamentally responsible for application of the information obtained [4].

This chapter will outline the different modalities of echocardiography available, discuss the implications of moving beyond focused cardiac ultrasound to more advanced applications, provide examples of the potential pitfalls and challenges of echocardiography in the critically ill, and outline some emerging echocardiographic techniques.

8.2 Modalities of Echocardiography and Thoracic Ultrasound

The choice of investigation in any critically ill patient depends upon not only the sensitivity and specificity of the test for a given potential diagnosis, but also the risks of transportation to potentially remote parts of the hospital. A number of different techniques are available (Table 8.2). Transthoracic echocardiography (TTE) should be regarded as the initial imaging modality of choice as it is widely available, carries no risk to the patient (other than misinterpretation of findings) and frequently provides all the required information4. Echocardiography in intensive care should be as comprehensive as possible and undertaken with a fully equipped machine (unless there is a specific requirement for Focused cardiac ultrasound (FoCUS) or a targeted study) and incorporate the full range of standard echocardiographic modalities (including 2D, PW/CW/colour Doppler, TDI/TVI) with careful qualitative and quantitative assessment of parameters as defined in the relevant curricula and guidelines [4–8]. Where TTE images are inadequate, TOE should be undertaken (not in patients who are hypoxic and/or unable to protect their own airways without prior intubation and ventilation). Care must be taken to exclude/correct significant coagulopathy prior to probe insertion, if necessary intubating the oesophagus using direct laryngoscopy and/or using paediatric probes to minimise potential trauma, particularly in those receiving mechanical cardiac and/or respiratory extracorporeal support.

Table 8.2 Techniques used in echocardiography

Technique	Description	Advantages	Disadvantages
FoCUS	Limited to basic imaging modalities (2D ± colour Doppler, qualitative, binary decision-making	Can provide key information in time-limited settings Can be undertaken by minimally trained operators	May result in missed diagnoses/ misinterpretation Provides only the most minimal information Limited in information provided to treating clinician
Targeted echocardiography	Echocardiography (and all potential techniques) used to answer a specific question (i.e. ? tamponade)	Directed study intended to provide specific information for treating clinician	If insufficiently experienced operator, potential to miss key, relevant information
TTE	Non-invasive bedside imaging, comprehensive evaluation of anatomical and physiological status of the heart	Relatively time-consuming Huge potential to answer anatomical and pathophysiological questions regarding the heart Readily available Non-invasive	Requires significant training Images frequently suboptimal in critical care setting Potential false negatives in certain conditions (i.e. LAA thrombus, endocarditis)
TOE	Invasive echocardiography allowing superior image quality (vs TTE)	High resolution images Technique easily teachable in the critical care setting May be initial imaging technique of choice in certain situations (i.e. ?LAA thrombus)	Oesophageal intubation Difficult alignment for evaluation of some structures (descending aorta, right ventricle) Potential complications (oesophageal perforation, oropharyngeal trauma etc)
Contrast echocardiography	Opacification of the: Left heart Right heart	endocardial border definition/exclusion of LAA thrombus) Evaluation of intracardiac/ intrapulmonary shunt	Risk of anaphylaxis Suboptimal opacification may lead to false negatives
Intracardiac echocardiography	Echo mounted within intracardiac catheter	Very high resolution of intracardiac structures	Invasive Expensive

(continued)

Table 8.2 (continued)

Technique	Description	Advantages	Disadvantages
Lung US	US imaging to evaluate lung and pleural structures	Easy to teach and apply Evaluation of interstitial fluid as well as pleural pathology	Not widely adopted by radiologists therefore potential missed collaboration in the field Can be difficult to differentiate cause of interstitial oedema
Pocket-sized imaging devices	Small, limited functionality machines	Portable	Limited applications and imaging quality FoCUS only

8.3 Levels of Expertise and Certification

Although image acquisition (both TTE and TOE) is relatively simple, interpretation, particularly in critical care, requires specific training. Beyond FoCUS, recommendations are such that given the complexity of the clinical context and potential ramifications of misinterpretation, the level of expertise for those undertaking echocardiography (TTE and/or TOE) should be at least those of undertaking imaging in the outpatient setting. When describing degrees of expertise, a number of levels have been defined, however, nomenclature can be confusing; advanced echo (frequently used to indicate 'beyond basic' in critical care) corresponds to the baseline standards for accreditation, representing the minimal requirement for independent practice in cardiology/cardiac physiology (Fig. 8.1). Certification in echocardiography is offered by a number of national and international bodies, however, the levels of knowledge and skill required for each vary significantly, and the differences in terminology are unlikely to be resolved in the immediate future [4–8]. Key is that every practicing clinician is aware of the scope of echocardiography (vs. FoCUS) in the ICU as well as their own limitations, and always uses the technique within an appropriate governance infrastructure.

8.4 Advanced Critical Care Echocardiography: Beyond Basic

Critical care echocardiography potentially uses information from all echocardiographic modalities to evaluate the patient. Unlike outpatient studies where the diagnosis is generally known, critical care studies are generally performed to evaluate either the cause of underlying symptoms/signs or, more frequently to assess the patient's pathophysiological status and guide interventions in various clinical scenarios. When moving from basic to more advanced echocardiography it

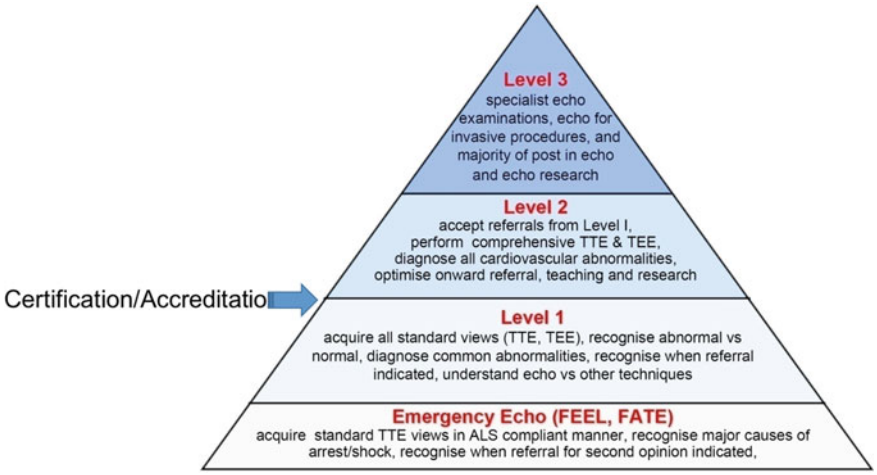

Fig. 8.1 Levels of knowledge and skill in ICU echocardiography. Note that for Level 1, both TTE and TEE are recommended. Certification/accreditation for comprehensive echocardiography required in intensive care is generally regarded as between Levels 1 and 2. For details, see text. TTE; transthoracic echocardiography, TEE; trans-esophageal echocardiography, FEEL; focused echo in emergency life support, FATE; focused assessed transthoracic echocardigoraphy, ALS; advanced life support

is important to be aware of the full range of modalities available, as well as the pitfalls when applying techniques which have been largely developed in the outpatient setting to the ICU (Table 8.3).

8.4.1 Left Ventricular Function

One of the commonest requests for ICU echocardiography is evaluation of left ventricular (LV) function. Of the more basic techniques, assessment of LV function generally either depends upon linear measures of changes in LV internal dimensions (fractional shortening) or differences between systolic and diastolic areas/volumes in the minor axis (ejection fraction). LV function is complex, with differing orientation of fibres at different muscle layers, comprising minor and long axis contraction, rotational contraction as well as differential basal and apical rotational vectors. Standard evaluation of LV ejection fraction includes the application of 2D and 3D echocardiography, however, its usefulness is limited, as normal values are not known for the critically ill patient population, are highly variable depending upon critical care interventions in addition to the preload and afterload status, and inherent contractility of the myocardium. Interpretation of findings must therefore take into account preload (including exclusion of inadequate stroke volume from the RV and estimation of left atrial pressure (see section

Table 8.3 FoCUS and advanced echocardiography: challenges and pitfalls in intensive care

Diagnosis	FoCUS	Advanced echo (additional)	Challenges in critical care
Hypovolaemia	Kissing LV walls IVC dimensions	E deceleration time E/A ratio E/E' ratio Pulmonary DT Colour Doppler propagation velocity	Demand absence of LV, pulmonary and RV disease to be valid Correlation with PCWP poor No absolute values—estimated ranges Not well-validated in critically ill Respiratory changes altered in IPPV Require combination of parameters Low values don't necessarily indicate tolerance to volume loading
Tamponade	Pericardial collection Dilated IVC RV diastolic collapse	Exaggerated reciprocal variation in trans-tricuspid and mitral velocities Swinging heart Pseudo-SAM	Demands global collection Presence of cardiac/pulmonary disease may mislead Respiratory changes altered in IPPV Not valid in low pulsatility states (ECMO)
Pulmonary embolism	Dilated RV	PASP PVR RV:LV dimensions	Concomitant pulmonary disease Effects of IPPV
Myocardial infarction/ischaemia	RWMA	Doppler changes in velocity Strain/strain-rate imaging DSE Contrast echocardiography TOE demonstration of first 2 cm of coronary arteries Perfusion imaging	Endogenous catecholamines Image quality RWMA challenging in offloaded heart (ECMO)

on RV assessment), afterload (including exclusion of significant mitral regurgitation which may be dynamic, Fig. 8.2), the level of inotropic agents being delivered (as the levels delivered may mimic submaximal or peak stress during a pharmacological stress echocardiogram), any negatively inotropic agents administered, the effects of positive pressure ventilation and the presence of any mechanical circulatory support.

Measurement of longitudinal (or long axis) function using M-mode and/or TDI, combined with Doppler interrogation of transmitral filling and evaluation of cardiac electromechanics provides additional information in evaluation of ventricular function, highly relevant to the ICU setting (Fig. 8.3). There is some evidence that

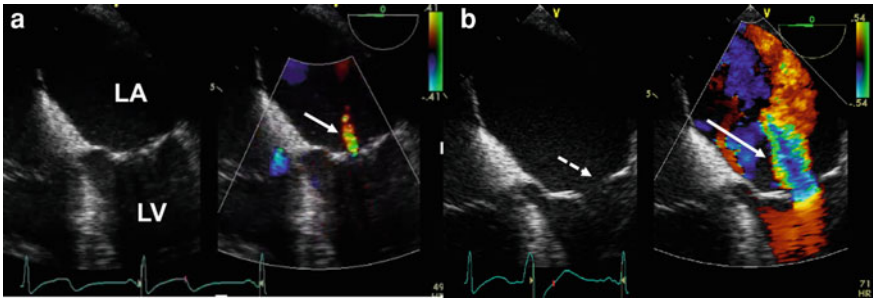

Fig. 8.2 Volume, ventilation and afterload and mitral regurgitation. The effects of ventilation, volume and afterload reduction on mitral regurgitation (and therefore LV afterload) in a patient with recurrent 'flash' pulmonary oedema and normal ejection fraction. **a** Immediately after intubation and ventilation there is trivial MR (arrowed). **b** With volume and pressor loading, the mitral leaflets do not coapt in systole (dotted arrow) and there is very severe MR (solid arrow). LA; left atrium, LV; left ventricle, MR; mitral regurgitation

parameters such as the total isovolumic time (tIVT) or Tei index (Fig. 8.4) may be less load-dependent than ejection fraction [9], and others (in combination) are used to assess left atrial pressure (see section on RV assessment) [10]. Abnormalities in long axis function relate to timing of onset, duration, magnitude and velocity of movement, and may be fixed (related to the underlying pathology) or dynamic (relating to inotropic or filling status) with a normal or abnormal response to pharmacological stress (Table 8.4) [11]. Calculation of indices of electromechanical efficiency (VTI, tIVT, Tei index) may demonstrate significant abnormalities even in the presence of a normal ejection fraction, suggest potential underlying causes (Fig. 8.5), and potentially guide interventions to optimise cardiac output (Figs. 8.5 and 8.6) [12, 13]. The critical care echocardiographer should be aware of the potential application of these techniques in the evaluation of a patient with inadequate cardiac output, particularly where standard measurements are normal and no other cardiac cause for a limited stroke volume is evident. Use of newer techniques including strain/strain-rate imaging may provide further insights in evaluation in this scenario.

8.4.2 Filling Pressures and Volume Status

The gold standards for estimation of left-sided and right-sided pressures are the pulmonary capillary wedge pressure, and right atrial pressures respectively. Unfortunately, echocardiography cannot measure absolute pressures, but merely differences in pressure between two chambers. Of the range of parameters used in comprehensive echocardiography to estimate left atrial pressure (including E wave deceleration time, E/A ratio, E/e', colour Doppler propagation velocity, pulmonary vein deceleration time), validation against pulmonary capillary wedge pressure of

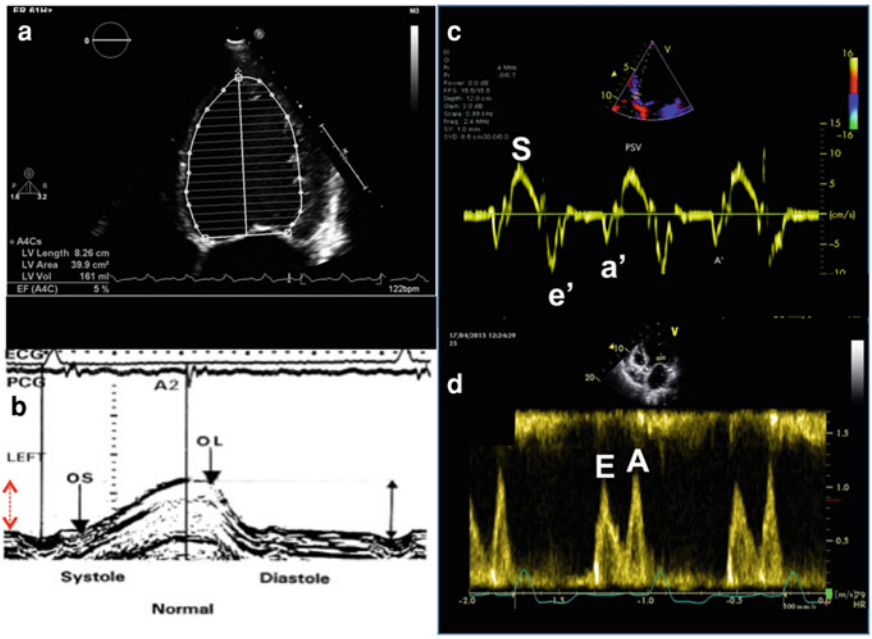

Fig. 8.3 Basic assessment of LV function using transthoracic echocardiography. **a** Ejection fraction measured using summation of discs in a severely impaired LV (5% EF). **b** Long axis function measured using M-mode in a normal left ventricle. The red arrow shows the extent of shortening in systole. **c** Tissue Doppler imaging recorded for the inter-ventricular septum of the LV. **d** Trans-mitral Doppler (PW) demonstating LV filling. EF; ejection fraction, ECG; electrocardiogram, PCG; phonocardiogram, OS; onset of shortening, OL; onset of lengthening, A2; aortic valve closure, S; systolic wave, e'; early diastolic, a' late diastolic components of annular velocities, E; early transmitral filling, A; late transmitral filling due to atrial contraction

each is variable and largely suboptimal [4, 14]. Further, few studies have been performed in the critical care setting. Here, a combination of a number of parameters is recommended (Fig. 8.7) [14]. None have been well-validated however in critically ill patients with cardiac disease, and therefore great care should be taken in their application, and always in the context of a comprehensive study. Where tolerance to volume loading (avoiding pulmonary oedema) is of concern, lung ultrasound may be useful [15]. Although widely used, most of the basic parameters used to determine volume status (or the potential to respond to a volume challenge with an increase in stroke volume) have significant limitations in the critically ill, in particular in the presence of cardiac and/or pulmonary disease (Table 8.3) and should be interpreted with appropriate caution.

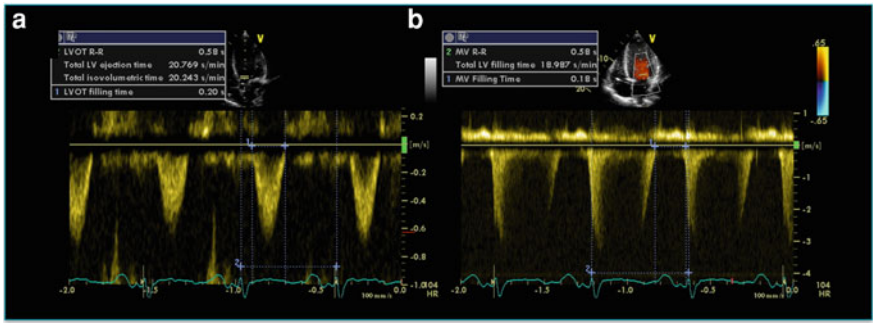

Fig. 8.4 Tei index and total isovolumic time measured using Doppler echocardiography. **a** LVOT PW Doppler taken from the apical 5-chamber view. **b** MR (CW Doppler) from the apical 4-chamber view. Tei index: [440 − 200]/200 = 1.2. ET: 0.2 × 014 = 20.8 s/min, FT; 0.18 × 104 = 18.9 s/min. tIVT: 60 − (20.8 + 18.72) = 20.2 s/min. LVOT; left ventricular outflow tract; PW; pulse wave, MR; mitral regurgitation, CW; continuous wave, ET; ejection time, FT; filling time, tIVT; total isovolumic time

8.4.3 Right Ventricular Function

The right ventricle (RV) is exquisitely sensitive to changes in afterload and reduction in coronary perfusion and in the ICU RV dysfunction is most commonly secondary to increased afterload due to pulmonary disease, mechanical ventilation and/or to left ventricular dysfunction. A range of conventional echocardiographic techniques are routinely used to assess right ventricular systolic function, including TAPSE, TDI and the right ventricular myocardial performance index, however due to the sensitivity of the RV to preload, afterload and coronary perfusion pressures, interpretation must be in the context of ventilation, arterial blood gases, inotropy and filling status (Fig. 8.8). Measurement of RV geometry and volumes is complex, and it may be that 3D echocardiography will transform how we assess the RV on the ICU [16–18]. As with the LV, a more physiological approach to the RV when using echocardiography, can provide information with potential to modulate interventions to improve RV performance, and/or monitor and modify interventions in order to minimise the adverse effects of therapies commonly used on the ICU (Fig. 8.8). Although all included in descriptions of standard echocardiographic examinations, they are not always systematically applied. These include measuring the duration of tricuspid regurgitation (TR), as well as peak velocity, and always in context of the RV systolic function, estimation of pulmonary vascular resistance using the pulmonary acceleration time, and evaluation for RV restrictive physiology (Table 8.4) [19].

Table 8.4 Additional parameters to standard acquisitions in the physiological assessment of ventricular function

Modality	Abnormality/finding	Utility
Left ventricular function		
M-mode long axis	• Timing of onset delayed • Duration prolonged • Excursion reduced	• BBB • Coronary ischaemia • LV function impaired (even if normal EF)
LV TDI	• Systolic (S') wave reduced • Diastolic filling: e' reduced	• LV contractility impaired • Estimation of LAP (combined with transmitral Doppler)
Transmitral Doppler	• Suppression of early filling—diastolic dysfunction • Combination of E/e'	• ?electromechanical dyssynchrony • ?ischaemia • Estimation of LAP
Aortic VTI (Doppler)	• Abnormally low • Combination with transmitral Doppler: prolonged tIVT	• Adequacy of CO • Potential to wean from MCS • Electromechanical dyssynchrony
Strain/strain rate imaging (Doppler or speckle tracking)	• Reduction in circumferential and longitudinal strain, strain rate, radial displacement and rotational velocity and displacement	• Subclinical ventricular dysfunction
Right ventricular function		
CW Doppler TV	• Prolonged duration of TR	• Pulmonary hypertension,
PW Doppler PV	• Short pulmonary acceleration time • Pre-systolic a wave: RV restriction	• High pulmonary vascular resistance • May indicate early RV dysfunction • Should prompt review of ventilatory parameters

8.5 3D and 4D Imaging

Technological advances in echocardiography have transformed image acquisition and quality, allowing the development of 3D and 4D (real-time 3D) imaging using both TTE and TOE. Potential applications relevant to the ICU include assessment of LV and RV dimensions and function, measurement of stroke volume, simultaneous assessment of all segments of both ventricles for regional wall motion abnormality and/or dyssynchrony and detailed examination of the cardiac valves [18, 20]. 3D is probably superior to 2D echocardiography for estimating ejection fraction, and diagnosing regional wall motion abnormalities, however limitations in

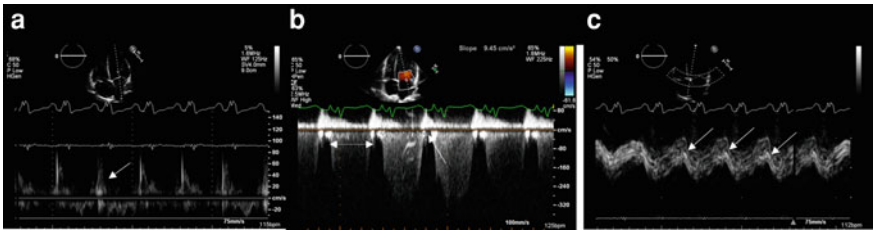

Fig. 8.5 Long axis and Doppler diagnosis of ischaemia. Doppler and long-axis function demonstrating LV ischaemia in a patient with pulmonary oedema and globally impaired LV systolic function receiving ECMO. **a** transmitral PW Doppler showing the unexpected finding of isolated late (A wave) transmitral filling. **b** CW Doppler of MR of 400 ms duration (dotted arrow). This prolonged duration of systole allows very little time for transmitral filling (solid arrow), explaining the absence of early diastolic filling in A. **c** M-mode of the long axis of the septum (apical 4-chamber view) demonstrating prolonged and reduced excursion, with post-ejection shortening (arrowed). This prolongation of systole in the long axis means the LV is generating tension into early diastole, and therefore MR is prolonged and early transmitral filling is suppressed. The reduction in long axis excursion in this patient and poor quality of transthoracic images, and the partial bypass from ECMO meant standard regional wall motion scoring and the TDI were uninterpretable. The patient underwent coronary angiography with subsequent revascularisation. LV; left ventricle, ECMO; extracorporeal membrane oxygenation, PW; pulse wave, CW; continuous wave, MR; mitral regurgitation, TDI; tissue Doppler imaging

the ICU setting are availability of machines, the need for specific training for its accurate application as well as the requirement high-quality images. 3D echo for assessment of LV dyssynchrony is based upon the regional time to minimum systolic volume, measured from the onset of the QRS complex, and is inferred from either the maximal difference between two regions, or standard deviation of up to 17 regional volumes, ascribed according to standardised nomenclature. The wider applicability of dyssynchrony assessment (using standard parameters as well as 3D echocardiography) is not yet known in critical care, however, recent evidence suggests that where electromechanical dyssynchrony is limiting stroke volume, resynchronisation may result in an acute improvement in haemodynamics. Assessment of the right ventricle using 3D imaging is superior to 2D echocardiography when assessing volumes and contractility, however 3D echocardiography systematically underestimates RV volumes (compared with the gold standard of cardiac magnetic resonance imaging) [12, 13]. 3D/4D echocardiography has revolutionised assessment of the mechanism and severity of valvular regurgitation, and detection/delineation of paraprosthetic valvular regurgitation (Fig. 8.9). Although advanced mitral valve assessment is more relevant to the cardiothoracic rather than general intensive care setting the potential for 3D/4D echocardiography to facilitate diagnosis and evaluation of regurgitation is evident.

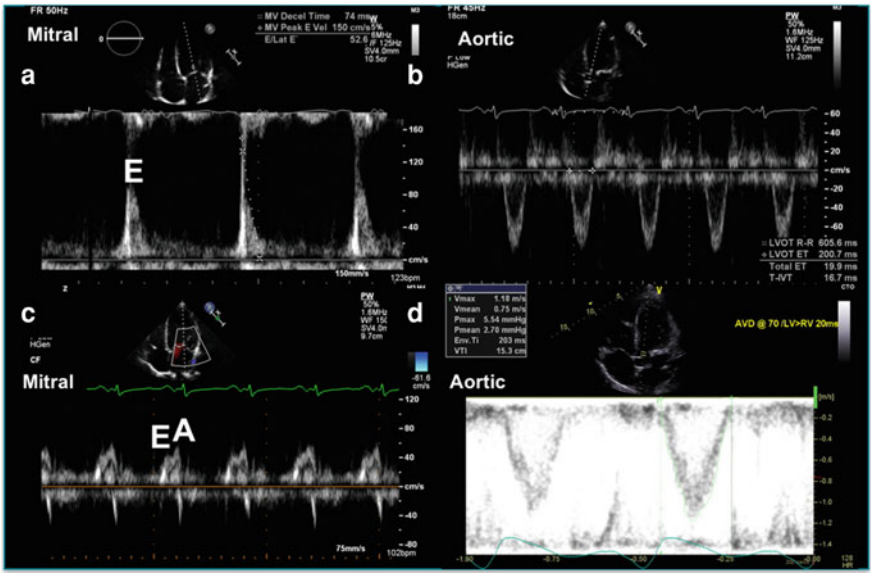

Fig. 8.6 Echocardiography-guided pacing optimization on the intensive care unit. Pacing optimisation to improve cardiac output in a patient with significant electromechancial dyssynchrony (the same patient as shown in Fig. 8.4), after biventricular pacemaker insertion, but before pacing optimisation. Upper panel, pre-optimisation: **a** transmitral PW Doppler showing an isolated E wave with a high velocity short deceleration time consistent with restrictive LV function and a high left atrial filling pressure. **b** Biventricular pacing has reduced the tIVT to 16.7 s. Lower panel, post-optimisation. Systematic alteration of heart rate, AV delay and VV delay has improved the electromechanics of the patient. **c** transmitral PW Doppler now demonstrates both E and A waves on transmitral filling. The tIVT has been reduced, and the aortic VTI increased to 15.3 cm. Pacing optimisation settings are shown in yellow: AV delay 70 ms and LV-RV delay 20 ms. PW; pulse wave, E; early transmitral filling, A; late transmitral filling, tIVT; total isovolumic time, LV; left ventricle, AV; atrio-ventricular, VV; ventriculo-ventricular, RV; right ventricle

8.6 Strain and Strain Rate Imaging

These techniques have been proposed to improve the ability to detect ischaemia and ventricular dysfunction not demonstrable by other more conventional echocardiographic techniques. They are measures of myocardial deformation that are basic descriptors of both the nature and function of cardiac tissue, and therefore differ significantly from more traditional methods of assessment of LV function. Strain/strain rate can be measured using Doppler or 2D (speckle tracking) echocardiography (Fig. 8.9) [21].

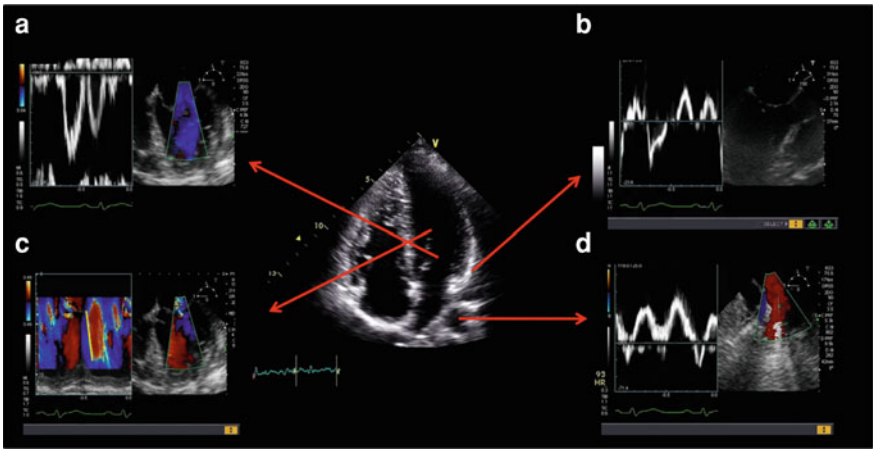

Fig. 8.7 Some parameters routinely used to estimate left atrial pressure. **a** Transmitral PW Doppler. **b** LV tissue Doppler imaging. **c** Colour M-mode velocity propagation. **d** Pulmonary vein PW Doppler. Of these, the best correlate with left atrial pressure is the deceleration time of the pulmonary vein D wave (white arrow), however, none are well-validated in the ICU and should generally be used in combination, and in the context of the comprehensive echocardiographic study. PW; pulse wave, LV; left ventricle, D wave; diastolic wave, ICU; intensive care unit

Strain rate is measured by obtaining a series of velocity curves (from tissue Doppler imaging (TDI) comprising isovolumic contraction, systolic, diastolic and atrial components) to demonstrate a velocity gradient along a length of ventricular wall. A regression calculation between adjacent tissue velocity data points along this length is used to generate strain rate, which is integrated to calculate strain. Strain (ε) is a unitless measure of lengthening and shortening only (defined as the change in distance between two points divided by the initial distance between those two points, $\varepsilon = (L1 - L0)/L0)$), assumes non-compressiblility of tissues, and can be calculated for three axes of myocardial motion, resulting in longitudinal, circumferential and radial strain [21]. The techniques have been well-validated with cardiac magnetic resonance scanning and animal models using sonomicrometry. As data are derived from TDI, certain caveats regarding their use exist; in particular sensitivity to signal noise and alignment. Speckle tracking uses 2D echocardiography to identify areas of correlation within signature blocks of backscattered echocardiographic tissue, and tracks tissue motion accordingly, allowing simultaneous longitudinal, radial, circumferential and also torsion analysis. It avoids the angle-dependency of Doppler, and allows interrogation of multiple vectors of movement simultaneously.

Currently strain rate imaging is regarded as a tool for understanding myocardial mechanics. It is highly sensitive in detecting changes in wall motion, and current clinical applications include potential identification of myocardial viability and detection of subclinical ventricular dysfunction [22]. There is little in the adult critical care literature regarding strain rate imaging, however, emerging studies have

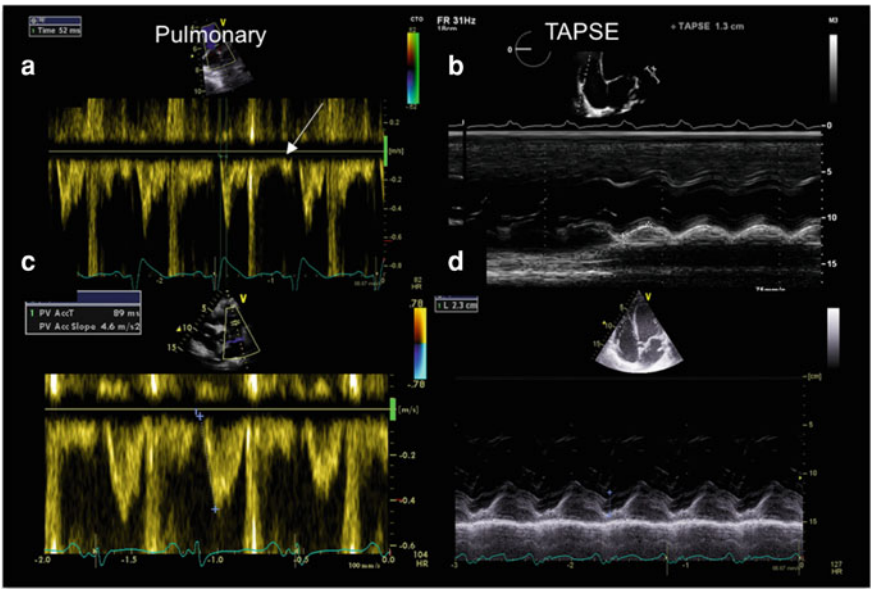

Fig. 8.8 The effects of altering coronary perfusion and RV afterload on echocardiographic parameters of RV function in a patient with cardiogenic shock. Upper panel before treatment. **a** Pulmonary arterial Doppler showing a short acceleration time (52 ms) and very short ejection time. A small pre-systolic A wave is also seen (arrowed) except during delivery of a positive pressure breath. **b** Corresponding TAPSE of 1.3 cm. In the context of significant inotropic support this is significantly impaired. Lower panel after treatment with iNO, levosimendan, nebulised prostacyclin and low-dose vasopressin plus insertion of an IABP, reduction in noradrenaline dosage and stopping adrenaline infusion. **c** The pulmonary artery Doppler shows the acceleration time to be normal, and the right heart VTI was significantly increased. **d** TAPSE has increased to 2.3 cm. The corresponding measured cardiac index in this patient increased from 1.3 to 2.6 L/min/m^2

demonstrated the feasibility of 2D longitudinal strain assessment in the ICU, further suggesting that abnormalities of strain and/or strain rate may identify patients at higher risk of death in both undifferentiated and septic shock [23, 24]. 2D strain speckle tracking has been shown to detect ventricular dysfunction in septic shock, not appreciated by conventional echocardiography. Here, despite other echocardiographic parameters being normal, significant abnormalities in circumferential and longitudinal strain, strain rate, radial displacement and rotational velocity and displacement were demonstrated.

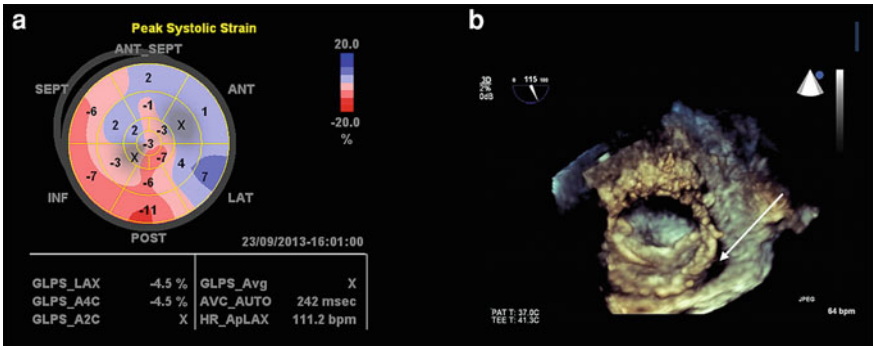

Fig. 8.9 3D and strain echocardiography in critically ill patients. **a** A bullseye plot demonstrating peak systolic strain in a patient admitted in pulmonary oedema. Abnormalities in strain are demonstrated in 17 regions of the heart. Each region is attributed a peak systolic strain value, and demonstrated according to the colour scale displayed. **b** 3D TOE looking down onto a single tilting disc mitral prosthesis from the left atrium taken from a patient with pulmonary oedema. A paraprosthetic gap is seen (arrowed) and this was confirmed as the site of paraprosthetic regurgitation using 3D colour Doppler imaging. ANT; anterior, SEPT; septal, LAT; lateral, POST; posterior, INF; inferior, TOE; transoesophageal echo

Although used in outpatient echocardiography, currently these techniques should be regarded as potential research tools in assessment of ventricular function in the critically ill. It seems possible however, that as the evidence emerges for its utility, particularly if it provides insights into how to optimise ventricular function in intensive care, its potential applicability as a standard advanced echo technique in this setting is huge.

8.7 Echocardiography for New Critical Care Techniques

Changing practice in advanced support of the heart and/or lungs using extracorporeal support (primarily extracorporeal membrane oxygenation, ECMO) demands a level of echocardiographic knowledge and expertise that, in effect, is a new area of specialisation. Areas to be addressed include confirming the underlying diagnosis, excluding contraindications to ECMO, guiding initiation of extracorporeal support (including positioning of cannulae), monitoring of the heart, diagnosis of complications and finally in those on cardiac ECMO differentiating patients who can be weaned from those who will need longer-term support/transplantation (Fig. 8.10). This exciting emerging area in critical care is likely to demand specific training, as seemingly minor echocardiographic findings can have profound implications for management of the patient.

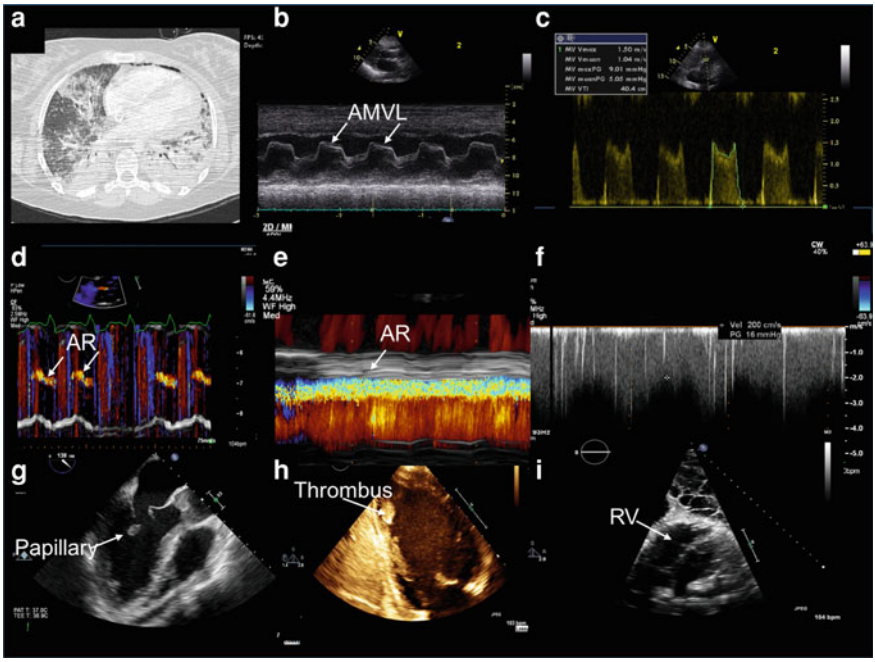

8.8 Conclusion

The step from basic to advanced echocardiography is not insignificant, demanding knowledge of the full range of echocardiographic techniques, as well as their limitations and potential pitfalls when used in the critical care setting. The scope for the application of advanced critical care echocardiography is, however, huge, and with increasing evidence emerging regarding the utility of comprehensive and physiological echocardiography, it is likely that our patients will benefit from its wider application in the future.

See also:

Chapter 5 Basic Lung Ultrasound
Chapter 6 Advanced Lung Ultrasound
Chapter 7 Focused Transthoracic Echocardiography
Chapter 9 Transoesophageal Echocardiography
Chapter 19 The Haemodynamically Unstable Patient
Chapter 22 The Patient Difficult to Wean from Mechanical Ventilation.

◂**Fig. 8.10** Examples of the utility of echocardiography in ECMO. Top panel. Shows images taken from a young patient with influenza receiving VV-ECMO who was disproportionately hypoxic for the level of pulmonary disease. **a** CT scan showing extensive lung involvement, but with some significant areas of sparing. **b** Trans-mitral M-mode showing characteristic movement of the anterior mitral valve consistent with previous rheumatic mitral valve disease (AMVL, arrowed). **c** PW Doppler showing an increased trans-mitral velocity. The mitral stenosis was confirmed by serial CW Doppler to be mild, but was over-estimated in her initial assessment due to her high cardiac output state. Middle panel demonstrating the challenges and importance of assessing valve disease in patients requiring VA-ECMO. **d** Colour M-mode across the aortic valve pre-ECMO showing mild AR (narrow height compared with the annulus and LVOT). **e** Colour M-mode across the aortic valve after initiation of ECMO the heart stops ejecting and the AR becomes continuous and more severe, resulting in progressive increase in LVEDP and LV dilatation, necessitating LV venting. **f** CW Doppler in the same patient between the LV and aorta showing continuous AR with a low pressure difference. Given a root pressure of 55 mmHg, the estimated LVEDP was 39 mmHg. Bottom panel shows three different patients with complications of ECMO. G. TOE (LVOT view) in a patient receiving VA-ECMO for presumed RV infarction (dilated, failing RV with a dynamic, underfilled LV on TTE). Two important findings are noted. First, there is a ruptured papillary muscle with associated free MR, second, the aortic valve is closed in systole and diastole with significant spontaneous contrast in the root. This should prompt correction of the underlying pathology and also a search for evidence of LV ischaemia. H. A patient who has received VA-ECMO and needs to be transitioned to VAD. Here, apical thrombus is noted (arrowed) which will influence the surgical approach. I. A patient receiving VV-ECMO for severe acute respiratory failure who was developing progressive multi-organ failure. The only echo view available was subcostal, and revealed a dilated, failing RV. The patient was 'upgraded' to VA-ECMO. AMVL; anterior mitral valve leaflet, AR; aortic regurgitation, RV; right ventricle, VV-ECMO; respiratory extracorporeal membrane oxygenation, CT scan; computerised tomography, PW; pulse wave, CW; continuos wave, VA-ECMO; cardiac extracorporeal membrane oxygenation, LVEDP; left ventricular end-diastolic pressure, TOE; trans-oesophageal echocardiography, LVOT; left ventricular outflow tract, RV; right ventricle, TTE; transthoracic echocardiography, VAD; ventricular assist device

References

1. Kristian Thygesen, Joseph S. Alpert, Allan S. Jaffe, Maarten L. Simoons, Bernard R. Chaitman, Harvey D. White and the Writing Group on behalf of the Joint ESC/ACCF/AHA/WHF Task Force for the Universal Definition of Myocardial Infarction. ESC/ACCF/AHA/WHF expert consensus document: Third Universal Definition of Myocardial Infarction. Circulation. 2012;126:2020–2035.
2. https://www.resus.org.uk/resuscitation-guidelines/adult-advanced-life-support/.
3. Ponikowski P, Voors AA, Anker SD, Bueno H, Cleland JG, Coats AJ, Falk V, González-Juanatey JR, Harjola VP, Jankowska EA, Jessup M, Linde C, Nihoyannopoulos P, Parissis JT, Pieske B, Riley JP, Rosano GM, Ruilope LM, Ruschitzka F, Rutten FH, van der Meer P; Authors/Task Force Members; Document Reviewers. ESC Guidelines for the diagnosis and treatment of acute and chronic heart failure: The Task Force for the diagnosis and treatment of acute and chronic heart failure of the European Society of Cardiology (ESC). Developed with the special contribution of the Heart Failure Association (HFA) of the ESC. Eur J Heart Fail. 2016 Aug;18(8):891–975. https://doi.org/10.1002/ejhf.592. Epub 2016 May 20. 2016.
4. Lancellotti P, Price S, Edvardsen T, Cosyns B, Neskovic AN, Dulgheru R, Flachskampf FA, Hassager C, Pasquet A, Gargani L, Galderisi M, Cardim N, Haugaa KH, Ancion A, Zamorano JL, Donal E, Bueno H, Habib G. The use of echocardiography in acute

cardiovascular care: recommendations of the European Association of Cardiovascular Imaging and the Acute Cardiovascular Care Association. Eur Heart J Acute Cardiovasc Care. 2014 Nov 6. pii: 2048872614549739.
5. http://www.echoboards.org.
6. http://www.bsecho.org/accreditation/types-of-accreditation/.
7. http://www.escardio.org/Sub-specialty-communities/European-Association-of-Cardiovascular-Imaging-(EACVI)/Certification-Accreditation.
8. http://www.esicm.org/education/edec.
9. Duncan AM, Francis DP, Henein MY, Gibson DG. Importance of left ventricular activation in determining myocardial performance (Tei) index: comparison with total isovolumic time. Int J Cardiol. 2004;95(2–3):211–7.
10. Vignon P, AitHssain A, François B, Preux PM, Pichon N, Clavel M, Frat JP, Gastinne H. Echocardiographic assessment of pulmonary artery occlusion pressure in ventilated patients: a transoesophageal study. Crit Care. 2008;12(1):R18.
11. Duncan A, Francis D, Gibson D, Pepper J, Henein M. Electromechanical left ventricular resynchronisation by coronary artery bypass surgery. Eur J Cardiothorac Surg. 2004;26 (4):711–9.
12. Tavazzi G, Kontogeorgis A, Bergsland NP, Price S. Resolution of cardiogenic shock using echocardiography-guided pacing optimization in intensive care: a case series. Crit Care Med. 2016;44(8):e755–61.
13. Mantziari L, Guha K, Senguttuvan NB, Sharma R. Cardiac resynchronization therapy for critically ill patients with left ventricular systolic dysfunction. Int J Cardiol. 2013;163(2):141–5. https://doi.org/10.1016/j.ijcard.2011.05.034.
14. Vignon P, AitHss ain A, François B, Preux PM, Pichon N, Clavel M, Frat JP, Gastinne H. Echocardiographic assessment of pulmonary artery occlusion pressure in ventilated patients: a transoesophageal study. Crit Care. 2008;12(1):R18.
15. Luna Gargani. PMCID: PMC305929. Lung ultrasound: a new tool for the cardiologist. Cardiovasc Ultrasound. 2011;9:6. Published online 2011 Feb 27. https://doi.org/10.1186/1476-7120-9-6.
16. Haddad François, Hunt Sharon A, Rosenthal David N, Murphy Daniel J. Right Ventricular function in cardiovascular disease, part I: anatomy, physiology, aging, and functional assessment of the right ventricle. Circulation. 2008;117:1436–48.
17. Haddad F, Doyle R, Murphy DJ, Hunt SA. Right ventricular function in cardiovascular disease, part II: pathophysiology, clinical importance, and management of right ventricular failure. Circulation. 2008;117(13):1717–31. https://doi.org/10.1161/CIRCULATIONAHA.107.653584.
18. Sebastian Schattke, Moritz Wagner, Robert Hättasch. Single beat 3D echocardiography for the assessment of right ventricular dimension and function after endurance exercise: Intraindividual comparison with magnetic resonance imaging. Cardiovasc Ultrasound. 2012;10:6. Published online 2012 February 22. https://doi.org/10.1186/1476-7120-10-6.
19. Cullen S, Shore D, Redington AN. Characterization of right ventricular diastolic performance after complete repair of tetralogy of Fallot: restrictive physiology predicts slow postoperative recovery. Circulation. 1995;91:1782–9.
20. Kapetanakis S, Kearney MT, Siva A, Gall N, Cooklin M, Monaghan MJ. Real-time three-dimensional echocardiography: a novel technique to quantify global left ventricular mechanical dyssynchrony. Circulation. 2005;112:992–1000.
21. Marwick TH. Measurement of strain and strain rate by echocardiography: ready for prime time? J Am Coll Cardiol. 2006;47(7):1313–27 Epub 2006 Mar 20.
22. Marciniak A, Sutherland GR, Marciniak M, Kourliouros A, Bijnens B, Jahangiri M. Prediction of postoperative left ventricular systolic function in patients with chronic mitral regurgitation undergoing valve surgery—the role of deformation imaging. Eur J Cardiothorac Surg. 2011 Nov;40(5):1131–7. https://doi.org/10.1016/j.ejcts.2011.02.049. Epub 2011 Apr 1.

23. De Geer Lina, Engvall Jan, Oscarsson Anna. Strain echocardiography in septic shock—a comparison with systolic and diastolic function parameters, cardiac biomarkers and outcome. Crit Care. 2015;26(19):122. https://doi.org/10.1186/s13054-015-0857-1.
24. Basu S, Frank LH, Fenton KE, Sable CA, Levy RJ, Berger JT. Two-dimensional speckle tracking imaging detects impaired myocardial performance in children with septic shock, not recognized by conventional echocardiography. Pediatr Crit Care Med. 2012;13(3):259–64. https://doi.org/10.1097/PCC.0b013e3182288445.
25. Sanfilippo Filippo, Santonocito Cristina, Panarello Giovanna, Arcadipane Antonio. The role of speckle tracking echocardiography for prognostication in patients with severe sepsis or septic shock. Crit Care. 2016;20(1):284.

Chapter 9
Transoesophageal Echocardiography

Farhan T. Husain and Maria-Magdalena Gurzun

Keywords Transoesophageal Echocardiography · Intensive care · TEE · Critical care

9.1 Introduction

Transoesophageal echocardiography (TOE) is a versatile tool in the armamentarium of the modern critical care physician and its role is finding more and more application in the intensive care unit (ICU). Although well established in the domains of cardiology and cardiac anaesthesia its penetrance into intensive care units has been slow. This could be down to financial constraints but is more likely due to paucity of training and lack of established guidelines. There is a growing opinion amongst experts that basic echocardiography and general echocardiography should be a mandatory part of training for junior doctors. Proficiency in the use of TOE is a prerequisite for advanced critical care echocardiography certification [1].

Most intensivists will be well aware of the limitations of transthoracic echocardiography (TTE) and the challenges that some of the patients pose making image acquisition very difficult due to limited acoustic windows and poor image qualities. TOE has the advantage of being able to provide excellent images of the heart and its structure making it easier to diagnose and treat patients. It is fast becoming a monitoring tool with clinicians using it to assess fluid responsiveness. Miniaturised disposable TOE probes have been developed and are available commercially to be used for haemodynamic monitoring of patients on ICU. TOE has a positive impact on patient management and maybe the only tool to provide the necessary information to intensive care physicians [2, 3].

F. T. Husain (✉) · M.-M. Gurzun
Department of Anaesthesia, Morriston Hospital, Heol Maes Eglwys, Swansea, SA6 6NL, West Glamorgan, UK
e-mail: Farhan_husain@hotmail.co.uk

A. Walden et al. (eds.), *Ultrasound in the Critically Ill*,
https://doi.org/10.1007/978-3-030-71742-1_9

TOE is a semi invasive procedure and care should be taken in patient selection as often the ICU patient is sedated precluding taking of a thorough history. It is however a very safe modality with very low complication rates when used appropriately [4].

The purpose of this chapter is to give the reader a taster of the potential applications of TOE for the intensive care setting and an idea of how to become proficient in the use of the probe and machine. A detailed description of all the techniques and diagnostic applications may not be necessary for use on ICU and is indeed beyond the remit of this narrative. But I would encourage the readers to access the tremendous amount of resources available on line and in well-established textbooks on the subject.

9.2 The TOE Probe

The TOE probe is a multiplane probe capable of providing several angles of insonation without having to move the transducer. This is achieved electronically by choosing which of the piezoelectric crystals are fired and how the acoustic lens focusses the ultrasound beam. Several sizes are commercially available and the adult probe is about 1 m long with graded markings in intervals of 10 cm to help guide insertion (Fig. 9.1). Typical operational frequencies of the TOE probe are between 2 and 7 MHz. The ultrasound waves are fired outwards in a fanwise manner repeatedly. The scan lines so produced are stitched together to form a fan/pie shaped sector which is projected on the screen with its apex at the top of the screen. The apex corresponds to the probe tip (Fig. 9.2) and the right side of the

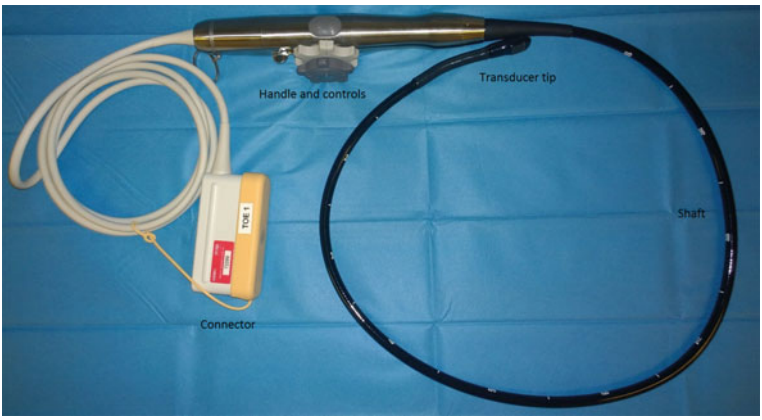

Fig. 9.1 TOE probe and components

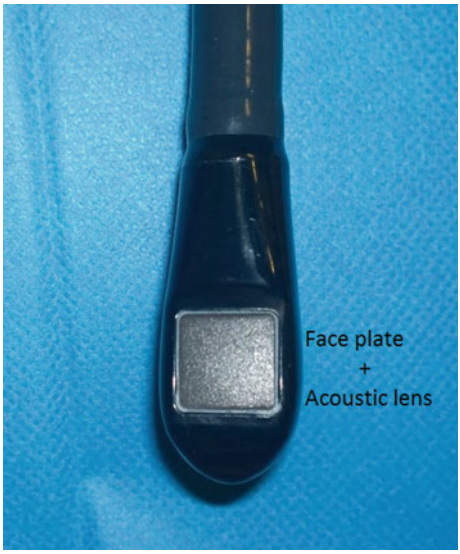

Fig. 9.2 TOE probe transducer tip

sector on the screen to the left of the patient. The default position of the probe is 0° which means the beam is insonating the structure immediately in front of/anterior to the probe tip in a horizontal / axial plane. Very much like a light house projects its light. It is helpful to visualise the ultrasound beam in your mind prior to starting the study as this will help you manipulate your probe in the right way to optimise your images.

The sector can then be rotated forward (anticlockwise) to 180° and rotated back (clockwise) to 0° using the 2 buttons on the handle (Fig. 9.3). The TOE probe is advanced *into* or withdrawn *out* of the oesophagus. It can be turned to the left or right to from the spindle in the long axis of the probe to see the structures on either side of the midline. The large wheel of the spindle can be used to anteflex (bend forward) or retroflex (bend back) so as to fire the beam above or below the midline at the set degree of rotation. The smaller wheel can be used to flex the probe to the left or right in the short axis of the probe/laterally (Fig. 9.4).

This enables you to change the position of the beam so as to optimise your view and centralise the area of interest into the middle of your field. Lastly there is a lever above the rotary knobs that will lock the tip into position once the desired amount of flexion has been achieved (Fig. 9.3). Always remember to put the lever back to the midline (neutral/unlocked) position prior to manipulations within the oesophagus or during insertion or removal of the probe so as to avoid damage to the patients firstly and also the probe. TOE probes are notoriously expensive and very fragile. It is good to remember that the probe you have in your hand may have cost rather more than that car you have parked outside the hospital.

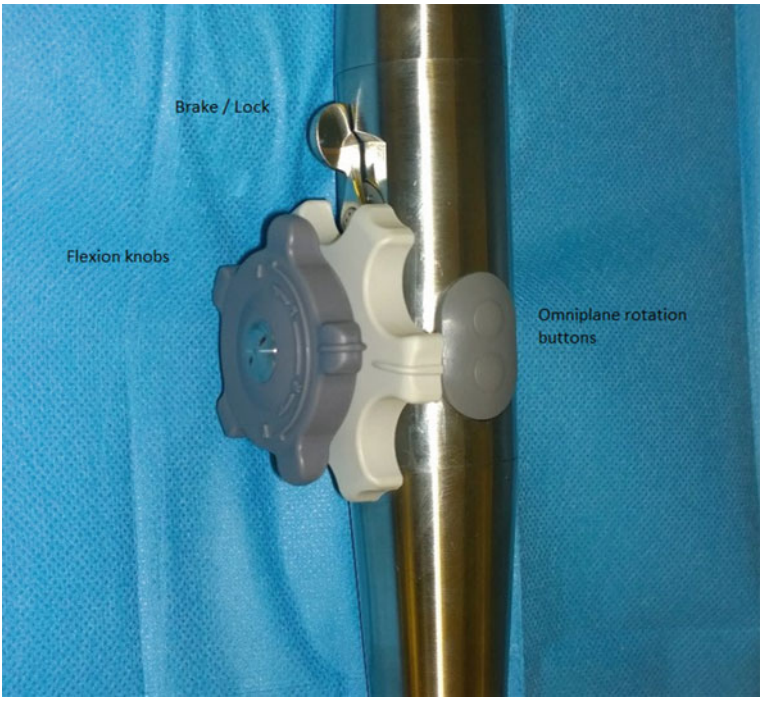

Fig. 9.3 TOE control levers and brake

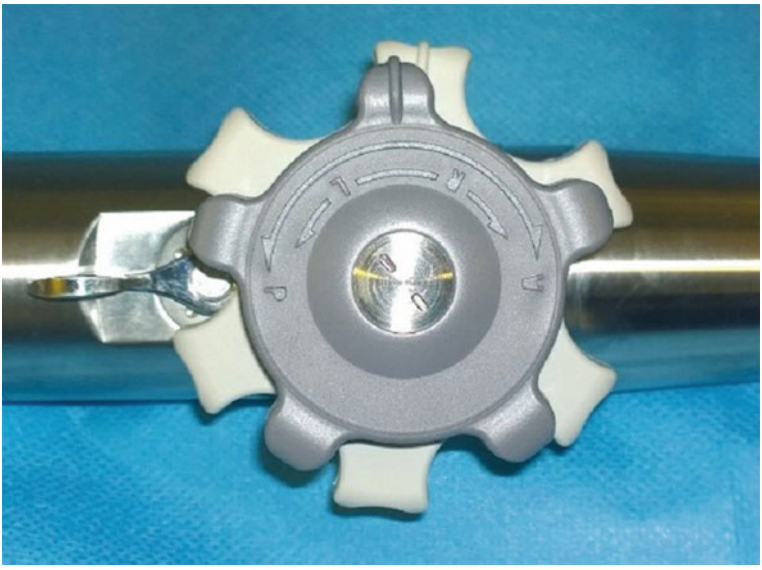

Fig. 9.4 Rotary knobs

9.3 Probe Insertion and Patient Preparation

The patients on the ICU are often already intubated and sedated but it is not uncommon to give additional doses of sedatives as well as a muscle relaxant to help with probe insertion. Having control of the ventilation is beneficial as respirophasic variations of flow may be studied more easily. The choice of agent is as per local protocols and should be done prior to commencing the procedure and enough time should be given for the drugs to have taken effect before attempting probe insertion to minimise trauma and any hemodynamic changes due to coughing/straining. [4].

The probe is visually inspected for any damage and then it is lubricated with an aqueous gel suitable for internal use and is prepared for insertion with or without a sheath. If a sheath is used, use the sterile gel provided ensuring that there is no air in front of the probe tip as this will result in poor picture quality, artefacts, acoustic dropout or lack of a picture all together. Ensure that a bite guard is used to prevent damage to the probe. Pass the probe into the oropharynx through to the hypopharynx along the midline with flexion to follow the curvature of the tongue and retro flexion to avoid the epiglottis. It is not unusual to feel some resistance at the level of the cricopharyngeus which should be overcome with gentle pressure. Never force the probe. Letting the cuff down of the endotracheal tube in an intubated patient maybe all that is needed. Use of a laryngoscope is advisable in the event of any resistance as is a jaw thrust using digital pressure on the tongue with forward mobilisation of the jaw. If you have the time, and resources are available, insertion of the probe can be done under direct visualisation using a video laryngoscope. This may help to reduce complications due to mechanical trauma during insertion. Nearly half of the complications of TOE are related to oropharyngeal trauma. Oesophageal perforation, although a devastating complication, is extremely rare. Developing a gentle approach and good patient selection will help minimise TOE related complication [5–7].

Once past the cricopharyngeus the probe is then advanced down the oesophagus in stages going through the upper ($\sim$15cm), middle ($\sim$20cm) and lower oesophagus ($\sim$30cm) before the probe advances into the stomach. A thorough examination will involve all the 28 recommended views but given time constraints and need for answers to specific clinical questions the examination can be modified to look at the views that are most likely to reveal the information required, and help to make patient management decisions [8, 9].

9.4 Image Acquisition

Once the probe has been positioned a thorough examination should be undertaken and all the views should be done expeditiously and in a systematic manner. The order of views could be based on the clinical question that needs to be answered, a focussed examination, or any other routine as long as all the required views have

been covered. It makes sense to start with views of the upper oesophagus and then proceed down the oesophagus till you reach the deep trans gastric view. Place the region of interest (ROI) in the middle of the field and as close to the transducer as possible. A useful starting point is the midoesophagus four chambered view (ME 4C) and it is also good to return to this view to re orient yourself should you have trouble visualising the anatomy or are 'lost'.

Ensure that the sector depth and width along with the gains are set so as to minimise the exposure of the patient to ultrasound energy and maximise the information gained. Heat generated by the probe head can be minimised this way ensuring that there is minimal thermal transfer to the oesophageal mucosa. All TOE machines have a thermal cut-out function to prevent this eventuality. As a general rule when the temperature of the probe is 5°higher than the body temperature ($\Delta T > 5$), a thermal index of 2.5, there is a risk of mucosal burn and study time should be limited to <1 min [9].

Set the gain so that the chambers appear dark like the screen outside the sector. Improving the quality of your images will ensure that the artefactual contributions are minimal. Ambient lighting should be minimised to try and achieve this otherwise the excessive gain might have you reaching for your sun glasses while reviewing your study in the lab.

2 Dimensional imaging (2D):

This is the bread and butter of the examination and as such serves as the foundation for your Doppler studies. Image optimisation is of paramount importance as the 2D image will act as a framework for M mode and Doppler interrogation. *You have to see it to D it*! This is where you put all your understanding of physics to good use. Higher frequency is better for axial resolution but lower will allow better penetrance. Use the lowest amount of gain and ensure that the area of interest is in the near field and within the focal length as the axial resolution will be best here. Blood/chambers should appear dark. Myocardium grey. Pericardium bright. Post processing controls can be used to further enhance your image (Fig. 9.5).

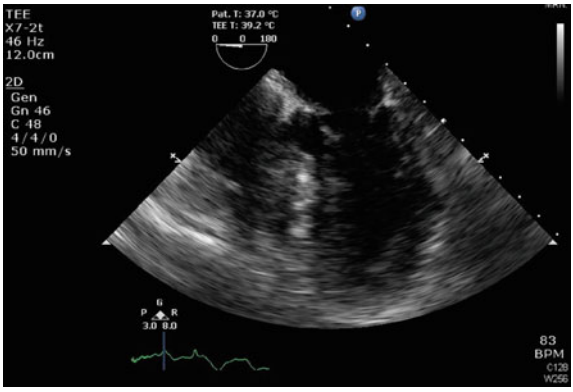

Fig. 9.5 TOE typical 2D image

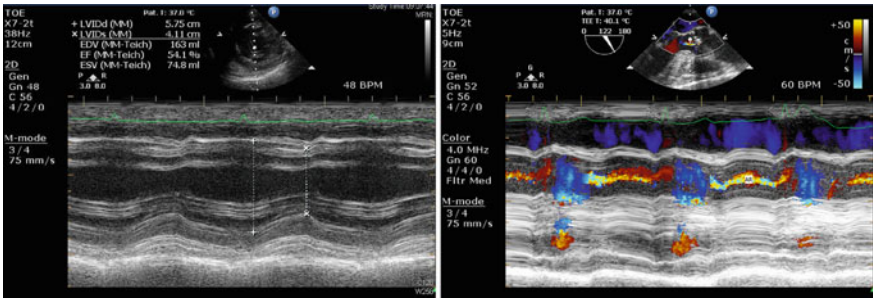

Fig. 9.6 **a** MMode through the left ventricle showing utilisation of the LV dimensions to calculate EF and analyse regional wall motion. **b** Colour MMode thought the LVOT showing holodiastolic flow of AR

Motion Mode Imaging (MM):

The motion mode is a mode of imaging that represents the variation with time of tissues along a single sample line. It is plotted in brightness mode, movement on the y axis is plotted against time along the x axis. As it has a higher sampling frequency and frame rate it results in very reliable measurements of and timing of the state of tissue. This is commonly used to study movement of valves and assess chamber size. Many machines can calculate ejection fractions in this mode but it should be remembered that it is representative of only the points along the sample line and not of the chamber as a whole. Application of colour flow Doppler to this can help identify the timing of events like regurgitation jets. Figure 9.6b shows a holodiastolic aortic regurgitation jet which is very central in origin.

Colour Flow Doppler (CFD):

CFD is used to visualise the flow of blood through the heart and a scale is set out on the top right hand corner of the screen to give a visual representation of the speed and character of the flow. This is achieved by superimposing the PWD onto the 2D imaging. Usually colour is coded as blue for blood moving away from the probe and red for blood moving towards the probe. Flow which does not have a solid colour with intermixing of colours and presence of colour from the entire spectrum usually means there is turbulent flow with eddy currents. When employing CFD always ensure that the Nyquist limit (the scale) is appropriate to the chamber being viewed. You may need to reduce it to see slow moving blood like the right side of the heart and venous drainage into right atrium. Equally, it is a bit embarrassing when a little tweak of the scale suddenly makes that regurgitant flow/turbulence you were excited about look rather tame. CFD sample boxes should be narrow and as close to the transducer as possible to minimise aliasing. In general blood moves fastest across aortic valve (AV) into the aorta (m/s) and slowest in the veins with the atrioventricular flow (cm/s) lying in between the two. CFD can be used to visualise flow, analyse the dynamics of flow and identify turbulence. It helps quantify regurgitant lesions and identify areas of turbulence which can then be analysed with spectral Doppler (Fig. 9.7a, b).

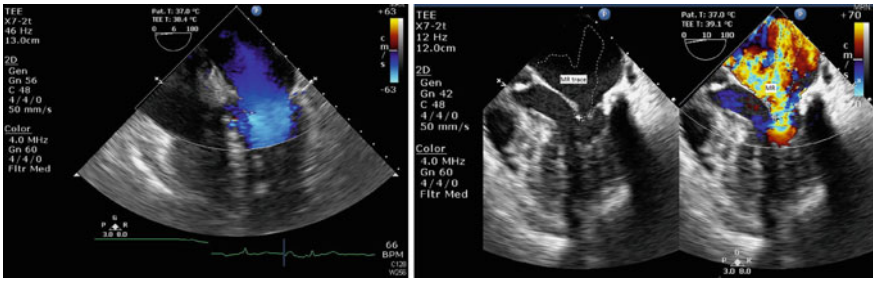

Fig. 9.7 **a** CFD showing laminar trans mitral flow in the ME 4C view. **b** CFD showing a large mitral regurgitation jet which has been traced to ascertain severity

Pulse Wave Doppler (PWD):

Here the same piezoelectric crystal will act as the transmitter and receiver listening for the echoes allowing for good depth discrimination. However, this limits the velocities that can reliably be detected and so any velocities >½ pulse repetition frequency (PRF) (Nyquist) will result in an aliasing artefact or wrap around (Fig. 9.8a).

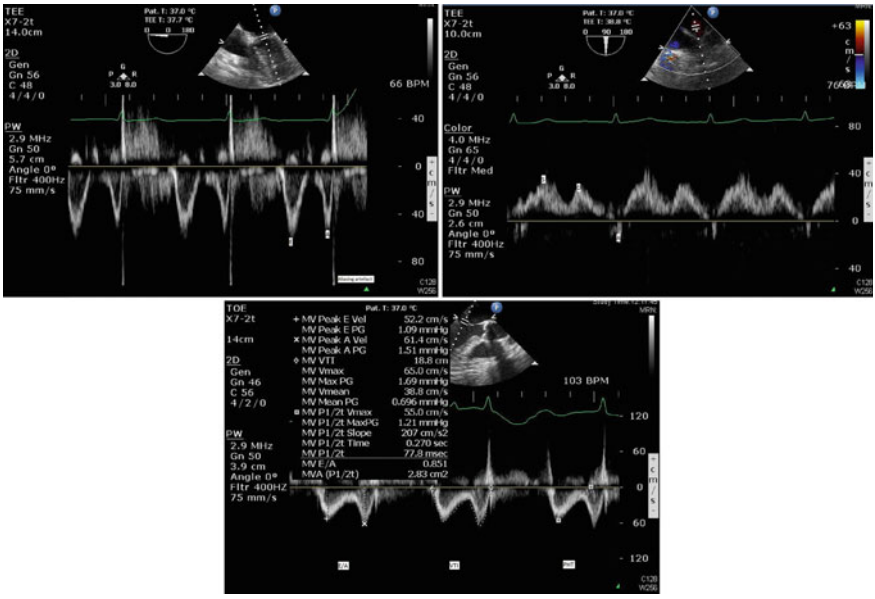

Fig. 9.8 **a** PWD trace of the transmitral flow showing diastolic flow (E) into the LV and the atrial contribution (A). The sample volume is placed at the level of the annulus and notice the aliasing artefact in the early systole. **b** PWD tracing of the left upper pulmonary vein showing systolic flow (S) and Diastolic flow (D) into the LA with and flow reversal (A) due to atrial contraction. **c** Application of PWD of the transmitral flow to estimate mitral annulus size (by PHT), pressure gradients across (by VTI) and ventricular diastolic function (by E/A)

CFD can be used to guide accurate placement of the sample volume of the PWD close to the region of interest. It is useful to remember that the Doppler will only reliably pick up the vector of flow that is parallel to it, so ensure that the sample beam is parallel to the flow to be able to get the classic envelope of a bright leading edge and a dark area under the curve.

Doppler Equation:

$$\frac{Fd = 2 \times Ft \times V \times \cos\theta}{C}$$

Fd = Doppler shift, Ft = Transducer frequency(MHz), V = Velocity (cm/s), cos θ = Angle between US (0° = 100% or maximal shift, 90° = 0% or no frequency shift) beam and the moving object (RBC) and C = Speed of sound in tissue (1540 m/s).

Most machines will have an angle correction to compensate for this but it is best to choose a view where the PWD alignment is perfect. Angle corrections of more than 20° will yield unreliable readings (Cos30° = 86% and Cos60° only 50% of maximal shift). PWD is used to interrogate slower moving blood like the atrio ventricular flow through the mitral and tricuspid valves or the venous drainage into the heart. It can be used to estimate the annular size of the valve by using the pressure half time (PHT) or the pressure gradient across a valve using the velocity time integral (VTI) which will give information about both the peak and mean pressure gradients accross the valves being interogated. Studying the characteristics of diastolic flow across the mitral valve by comparing the relative contributions of ventricular relaxation (E) and atrial systole (A), the E/A ratio (Normal = 2), one can make a judgement on the diastolic function of the LV Figure 9.8c.

Continuous Wave Doppler (CWD):

This technique uses 2 separate piezoelectric crystals, separate transmitting and listening, therefore it has no upper limit to velocity and is able to accurately assess faster flows without aliasing. Unlike PWD it has poor depth discrimination as it is sampling the entire Doppler beam. CWD is used to interrogate faster moving blood like that in the aorta or past a stenotic valve. Generally, CWD should be used where the flow is expected to be >1.5–2 m/s to ensure that there is no aliasing artefact. The choice of which Doppler to use is therefore dictated by patient factors and the clinical situation. Fast flowing blood in a hyperdynamic circulation or a tachycardic patient is better interrogated with CWD. It can also be used to calculate the aortic valve area in patients with aortic stenosis. The acceleration of flow past the AV can be seen when the sample line is placed with the LVOT, AV and aorta in line (Fig. 9.9a, b).

Tissue Doppler Imaging (TDI):

Here, unlike the faster moving blood in the two techniques above the Doppler beam is focussed on slower moving heart tissue. So the machine filters out all the high frequency and low amplitude signals in favour of the lower frequency echoes.

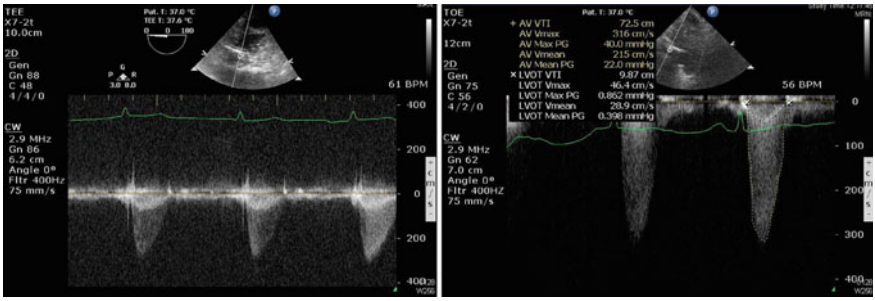

Fig. 9.9 **a** CWD trace through aortic valve. Note the double shadow signifying the acceleration past the AV. **b** CWD double shadow being analysed using VTI which will be used to calculate the valve area

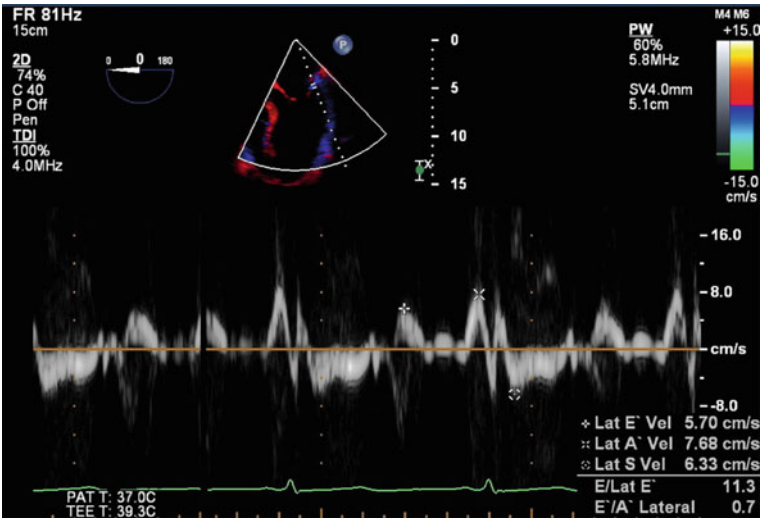

Fig. 9.10 TDI with sample volume at the lateral MV annulus

Classically the lateral mitral annulus is used to determine the contractility of the left ventricle. The advantage of this modality is that it is not affected as much by the preload or volume status of the patient. Applying a colour code to TDI can help visualise the movement better. Faster moving areas are coded bright [11] (Fig. 9.10).

3 Dimension Echocardiography (3DE):

This modality has become increasingly available and the matrix array probe yields a pyramidal shaped sector that after cropping can display a real time 3D image of the region of interest (ROI). It is excellent in localising the origin of regurgitant lesions and studying leaflet morphology in detail. Once the 3D picture has been produced it

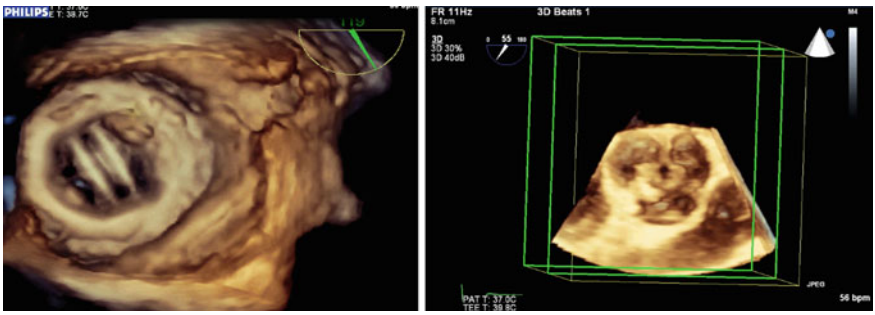

Fig. 9.11 **a** 3D reconstruction of a mechanical prosthesis in situ with both mechanical leaflets clearly visible. **b** 3D reconstruction of a tricuspid aortic valve rotated so that it appears as it would from the aortic side

can be rotated to study the ROI from several views. A full description is beyond the scope of this narrative (Fig. 9.11a, b).

Once completed and all the images have been saved and video loops recorded, withdraw the probe and check the sheath for any signs of damage. Remove the sheath and then wipe down the probe with the recommended wipes before sending it for disinfection as per the local protocol. It is also useful to maintain a log of which probe has been used for patients as it will help with infection control audit and is considered good practice. Store the probe hanging up in custom built cupboards with provision for protection of the tip from damage. Commercially available sterilizing units help reduce the turnaround time of probes and provide a printed report on the sterilisation cycle, agent used and the electrical integrity of the probe.

9.5 Indications for TOE in ICU

The main findings in which TOE examination is highly recommended for critically ill patients are aortic dissection, valvular lesions, infective endocarditis, prosthetic valve dysfunction, intracardiac masses and to investigate source of thromboembolism [27] 29. There are several situations that you may encounter in intensive care that make the use of TOE favourable [12]. Indeed, many of these situations might call for use of TOE as a monitor to therapy too [13]. However more research is needed to validate the use of TOE as a monitor of cardiac output in the ICU setting.

Clinical settings where TOE maybe a useful adjunct are:

Hypotension/Haemodynamic lability

Congestive Heart Failure

Respiratory failure/Un explained persistent hypoxemia

Suspected Thrombo Embolic event/Pulmonary Embolism/Cause of stroke

Sepsis where no clear cause can be identified/Strong suspicion of endocarditis

Pericardial Effusion/Tamponade

Trauma/Suspected cardiac contusion

Suspected aortic dissection

Guide placement of Intra-Aortic Balloon Pump (IABP)

Confirm/Guide placement of intra cardiac catheters/Pace maker wires

TTE not able to provide information/Prone patient/Circumferential burns

9.6 Contra-indications to Use of TOE

TOE is a semi invasive procedure and has a very low complication rate. The list below is to encourage you to decide and weigh the risk and benefit of undertaking a TOE.

Absolute contraindications

Oesophageal disease

Strictures/Bleeding varices/Tumour/Diverticulum/Laceration/Perforation

Other

Perforated bowel/Active upper GI Bleed.

Relative contraindications

Oesophageal

Barret's disease/Varices/Dysphagia/Oesophagitis

Gut related

Upper GI surgery/Symptomatic Hiatus hernia

Cancer

Oral/Buccal/Laryngeal/Mediastinal/Radiation to neck or mediastinum

Musculoskeletal

Restricted neck mobility/Severe cervical arthritis/Unstable C spine

Haematological

Thrombocytopenia/Marked coagulopathy

The above list is merely to remind the echocardiographer of the importance of taking a thorough history and develop a meticulous technique to prevent development of complications by considering each individual patient in the context of his/her clinical situation. Dire situations like imminent cardiac arrest might weight the decision in favour of use while availability of alternate modalities might dictate

exercising caution. TOE should not be used without due consideration and in an evidence based manner. Alternative techniques and methods using different types of probes for instance, can be employed when true contraindications to TOE exist [30].

9.7 TOE Examination on the ICU

There is no consensus on which order to view the heart during an examination. The order in which the examination is conducted is not important so long as all the relevant views for the question being asked have been covered. It should be borne in mind that all 28 views recommended might not be required or indeed practical. It is perfectly acceptable to adapt the routine to fit in with locally devised and agreed protocols. Therefore, a focussed TOE examination may yield the best results in a timely manner. A more thorough examination can be done after the questions sought have been addressed and the indicated management plans have been put in place.

A useful starting point is in the middle oesophagus as it is not uncommon for the upper oesophageal views to be difficult to obtain and a beating heart is slightly easier to locate. The markings on the probe should help locate the midoesophagus, usually being between 20 and 30 cm from the incisors. It is useful to remember that only slight movements of the probe and rotation are needed when trying to develop the picture. If you lose the image and get 'lost' it is best to return back to the previous best view and start again.

Midoesophageal 4 chamber view (ME 4C):

Rotation 0°. The probe can be gently manipulated to get the optimal position with the MV in the centre of the sector. The probe is immediately behind the left atrium (LA) which appears as the chamber at the apex of the sector. Try and ensure that the mitral valve (MV) and left ventricle (LV) apex are in the centre of the screen. This will ensure that the Doppler alignment will be parallel, or require least angle correction, when it is used to interrogate atrioventricular flow. 2D zoom can be used to evaluate any pathology of the valve leaflets seen. Study the leaflet mobility and the nature of the coaptation point between the valve leaflets. CFD box is positioned to cover both valves with a Nyquist limit $\sim$60 cm/s to show laminar ante grade (diastolic) flow as a solid blue colour. Any retrograde/regurgitant flow will appear red or more commonly as a mosaic as it is generally turbulent. As the blood flows forward in systole into the aorta (Ao) through the left ventricular outflow tract (LVOT) it is generally laminar and appears a solid red. Any septal pathology like a post infarct muscular VSD can be visible here too. Regurgitant jets can be further analysed using PWD and CWD and more information about the ventricular performance so gained (Fig. 9.12, Table 9.1).

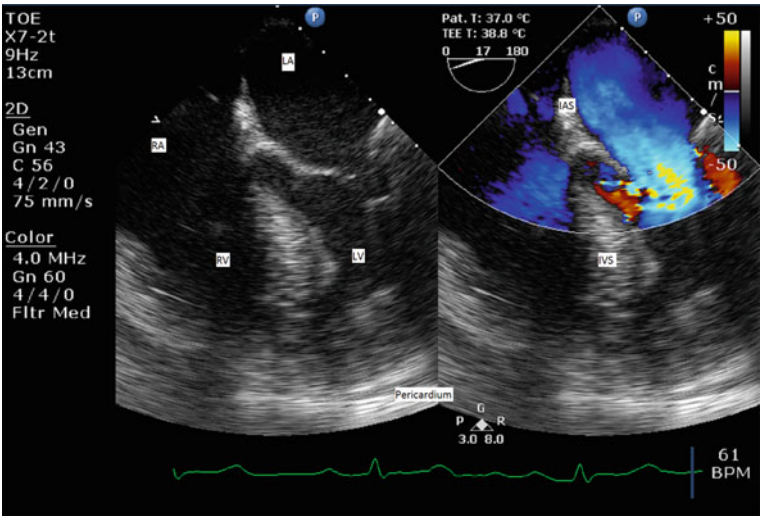

Fig. 9.12 ME 4C View with CFD showing laminar transmitral flow into the LV appearing as a solid blue colour. LA = Left Atrium, RA = Right Atrium, LV = Left Ventricle, RV = Right Ventricle, IVS = Inter Ventricular Septum, IAS = Inter Atrial Septum

Table 9.1 ME 4C

Structures	Pathology	Application
Left Atrium (LA) Left Ventricle (LV)—Inferoseptal/ Anterolateral/Lateral walls Anterior Papillary Mitral Valve (MV)— Anterior + Posterior leaflet (A2/P2) Tricuspid Valve (TV)— Anterior/Posterior + Septal leaflet Right atrium (RA) Right ventricle (RV)— Freewall Septum— Interatrial septum (IAS) Interventricular septum (IVS)	Chamber size— Dilatation/collapsing Valvular pathology— Stenosis/Regurgitation Ventricular function— RWMA 3,9,14 (Inferoseptal), 6,12 (Anterolateral), 16 (Lateral), 17 (Apical) Pericardial collection Septal defects Tumours—Atrial myxoma Vegetations—MV/TV	PWD— MV—E/A, PHT, VTI TV—E/A CFD— MR/TR/MS CWD— MR V max/ RVSP TDI—MAPSE/ TAPSE Caliper— MVA/TVA Trace— Simpsons (EDV/ESV/EF) MR/TR

Midoesophageal Mitral Commissural view (ME MC):

Rotation $\sim 60°$. From the ME4C view the plane is rotated forwards keeping the MV and LV in the centre of your field till both papillary muscles are visible. The posterior mitral valve leaflet (PMVL), P1 to the right and P3 to the left, are seen

enclosing the central portion, A2, of the anterior mitral valve leaflet (AMVL) The lateral LV wall is to the right of the image and the inferior LV wall is on the left.

Midoesophageal two chamber view (ME 2C):

Rotation ~90°. Leaving the probe where it is in the oesophagus, continue to rotate forward till the left atrial appendage (LAA) comes into view on the right of your field. The LA is in the near field and the LV in the far field. Anterior LV wall is now on the right and the Inferior LV wall is on the left. The coronary sinus (CS) is visible in the atrio ventricular groove on the left and the LAA is seen overhanging the LV. The A2 and P2 scallops have now reversed position on the screen from where they were in the ME4C view. The A2 is now on your right and P2 to the left. The posterior papillary muscle is visible in the LV. This view is good for studying flow into LAA and to rule out LA thrombus. In addition, this view can be used to confirm the EF calculations that might have been done in the ME 4C view using the Simpsons' disc method (Fig. 9.13, Table 9.2).

Midoesophageal Bicaval view (ME BC):

Rotation ~100°. From the ME2C turn the probe from the handle to look right until you can see the superior vena cava (SVC) on the right side (cephalad) of the image and inferior vena cava (IVC) to the left (caudad). The LA in the near field above is separated by the IAS from the RA in the far field below. If in doubt, follow the flow on CFD into the chamber. SVC flow appears blue as it moving away from your probe while the IVC flow appears red as it is moving towards the probe. Remember to reduce the Nyquist to ~40 cm/s as the flow here is slower. Any flow across the

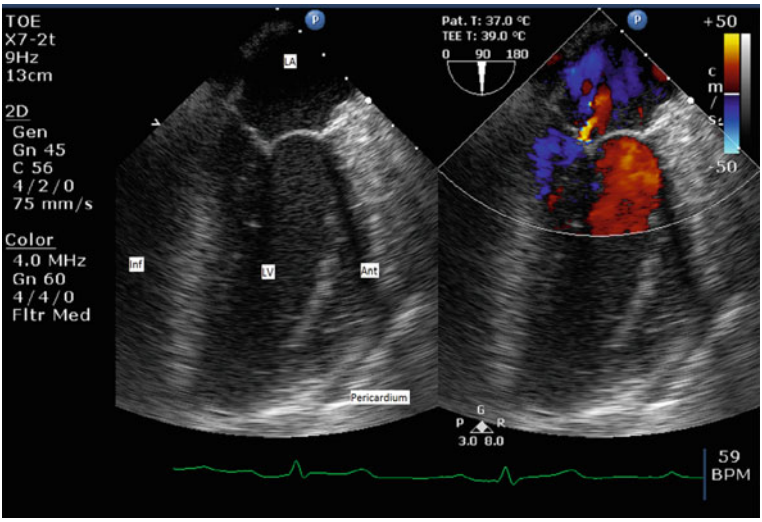

Fig. 9.13 ME 2C view showing the MV closed shut in systole with a tiny bright yellow closure jet of mitral regurgitation. The solid red colour signifies flow of blood in the left ventricular outflow tract. LA = Left Atrium, LV = Left ventricle, Inf = Inferior Wall, Ant = Anterior wall

Table 9.2 ME 2C

Structures	Pathology	Application
LA LAA MV—A2/P2 LV—Anterior wall/Inferior wall LV apex CS	LV systolic function— RWMA 1,7,13 (Anterior) 4,10,15 (Inferior) 17 (Apical) MV pathology LAA thrombus	PWD— MV (VTI/EA/PHT) LAA contractility CFD— MR/MS LAA flow Trace—Simpsons (EDV/ESV/EF)

IAS is abnormal and may suggest the presence of a patent foramen ovale (PFO)/ASD. If you continue to rotate forward to ~110° you should be able to bring the right lower pulmonary vein into view. As the 2D is often very subtle it is helpful to use the CFD box. Pulmonary venous drainage will appear red and laminar as it is flowing into the LA towards your probe. It is well positioned to be interrogated with PWD. MMode of the SVC can help asses filling by looking for respirophasic variations of venous drainage into the RA and fluid responsiveness. Small calibre and collapsibility of the SVC and IVC suggest hypovolemia (Fig. 9.14, Table 9.3).

Midoesophageal Long Axis view (ME LAX):

Rotation ~120°. Return from the ME BC view to the ME 2C view and then rotate forward until the LVOT and aortic valve (AoV) begin to come into view. In

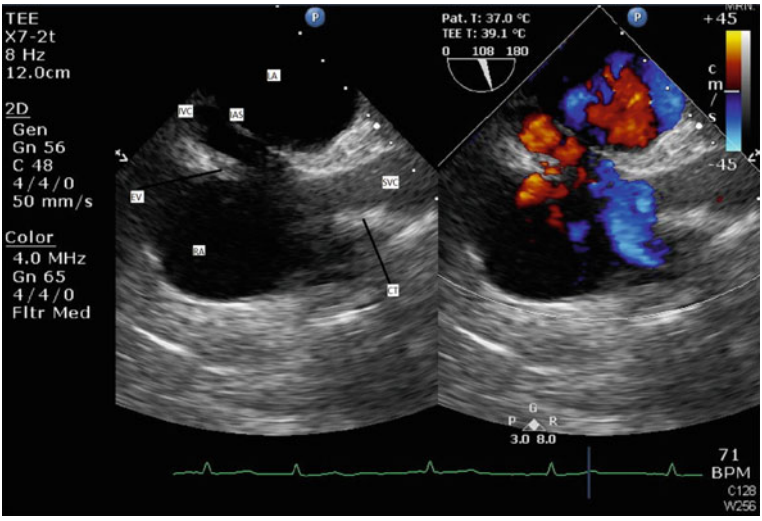

Fig. 9.14 ME Bicaval view showing laminar venous blood flow into both atria. SVC = Superior Vena Cava, IVC = Inferior Vena Cava, LA = Left Atrium, RA = Right Atrium, IAS = Inter Atrial septum, CT = Christa Terminalis and EV = Eustachian Valve

Table 9.3 ME Bicaval

Structures	Pathology	Application
LA IAS RA Free wall/Right atrial appendage (RAA) Christa Terminalis (SVC) Eustachian valve (IVC) SVC IVC	Atrial masses Caval flow ASD Indwelling catheters— Central venous line tip/PAC/ Pacing wires	PWD— TV (E/A, TR Vmax, RVSP) IVC and PV flow CFD— TR IAS (ASD/PFO) Mmode—SVC/IVC (collapsibility)

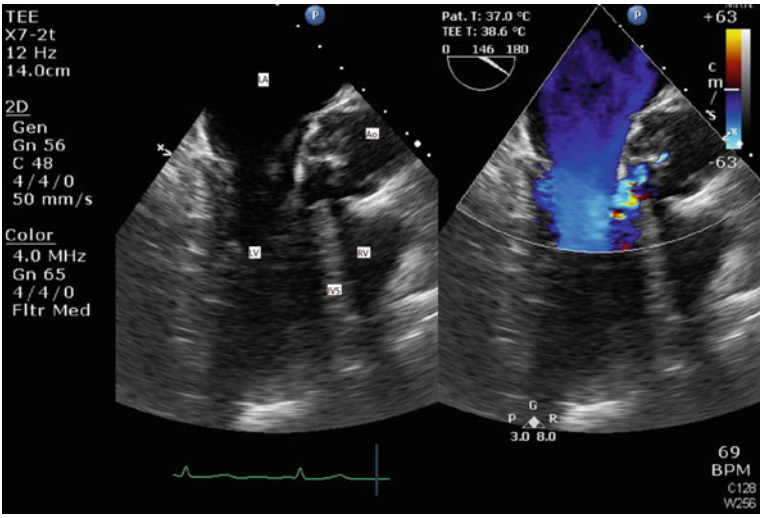

Fig. 9.15 ME LAX view showing laminar diastolic flow into the LV and a hint of Aortic Regurgitaton flow in the Left Ventricular Outflow Tract. LA = Left Atrium, LV = Left ventricle, RV = Right ventricle, IVS = Inter Ventricular Septum, Ao = Aorta

addition, the RV will start to appear, adjacent to the anterosptal LV wall on the right of screen. The posterior LV wall is to the left. The A2 and P2 portions of the MV are visible. The CFD box is positioned over the MV, LVOT and AoV with Nyquist ~60 cms. Any acceleration of flow in the region of the LVOT can be a sign of hypovolemia (Fig. 9.15, Table 9.4).

Midoesophageal Aortic Valve Long Axis (ME AV LAX):

Rotation ~130°. With a little forward rotation and gentle turning of the probe to look left you will be able to line up the LVOT, AoV and proximal ascending aorta. Reduce the depth to try and centralise the AoV. CFD box is applied to the AoV and MV with Nyquist ~60 cm/s. The distal cusp of the AoV is the right coronary

Table 9.4 ME LAX

Structures	Pathology	Application
LA MV—A2/P2 LV—Posterior wall/Anteroseptal wall IVS LVOT AV Aortic root/Proximal ascending segment	Valvular pathology—Mitral/Aortic Ventricular function—RWMA 2,8,14 (Anterospetal) 5,11,16 (Posterior) 17 (Apical) Septal defects—VSD Aortic root pathology Systolic anterior migration (SAM)	PWD— MV (E/A, VTI, PHT) CFD— MV (VC/PISA) AV (VC/Jet hieght) Mmode—AV Trace—MR Calliper—MVA

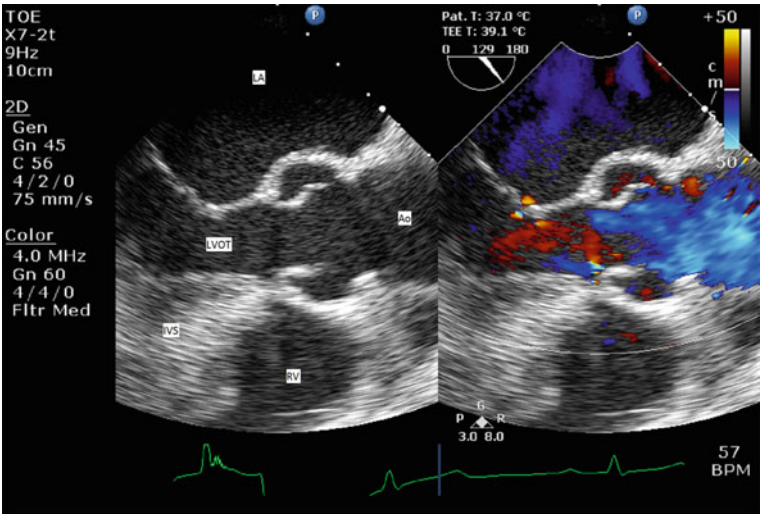

Fig. 9.16 ME AV LAX view showing the AV open in systole with blood flow through the left ventricular outflow tract coloured red and laminar blood flow in the aorta appearing blue. LA = Left Atrium, IVS = Inter Ventricular Septum, RV = Right Ventricle, LVOT = Left Ventricular Outflow Tract, Ao = Aorta

cusp. The transverse sinus lays between the LA and ascending aorta (Fig. 9.16, Table 9.5).

Midoesophageal Aortic Valve Short Axis view (ME AV SAX):

Rotation ~40°. From the ME AV LAX view rotate the omniplane angle back by ~90°. The AV that was appearing in its long axis should now appear in its short axis with its 3 leaflets visible. Develop this image with gentle probe withdrawal and forward flexion till the sinuses are equal and symmetrical when the cusps are closed, the 'Mercedes Benz' sign. The AV should be in the centre of screen and the depth adjusted to achieve this. If you desire to see the coronary ostia, then you may

Table 9.5 ME AV LAX

Structure	Pathology	Application
LA Transverse sinus MV—A2/P2 AV Aortic root Ascending aorta	Valvular pathology— MV/SAM AV Aortic root— Aneurysm/Dissection/Abscess LVOT pathology— Subaortic membrane Septal pathology— VSD/Asymmetric septal hypertrophy/ Fistulae	PWD CFD—MS (PISA/VC) Mmode Trace—MR Caliper— Ao Annulus/Sinus/STJ/ Ascending AV—AR (VC/JH)

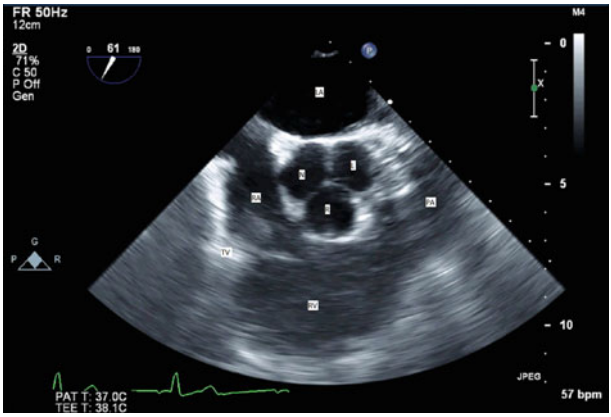

Fig. 9.17 ME A SAX in diastole with a closed tricuspid AV surrounded by the right heart. LA = Left Atrium, RA = Right Atrium, RV = Right Ventricle, L = AV Left Coronary Cusp, R = AV Right Coronary Cusp, N = AV Non Coronary Cusp, PA = Pulmonary Artery, TV = Tricuspid Valve

need to withdraw the probe ever so slightly. CFD interrogation should show laminar red flow through the AV. Nyquist ~60 cm/s (Fig. 9.17, Table 9.6).

Midoesophageal Right Ventricular Outflow view (ME RVOT):

Rotation ~60°. From the ME AV SAX view rotating the omniplane forward will bring the TV, on the left, and pulmonary valve (PV), on the right, into view with the RVOT in the far field just below the AV. It has the advantage of being able to visualise the flow throughout the RV from its inflow at the TV appearing blue and turning red as it flows past the RVOT into the pulmonary artery (PA) past the PV. CFD with Nyquist ~60 cm/s. The AV will appear in the centre and with some loss of leaflet symmetry (Fig. 9.18, Table 9.7).

Table 9.6 ME AV SAX

Structure	Pathology	Application
AV— 3 cusps Non/Right/Left (coronaries) Commissures Coronary arteries— Right and Left main stem IAS LA RA	LA size (Anteroposterior) AV pathology— Stenosis/Regurgitation/Bicuspid ASD/PFO VSD—Membranous/Muscular/ Fistulae	CFD— AS/AR position Calliper— Dimension Trace— AVA (Planimetry)

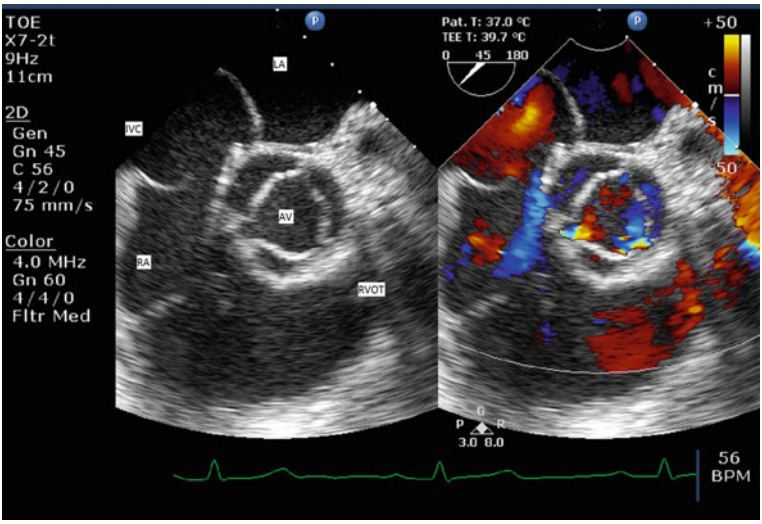

Fig. 9.18 ME RVOT view showing the right atrium, right ventricle and the pulmonary artery wrapping around the AV located centrally. LA = Left Atrium, RA = Right Atrium, IVC = Inferior Vena Cava, RVOT = Right ventricular Outflow Tract

Upper oesophageal Ascending Aortic Short Axis view (ME AsAo SAX):

Rotation 0°. This view can be developed form the ME AV SAX view by withdrawing the probe slightly into the upper oesophagus and turning the rotation back to 0°. It is ideal for viewing the bifurcation of the PA into the Rt and Lt branches. The right branch can be seen arching over the AsAo in the near field and the superior vena cava (SVC) is visible as a collapsible structure in between the two on the left of screen. This view can be utilised to confirm position of pulmonary artery catheter (PAC) or to rule out PE. Rotating the plane forward ~90° can help visualise the Rt PA in its short axis and open up the ascending aorta along its long axis (Fig. 9.19).

Table 9.7 ME RVOT

Structure	Pathology	Application
LA IAS RA TV— Posterior + Anterior or septal leaflet PV— Anterior + Left cusp RVOT	PV/PA pathology TV— Stenosis/Regurgitation Septal defects— Atrial/Ventricular (Membranous/ Muscular) Catheters— PAC/Pacing wires	PWD— TR (E/A, VTI)/ RVSP CFD—TR/AR/PR Calliper—TVA/ PA Trace—TR

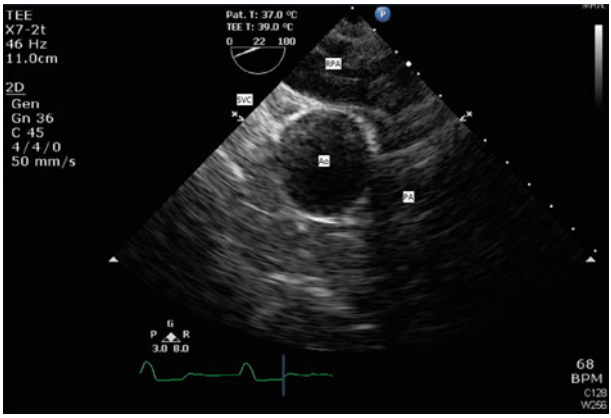

Fig. 9.19 UE As Ao SAX view showing the right pulmonary artery arching over the ascending aorta with the pulmonary artery and superior vena cava also visible. Ao = Ascending aorta, PA = Pulmonary artery, RPA = Right pulmonary branch and SVC = Superior Vena Cava

Trans gastric Mid Short Axis view (TG Mid SAX):
Rotation 0°. Return the omniplane angle to 0°, ensure the brake is disengaged and the probe is in neutral position before advancing the probe gentle into the stomach. You should be able to visualise the coronary sinus (CS) coming into view on the right side of the image as you go past the lower oesophagus. CFD with Nyquist ~40 cm/s should help you locate blue laminar flow into the RA from the right of screen. The CS is the most basal structure of the heart and visualised just prior to the probe entering the stomach. Once in the stomach the TG Mid SAX view will come into view with a bit of forward flexing of the probe tip. If the stomach lining is visible it usually means that stomach aspiration and preparation has been suboptimal, requiring you to use more ante flexion than is normally required. Manipulate the probe so that the LV is in the centre of the screen and a bit of rotation might be required to obtain a symmetrical circular LV with both papillary muscles visible. This is an excellent view to assess LV contractility and gentle ante

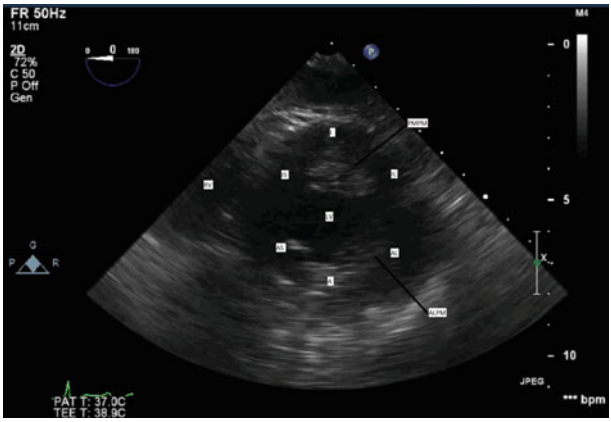

Fig. 9.20 TG Mid SAX view showing the circular profile of the LV cut in transverse section with the papillary muscles and all 6 mid LV segments [7–12]. RV = Right Ventricle, LV = Left Ventricle, A = Anterior LV Segment, AS = Antero Septal, IS = Infero Septal, I = Inferior, IL = Inferolateral, AL = Antero Lateral, PMPM = Postero Medial Papillary Muscle, ALPM = Antero Lateral Papillary Muscle

flexion and retro flexion will ensure that you can visualise the basal and the apical LV segments respectively. In this way the all 16 LV segments can be visualised and analysed for regional wall motion anomalies (RWMA). The posteromedial papillary muscle (PMPM) appears near the apex of the sector posteriorly and the anterolateral papillary muscle (ALPM) anteriorly and to the right of screen. The RV may appear on the left of the image separated from the LV by the septal wall. CFD although not needed may be used if a VSD is suspected with Nyquist set ~60 cm/s. Basal views in the TG position will show the MV in its entirety with both the AMVL and the PMVL visible and also the anterior (AC) and posterior commissures (PC). Application of CFD box with Nyquist ~60 cm/s will help reveal origins of any mitral regurgitation (MR) jet/s if present. The apical view will help diagnose any apical pathology like an aneurysm and rarely any thrombus (Fig. 9.20, Table 9.8).

Trans Gastric Two chamber view (TG 2C):

Rotation ~90°. With a clear and symmetrical 2D view of the TG Mid SAX rotate forward by ~90°. This should open out the LV in its long axis and is very much like developing the AV in the ME views. The anterior LV wall will be in the far field and the inferior wall is visible adjacent the apex of the sector. The PMPM is visible in the near field and a little rotation of the omniplane angle will develop the ALPM in the far field. The mitral valve is just visible to the right of screen and often the papillary heads and chordae are clearly visible. This is an excellent view to diagnose any involvement of the subvalvular/papillary apparatus as a cause for any MV pathology like MR (Fig. 9.21, Table 9.9).

Table 9.8 Transgastric SAX views (TG Basal SAX + TG Mid SAX + TG Apical SAX)

Structure	Pathology	Application
Mid LV—6 Mid segments clockwise Inferior—Inferolateral—Anterolateral—Anterior—Anteroseptal——Inferoseptal Papillary Muscle—PMPM/ALPM IVS RV	Mid RWMA [7–11] LV—Hypertrophy VSD Papillary pathology Dimensions and IVS—Haemodynamics	MMode—EF/FS/LVH Trace—FAC/FS/EF EDV/ESV CFD—MR origin AR
Basal LV—6 Basal segments as above IVS MV— AMVL/PMVL Anterior + Posterior commissure (AC/PC)	Basal RWMA [1–6] MV—Pathology/Origin of MR VSD	
Apical LV—4 Apical Segments clockwise Inferior—Lateral—Anterior—Septal	Apical RWMA [17] Aneurysm	

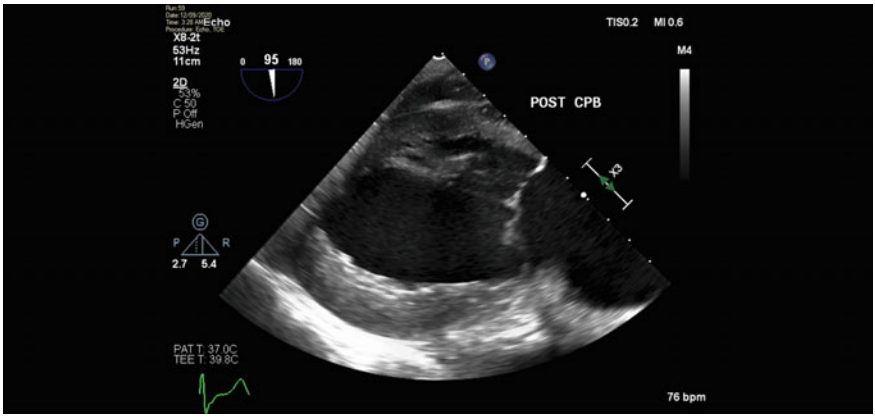

Fig. 9.21 TG 2C view

Trans Gastric Long Axis (TG LAX):

Rotation ~120°. From the TG 2C view above rotate the plane forward till the LVOT appears in the far field below and to the right of screen. The basal segment of the posterior wall is in the near field closest to the probe and the RV visible adjacent the LVOT and separated from the LV by the anteroseptal wall. The MV and AV may also be visible. The advantage of this view is that it allows for Doppler alignment for interrogation of LVOT and AV flow with CWD. Blood flowing into the LVOT appears a laminar red and the trans mitral diastolic flow is blue (Fig. 9.22).

Table 9.9 TG LAX views

Structure	Pathology	Application
TG 2C	TG 2C	CFD—
LV—	LV—	AR
Anterior + Inferior walls (Basal and	RWMA/Systolic function	Mmode
Mid segments)	MV pathology	CWD—
PMPM	Sub valvular apparatus	AV (AS/AR)
MV—	TG LAX	CFD—
AMVL /PMVL/Chordae	LV—Systolic function/RWMA	AS/AR/SAM
TG LAX	Valvular pathology—	CWD—
LV—	AV/MV/Prosthetic valve	AS/AR
Posterior (Basal) + Anteroseptal wall	VSD	CFD—
LVOT	TG Deep LAX	AR/Wash jets
IVS	Valvular pathology—	/AS
RV	AV/MV/Prosthesis	Paravalvular
TG Deep LAX	VSD	CFD—
LV—Apex	ASH	IVC/HV flow
IVS	TG IVC	TR
LVOT	IVC pathology	PWD—
AV	Haemodynamic variations with	IVC flow
Proximal Ascending Aorta (PAA)	respiration	Mmode—
TG IVC	TR	IVC
IVC		
Hepatic vein		

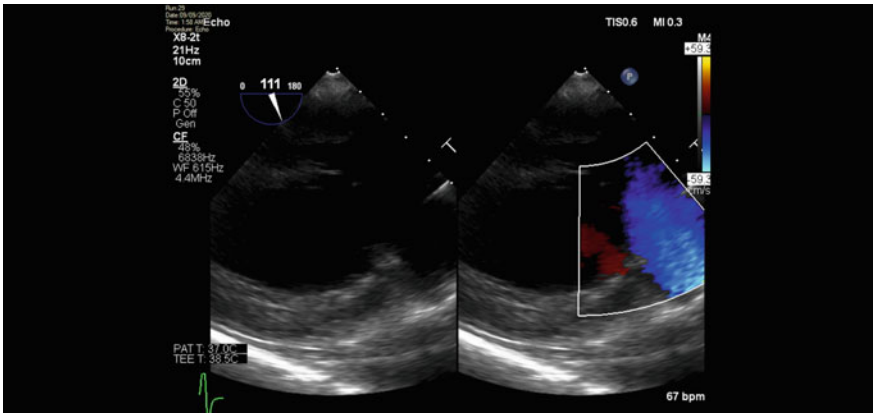

Fig. 9.22 TG LAX view

Deep Trans Gastric Long Axis View (Deep TG LAX):

Rotation 0°. The probe is advanced into the stomach further past the apex of LV and then ante flexed to look back upon itself and the heart. Try and get the LVOT and AV in the centre of the screen. This may well require leftward flexion in addition to marked ante flexion. The IVS is seen separating the LV, on the right,

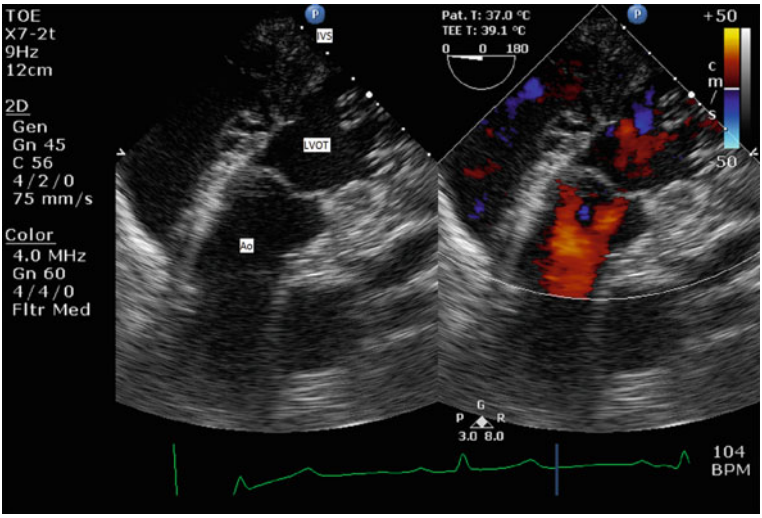

Fig. 9.23 TG Deep LAX view showing the AV closed in diastole and the left ventricular outflow tract in line with the ascending aorta. IVS = Inter Ventricular Septum, LVOT = Left Ventricular Outflow Tract, Ao = Aorta

from the RV on the left. The MV is visible to the right of the AV and the papillary muscles with their chordal attachments maybe seen in the near field. This is the best view to interrogate the blood flowing through the LVOT into the proximal ascending aorta past the AV as the Doppler alignment is closest to ideal. The trans mitral flow into the LV appears red and the LVOT and AV flow appears blue. Any turbulence can be seen as a mosaic pattern. CFD box is positioned with the AV in the centre and Nyquist $\sim$60 cm/s. CWD is often used and a velocity time integral (VTI) will yield the maximum and mean pressure gradient across the AV (Fig. 9.23).

Trans gastric Inferior Vena Cava view (TG IVC):

Rotation $\sim$40°. This view can be obtained by returning the probe to the TG Mid SAX view and then turning it to the right to see the liver. Remember to always disengage the brake/locking mechanism if this has been used and allow the probe to return to its neutral position prior to withdrawal of the probe. Once the liver is visible adjust the plane and probe in such a way so as to be able to visualise the course of the IVC as you withdraw the probe to locate the junction of the IVC with the RA. The hepatic vein can be seen draining into the IVC from the left of screen. IVC flow and collapsibility can be studied here to help guide fluid resuscitation and access the filling status of your patient (Fig. 9.24).

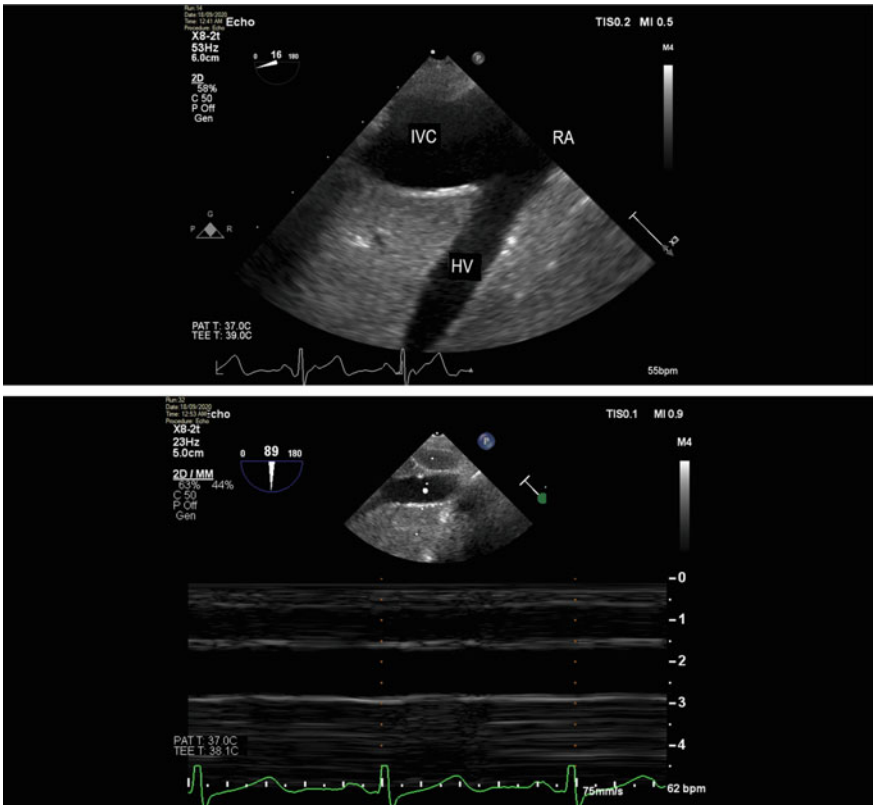

Fig. 9.24 **a TG IVC view** and **b** M Mode interogation of IVC for collapsibility. IVC = Inferior Vena Cava, HV = Hepatic Vein, RA= Right Atrium

Midoesophageal Descending Aorta Short and Long Axis views (ME Des Ao SAX/LAX):

Rotation 0° for SAX, ~90° for LAX. Withdraw the probe in the oesophagus till you get to the ME 4C view and then turn the probe to your left till the descending aorta comes into view at the apex of the sector. You will need to reduce the sector depth to help with spectral resolution and CFD will help localise it if it is indistinct. Any atheromatous disease will be visible and can be classified as it has embolic implications. Presence of mobile atheromas are highly likely to embolise and are classified as severe atheromatous disease irrespective of the size of the plaque. This is also a good view to assess the flow reversal with PWD which signifies physiologically significant AR. In the LAX view the distal part of the Des Ao is on the left of screen and the proximal is on the right. CFD with Nyquist ~60 cm/s will yield laminar flow with proximal aortic flow a solid red and distal flow appearing blue with a black line separating the two where the flow is perpendicular to the probe. This view will help confirm the position of IABP and withdrawing the probe

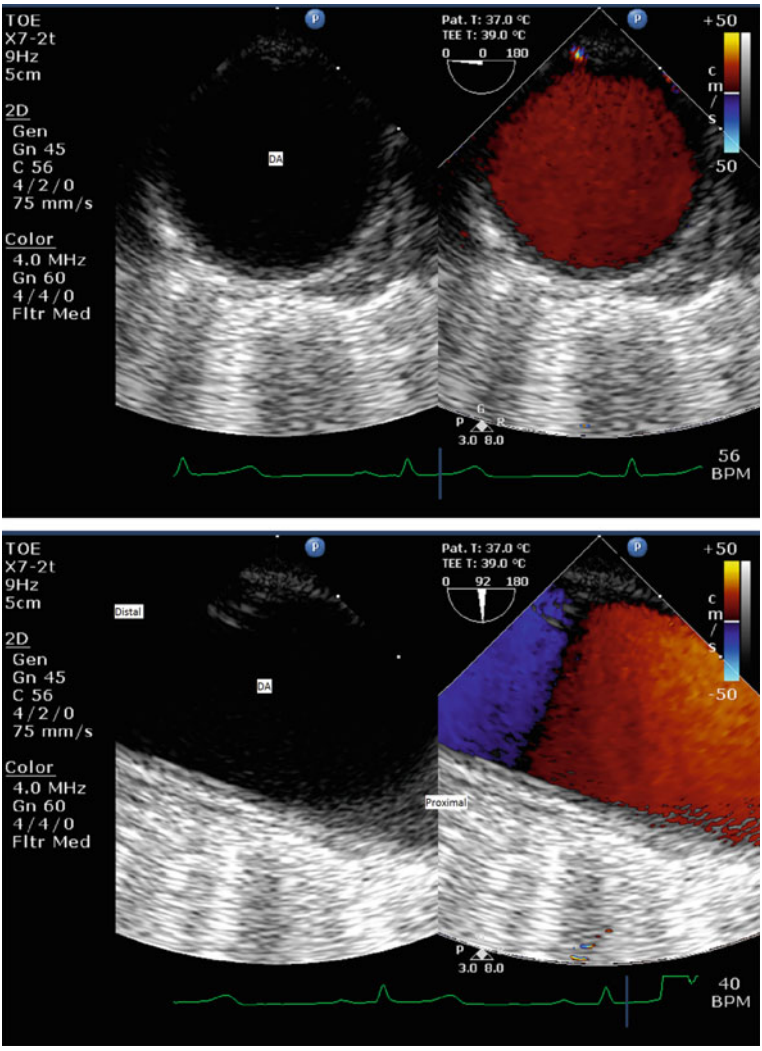

Fig. 9.25 **a** ME Descending Aorta in SAX view with CFI (Colour Flow imaging). **b** ME Descending Aorta in LAX view with CFI. DA=Descending Aorta

further into the proximal descending aorta will help position the balloon optimally. Often any dissection flap can be seen clearly and the true and false lumen can be interrogated for flow. Colour Mmode, timing the pulsatility and CFD will help identify the true lumen (Fig. 9.25a, b).

Upper oesophageal Aortic Arch Short and Long Axis views (UE AA SAX/LAX):

Rotation 0° (LAX) and ~90° (SAX). With the DesAo in short axis withdraw the probe slowly till the aorta begins to open out becoming elliptical. You have reached

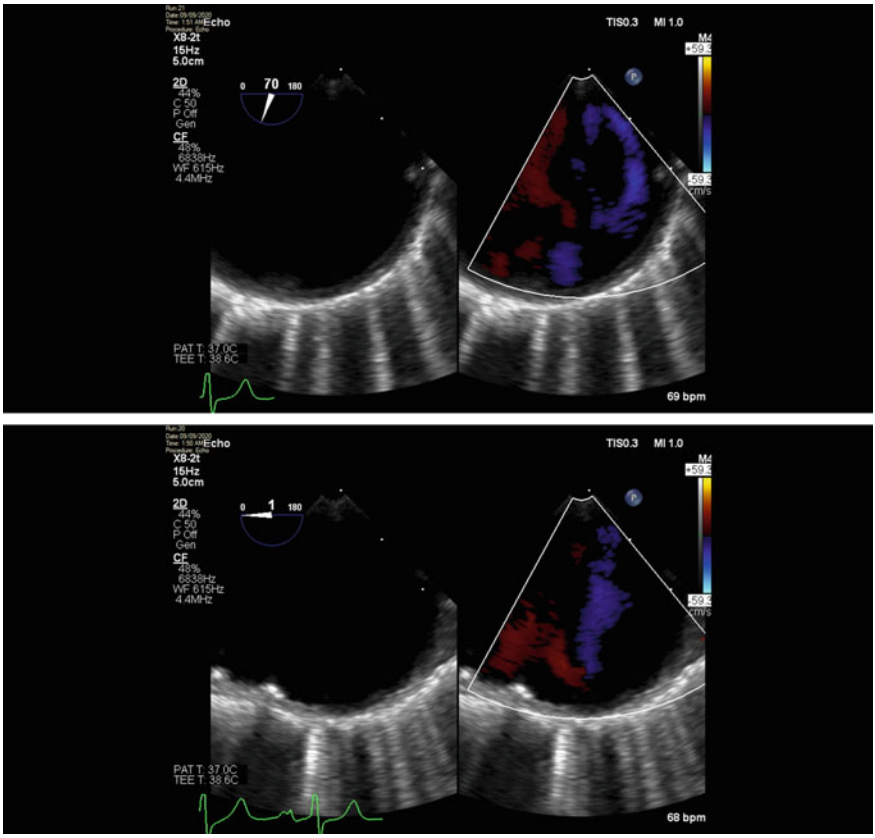

Fig. 9.26 **a** UE Aortic Arch SAX. **b** UE Aortic Arch LAX

the level of the AA and this can be confirmed by getting the circular profile in the SAX by rotating the probe to ~90°. Proximal portion of the arch will be to the left of screen and the distal arch will be in the centre near the apex or to the right of screen. If the IABP is visible in this view it is prudent to have it withdrawn as it might compromise cerebral blood flow by obstructing flow to left common carotid and left subclavian arteries. The origin of the left subclavian artery is visible in the SAX view and the innominate vein can be found just anterior to it in the apex of the sector or to the right. The pulmonary artery is to the left and in the far field. Increasing the sector depth will help develop the PV and visualise flow in the PA. This is a good view to confirm the position of the pulmonary artery catheter (PAC). When using CFD remember to use an appropriate Nyquist for the structure being interrogated. Nyquist ~60 cm/s for arterial and ~30 cm/s for venous flow (Fig. 9.26).

9.8 Clinical Applications

The ACC/AHA/ASE 2003 guidelines for the clinical application of echocardiography [13] recommend the utilization of echocardiography in all hemodynamically unstable patients, in patients with multiple trauma/chest trauma with suspected aortic dissection or aortic injury, suspected pericardial effusion and suspected or pre-existing valvular or myocardial disease. Although it is considered a semi-invasive diagnostic tool, TOE should be used for critically ill patients when information essential for patient management cannot be obtained by transthoracic echocardiography [8] due to patient factors resulting in inadequate visualization of relevant structures [27, 28]. Be that as it may, there are several useful applications of the TOE in the everyday practise of the intensivist. Some of the more common ones are discussed below.

1. Assessment of ventricular volume status and loading conditions:

The left ventricle function and volume status may be estimated by visualization of left ventricle end-diastolic (EDD) and end-systolic dimensions (ESD) [14]. This method for estimating loading conditions was demonstrated to be more accurate than pulmonary capillary wedge pressure [15] (Fig. 9.27).

Hypovolemic patients have both reduced end systolic and end diastolic left ventricle dimensions, with hyper contractile left ventricle and kissing papillary muscle in systole. On the other hand, the septic patients have reduced end systolic dimensions due to reduced afterload with normal end diastolic dimensions [14, 16]. Moreover, TOE can identify the patients who are responders to fluid therapy. These are the patients with lack of increase of left ventricle diastolic dimensions after fluid administration [17]. Some other data offered by TOE examination like trans mitral flow (PWD) and mitral annular tissue velocities ratio or trans mitral flow propagation velocity ratio may accurately estimate the left ventricle end-diastolic pressures [17]. There can be several reasons for increased dimensions of the LV including coronary artery disease, cardiomyopathy, valvular pathology and drug abuse. Flattening of the IVS suggest RV volume over load. It is worth noting that only a dilated RV contributes to the apex of the heart as seen in the ME 4C view. Normally the RV apex lies around the middle third of the IVS. Estimation of the stroke volume can yield the cardiac output and can be determined by using the velocity time integral (VTI) obtained by PWD/CWD assessment of flow past the PV and AV.

$$Cardiac\ Output = Stroke\ Volume \times Heat\ Rate$$

Since the aorta and pulmonary arteries are tubular structure an idea of the volume can therefore be calculated as the volume of a cylinder ($\pi r^2 h$). The diameter (d) can be measured by calliper and the VTI can be used as the height of the cylinder to define a volume.

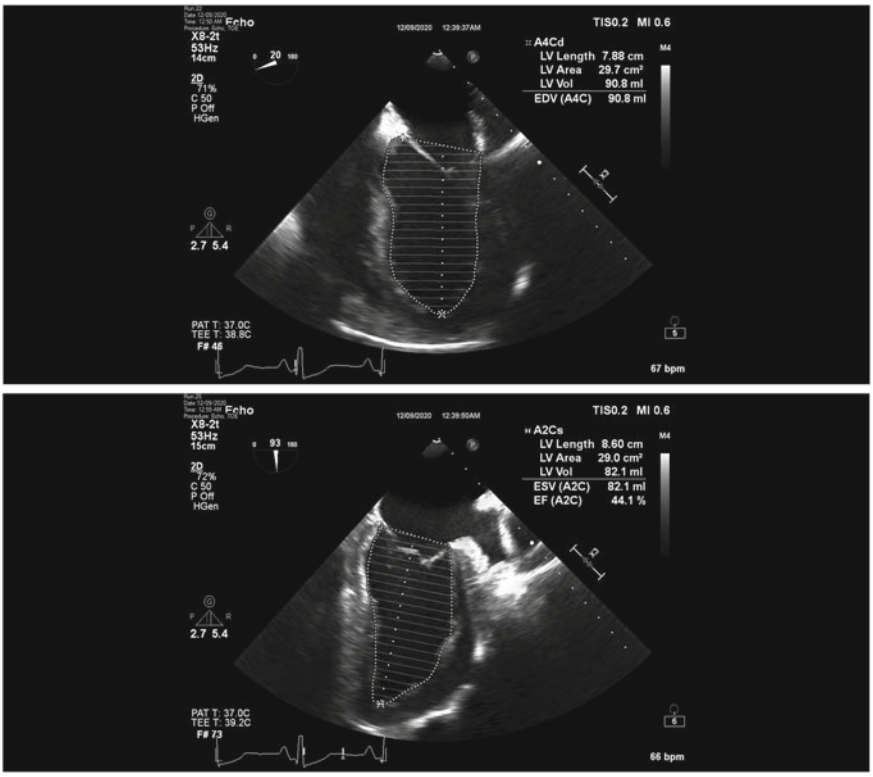

Fig. 9.27 **a** Simpsons method used to map EDV 2C. **b** Simpsons method used to map ESV and obtain the Ejection Fraction

$$\text{Stroke Volume (SV)} = VTI \times \pi(LVOTd/2)^2 = \text{VTI} \times 0.785\text{d}^2$$

2. Ventricular function:

TOE is a very useful tool for assessment of left ventricle global or regional systolic function. When considering contractility look for both the inward movement of the walls as well as the thickening of the segments. Usually eye balling the moving ventricle is the most practical way of quickly assessing the ventricular contractility and ejection fraction. Fractional area change (FAC) is the area change with systole from it diastolic dimensions and can be traced in the TG Mid SAX by excluding the papillary muscles form your trace of the endocardial border. This is an area and not a volume.

$$FAC(\%) = \frac{LVED\ area - LVES\ area \times 100}{LVED\ area}$$

Normal values are 50–80%.

Fractional shortening (FS) is best measured from an Mmode of the TG Mid SAX view. Since this sample line only crosses 2 segments it is a poor indicator of overall LV function.

$$FS(\%) = \frac{LVIDd - LVIDs \times 100}{LVIDd}$$

Normal values are $\geq 30\%$.

For more precise data, the calculation of left ventricle ejection fraction (EF) by Simpson's method in ME 4C and ME 2C view may be performed. Alternatively, the area length method can be used by tracing the endocardial border of the LV and then using the calliper to estimate the length of the LV from MV annulus to apex. The TG Mid SAX view can also be used to measure the end diastolic (EDD) and the end systolic (ESD) dimensions to calculate the EF.

$$EF(\%) = \frac{EDD - ESD \times 100}{EDD}$$

Normal values 55–75%.

Often there is some functional MR which can be interrogated by CWD and the velocity change from 1 to 3 m/s can be used to estimate pressure difference (DP) and the time taken to achieve this (dT). The ratio DP/dT provides an estimate of LV systolic function. Normal values $\geq$ 1000–1200 mmHg/s.

Other methods like measuring the strain/strain rate and speckle tracking offer the advantage of being unaffected by the angle of Doppler beam although maybe time consuming and therefore not as applicable as the quicker methods above. In addition, 3D TOE allows more accurate estimation of left ventricle ejection fraction by triplane or 3D volumes (Fig. 9.28).

For appreciation of left ventricle regional wall motion abnormalities, the mid-oesophageal (ME 4C, ME 2C, ME LAX) as well as the trans gastric views (TG Basal SAX, TG Mid SAX, TG Apical SAX) should be used. This allows for the visualisation of every segment in at least two views (Fig. 9.29).

The right ventricle function is generally appreciated by eye balling it and analysing the movement of right ventricular free wall in the ME 4C and RVOT views, by measuring tricuspid annular plane systolic excursion (TAPSE>1.5 cm being normal) and fraction area change in ME 4C view.

Regional wall motion abnormalities (RWMA) if present are usually due to the presence of coronary artery disease (CAD) and can be mapped to the coronary artery branch involved. The RV and inferoseptal wall of the LV are supplied by the right coronary artery (RCA). The septal wall, anterior and anteroseptal walls and apex are supplied by the left anterior descending artery (LAD). The anterolateral, lateral and inferolateral walls are supplied by the left circumflex artery (LCx). There is often shared supply to adjacent segment for adjoining territories which often appears as retrograde filling on coronary angiography. Other signs of ischaemia are

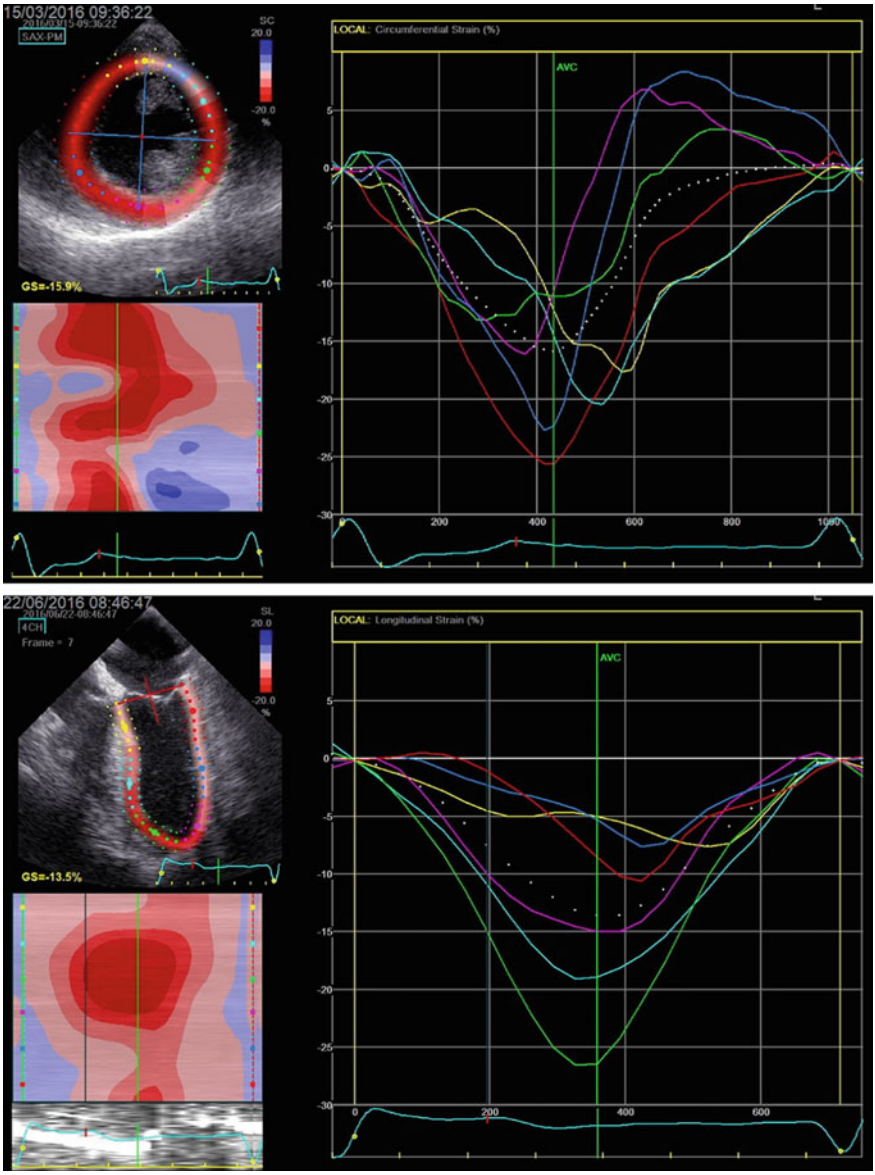

Fig. 9.28 **a** Circumferential Strain imaging. **b** Longitudinal Strain imaging

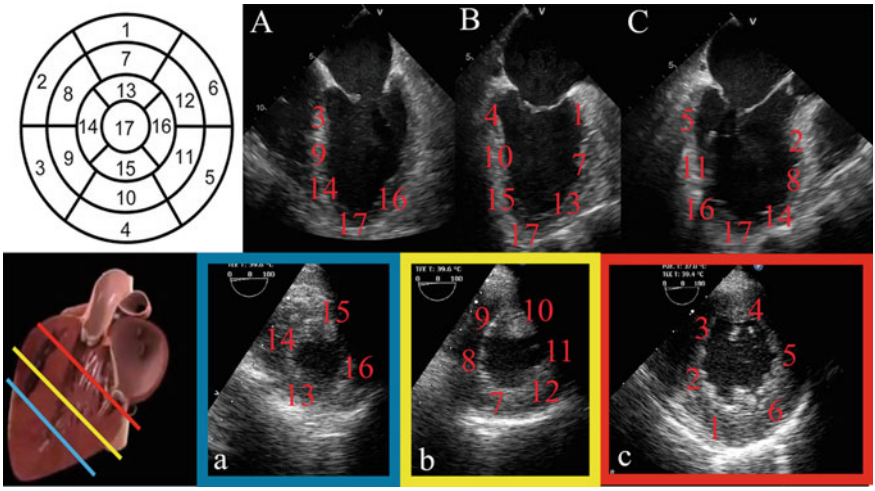

Fig. 9.29 Demonstrating LV Segments in the ME 4C(A), 2C(B) & 3C LAX(C) & Apical(a), Mid (b) & Basal TG SAX views

chronic segmental dysfunction, ventricular dilatation, functional MR, papillary muscle dysfunction/rupture, VSD, haemorrhagic effusion and LV aneurysm.

3. Cardiac tamponade:

Cardiac tamponade is a medical emergency and its timely diagnosis and management, with percutaneous or surgical evacuation, are vital to prevent further end organ damage due to the resultant low output state. The diagnosis is established based on clinical and echocardiographic signs [18]. The TOE exam may reveal the presence of pericardial fluid surrounding the heart and also may show echocardiographic signs suggestive of hemodynamic significance like compressed right or left heart cavities. PWD measured transmitral/tricuspid inflow respiratory variations of more than 25% (mitral E wave decreases and tricuspid E wave increases with inspiration) suggest compromise. Decreases of the flow across the aortic valve by more than 10% during inspiration (measured by VTI) is another sign along with paradoxical septal movement [19]. It is important to remember that the findings will differ based on whether the patient is breathing spontaneously or is being ventilated. Chamber collapse is evident when the pressure within it is minimum. So for ventricles it would be during diastole and for atria it would be during systole. Respirophasic variations are best visualised by decreasing the sweep speed to fit multiple inflow spectral profiles on the screen allowing for better comparison (Fig. 9.30).

4. Other Left Ventricular Pathology:

Often patients on the ICU are septic and under filled which may give rise to a dynamic obstruction of the LVOT. This may result in the systolic anterior migration (SAM) of the AMVL which is due to the fast moving blood in the LVOT. The

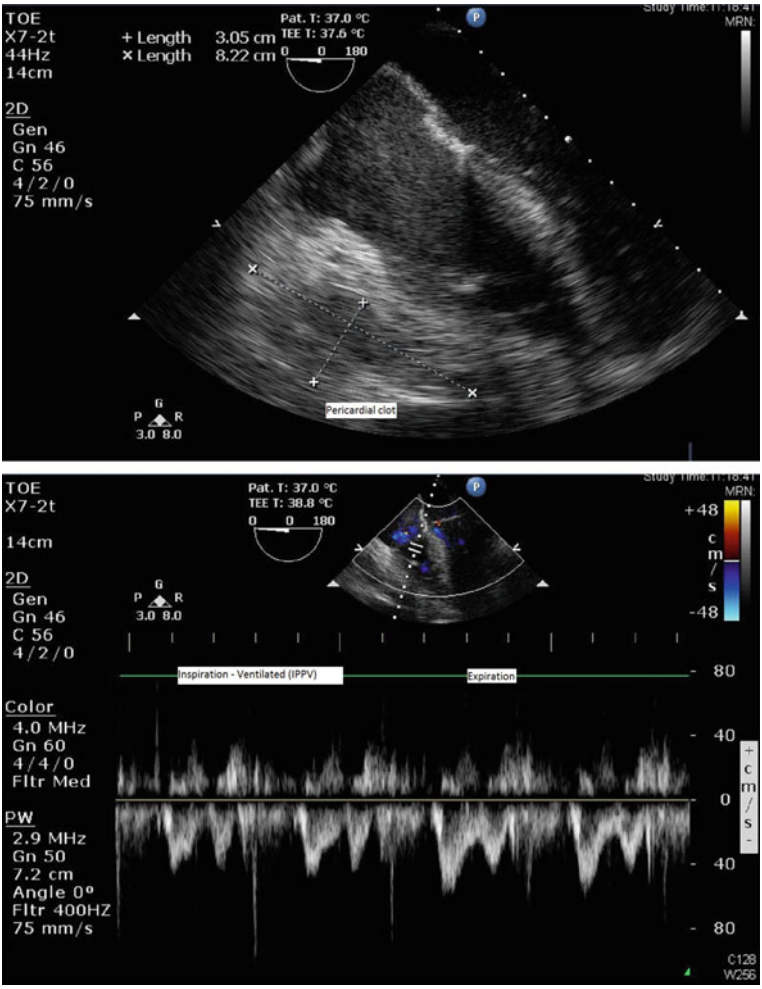

Fig. 9.30 **a** ME 4C showing a large clot sitting the pericardium adjacent the RV and affecting the transtricuspid flow with respiration. **b** PWD of the transtricuspid flow showing a reduction of RV inflow with ventilated breath and increased flow with passive expiration

resultant pressure difference across the AMVL forces it into the LVOT, thereby preventing blood from entering the aorta. This diagnosis can easily be made with TOE and is vital as the management plan, of fluid loading and vasoconstrictor with consideration for β blockers, is very different from what could be the natural response to a low output state. Inotropic agents are usually not indicated [14]. The worsening of any MR jet with turbulence in the LVOT on CFD should raise the suspicion of SAM. Sometime the deflection of the AMVL can be clearly seen on 2D when the clip is slowed down. Patients with cardiogenic shock after MI can develop

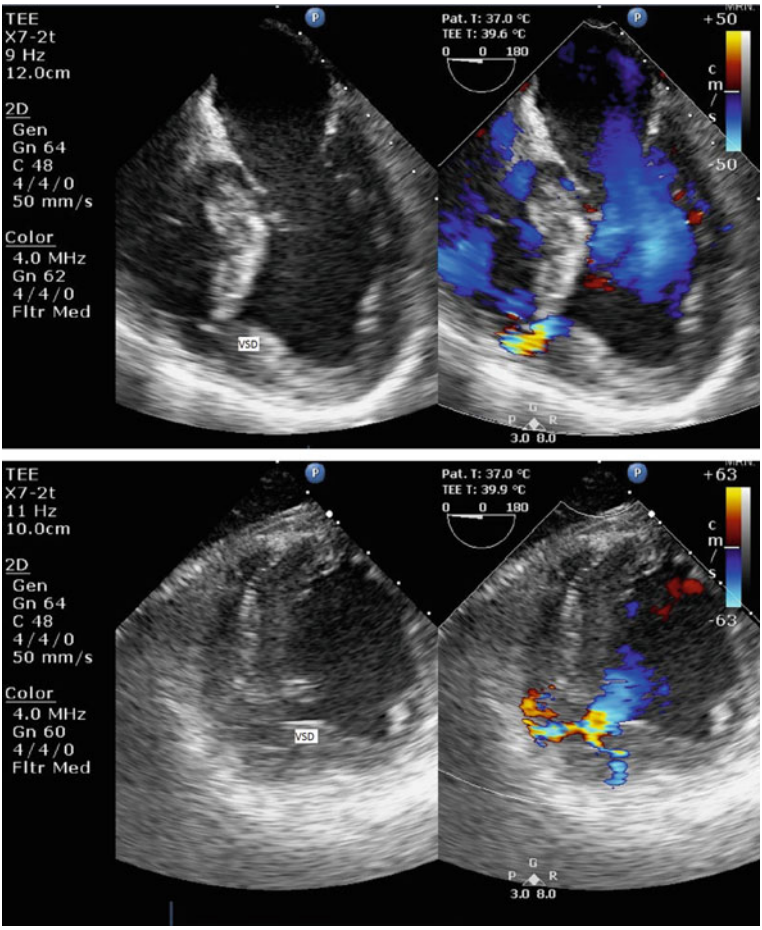

Fig. 9.31 **a** ME 4C view showing a muscular ventricular septal defect (VSD) in the distal septum with continuous flow across into the right ventricle. **b** TG Mid SAX view showing the ventricular septal defect to be in the mid anteroseptal segment of the LV wall with shunting of blood into the RV

septal defects typically in the first week post MI. New systolic murmurs should be investigated aggressively as VSD has a very poor prognosis (Fig. 9.31a, b).

5. Infective endocarditis:

TOE has excellent spatial and temporal resolution compared to TTE and other imaging modalities which makes it the perfect diagnostic tool for infective endocarditis. A not uncommon clinical scenario encountered in critically ill patients on the ICU. TOE is a class I indication for patients with clinical suspicion of infective endocarditis and a negative or non-diagnostic TTE or for patients with clinical suspicion of infective endocarditis when intracardiac devices or prosthetic valves are present [20].

The echocardiographic findings suggestive of infective endocarditis are vegetations (infected mass attached to an endocardial structure that echocardiographically appears as oscillating or nonoscilating masses), abscesses (cavity with necrosis and purulent material that echocardiographically appears as nonhomogeneous perivalvular area) and pseudo aneurysms (perivalvular cavity communicating with the cardiovascular lumen that echocardiographically appears as pulsatile, echo-free perivalvular space) [20, 21].

6. Cardiac masses:

TOE is a useful tool for diagnosis of cardiac masses as well as masses adjacent to the heart. Although for the latter, additional imaging modalities are frequently necessary [22]. Having a high spatial and temporal resolution, TOE is a reliable technique to detect and characterize the intracardiac masses like thrombi, tumours, marantic vegetations and fibro-elastomas [23]. This diagnosis is particularly important in patients with previous stroke, taking into account the fact that 15–30% of ischemic strokes are due to emboli of cardiac origin [24]. It is not uncommon for patients in ICU to go into atrial tachyarrythmias. Loss of pulsatility will render atria at a high risk of retaining clots and these may pose a danger especially if these patients are considered for synchronised DC cardioversion in the setting of severe haemodynamic compromise. TOE is a useful tool to exclude the presence of an intra cardiac clot, most commonly found in the LAA, which might give rise to a catastrophic embolic event after DCC (Figs. 9.32 and 9.33).

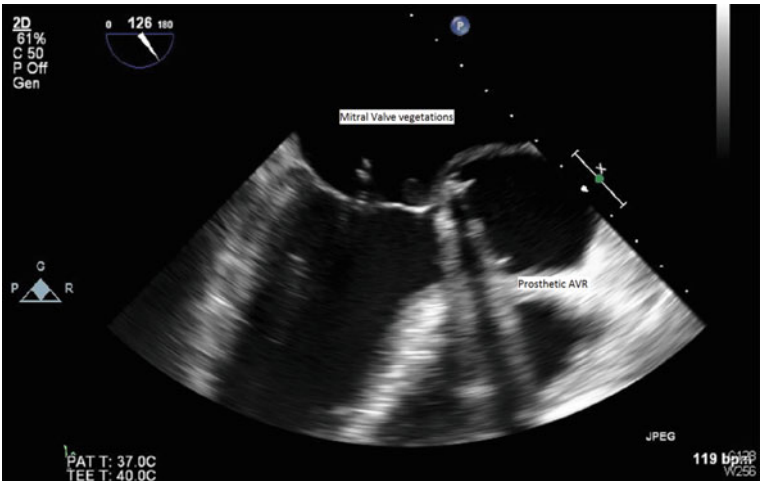

Fig. 9.32 ME AV LAX view showing a large vegetation on the atrial surface of the mitral valve due to the infection of the mechanical prosthetic aortic valve

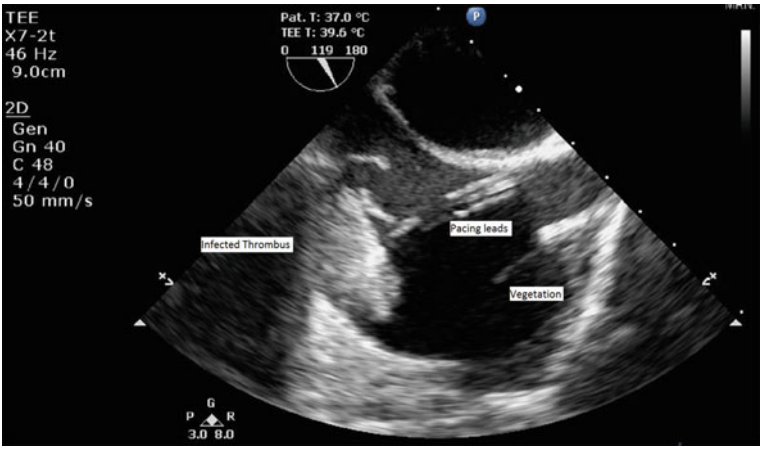

Fig. 9.33 ME BC view showing a right atrial mass, most likely a thrombus, associated with in dwelling pacing leads with evidence of vegetations

7. Valvular disease:

The majority of patients in ICU have normal leaflet morphology. Age related changes may be seen ranging from myxomatous degeneration to restrictions most commonly due to ventricular dilatation and fibrosis. Valvular pathology frequently accompany infective endocarditis of any origin. Destruction of the valve leaflets can be catastrophic resulting in flash pulmonary oedema and LVF. Leaflets are more commonly interrogated with 2d zoom to exclude subtle vegetations and to exclude intra cardiac abscesses as above. Often the character of regurgitant jets can hint at the underlying pathology. Ischaemic regurgitation is often central due to failure of coaptation affecting both leaflets equally. Eccentric jets are usually pathological due to defects of the leaflets itself like prolapsing myxomatous leaflets or restricted rheumatic ones. If the valve leaflets rise above the annular plane, they are said to be prolapsing but if the leaflet tips are free of their chordal attachment and are seen pointing into the atria they are termed flail.

8. Aortic dissection:

Acute aortic dissection has a high mortality and its detection and classification are vital for formulating the appropriate action plan. Ascending aortic dissections are treated surgically while the descending thoracic dissections are often treated conservatively or with endovascular stenting. TOE is sometimes the preferred technique compared to CT or MRI as it is quick, can be done on the ICU and does not need use of contrast agents [25]. The diagnostic element for classical aortic dissection is the presence of an aortic flap. TOE can provide morphological information which is very important for surgical management. It is helpful in identifying the intimal tear location, the true lumen of the aorta, the presence and the mechanism of aortic regurgitation, the arterial vessel involvement or extension and the presence of a pericardial effusion or periaortic bleeding [25, 26] (Fig. 9.34).

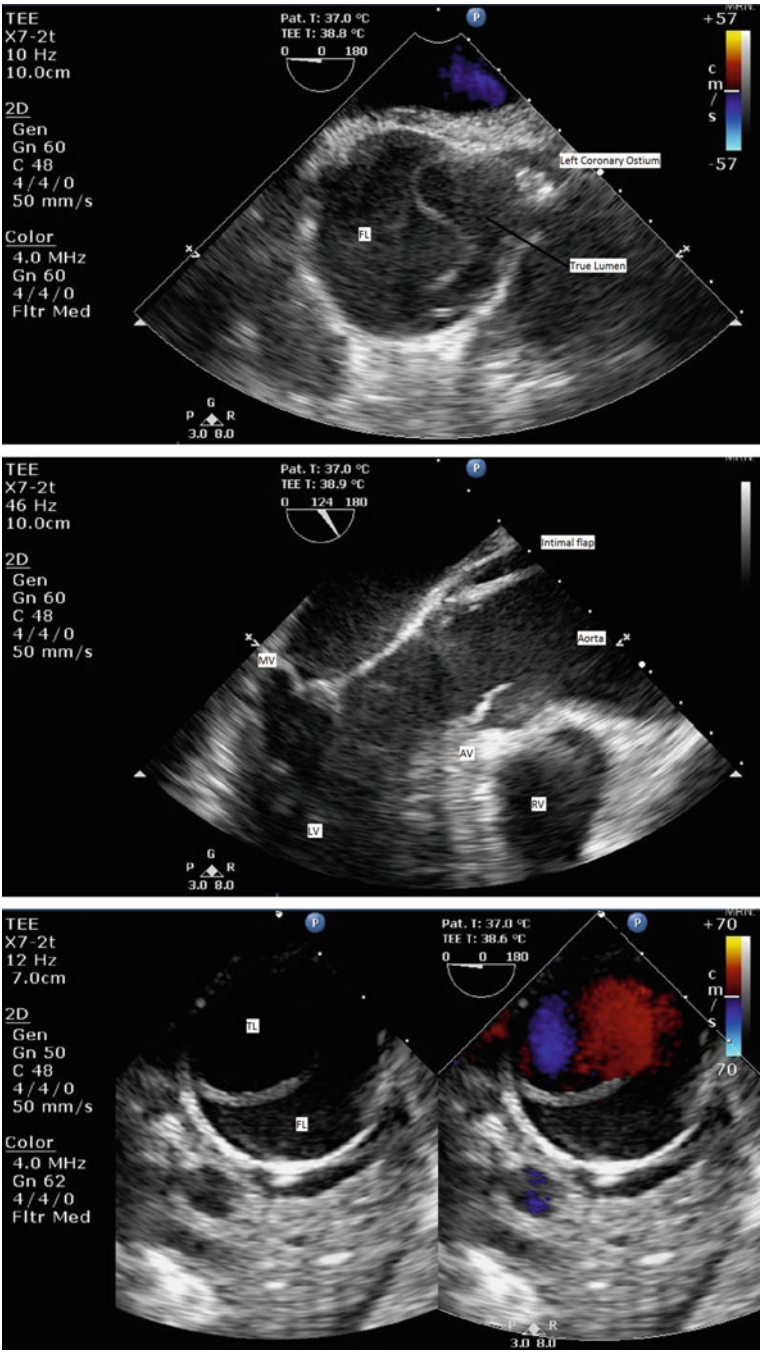
TEE
X7-2t
10 Hz
10.0cm
2D
Gen
Gn 60
C 48
4/4/0
50 mm/s
Color
4.0 MHz
Gn 60
4/4/0
Fltr Med
Pat. T: 37.0 °C
TEE T: 38.8 °C
0 0 180
+57
cm/s
-57
Left Coronary Ostium
FL
True Lumen
G
P R
3.0 8.0
TEE
X7-2t
46 Hz
10.0cm
2D
Gen
Gn 60
C 48
4/4/0
50 mm/s
Pat. T: 37.0 °C
TEE T: 38.9 °C
0 124 180
Intimal flap
Aorta
MV
AV
RV
LV
G
P R
3.0 8.0
TEE
X7-2t
12 Hz
7.0cm
2D
Gen
Gn 50
C 48
4/4/0
50 mm/s
Color
4.0 MHz
Gn 62
4/4/0
Fltr Med
Pat. T: 37.0 °C
TEE T: 38.6 °C
0 0 180
+70
cm/s
70
TL
FL
P R
3.0 8.0

◂**Fig. 9.34** **a** ME As Ao SAX showing a dissection flap involving more than 2/3rd of the circumference of the ascending aorta. Notice that the flap does not progress into the left coronary artery. TL = True Lumen, FL = False Lumen. **b** ME As Ao LAX showing the intimal flap in the aortic root. MV = Mitral Valve, LV = Left Ventricle, RV = Right Ventricle, AV = Aortic Valve. **c** ME Des Ao SAX view showing progression of the dissection flap into the descending aorta. TL = True Lumen, FL = False Lumen

9.9 Conclusion

It is clear that TOE is of immense value to the intensive care physician. The applications for TOE continue to expand and with improvement of technology and development of powerful software packages to analyse the data gathered, it will become more and more reliable. It is already the investigation of choice for diagnosis of infective endocarditis, exclusion of LA thrombus and confirmation of aortic dissection. Immensely beneficial for evaluating LV function and guide fluid management in the haemodynamically compromised patient. It is just a matter of time before it becomes routine to use TOE to monitor and treat patients in the ICU. Future training programmes for doctors on ICU will have to cater to this aspect of their skill. It is vital that doctors of tomorrow are competent in the use of ultrasound and can use it to its fullest potential to help with the management of patients on ICU. Although there is no standard protocol for the use of TOE on ICU as yet there is an opportunity to help in the development of a programme that will fulfil the needs of the ICU physician. There are commercially available simulators and online resources that can help augment any training programme for TOE on ICU, but hands on training is by far the most realistic and the provision of this opportunity is paramount to the success of any programme. In conclusion TOE is an excellent tool for the use of intensive care physicians to confirm their clinical suspicions and help guide therapy. It is not however, a replacement for sound clinical judgement, detailed history taking and a thorough physical examination. Used prudently it is safe and of immense benefit to patient care [31, 32].

References

1. International expert statement on training standards for critical care ultrasonography. Intensive Care Med. 2011;37(7):1077–83.
2. Khoury AF, Afridi I, Quiñones MA, Zoghbi WA. Transesophageal echocardiography in critically ill patients: feasibility, safety, and impact on management. Am Heart J. 1994;127 (5):1363–71.
3. Hüttemann E. Transoesophageal echocardiography in critical care. Minerva Anestesiol. 2006;72(11):891–913.
4. Hüttemann E, Schelenz C, Kara F, Chatzinikolaou K, Reinhart K. The use and safety of transoesophageal echocardiography in the general ICU—a minireview. Acta Anaesthesiol Scand. 2004;48(7):827–36.

5. Aviv JE, Di Tullio MR, Homma S, Storper IS, Zschommler A, Ma G, Petkova E, Murphy M, Desloge R, Shaw G, Benjamin S, Corwin S. Hypopharyngeal perforation near-miss during transesophageal echocardiography. Laryngoscope. 2004;114(5):821–6.
6. Daniel WG, Erbel R, Kasper W, Visser CA, Engberding R, Sutherland GR, Grube E, Hanrath P, Maisch B, Dennig K, et al. Safety of transesophageal echocardiography. A multicenter survey of 10,419 examinations. Circulation. 1991;83(3):817–21.
7. Sainathan S, Andaz S. A systematic review of transesophageal echocardiography-induced esophageal perforation. Echocardiography. 2013;30(8):977-83.
8. Hahn RT, Abraham T, Adams MS, Bruce CJ, Glas KE, Lang RM, Reeves ST, Shanewise JS, Siu SC, Stewart W, Picard MH. Guidelines for performing a comprehensive transesophageal echocardiographic examination: recommendations from the American Society of Echocardiography and the Society of Cardiovascular Anesthesiologists. J Am Soc Echocardiogr. 2013;26(9):921–64.
9. Mayo PH, Narasimhan M, Koenig S. Critical Care Transesophageal Echocardiography. Chest. 2015;148(5):1323–32.
10. Nelson TR1, Fowlkes JB, Abramowicz JS, Church CC. Ultrasound biosafety considerations for the practicing sonographer and sonologist. J Ultrasound Med. 2009 Feb;28(2):139–50.
11. Sutherland GR, Stewart MJ, Groundstroem KW, Moran CM, Fleming A, Guell-Peris FJ, et al. Color Doppler myocardial imaging: a new technique for the assessment of myocardial function. J Am Soc Echocardiogr. 1994;7:441–58.
12. Cheitlin MD et al. ACC/AHA/ASE 2003 guideline update for the clinical application of echocardiography: summary article: a report of the American College of Cardiology/ American Heart Association Task Force on Practice Guidelines. Circulation. 2003;108 (9):1146–62.
13. Porter TR, Shillcutt SK, Adams MS, Desjardins G, Glas KE, Olson JJ, Troughton RW. Guidelines for the use of echocardiography as a monitor for therapeutic intervention in adults: a report from the American Society of Echocardiography. J Am Soc Echocardiogr. 2015;28 (1):40–56.
14. Roscoe A. Strang T Echocardiography in intensiv care Anaesteis. Critical CAre and Pain. 2008;8:46–50.
15. Benjamin E, Griffin K, Leibowitz AB, et al. Goal-directed transesophageal echocardiography performed by intensivist to assess left ventricular function: comparison with pulmonary artery catheterization. JCardiothorac Vasc Anesth. 1998;10–5:12.
16. Hilton A. Echocardiography is the Best Cardiovascular 'monitor' in Septic Shock Crit Care REsusc. 2006;8:247–51.
17. Mahmood F, Chiristie A. Matyal R Transesophageal Echocardiography and Noncardiac Surgery Cardiothoracic and Vascular Anesthesia. 2008;12:265–89.
18. Gray R, Baldwin F, Bruemmer-Smith S. Diagnostic echocardiography in an unstable intensive care patient. Echo Res Pract. 2015; 2(1): K11–6.
19. Popescu B. Ginghina C Enache R. Editura Medicala: Pericardial diseases in Doppler Ecocardiography; 2011.
20. The 2015 ESC Guidelines for the management of infective endocarditis. Eur Heart J. 2015;36 (44):3036–7.
21. Thanavaro KL, Nixon JV. Endocarditis 2014: an update. Heart Lung. 2014;43(4):334–7.
22. Sengupta P. Khandheria B Transesophageal Echocardiography Heart. 2005;91:541–7.
23. Pepi M, Evangelista A, Nihoyannopoulos P, Flachskampf FA, Athanassopoulos G, Colonna P, Habib G, Ringelstein EB, Sicari R, Zamorano JL, Sitges M, Caso P. European Association of Echocardiography. Recommendations for echocardiography use in the diagnosis and management of cardiac sources of embolism: European ssociation of Echocardiography (EAE) (a registered branch of the ESC). Eur J Echocardiogr. 2010;11 (6):461–76.
24. Ferro JM. Cardioembolic stroke: an update. Lancet Neurol. 2003;2:177–88.
25. Evangelista A, Flachskampf FA, Erbel R, Antonini-Canterin F, Vlachopoulos C, Rocchi G, Sicari R, Nihoyannopoulos P, Zamorano J, ofEchocardiography, European Association and

Document Reviewers: Pepi M, Breithardt OA, Plonska-Gosciniak. Echocardiography in aortic diseases: EAE recommendations for clinical practice. Eur J Echocardiogr. 2010;11 (8):645–58.
26. Hiratzka LF, Bakris GL, Beckman JA, Bersin RM, Carr VF, Casey DE Jr et al 2010 ACCF/AHA/AATS/ACR/ASA/SCA/SCAI/SIR/STS/SVM Guidelines for the diagnosis and management of patients with thoracic aortic disease. J Am Coll Cardiol. 2010 Apr 6;55(14).
27. Practice guidelines for perioperative transesophageal echocardiography. An updated. by the American Society of Anesthesiologists and the Society of Cardiovascular Anesthesiologists Task Force on Transesophageal Echocardiography. Anesthesiology. 2010;112(5):1084–96.
28. Douglas PS, Garcia MJ, Haines DE, Lai WW, Manning WJ, Patel AR, Picard MH, Polk DM, Ragosta M, Ward RP, Weiner RB. ACCF/ASE/AHA/ASNC/HFSA/HRS/SCAI/SCCM/SCCT/SCMR 2011 Appropriate Use Criteria for Echocardiography. J Am Coll Cardiol. 2011;57(9):1126-66.
29. Piérard L. Flachskampf FA, Badano L, Daniel WG, Feneck RO, Fox KF, Fraser AG, Pasquet A, Pepi M, Perez de Isla L, Zamorano JL, Echocardiography, European Association of and Echo Committee of the European Association of Cardiothoracic Anaesthesiologists, Roelandt JR. Recommendations for transoesophageal echocardiography:update 2010. Eur J Echocardiogr. 2010;11(7):557–76.
30. Hilberath JN, Oakes DA, Shernan SK, Bulwer BE, D'Ambra MN, Eltzschig HK. Safety of transesophageal echocardiography. J Am Soc Echocardiogr. 2010;23(11):1115–27.
31. Kallmeyer IJ, Collard CD, Fox JA, Body SC, Shernan SK. The safety of transesophageal echocardiography: a case series of 7200 cardiac surgical patients. Anesth Analg. 2001;92:1126–30.
32. Seward JB, Khandheria BK, Oh JK, Freeman WK, Tajik AJ. Critical appraisal of transesophageal echocardiography: limitations, pitfalls, and complications. J Am Soc Echocardiogr. 1992;5:288–305.

Chapter 10
FAST Scanning

Jane Brenchley

Keywords FAST · e-FAST · FAFF · Trauma · Ultrasound

10.1 Introduction

The use of ultrasound to evaluate the trauma patient in the resuscitation room was first described in the Archives of Emergency Medicine by Chambers and Pilbrow in 1988 [1].

Initially performed by radiologists the technique was seized upon by both trauma surgeons and emergency physicians with adoption of the focused assessment with sonography in trauma (FAST) protocol in continental Europe and the Far East followed by North America and the UK. This has been backed up in a randomised trial of FAST scanning versus standard care which demonstrated a reduction in use of CT scanning, time to definitive surgery and reduction in hospital days [2].

The FAST scan is a rule in technique—the sole aim is the identification of free fluid. A positive fast scan denotes a significant amount of bleeding and may change management priorities. A negative scan does not exclude intra-abdominal injury and studies performed during diagnostic peritoneal lavage have shown that in excess of 600 mL of fluid is required before it is demonstrated by sonography [3].

There are several limitations to be aware of: The FAST exam is not useful in diagnosing retroperitoneal fluid or hollow viscus injury and the patient's body habitus may make the exam challenging.

J. Brenchley (✉)
Department of Emergency Medicine, Royal Berkshire Hospital, Reading, Berkshire RG1 5AN, England
e-mail: jane.brenchley@nhs.net

A. Walden et al. (eds.), *Ultrasound in the Critically Ill*,
https://doi.org/10.1007/978-3-030-71742-1_10

10.2 Equipment

Ensure the machine is set up on an abdominal preset and use the curvilinear abdominal probe. Generally the entire exam is completed with this probe rather than switching to a phased array part way through, although this is an option if the cardiac view is difficult.

10.3 FAST Scan Principles

The rationale behind the FAST exam is the identification of free intra-peritoneal fluid. In the context of trauma this is assumed to be blood until proven otherwise. The exam now involves four standard views (RUQ, LUQ, pelvis and pericardial). The earlier descriptions included two paracolic views, but by the time free fluid was visualised here the other views were always positive, so these extra views were abandoned.

The purpose of FAST is the binary assessment of the presence or absence of free fluid. Fluid is hypoechoic and thus appears black on ultrasound (fresh bleeding is hypoechoic and appears black until it starts to clot). Fluid seen on any view denotes a positive FAST scan. If all views are negative the scan is negative. Once one abdominal view is positive there is no diagnostic benefit in continuing the scan. The scan is limited to these four standard views. No attempt is made to examine the texture of the solid organs—ultrasound is less sensitive early in the post injury period and requires more time and skill. The site of fluid is determined by the peritoneal reflections rather than specific organ injury, so in the supine patient the most dependent areas are the RUQ and the pelvis, and fluid will collect here first. The RUQ view is the most sensitive area, adding the other views improves sensitivity slightly. The scan usually takes less than two minutes in experienced hands and can be repeated as necessary before patient transfer or after deterioration.

10.4 FAST Scan Views

10.4.1 Right Upper Quadrant

The probe is placed in a longitudinal orientation between the sagittal and coronal planes. Using the liver as a sonographic window, the beam is aimed towards the kidney until a view of Morison's pouch is obtained. The beam is then fanned through the kidney from front to back. Figure 10.1 shows probe position.

Figure 10.2 shows a normal right upper quadrant view of liver, right kidney and diaphragm showing mirror image artefact above the diaphragm.

A positive scan is indicated by a black stripe of free fluid between the kidney and liver. Any free fluid around the tip of the liver is also noted.

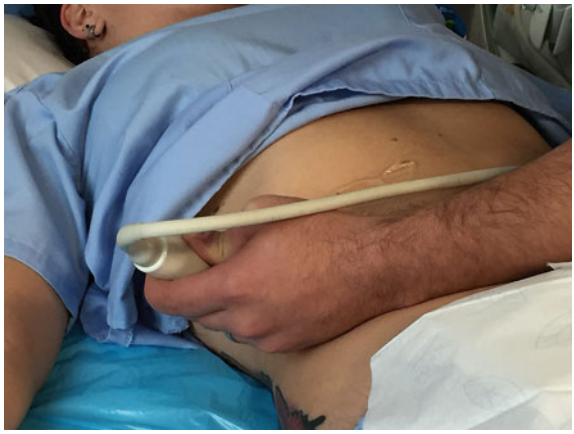

Fig. 10.1 Probe position for RUQ view

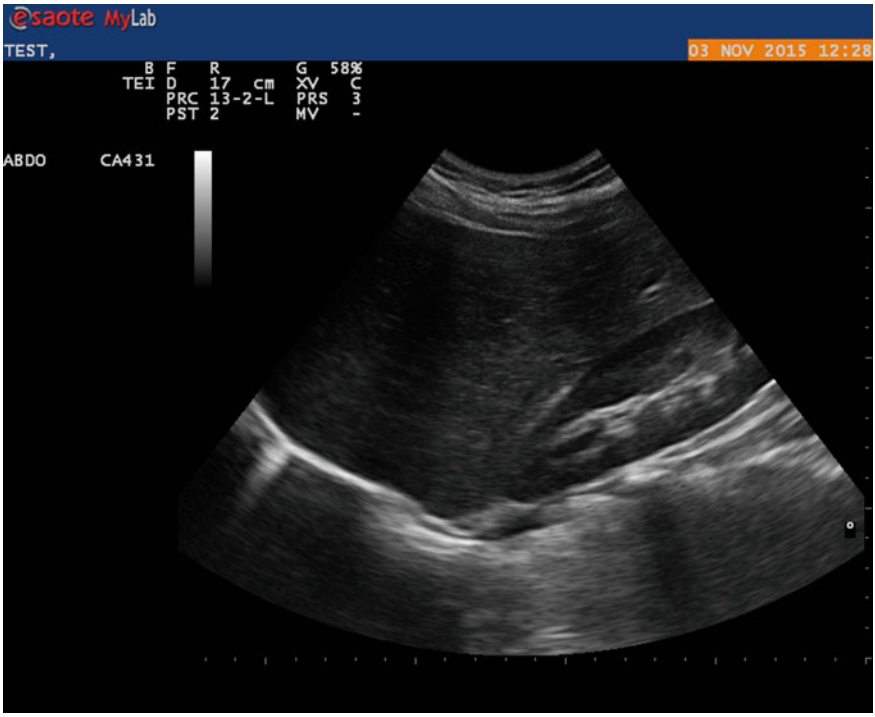

Fig. 10.2 Normal RUQ view showing liver, R kidney and Morison's pouch

10.4.2 Left Upper Quadrant

The probe position for the LUQ view is further cephalad and posterior than expected to avoid shadows from the stomach. This is shown in Fig. 10.3. Again using the spleen as a window the beam is orientated towards the kidney and any fluid between the spleen and kidney noted. Any fluid around the spleen is noted.

Figure 10.4 shows a normal left upper quadrant view of spleen, left kidney, diaphragm and mirror image artefact above the diaphragm.

10.4.3 Pelvis

The probe is placed suprapubically and angled down into the pelvis to visualise the bladder. The probe position is demonstrated in Fig. 10.5. Ideally the examination is performed before the insertion of a urinary catheter allowing improved visualisation of the structures behind the bladder. Any fluid collects initially in the peritoneal reflection behind the bladder, so in the pouch of Douglas or the recto-vesical pouch. As the quantity of fluid increases fluid is seen cephalad to the bladder and bowel loops may be seen floating in fluid.

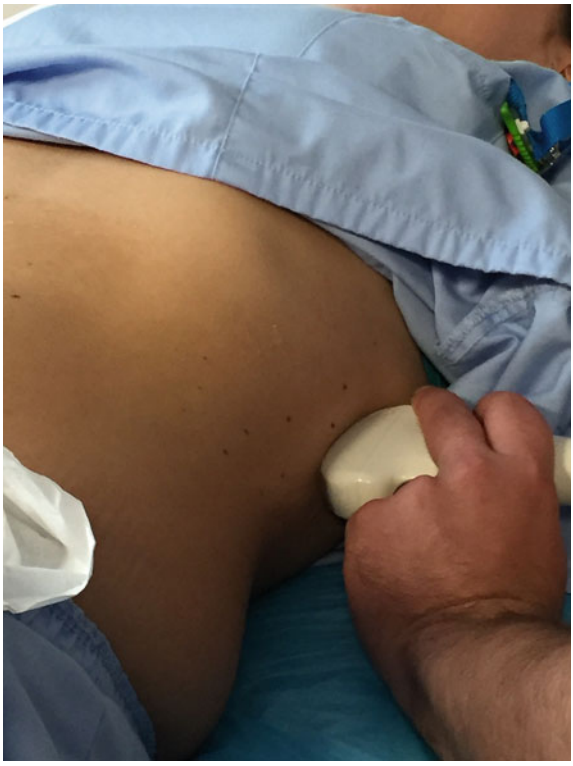

Fig. 10.3 Probe position for LUQ view

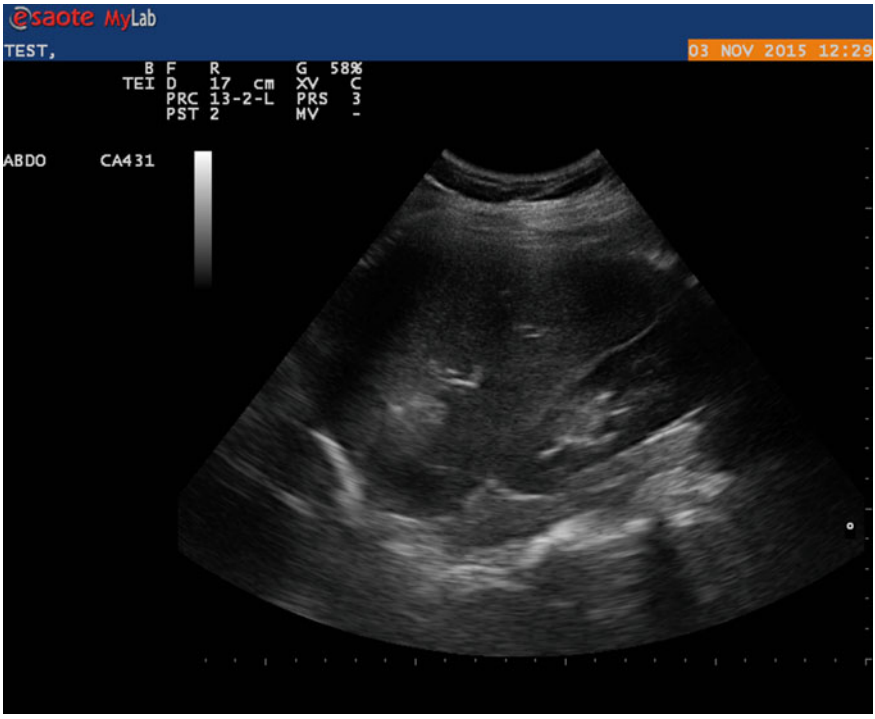

Fig. 10.4 Normal LUQ view showing spleen, L kidney and the spleno-renal recess

Fig. 10.5 Probe position for transverse pelvic view

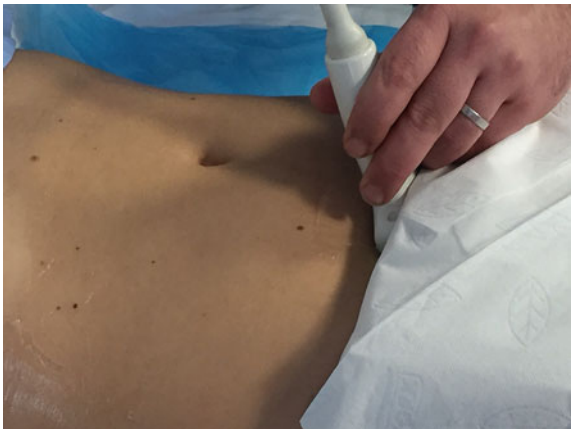

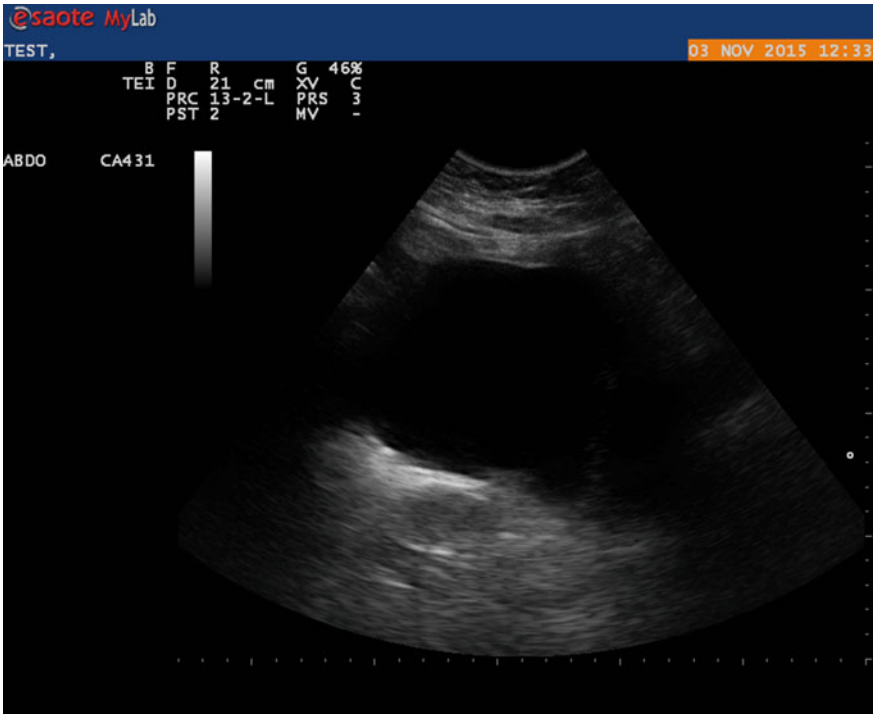

Fig. 10.6 Normal transverse pelvic view showing bladder, uterus and pouch of Douglas

Figure 10.6 shows a normal pelvic view—note the gain is turned down so the bladder appears black (as it is fluid filled) and to see contrast in the structures behind the bladder.

It is important to visualise the bladder as it is easy to assume any pelvic fluid collection seen will be the bladder when it may instead be free fluid.

10.4.4 Pericardium

The purpose of the pericardial view is to visualise fluid in the pericardial sac. This is less often seen in blunt trauma.

The standard view described is the subxiphoid view. This is shown in Fig. 10.7. The probe is placed below the xiphoid process and using the left lobe of the liver as an acoustic window the beam is pointed up towards the heart.

Figure 10.8 shows the normal pericardial view—pericardial fluid appears as a black stripe between the liver and myocardial wall anteriorly and between the bright pericardium and the myocardium posteriorly.

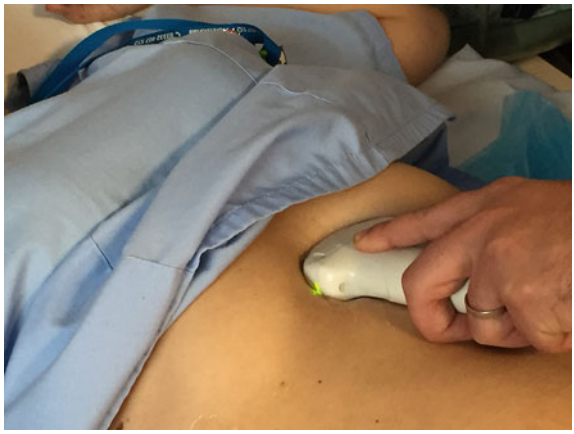

Fig. 10.7 Probe position for sub-xiphoid pericardial view

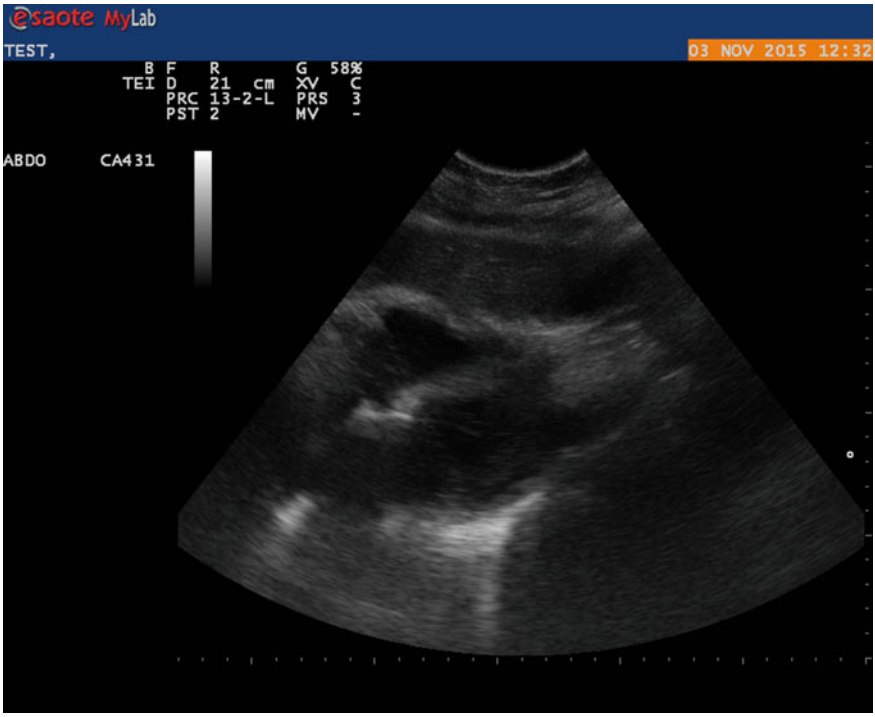

Fig. 10.8 Normal subxiphoid view

This can be a difficult view to achieve in the supine patient (and FAST is usually performed at the end of the primary survey when the patient is still flat). An alternative is to use a parasternal window—select any rib space which affords an

image of the anterior and posterior myocardium and pericardium. This is usually much easier, although in a patient with penetrating trauma, an anterior pneumothorax may be present meaning that this view is unobtainable, so practitioners should be adept in both techniques.

10.4.5 Extended FAST—eFAST

The standard FAST exam has been extended to include the pleural spaces. Ultrasound is accurate in diagnosing pneumothorax and haemothorax.

In both RUQ and LUQ views the diaphragm is visualised. Where there is air above the diaphragm (either normally within the lung or as a pneumothorax) the diaphragm becomes a highly reflective structure and mirror image artefact is seen 'above' it. This is seen in both RUQ and LUQ views above—above the bright reflection of the diaphragm is seen a similar appearance to the liver and spleen below it. If there is fluid above the diaphragm (assumed to be blood in the context of trauma) the diaphragm is less bright and there is a black (hypoechoic) space above it.

10.4.6 Focussed Assessment for Free Fluid—FAFF

Similar principles may apply to the use of ultrasound in non-traumatic emergency situations in patients presenting with abdominal pathology. Free fluid may be blood e.g.—in a patient with ectopic pregnancy or ascites. The same three or four view limited scan is performed depending on indication.

10.5 Conclusion

Ultrasound scanning for free fluid in a trauma situation (FAST) is a quick and dichotomous decision making tool which can help in decision making about the need for emergency surgery. An extended examination can also be used to rule out pneumothorax and haemothorax.

See also:
Chapter 5 Basic Lung Ultrasound.
Chapter 6 Advanced Lung Ultrasound.
Chapter 7 Focused Transthoracic Echocardiography.
Chapter 19 The Haemodynamically Unstable Patient.
Chapter 20 The Unconscious Polytrauma Patient.

References

1. Chambers JA, Pilbrow WJ. Ultrasound in abdominal trauma: an alternative to peritoneal lavage. Arch Emerg Med. 1988;5(1):26–33.
2. Melniker LA, Leibner E, McKenney MG, Lopez P, Briggs WM, Mancuso CA. Randomised controlled clinical trial of point-of-care limited ultrasonography for trauma in the emergency department: the first sonography outcomes assessment program trial. Ann Emerg Med. 2006;48 (3):227–35.
3. Branney SW, Wolfe RE, Moore EE, Albert NP, Heinig M, Mestek M, Eule J. Quantitative sensitivity of ultrasound in detecting free intraperitoneal fluid. J Traums - Inj Infect Crit Care. 1995;39(2):375–89.

Chapter 11
Renal Tract Ultrasound

Hefin Jones

Keywords Renal · Hydronephrosis · Renal ultrasound · Urosepsis

11.1 Introduction

The kidneys and urinary tract are a common source for occult pathology in the acutely unwell patient, urosepsis is frequently encountered and being able to demonstrate the presence of urinary calculi or obstruction could lead to more rapid source control. Equally, oligouria, anuria and acute kidney injury (AKI) may occur as a consequence of other conditions remote from the kidney due to hypovolaemia, pre-renal hypoperfusion and the toxic effects of some medications. Ultrasound is a simple and effective way of attributing pre-renal, post-renal and intrinsic renal factors to the cause of the acute kidney injury and dysfunction.

11.2 Equipment

The optimal probe is the curvilinear probe at 5 MHz setting but higher frequency probes, such as a 9 MHz can be used in the neonatal and infant setting. The curvilinear array is superior in demonstrating anatomy, particularly when imaging near the ribs. When faced with challenging anatomy, using a thick "footplate" of US gel can allow imaging around the ribs of shallow-lying structures immediately behind them. Use of pre- and post-processing techniques, such as harmonics and lower frequency selection can improve image quality in difficult-to-image patients. Patient positioning can improve imaging windows, such as elevating the ipsilateral arm to increase the sonographic window between the ribs. Use of other solid

H. Jones (✉)
Consultant in Radiology, University Hospitals of North Midlands, Newcastle Road, Stoke-on-Trent, Staffordshire ST4 6QG, UK
e-mail: Hefin.Jones@uhnm.nhs.uk

A. Walden et al. (eds.), *Ultrasound in the Critically Ill*,
https://doi.org/10.1007/978-3-030-71742-1_11

organs, such as the liver and spleen, can improve US wave transmission and also ensures absence of interference from bowel gas. Use of simple colour imaging can demonstrate appropriate and universal perfusion of the kidneys but Doppler imaging of the spectral waveform can be challenging, particularly in the acute setting and is not covered in this chapter.

11.3 Sonoanatomy

There should be three clearly defined sonographic zones in the kidneys (see Figs. 11.1, 11.2 and 11.3): the most peripheral cortex should have a clear external contour and have an iso-echogenicity (dark-grey); focal areas seen in regular but intermittent intervals medial to the cortex represent the medullary pyramids and should be significantly more hypoechoic (almost black). The antero-posterior (AP) diameter can be measured and is shown in Fig. 11.3; the more medial renal pelvis contains a large amount of fat and this should provide high echogenicity (white). Loss of this distinction is indicative of intrinsic renal parenchymal disease (see Fig. 11.4). The peripheral collecting system is virtually invisible in normal patients and the pelvi-ureteric junction should be visible exiting the renal hilum near the main renal artery and vein. Simple colour imaging should demonstrate pulsatile arterial and venous flow out to the cortex in all segments. There is a thin relatively avascular zone within the kidney in a coronal plane, which is a normal finding.

Ureters should only be visible at the pelvi-ureteric junction and if they are visible beyond this, should be considered dilated (see Fig. 11.5). Ureters can be seen to insert into the postero-basal aspect of the urinary bladder, often only demonstrated as small protrusions in a para-midline location. In patients with normal ureteric peristalsis, bilateral ureteric jets may be intermittently demonstrated to cause turbulence within the bladder, a finding that can be more easily seen using simple colour imaging.

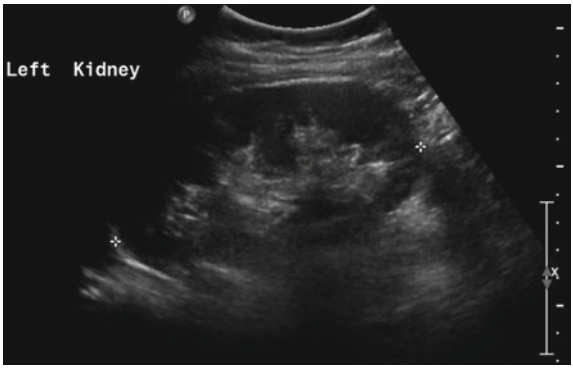

Fig. 11.1 Normal appearance of the renal parenchyma

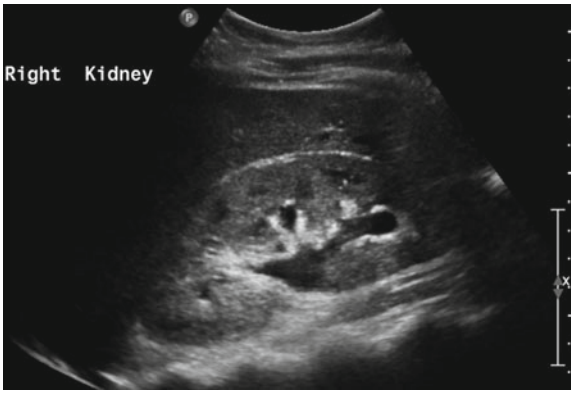

Fig. 11.2 Normal appearance of the renal parenchyma

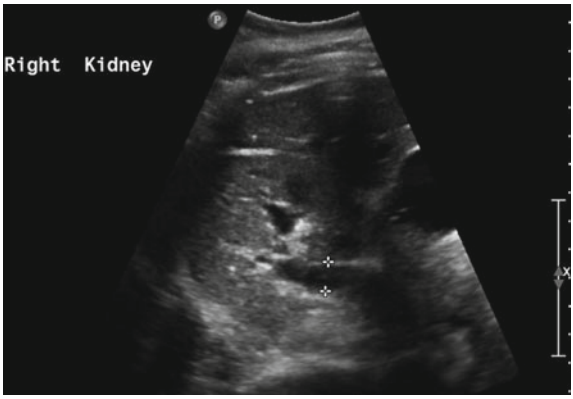

Fig. 11.3 Normal AP diameter

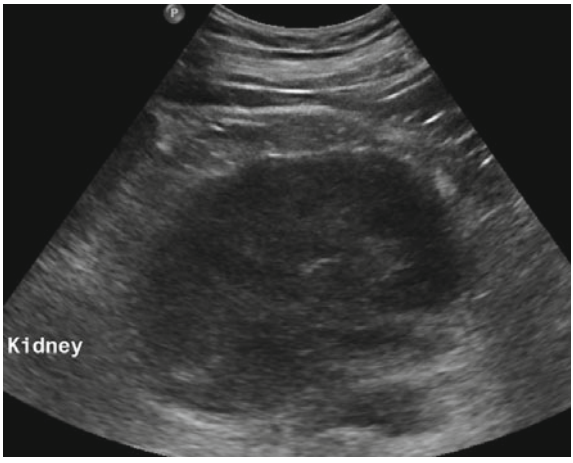

Fig. 11.4 Example of loss of the normal corticomedullary differentiation

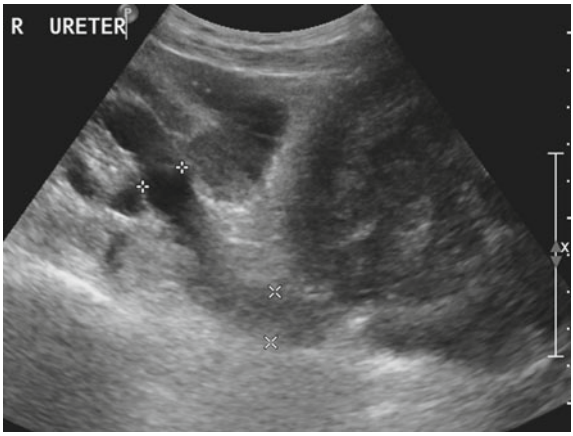

Fig. 11.5 Proximal ureteric dilatition

11.4 Pathology

Hydronephrosis is a relatively uncommon finding but one which should be eliminated as a cause for AKI. Assessment is relatively straightforward, as the dilated renal pelvis and calyceal system should become apparent as a branching and often rounded structure, with an AP diameter of more than 10 mm in adults (see Fig. 11.6). Care should be taken, however, as para-pelvic cysts can have somewhat similar appearances and referral to other imaging studies is often useful. A useful discriminator is that the hydronephrotic kidney is often larger in overall length and the calyces should also be dilated (see Fig. 11.7). Calculi are a common cause (see Fig. 11.8) and, to aid diagnosis, there may be further non-obstructive calyceal calculi visible as hyperechoic foci, with posterior acoustic shadowing, seen as a band of anechoic signal loss distal to the hyperechoic focus. Other causes potentially visible are red-cell casts from haemorrhagic lesions, such as transitional cell or renal cell carcinomata, which may be directly visible or the casts themselves can be seen as hyperechoic filling defects in a dilated collecting system (see Fig. 11.9).

Hydronephrosis can be focal, limited to a discrete pole, particularly in duplex systems, which have either partially or entirely separate ureteric drainage. In duplex systems, the ureter draining the upper moiety is likely to have ectopic distal insertion and the lower moiety is more prone to reflux and associated scarring.

Hydronephrosis may be seen without hydroureter, suggestive of pelvi-ureteric junction obstruction, which is often longstanding and associated with a differential renal function, or be associated with hydroureter, suggesting more distal obstruction, so care should be taken to look for proximal hydroureter. Any ureter measuring more than 3 mm beyond the pelvi-ureteric junction should be considered as hydroureter. If the ureter at the vesicoureteric junction (VUJ) is also dilated, this would suggest a VUJ or bladder cause (see Fig. 11.10). Calculi most commonly become impacted within the few centimetres proximal to the VUJ, and can

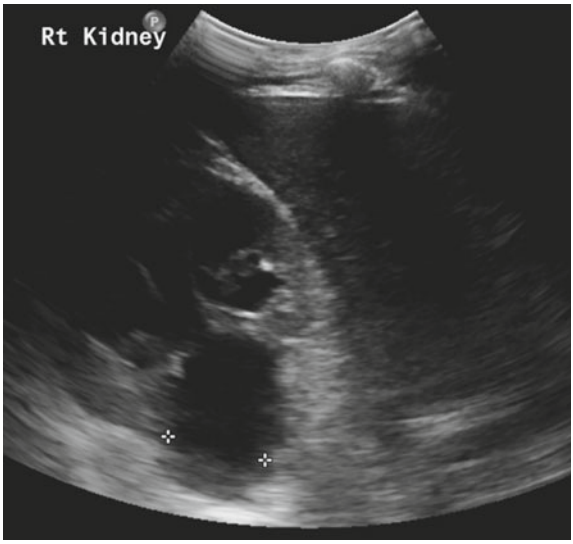

Fig. 11.6 Hydronephrosis with enlarged AP diameter

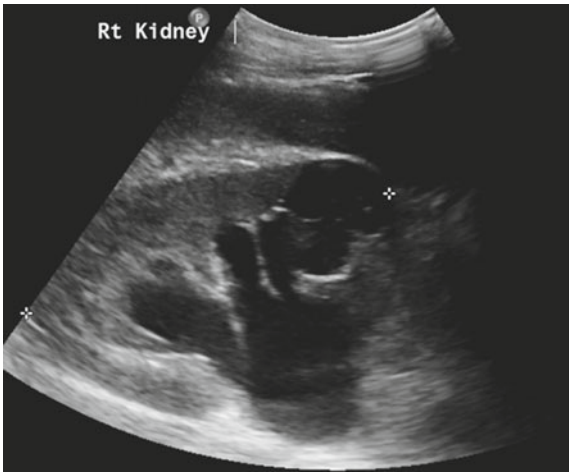

Fig. 11.7 Hydronephrosis

potentially be visualised at this site. Malignant encroachment of the VUJ can cause a spectrum of occlusion, both directly, and via external compression of the ureters away from the VUJ.

Non-calcular causes of hydroureter, include deficiencies of ureteric implantation, such as ureterocele and ureteric reflux, sometimes associated with ectopic implantation. Ureteroceles are seen as abnormally large bulges into the bladder and an ectopic VUJ will have an abnormal site.

In cooperative patients, bladder can be imaged pre- and post-micturition to derive a residual post-micturition volume, which should be less than 65 ml in

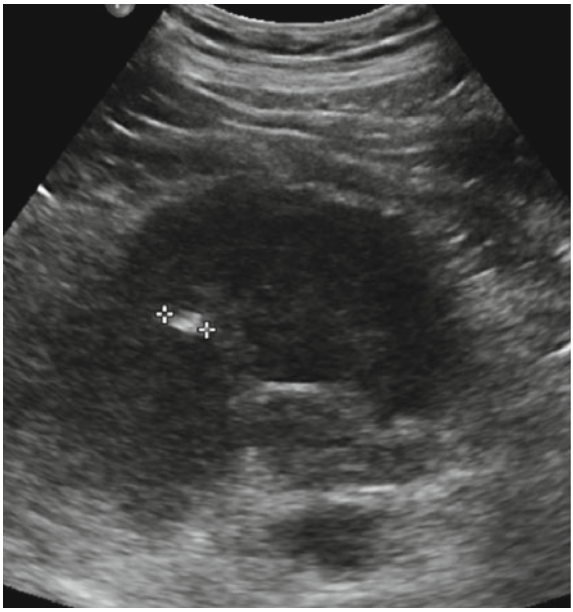

Fig. 11.8 Example of calculus

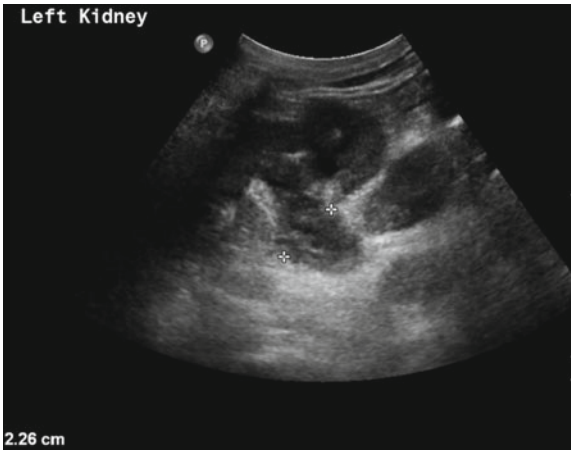

Fig. 11.9 Proximal hydroureter caused by haematoma

young patients and 100 ml in older patients (see Figs. 11.11 and 11.2). Benign prostatic hypertrophy is the most common cause in men and this can lead to bilateral hydroureter and hydronephrosis.

Haemorrhage into the bladder can occur from the bladder wall, prostate or from the upper tracts and differentiating the swirled heterogeneous pattern of haematoma from tumour can guide appropriate further imaging (see Figs. 11.13 and 11.4).

Obstructed collecting systems are more prone to becoming infected and gross hydronephrosis can lead to medullary infarction through the pressures involved.

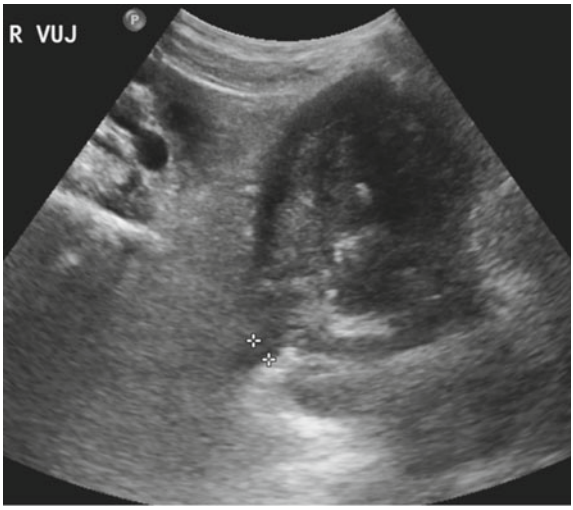

Fig. 11.10 Hydroureter extending to the vesico-ureteric junction

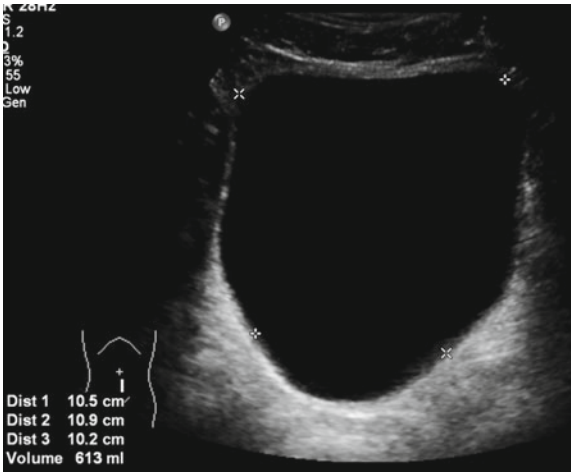

Fig. 11.11 Coronal bladder volume

Often the proximal ureter will rupture, which can be visualised as a perinephric collection, without septations. Septated peri-nephric collections are suggestive of either haematoma or abscess. Active extravasation can be demonstrated with simple colour imaging, as a high velocity jet within the collection. Abscesses will have hyper-perfusion in the periphery but should have no internal flow, often with hyperechoic contents.

Traumatic injury to the kidneys is generally manifested as disruption of the normal cortico-medullary pattern, with or without features of active extravasation. Peri-nephric collections (see Fig. 11.15) may be due to haematoma or due to extension of the laceration into the collecting system, resulting in a urinoma. CT is the optimal modality for confirmation and further assessment.

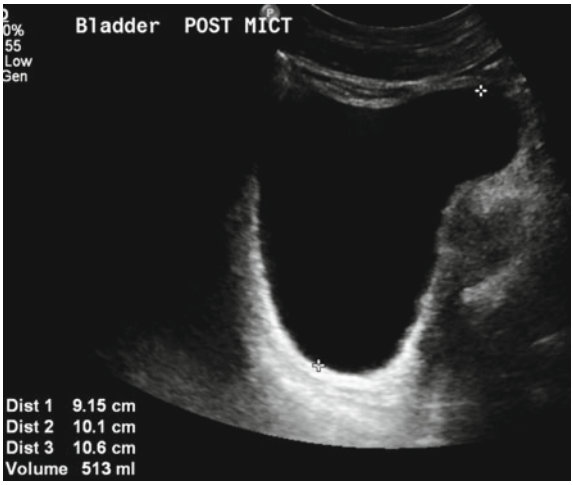

Fig. 11.12 Sagittal bladder volume

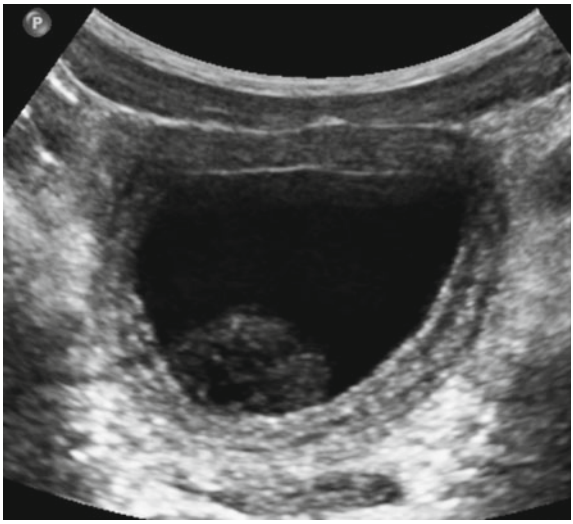

Fig. 11.13 Haematoma within the bladder

Renal cysts are common and most commonly are benign. Features of concern include septations within the cyst, particularly if thick and with vascularity on colour imaging (see Fig. 11.16). Thin calcifications in the wall are not of concern but more coarse calcifications can indicate worrying features. Any obvious soft-tissue components within a cyst is of concern and should warrant prompt referral for CT for further assessment (see Fig. 11.17). Additional renal cortical tissue known as a hypertrophic column of Bertin is a recognised normal developmental finding (see Fig. 11.18).

A relatively common markedly hyperechoic lesion is an angiomyolipoma, which is generally thought of as a benign incidental finding, but larger lesions (>4 cm)

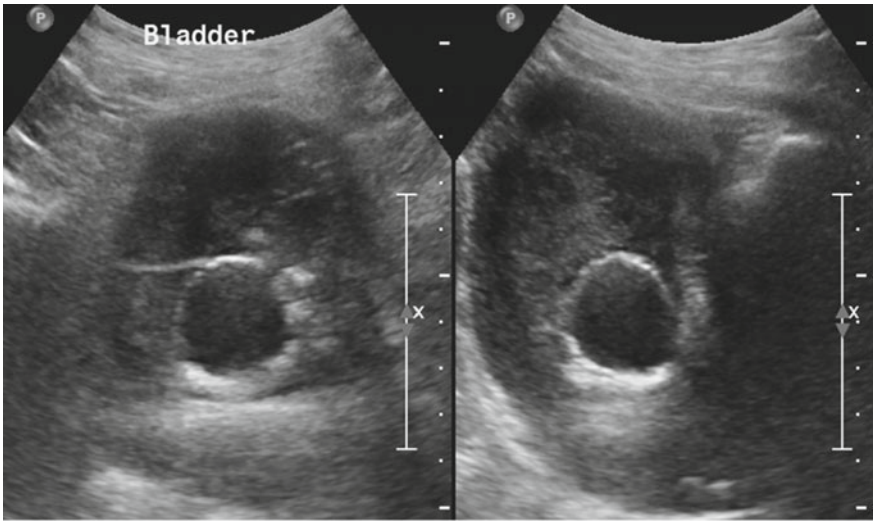

Fig. 11.14 Catheterised bladder with intraluminal haematoma

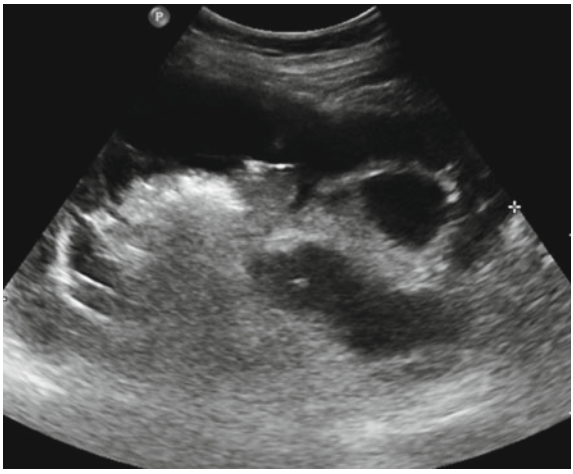

Fig. 11.15 Traumatic peri-nephric collection

warrant further investigation, due to the risk of catastrophic haemorrhage (see Fig. 11.19). Intra-parenchymal haematoma appears as a swirled coarsely heterogeneous echogenic mass, displacing normal parenchyma, particularly when large (see Fig. 11.20).

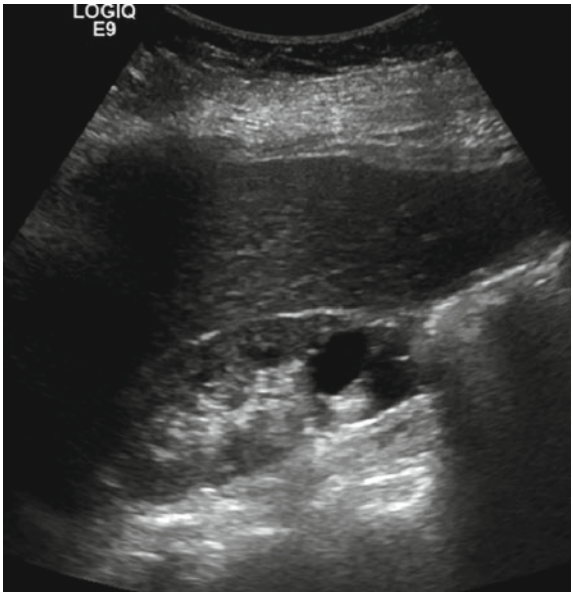

Fig. 11.16 Benign renal cortical cysts

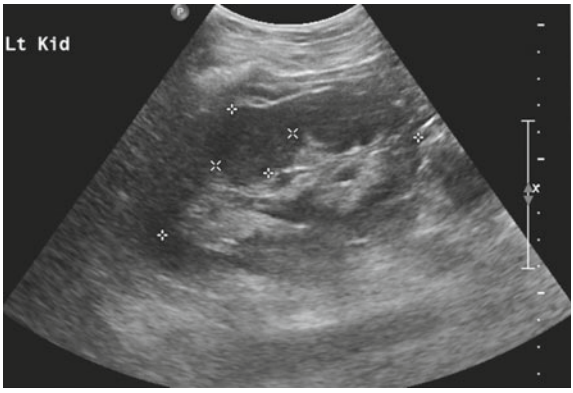

Fig. 11.17 Solid renal tumour

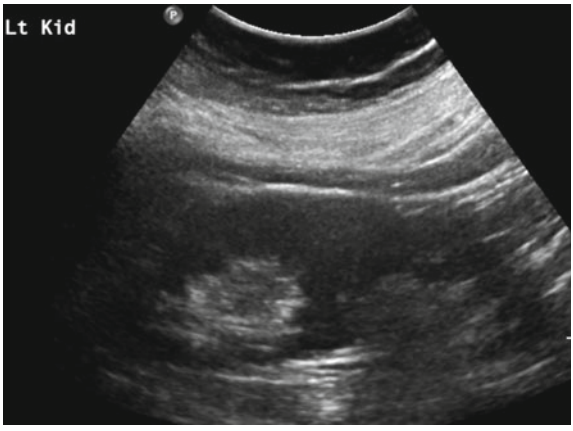

Fig. 11.18 Benign hypertrophic column of Bertin

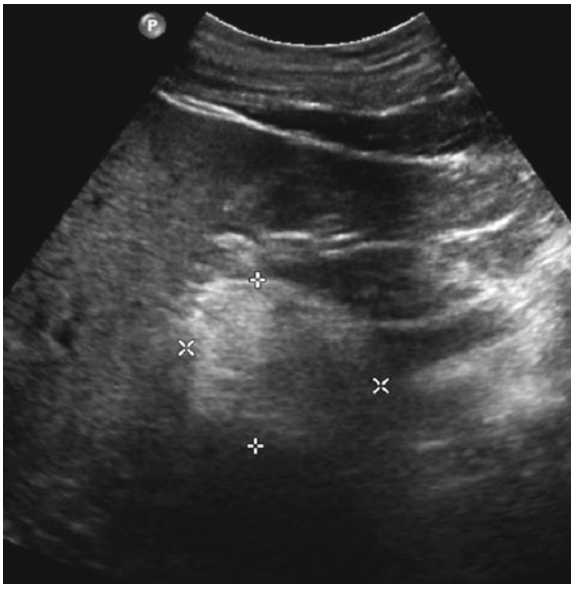

Fig. 11.19 Large angiomyolipoma

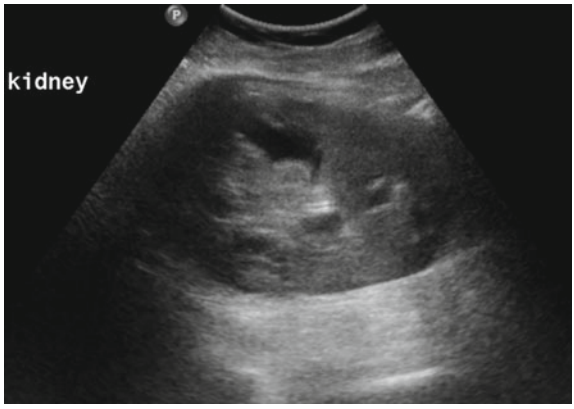

Fig. 11.20 Intra-parenchymal haematoma

11.5 Conclusion

Renal tract ultrasound is an essential investigation for patients with acute kidney injury but also where there is a concern about trauma or urosepsis. Establishing whether a patient has hydronephrosis early on in their admission can mitigate the need for renal replacement therapy if obstruction is relieved.

See also:

Chapters 12 and 13 Abdominal Ultrasound Chapters 10 FAST Scanning.

Chapter 20 The unconscious, Polytrauma Patient.

Chapter 23 The Patient with Acute Kidney Injury.

Chapter 24 The Patient with Acute Abdominal Pain.

Chapter 12
Abdominal Ultrasound—Liver, Spleen and Biliary Tree

James M. Pilcher and Pawan Patel

Keywords Abdominal ultrasound · Scanning technique · Liver parenchyma · Hepatic masses · Biliary obstruction · Splenic masses

12.1 Introduction

Focused abdominal ultrasound in critically unwell patients, can provide valuable diagnostic information regarding specific pathologies of the abdominal viscera or peritoneal cavity; evaluate blood flow within the main arteries and veins of the abdomen and be used to guide intervention procedures, such as percutaneous drainages [1]. The technique differs to that practised in radiology departments, where traditionally a comprehensive survey of the whole abdomen and pelvis is performed, instead targeting individual organs or quadrants of the abdomen, to answer specific clinical questions. In addition abdominal ultrasound in the acutely ill has its own challenges, with oedematous tissues, excessive bowel gas or free air in the post-operative patient, external monitoring devices, open wounds, limited patient positioning and ability to breath hold; all compromising either image quality or access to adequate views. In this chapter an approach to abdominal ultrasound in acutely unwell patients, followed by a description of ultrasound findings in a selection of pathologies affecting the liver, biliary system, spleen, bowel and peritoneum. The pathologies chosen are those that the author believes not infrequently arise as clinical queries and that can often be answered with the careful use of targeted ultrasound.

J. M. Pilcher (✉)
Consultant Radiologist, St George's University Hospitals NHS Foundation Trust, Blackshaw Road, Tooting, London SW170QT, UK
e-mail: James.Pilcher@stgeorges.nhs.uk

P. Patel
Locum Consultant, St George's University Hospitals NHS Foundation Trust, Blackshaw Road, Tooting, London SW170QT, UK

A. Walden et al. (eds.), *Ultrasound in the Critically Ill*,
https://doi.org/10.1007/978-3-030-71742-1_12

12.2 Artefacts

When scanning the upper quadrants of the abdomen, the operator should be aware of potential artefacts generated by air-tissue and fluid-tissue interfaces. The mirror image artefact can potentially be generated at any air-tissue interface, which in the upper quadrants is typically the interface between either the liver or spleen and the pleura-aerated lung interface against the diaphragm. The artefact generates a faint image of the liver or splenic architecture on the cranial side of the diaphragm i.e. within the aerated lung (Fig. 12.1). This artefact will be lost in the presence of a pleural effusion, which itself can be a helpful diagnostic finding. If the is a small amount of fluid partially surrounding the liver or spleen, at certain scanning angles a diffraction artefact can be generated, giving the impression of a defect/step in the adjacent hemi-diaphragm (Fig. 12.2) [2]: this is a particular potential pitfall when scanning trauma patients.

Some of the artefacts encountered in the abdomen can be helpful by increasing diagnostic confidence. Acoustic shadowing is the loss of sonographic information beyond an interface or structure that is either strongly reflective or absorptive of ultrasound. Within the gallbladder, gallstones will generally generate this artefact, seen as a well-defined black/dark-grey line radiating down beyond the gallstone (Fig. 12.3). Likewise renal stones, if large enough, will also generate this artefact. Unfortunately gas within the bowel will do the same, preventing visualisation of deeper structures: although the nature of the shadowing is different, being less defined and more mixed in its reflectivity (dirty shadowing). Acoustic enhancement occurs beyond structures that allow more sound through than the adjacent tissue interfaces, resulting in an increase in the brightness of the tissue beyond. Structures that are very uniform in their acoustic properties, or are low in density will typically

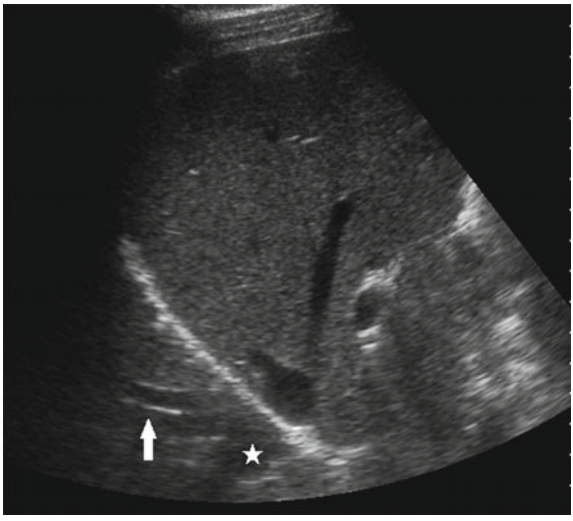

Fig. 12.1 Longitudinal oblique view of the right lobe of the liver and hemidiaphragm, the latter is seen as a curvilinear echogenic interface. The hepatic veins (arrow) and IVC (star) are seen cranial to the hemidiaphragm due to mirror artefact

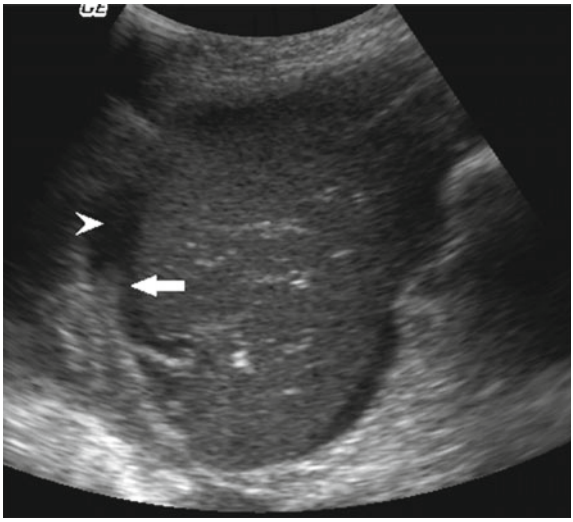

Fig. 12.2 Longitudinal oblique view of the spleen and left hemidiapharagm. There is a small volume of free fluid partially surrounding the spleen (arrowhead), which causes a diffraction artefact between the spleen and the left hemidiaphragm, making the latter appear fractured (arrow)

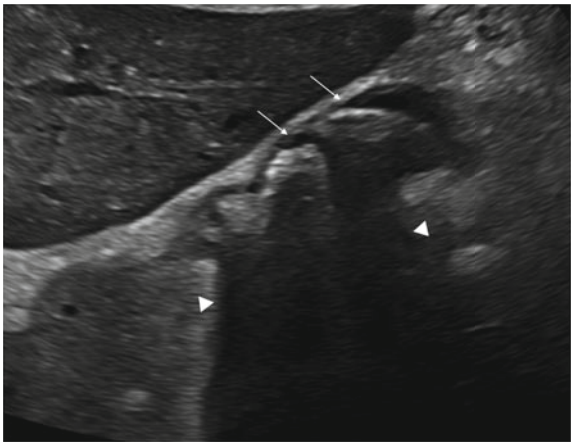

Fig. 12.3 Longitudinal oblique view through the gallbladder containing multiple echogenic gallstones (arrows). These are causing acoustic shadowing (arrowheads), with loss of tissue information beyond the gallstones

do this: such as a cyst in the liver (Fig. 12.4), or a solid mass with very uniform cell content within it such as lymphoma. Reverberation artefact occurs where the returning echo from a strongly reflecting surface, reflects back and forth between that interface and another strongly reflecting surface (usually the skin surface-probe interface) to produce equally spaced linear echoes that weaken over depth. Intensivists are very familiar with this artefact in lung ultrasound and likewise in the abdomen this can be seen distal to a straight, continuous air interface in the bowel, or when there is free air adjacent to the anterior peritoneum.

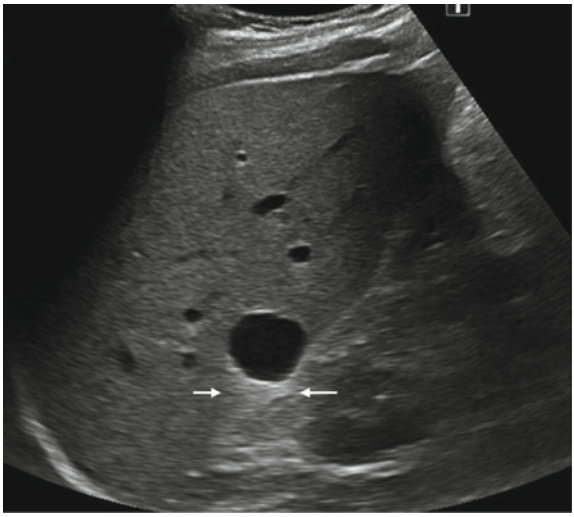

Fig. 12.4 A simple cyst in the liver demonstrates increased parenchymal reflectivity beyond the posterior wall of the cyst (arrows), known as acoustic enhancement

12.3 Scanning Technique

The vast majority of abdominal ultrasound examinations carried out on the intensive care unit can be performed to a satisfactory diagnostic standard using a standard curvilinear array, operating in a frequency range of between 2 and 6 MHz. Occasionally it is useful to have the option of a higher frequency linear array, such as the vascular access probe, to perform targeted assessment of the liver surface, bowel loops, and peritoneum. The abdominal preset should be selected and the operating frequency of the probe optimised for the patient being scanned: the lower frequency option being selected for the more challenging patient. On modern machines this is often labelled as either: resolution, general, penetration setting; or easy, medium and difficult. There is also usually the option of turning on or off harmonic imaging, which can improve tissue contrast and reduce clutter in the image. Further adjustments to the grey scale image can be made by adjusting the extent of compound imaging used in generating the image, improving edge definition, but also smoothing the image (Fig. 12.5). The depth should be adjusted to display the entire organ under investigation and as a general starting point setting the depth to 15 cm should allow adequate visualisation of most of targeted organs described in this chapter. If the focal zone can be adjusted, this needs to be set at the level of diagnostic interest and therefore may require repeat adjustment during the examination. If colour Doppler is being used the assess flow in the hepatic vessels, the colour box should be adjusted to only cover the area of interest and thought given to optimising the scale setting and gain control.

Although the intensivist will frequently perform a targeted approach to abdominal ultrasound in order to answer a specific question about one organ, the following description outlines a more general approach to the upper abdominal

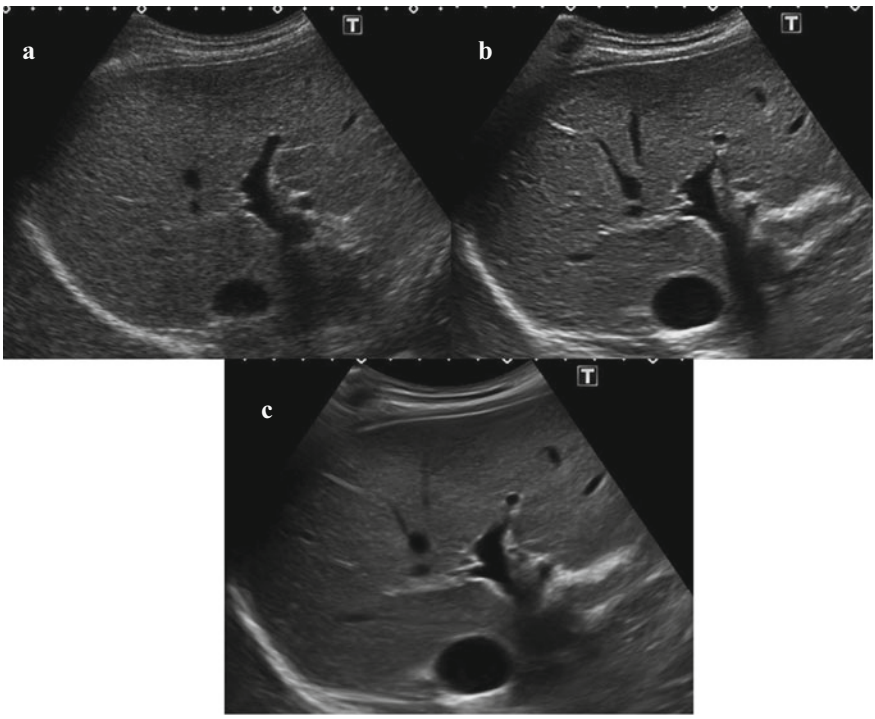

Fig. 12.5 Three identical views through the right lobe of the liver, with increasing image compounding (**a**, **b**, **c**). This progressively reduces the speckle (graininess) in the liver parenchyma and increases vessel wall definition

organs in an attempt to highlight their spatial relationship on ultrasound. The initial scan is performed with the patient in the supine position. The abdominal probe is placed transversely in the midline, just below the xiphisternum, with the side marker on the probe orientated towards the right side of the patient. By rocking the probe in an up and down motion, angled sweeps through the left lobe of the liver can be obtained without having to move the probe across the skin surface (Fig. 12.6): This sweeping approach will also usually cover the base of the heart, gastro-oesophageal junction, proximal aorta with its mesenteric branches, and part of the pancreas. The probe is then slid laterally to sit directly below the right costal margin and the same rocking action repeated to image the right lobe of the liver. This is repeated, sequentially repositioning the probe more laterally, until the whole of the right lobe of the liver has been covered. If the patient is able to breath-hold, then the image quality can be enhanced by performing these scan sweeps in suspended deep inspiration. If this is not possible, then further views of the liver can be obtained by placing the probe into one of the lower rib spaces, although the angled

sweep is then limited by acoustic shadowing from the ribs. The liver is then scanned in longitudinal section, by either sliding and rocking the probe along below the costal margin, preferably with the patient in arrested inspiration; or if the subcostal approach is limited, by scanning across the lower ribs while altering the angle of the probe to compensate for the rib shadows. Views of the far right lateral edge of the liver can also be obtained by placing the probe in the subcostal midclavicular line and angling the probe face towards the right shoulder to catch the posterior superior region of the right lobe (Fig. 12.6). Rolling the patient onto their left side, may also improve views of the lateral aspect of the liver, with the probe placed longitudinally along the anterior axillary line (subcostal or intercostal) and angled posteriorly. This latter approach is can also be used for gaining a longitudinal image of the gallbladder, although this is usually demonstrated just as well when the patient is supine, with the probe placed in an identical location. Transverse views of the gallbladder are obtained, using probe positioning as for transverse views of the right lobe of the liver. The porta hepatis can usually be seen with a longitudinal oblique approach similar to that for the gallbladder, but with the probe orientated less posteriorly. The common bile duct (CBD) can sometimes be seen well enough with this approach, but if not the patient is then rolled onto their left side and the probe placed directly over the line of the CBD in a midclavicular subcostal location, with the probe rotated slightly clockwise off the transverse (Fig. 12.6). A longitudinal positioning of the probe, just to the right of the midline can sometimes demonstrate the distal CBD as it passes through the head of the pancreas (Fig. 12.6). Going back to the starting position and moving to the left, identical positioning of the probe along the left costal margin and lower rib spaces, will afford views of the stomach, tail of pancreas and most of the spleen. A good longitudinal view of the spleen can be obtained, by placing the probe between the mid and posterior axillary line and rotating the probe obliquely so that it lies in one of the lower rib spaces: Sometimes this is easier to perform with the patient rolled slightly onto their left side, again rocking the probe to sweep through the spleen from anterior to posterior. Rotating the probe 90° in this location will enable transverse sweeps of the spleen, while sliding the probe caudally from this position will bring the left kidney into view. Because of the more posterior location of the spleen, breath holding is often unhelpful in improving its visualisation on ultrasound, as the lower lobe of the left lung extends down around it casting an acoustic shadow.

By adopting the above approach it is usually possible to fully assess the liver, gallbladder, biliary tree, stomach and spleen, with other abdominal structures captured during the sweeping motion at each probe position. For ultrasound of the bowel a more targeted approach is required and this is outlined in the section in the subsequent chapter on bowel. Likewise for the detection of intraperitoneal free fluid a more focused approach can be used, which includes the pelvis and this is also described in the subsequent chapter.

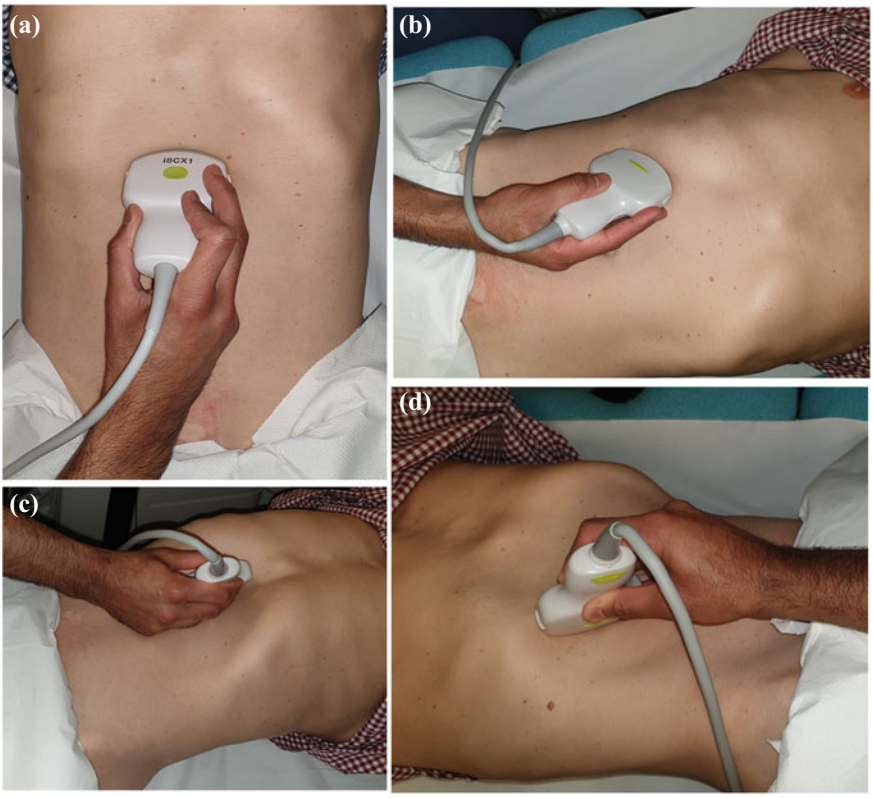

Fig. 12.6 Abdominal probe positions for: **a** Transverse sweep through the left lobe of the liver; **b** Additional views of the posterior superior right lobe of liver; **c** Longitudinal view along the common bile duct, with patient in the left lateral decubitus position; **d** Longitudinal view through the head of the pancreas to demonstrate the distal CBD

12.4 Liver

Ultrasound is the first line imaging technique for the liver on the intensive care unit, whether in the evaluation of the jaundiced patient, looking for a source of sepsis, confirming portal vein patency or assessing suspected hepatic venous congestion.

12.4.1 Anatomy

The liver lies in the right upper quadrant, and is made up of three lobes: the right and left lobe separated by the main lobar fissure, and the caudate lobe. The right and left lobes are further subdivided into anterior and posterior segments, and medial

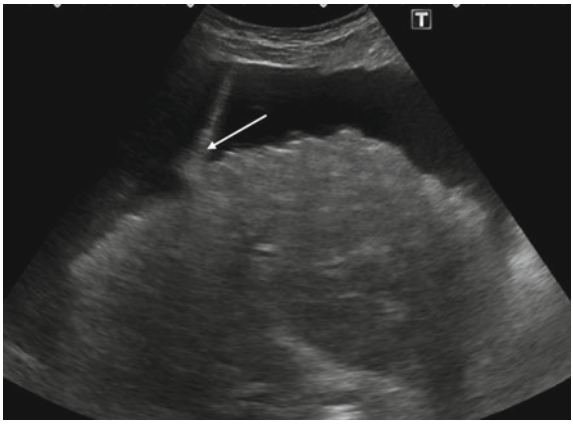

Fig. 12.7 Transverse scan through a cirrhotic liver, in a patient with abdominal ascites. The ligamentum teres and falciform ligament are seen as an echogenic triangle arising off the liver surface to reach the anterior abdominal wall (arrow)

and lateral segments respectively. It has a domed smooth superior surface, in contact with the right hemi-diaphragm and adjacent ribs, and a more contoured inferior or visceral surface that is orientated to face postero-medially. The liver is surrounded by Glisson's capsule, which on high resolution ultrasound can be appreciated as a thin linear echo along the liver surface. Adherent peritoneum then overlies most of the liver, except for the bare area posteriorly, which is bordered by folds in the peritoneum, namely the right and left triangular ligaments and the coronary ligament, which divide the subphrenic and subhepatic peritoneal spaces. Although these ligaments are not seen at ultrasound, anteriorly the falciform ligament and ligamentum teres can be seen in the presence of ascites, as an echogenic triangular structure arising off the anterior surface of the liver and extending down to the umbilicus (Fig. 12.7). The ligamentum teres contains tiny veins, normally invisible at ultrasound, but these dilate in patients with portal hypertension and can then be identified with colour Doppler, shunting portal venous blood to the umbilicus (Fig. 12.8).

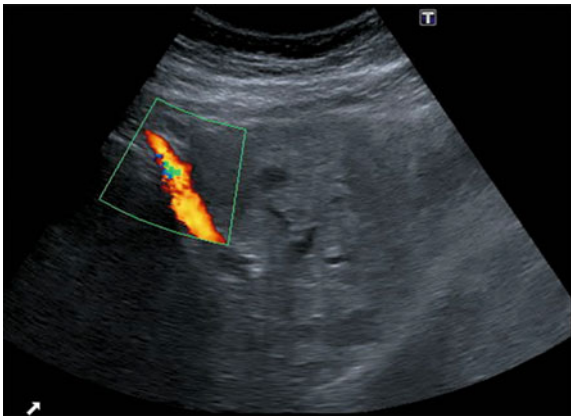

Fig. 12.8 Transverse view through the left lobe of the liver with colour Doppler showing large collateral vein exiting the liver in the ligamentum teres towards the umbilicus

Vascular input to the liver is from the portal vein (approximately 75% of inflow) and the hepatic artery (25%).These enter the liver at the porta hepatis, with the portal vein positioned posterior to the hepatic artery and the adjacent common hepatic duct. Positioning the abdominal probe in an oblique orientation along the right anterior axillary line can demonstrate this vascular anatomy nicely and enable Doppler assessment of the main portal vein (Fig. 12.9). On this view the portal vein is relatively straight, while the hepatic artery is more tortuous and may not be seen in its entirety. Just before entering the porta the hepatic artery divides into right and left branches, with the right hepatic artery passing between the portal vein and common hepatic duct to enter the liver: although there are a number of anatomical variations recognised. Within the liver the portal vein divides into right and left branches, with the right passing transversely through the liver for a short length before dividing into anterior and posterior branches, while the left branch curves anteriorly through the left lobe of the liver to divide into segmental branches. The intrahepatic portal veins have echogenic walls on ultrasound due to their fibromuscular walls, while the accompanying hepatic artery and bile duct increases the number of adjacent reflective interfaces. Three main hepatic veins drain the liver: the left runs between the medial and lateral segments of the left lobe of the liver, the middle hepatic vein lies in the sagittal plane between the right and left lobes of the liver and the right runs in a coronal plane between the anterior and posterior segments of the right liver. The left and middle hepatic veins usually join together before draining into the IVC. Due to their orientation and thin walls the hepatic veins usually appear as echolucent tubular structures on ultrasound (Fig. 12.10), with no wall interface, this appearance and their orientation within the liver enables their distinction from portal veins at ultrasound.

As already alluded to, the lobes of the liver are divided into segments using a classification originally described by a French surgeon Claude Couinaud [3]. A detailed description of this classification is beyond the scope of this text, but both the right and left lobes of the liver contain four segments; each with a central

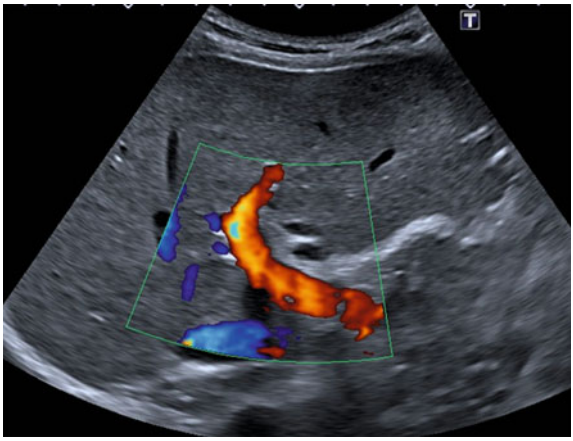

Fig. 12.9 Longitudinal oblique view through the main portal vein with colour Doppler confirming flow towards the liver i.e. coded red

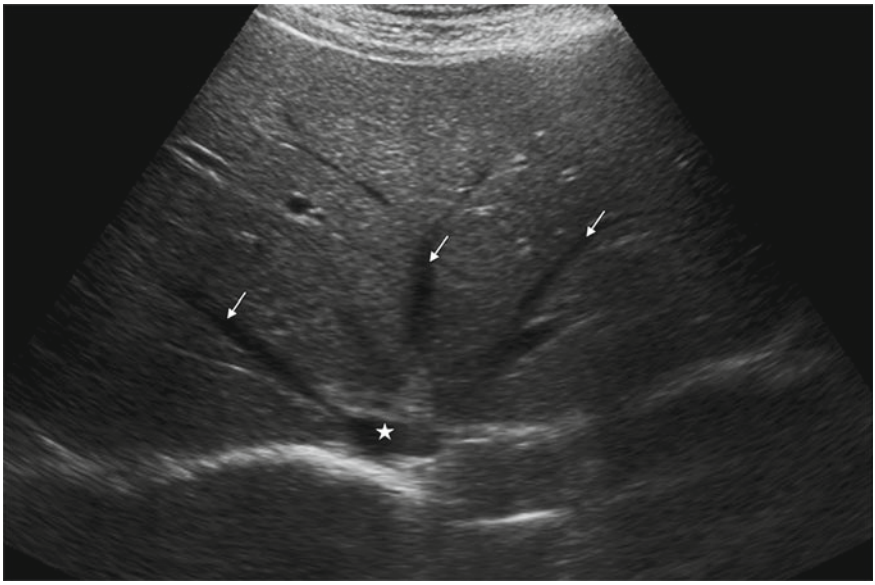

Fig. 12.10 Right subcostal transverse view through the liver showing the hepatic veins (arrowed) confluence with the IVC (star)

feeding portal vein, with adjacent segments margined by one of the hepatic veins (Fig. 12.11). The segments are numbered I–VIII, with segment I representing the caudate lobe, this lies posterior to the rest of the left lobe of the liver, which contains segments II–IV. The right lobe contains segments V–VIII, with V and VIII

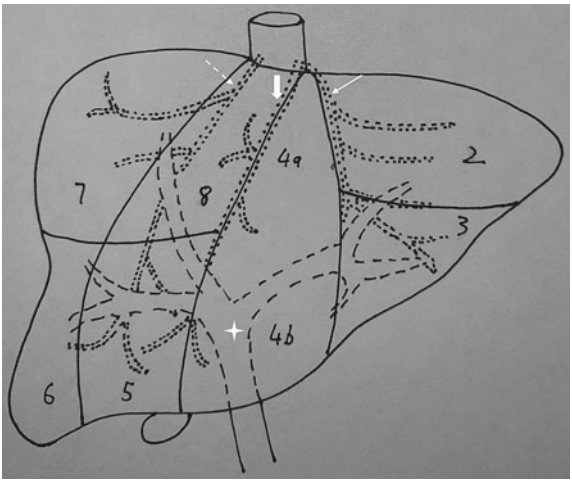

Fig. 12.11 The Couinaud classification divides the liver into eight segments, each of which has its own blood supply and biliary drainage. The centre of each segment contains the portal triad, consisting of a branch of the hepatic artery, portal vein and a bile duct. Venous drainage is at the periphery of the segments from hepatic vein branches. The middle hepatic vein (thick arrow) divides the liver into the right and left lobes. The left hepatic vein (thin arrow) divides the left lobe into a medial (segment 4a and b) and lateral part (segment 2 and 3). The right hepatic vein (dashed arrow) divides the right lobe into anterior (segment 8 and 5) and posterior (segments 7 and 6) parts. The portal vein (star) divides the liver into superior and inferior segments. The caudate lobe is segment 1

Table 12.1 Dimensions of normal liver at abdominal ultrasound [4]

Diameter	Mean ± SD (cm)
Midclavicular Longitudinal	10.5 ± 1.5
Midclavicular anteroposterior	8.1 ± 1.9
Midline Longitudinal	8.3 ± 1.7
Midline anteroposterior	5.7 ± 1.5

positioned anterior to VII and VI. When scanning the liver, the right and left lobes can be targeted individually, allowing the segmental anatomy to be appreciated as described in the section on scanning technique.

12.4.2 Liver Size

Wide variation in the configuration of the liver makes overall assessment of liver size difficult. There are defined linear values, based upon measurements taken from 1000 healthy volunteers [4], enabling some assessment of right and left lobe size measured at the midclavicular line and midline respectively; this can be useful in certain situations, such as assessing chronic liver disease (Table 12.1). Comparing the relative size of the caudate lobe to the right and left lobe is also useful in this situation as the caudate may enlarge in cirrhosis or hepatic vein occlusion. Normally when scanning in the transvers plane, at the level of the porta, the diameter of the caudate should be less than two-thirds the diameter of the right lobe; while the anteroposterior distance of the caudate should be less than half that of the left lobe.

12.4.3 Normal Liver Parenchyma

It is important for the operator to be comfortable with how normal hepatic echotexture appears on their ultrasound system (it will differ slightly between ultrasound units), in order to detect parenchymal changes that may indicate disease. This may be due to underlying chronic inflammation, deposition disorders, end stage fibrotic disease or a reflection of altered metabolism. The main two patterns to recognise however are fatty change and cirrhosis.

Normal liver echotexture consists of fine interleaving echoes, producing a fairly consistent speckle pattern from the front to the back of the liver. However this pattern can be altered by the operator changing the scanning frequency, turning on/off harmonic imaging or altering the spatial compounding level and the operator should be comfortable with the impact these adjustments may have on the final image (Fig. 12.5). Normal liver reflectivity is described as similar or slightly brighter than that of the adjacent right kidney, providing the latter is normal, and therefore possibly a more reliable comparison is the spleen, which is typically slightly more echogenic than the liver. Within the liver, the portal tracts are usually quite reflective, seen as bright lines outlining the portal veins, while the hepatic veins usually have no reflective wall, unless they are scanned in a perpendicular orientation, with respect to the ultrasound probe.

12.4.4 Abnormal Liver Parenchyma

Fatty liver is one of the commonest abnormalities found on abdominal ultrasound, with many associations (Table 12.2), and is due to increased levels of triglycerides within the hepatocytes. It results in a diffuse increase in parenchymal reflectivity, the liver becoming more echogenic than the adjacent kidney and spleen, although the texture remains fine and uniform. In some cases however areas of focal fatty sparing can occur, typically around the gallbladder, next to the ligamentum teres and at the bifurcation of the main portal vein. These cause focal areas of relatively reduced reflectivity in the liver with rather geometric shapes, typically having straight edges (Fig. 12.12). Colour Doppler can be used to confirm normal anatomy of hepatic vessels passing through these areas of reduced reflectivity. Occasionally fatty change can take on a more rounded appearance within the liver and then closer interrogation is required, including the use of contrast enhanced imaging, to exclude an underlying mass lesion.

Diffuse fatty change is usually described as mild, moderate or severe; mild showing a slight increase in liver reflectivity, moderate when there is loss of hepatic vessel wall definition, with poor visualisation of the posterior liver and severe when there is very limited visualisation of the hepatic vessels, posterior liver and hemidiaphragm [5] (Fig. 12.13). Sometimes fatty change is more focal in the liver, when its shape and location is similar to that described above for focal fatty sparing, although these locations now appear brighter than the adjacent liver parenchyma. Again, as with focal sparing, normal hepatic vessels can be shown to pass through these areas on colour Doppler.

Cirrhotic patients carry significant co-morbidities and therefore it is important to be able to recognise these parenchymal changes in patients who are as yet undiagnosed. The cirrhotic liver can take on a number of appearances, depending upon it aetiology, presence of portal hypertension and associated malignancies. Typically

Table 12.2 Conditions associated with fatty liver

Common	Rare	Congenital
Alcohol	Pregnancy	Organic aciduria
NAFLD	Starvation	Aminoacidopathy
Obesity	Rapid weight loss	Glycogen storage disorders
Hyperlipidaemia	Total parenteral	α1—antitrypsin deficiency
Hepatitis B and C	nutrition Jejunal-ileal bypass Radiotherapy	Wilson's disease Haemochromatosis Cystic fibrosis
Drugs		
Steroids Chemotherapy		
Amiodarone Valproic acid		

NAFLD = Non-alcoholic fatty liver disease

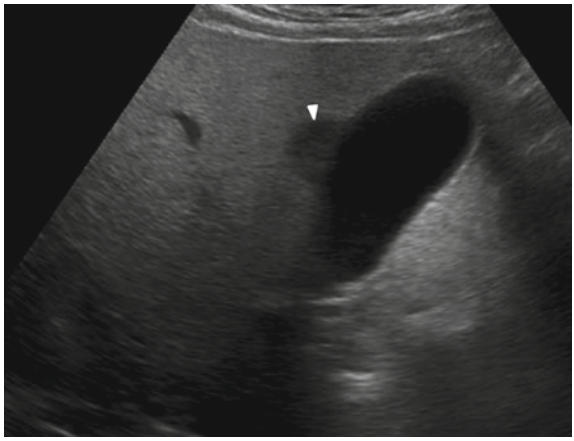

Fig. 12.12 Longitudinal oblique view through segment 5 of the liver shows a well-defined area of relatively reduced reflectivity, with respect to the background liver, adjacent to the gallbladder. The shape and location is typical for focal fatty sparing (arrowhead). The background liver shows diffuse increased reflectivity indicating steatosis

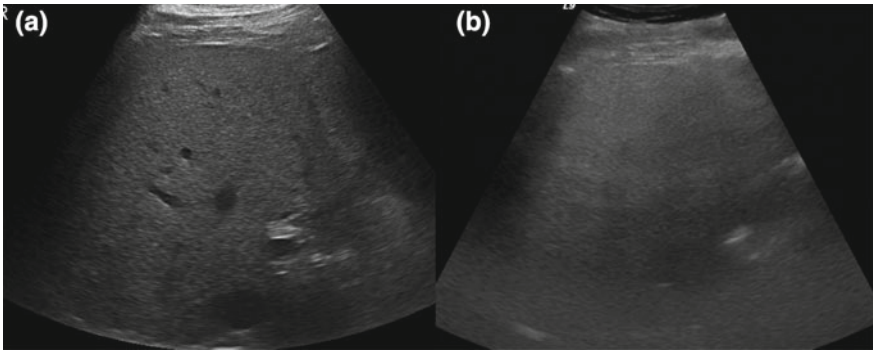

Fig. 12.13 Diffuse fatty liver: **a** Moderate fatty liver, with loss of vessel wall definition in the periphery of the liver and some loss of parenchymal detail towards the back of the liver. **b** Severe fatty change, with marked attenuation and almost no appreciation of hepatic vessels

there is a "coarsening" of the parenchymal liver texture due to focal regenerating nodules and surrounding fibrosis. Careful scrutiny of the liver surface shows an irregular contour due to focal nodules: which are seen more clearly in the presence of ascites (Fig. 12.14). If available, a more detailed evaluation of the liver surface contour can be made by switching to a higher frequency linear array probe (Fig. 12.15). There is often a reduction in size of the right lobe of the liver, with relative enlargement of the caudate lobe and with the onset of portal hypertension the portal vein becomes dilated (> 13 mm). If spectral Doppler interrogation is

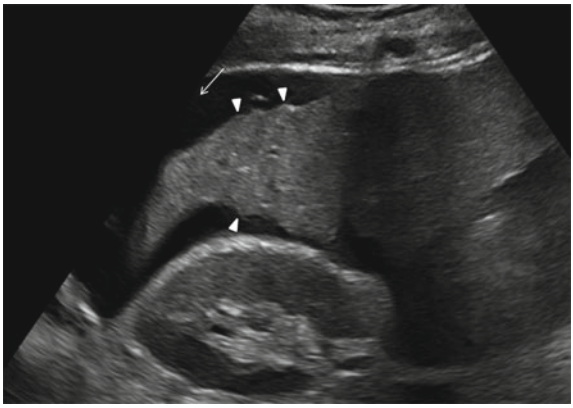

Fig. 12.14 Transverse view of a cirrhotic liver, with surrounding ascites (arrows) and underlying right kidney. The liver surface demonstrates a nodular contour in keeping with cirrhosis (arrowhead)

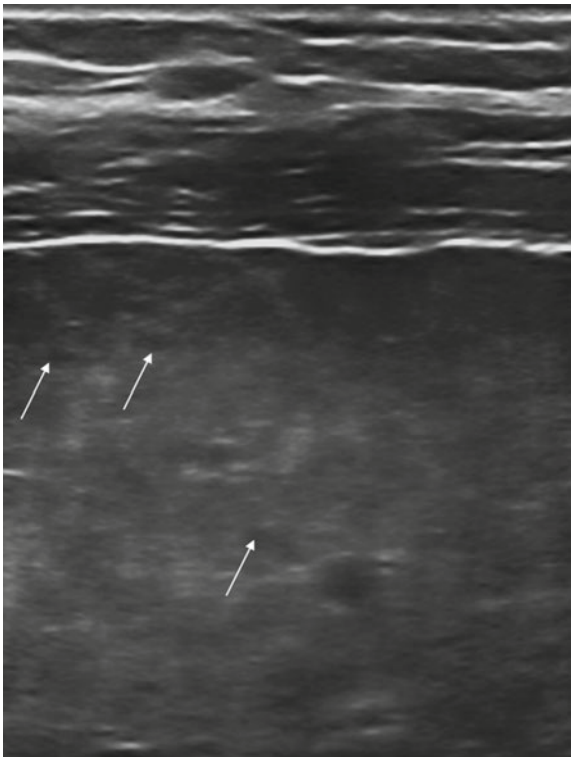

Fig. 12.15 Higher frequency linear array scan through liver that initially looked mildly heterogeneous on a curvilinear array. This confirms multiple low reflective nodules (arrows), surrounded by echogenic reticular pattern of fibrosis, consistent with cirrhosis

applied to the portal vein, an angle corrected peak portal vein velocity of <15 cm/s is consistent with portal hypertension (Fig. 12.16). Colour Doppler can be used to identify collateral vessels around the left lobe of the liver, small bowel mesentery and at the splenic hilum, where there may also be splenomegaly.

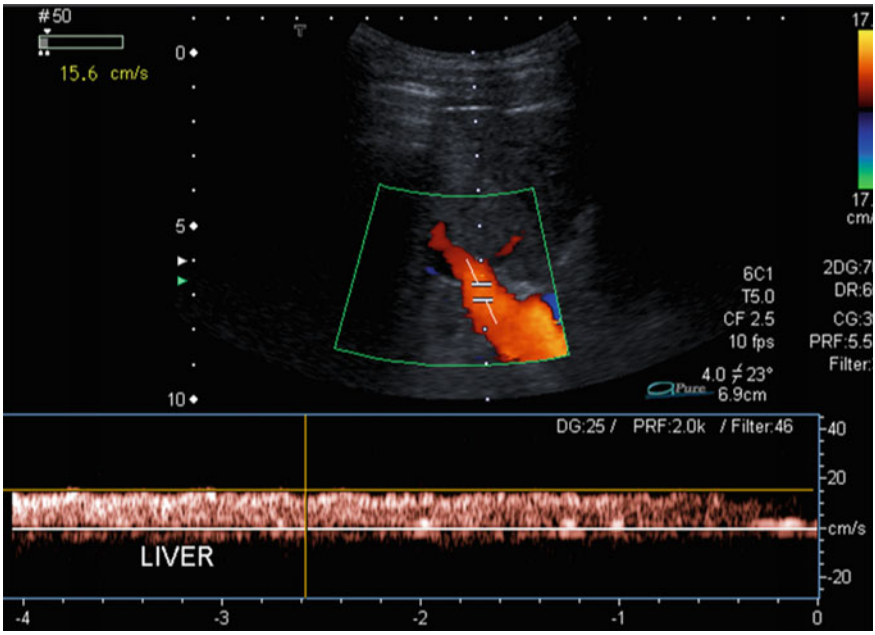

Fig. 12.16 Angel corrected spectral Doppler trace through the main portal vein, in a patient with cirrhosis, demonstrating a reduced peak portal vein velocity of 15.6 cm/s. The main portal vein is also dilated

12.4.5 Inflammatory Conditions

Inflammatory/infective conditions of the liver tend to be either diffuse or focal and ultrasound has an important role to play in both the initial identification of these and sometimes their management.

The inflammatory liver is a well-recognised, but non-specific pattern change seen in liver parenchymal echotexture and is likely to be a finding in a number of intensive care patients. Also known as the "starry sky" appearance, this represents an increase in periportal tract reflectivity, sometimes associated with a thickening of the bright interfaces outlining the portal veins. The background liver parenchyma is perceived as being darker than its usual mid-grey reflectivity (Fig. 12.17), and depending upon the underlying cause, the liver may also be slightly enlarged. Although these findings are often attributed to a diagnosis of viral hepatitis, when there is also typically gallbladder wall thickening [6], this has a broad differential diagnosis, including a normal variant in slim individuals (Table 12.3).

Pyogenic liver abscesses may result from direct extension of an infective process in the biliary tree, portal venous dissemination from an abdominal source, or haematogenous spread from a distant infection. On ultrasound pyogenic liver abscesses are highly variable in their appearance: sometimes resembling a simple

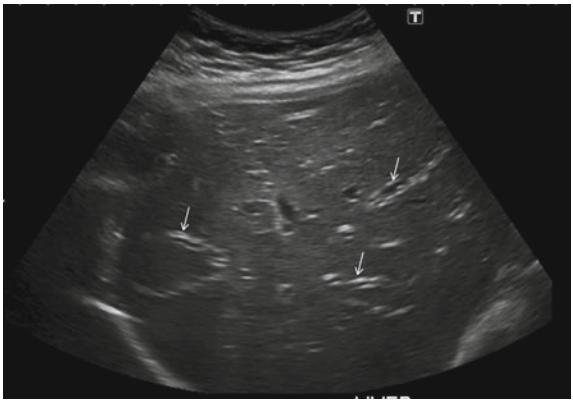

Fig. 12.17 Transverse view of the liver, showing increased reflectivity of the periportal tracts right out to the periphery of the liver (arrows)

Table 12.3 Differential for increased periportal reflectivity at liver ultrasound

Diagnosis	Additional findings
Acute viral hepatitis Infectious mononucleosis	Thick walled gallbladder Splenomegaly and lymphadenopathy
Toxic shock syndrome	
Congestive cardiac failure	Hepatic vein enlargement ± ascites
Periportal fibrosis Cholangitis	Coarsened liver parenchyma Thick walled common bile duct
Inflammatory bowel disease	Bowel wall thickening and hyperaemia
Schistosomiasis	
Burkitt'slymphoma	
Normals	

anechoic cyst to a solid echogenic mass, or multiple partially cystic nodules suggestive of metastatic disease. Early abscess formation often appears solid on ultrasound, but frequently demonstrates slightly reduced reflectivity and posterior acoustic enhancement, suggesting a more cystic content (Fig. 12.18). With progressive necrosis they become more heterogeneous in echotexture, with central cystic change containing debris, echogenic septations and if it is a gas forming organism, highly reflective foci showing reverberation artefact or shadowing [7]. Certain pathogens (e.g. Klebsiella Pneumoniae) however can result in a deceptively solid appearing lesion, with no through transmission of sound [8], although circumferential increased vascularity on colour/power Doppler may suggest an inflammatory process.

The sensitivity of ultrasound for detection of liver abscess is up to 97% [9], but the variable ultrasound appearances can overlap with those seen in haemorrhagic liver cysts, focal haematoma and malignant tumours. Where there is diagnostic uncertainty, further imaging with CT or MRI may be required, or if there is the relevant experience a contrast enhanced ultrasound (CEUS) study reveals a fairly

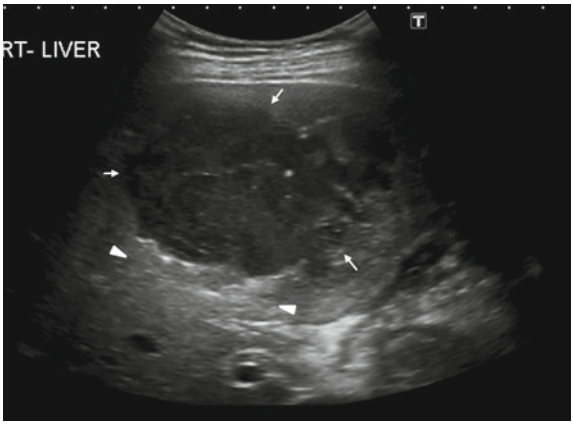

Fig. 12.18 Early liver abscess (arrows), with a mainly solid appearance, but through transmission of sound indicating this may be party liquefied (arrowheads). No internal vascularity was seen on subsequent Doppler interrogation

characteristic enhancement pattern in the region of the liver abscess [10]. Once confirmed, ultrasound can be used to guide either needle aspiration of the abscess or insertion of a pigtail drainage catheter. Although both of these techniques can expedite resolution of the abscess, a greater reduction in abscess volume can be achieved with single pigtail drainage [11] using ultrasound monitoring to ensure the drain remains correctly sited. If heavily loculated, or multi-focal in nature, attempts at percutaneous drainage may only produce a few millilitres of abscess content.

12.4.6 Focal Hepatic Masses

Focal liver lesions are not infrequently seen when assessing the liver with ultrasound and familiarity with some of the more common lesions and when to ask for further imaging is important for the operator. When assessing focal liver lesions, as for mass lesions elsewhere in the abdomen, the operator should determine: it's location in the liver, the relative reflectivity of the lesion with respect to the background visceral parenchyma; it's uniformity of texture; shape and margins; whether it is solitary or multifocal; look for any associated artefacts e.g. acoustic shadowing and use colour/power Doppler to determine whether it has increased or reduced vascularity. Some focal liver lesions can be confidently diagnosed with standard ultrasound alone, but many have features that overlap between benign and malignant. These will require further evaluation with CEUS, CT or MRI.

12.5 Haemangiomas

Cavernous haemangiomas are the commonest benign mass lesion in the liver with a prevalence of 0.5–20%. These can be multifocal in 10–50% of cases [12], more commonly seen in the right lobe and towards the periphery of the liver. The multiple interfaces generated by a combination of blood spaces and fibrous septae results in a relatively uniform echogenic, rounded, lobular mass, typically <3 cm in size (Fig. 12.19). This may show some posterior through transmission of sound on grey scale imaging, but due to the sluggish flow of blood within it, rarely demonstrates any flow on colour/power Doppler. If the ultrasound appearances are typical then no further imaging is required; however as they get larger, central areas of haemorrhage, necrosis and fibrosis, can result in a more heterogeneous pattern of reduced central reflectivity, although often maintaining their echogenic margin. These changes make confident diagnosis with ultrasound more challenging and will require either CEUS or MRI with contrast to confirm the typical enhancement pattern seen with haemangiomas. If very large, as with other benign liver masses, haemangiomas can cause symptoms through compression of the biliary tree, inferior vena cava, portal vein or adjacent viscera; all of which can potentially be demonstrated at ultrasound.

12.5.1 Hepatic Cyst

Seen in 2–4% of the population, simple hepatic cysts have a classical appearance on ultrasound of a rounded, anechoic structure, with an imperceptible wall and posterior acoustic enhancement. A single thin septation may be seen, but thick septations or echogenic mural nodules raise the possibility of a cystic mucinous tumour and require further evaluation with CEUS or contrast enhanced CT/MRI.

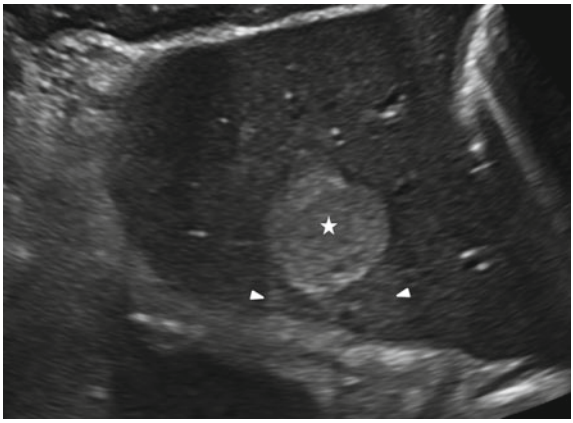

Fig. 12.19 Well defined, lobular, uniformly echogenic focal liver lesion (star), with posterior acoustic enhancement (arrowheads) in keeping with a hepatic haemangioma

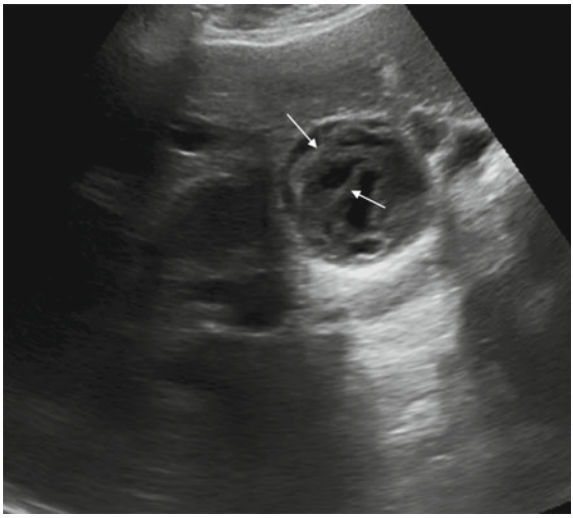

Fig. 12.20 Transverse view through left lobe of the liver showing a haemorrhagic cyst, with thick septations (arrows) and through transmission of sound, deep to the cyst. This will require further characterisation with contrast imaging (ultrasound, CT, MRI) to confirm there is no blood flow in the septations

Haemorrhagic change can also cause thickened septations, internal echoes and wall thickening, which requires further evaluation to confirm lack of enhancement in the septations (Fig. 12.20). Other complications of hepatic cysts are rupture and infection, both of which are rare in patients with only one or two cysts, but in patients with polycystic liver disease these complications become more common.

Polycystic liver disease is an autosomal dominant condition, sometimes associated with autosomal dominant adult polycystic kidney disease, resulting in multiple hepatic cysts throughout the liver (Fig. 12.21). Due to the sheer number of cysts, the complications already described are more likely to occur along with

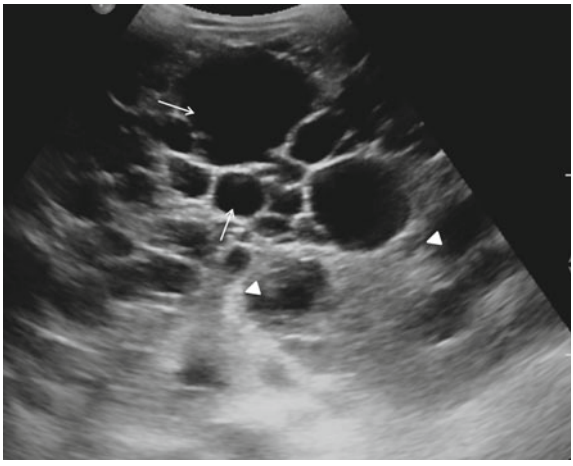

Fig. 12.21 Polycystic liver disease. The liver parenchyma is almost completely replaced by innumerable, well circumscribed, anechoic cysts (arrows). There are regions of posterior acoustic enhancement, in keeping with features of fluid content (arrowheads)

extrinsic compression of adjacent structures, namely the IVC, portal vein, biliary system and adjacent stomach.

12.5.2 Malignant Focal Liver Lesions

Liver metastases are the most common malignant liver lesion by a significant percentage, with the two most common primary tumours being hepatocellular carcinoma and cholangiocarcinoma. Liver metastases are typically multifocal, discrete lesions detected incidentally as they are usually asymptomatic. They are variable in their sonographic appearance, ranging from hypoechoic to hyperechoic or a mixed reflectivity; the classic pattern of the latter is of an echogenic centre, with hypoechoic margin (Fig. 12.22), also referred to as target lesions. Most metastases will show little if any vascularity on colour or power Doppler and assessment of vascularity in these lesions requires the addition of microbubble contrast or alternative cross-sectional imaging. Rarely extensive metastatic infiltration of the liver can present with obstructive jaundice due to intrahepatic compression of numerous biliary radicals. Hepatocellular carcinoma may present acutely with spontaneous rupture and subsequent haemoperitoneum, or portal vein thrombosis as a result of portal vein invasion. Both of these complications can be diagnosed at ultrasound (see later text). As with liver metastases, hepatocellular carcinoma is variable in its sonographic appearance, tending to be hypoechoic when small, with a more mixed, increased reflective pattern centrally as it grows in size [13]. The additional findings of satellite nodules, thrombosed adjacent veins and

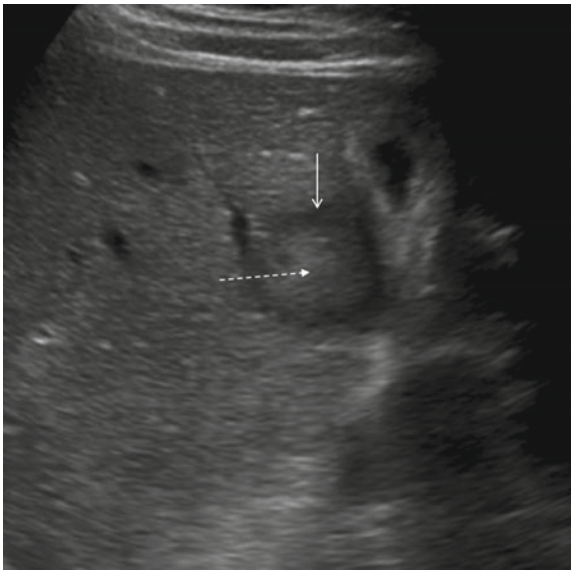

Fig. 12.22 "Target lesion": Focal liver lesion with an echogenic centre (dashed line) and hypoechoic peripheral rim (arrow). This appearance is strongly suggestive of a liver metastasis

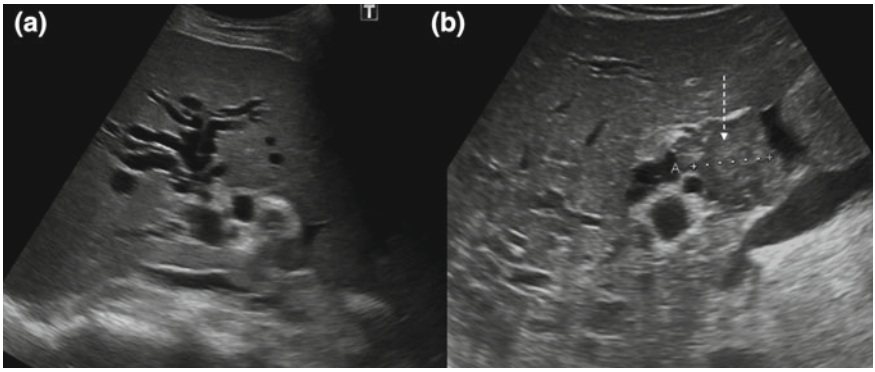

Fig. 12.23 **a** Transverse image through right lobe of liver showing numerous branching tubular structures (too many), in keeping with intrahepatic bile duct dilatation. **b** This is seen to be secondary to an obstructing lobulated mass at porta hepatis (dashed arrow)

detectable vascularity on colour/power Doppler also support a likely diagnosis of hepatocellular carcinoma, particularly in the presence of background cirrhosis. Intrahepatic cholangiocarcinomas are classified as either periductal -infiltrating or intraductal-mass forming and most commonly arise at the bifurcation of the hepatic ducts, resulting in intrahepatic duct dilatation in both lobes of the liver, obstructive jaundice and episodes of cholangitis. Sonographically the dilated intrahepatic bile ducts produce a crab-like pattern within the liver on transverse scanning, with the dilated bile ducts seen as black tubular structures radiating out from the porta (Fig. 12.23). The actual tumour itself can be difficult to appreciate on ultrasound, particularly the periductal type, often being relatively isoechoic to adjacent liver parenchyma, with the abrupt cut-off of the dilated intrahepatic bile ducts the only clue to the cause. Larger or intraductal tumours are more apparent on ultrasound and are of variable reflectivity. More peripherally located, lobar intrahepatic tumours tend to be clinically silent and at ultrasound there may be regional atrophy of the liver parenchyma, with crowding of the dilated bile ducts, adjacent portal veins and hepatic artery (Fig. 12.24). As with liver metastases, ultrasound suspected hepatocellular carcinoma or cholangiocarcinoma will require further characterisation with additional contrast enhanced cross-sectional imaging.

12.6 Portal Vein Gas

Gas within the portal vein is a rare finding on ultrasound and is associated with a number of conditions (Table 12.4), including bowel ischaemia, gastrointestinal sepsis and obstruction. Initially viewed as an imaging sign of mortal disease, there are increasing reports of reversible or more benign disease processes that can temporarily cause this phenomenon to be observed sonographically [14]. At

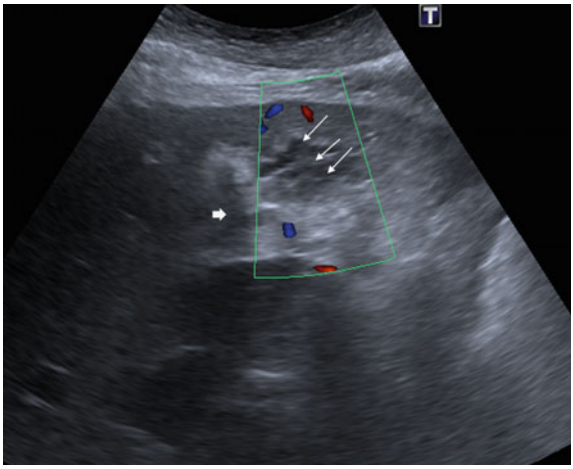

Fig. 12.24 Transverse view of the left liver, showing crowding of dilated ducts and port vein branches (arrows), due to atrophy of the left lobe. No flow is seen with any of these on Colour Doppler and the left portal vein (thick arrow), was also occluded. A central infiltrating mass was subsequently demonstrated on contrast ultrasound

Table 12.4 Conditions associated with portal vein gas [14]

Condition
Necrotising enterocoltis
Mesenteric artery occlusion
Hypertrophic pyloric stenosis
Ventral hernia Diverticulitis
COPD
Blunt abdominal trauma
Appendicitis
Crohn's disease Enterovascular fistula Perforated gastric ulcer Liver abscess

ultrasound tiny echogenic foci are seen to stream through the portal vein in the direction of portal vein flow, fanning out into periphery of the liver, causing multiple pinpoint echoes, which are more marked in the subscapular parenchyma. Spectral Doppler interrogation of the portal vein, will demonstrate thin spikes of high signal imposed on the normal portal vein trace and a distinctive cracking sound described as "the bubbling cauldron" (Fig. 12.25). This appearance can be distinguished from pneumobilia, which tends to be more central in its location in the liver and only moves with changes in patient position.

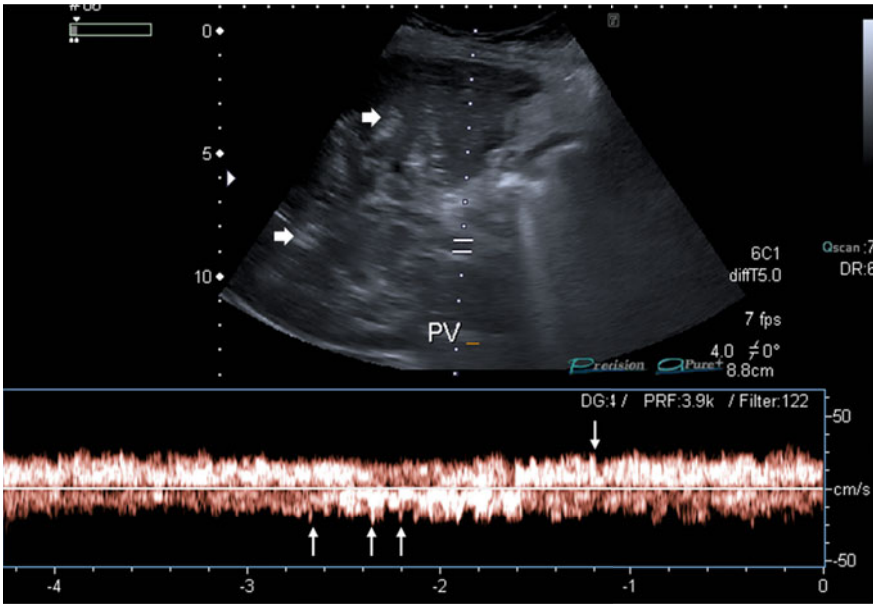

Fig. 12.25 Spectral Doppler trace of portal vein, showing multiple sharp spikes in the trace (arrows), due to portal vein gas. Branching echogenic regions are seen in the liver parenchyma (thick arrows) due to multiple gas interfaces

12.7 Portal Vein Occlusion

The two main causes for portal vein occlusion are thrombosis and tumour invasion, with the most common underlying pathology being portal hypertension secondary to cirrhosis. The more advanced the stage of cirrhosis the higher the risk for this complication to occur. In an acute thrombosis the portal vein may still appear anechoic and Doppler parameters will need to be optimised to ensure that there is not still very slow flow present: by reducing the Doppler scale, increasing the colour or spectral gain and if possible altering the Doppler frequency. If there is still uncertainty, then the use of an ultrasound contrast agent or contrast enhanced CT/MRI should be considered. In more chronic thrombosis the clot is more echogenic and may retract, with partial recanalization of the portal vein. A network of collaterals can develop around a chronically thrombosed main portal vein within a few weeks, seen on colour Doppler as a cluster of tortuous vessels, with continuous low flow entering the liver (Fig. 12.26).

Tumour thrombus tends to cause significant expansion of the involved portal vein and can be confirmed by the detection of arterial Doppler traces within the thrombus.

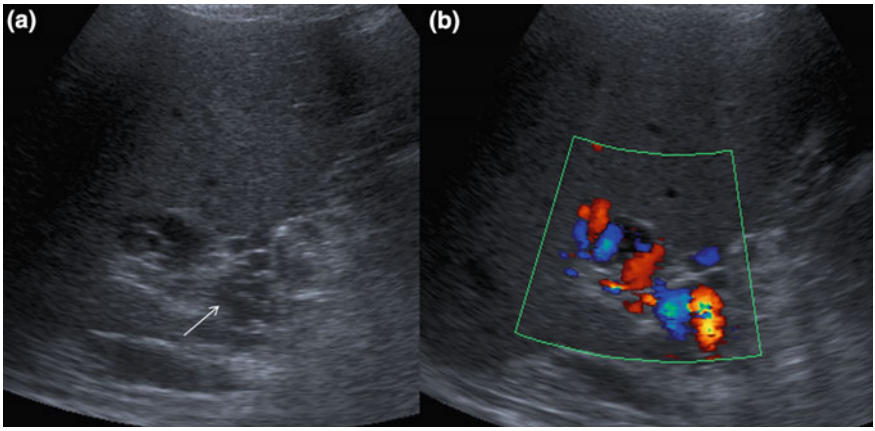

Fig. 12.26 **a** Longitudinal oblique view of the porta, showing a cluster of tortuous vessels at the hepatic porta indicated by serpiginous anechoic structures (arrow). **b** Colour Doppler confirms flow within these structures and absence of flow in the main portal vein, consistent with cavernous transformation

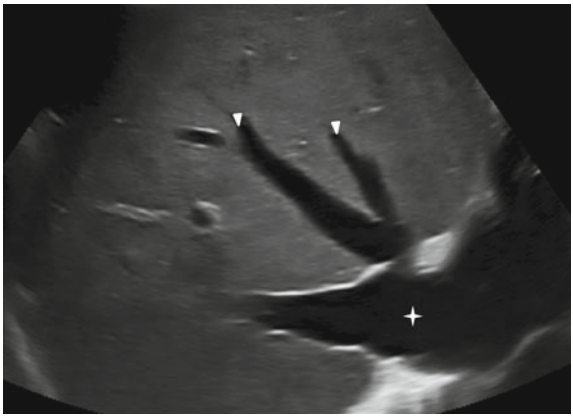

Fig. 12.27 Transverse view of liver showing dilated hepatic veins (arrowheads) at their confluence with the dilated IVC (star)

12.8 Hepatic Venous Congestion

Abnormal liver function tests are often found in patients with congestive cardiac failure due to passive hepatic venous congestion. Ultrasound of the liver will demonstrate dilatation of the hepatic veins, with no tapering of the veins at their confluence with the IVC (Fig. 12.27); this is best appreciated on a transverse view

through the liver at the hepatic vein confluence and has been referred to as "the playboy bunny sign" [15]. The retrohepatic IVC is also distended—adopting a rounded as opposed to oval contour on transverse scanning. The liver may be mildly enlarged and demonstrate increased periportal reflectivity.

12.9 Hepatic Venus Outflow Obstruction

In addition to hepatic venous congestion, veno-occlusive disease and Budd Chiari syndrome can also cause venous outflow obstruction and result in hepatomegaly. The former involves the venules at sinusoidal level, while in Budd Chiari the occlusion occurs at the level of the hepatic veins and/or the IVC between the liver and the right atrium, which can be acute or chronic. The findings at ultrasound therefore differ between these conditions. In veno-occlusive disease normal flow is seen on colour Doppler in the hepatic veins, but there may be reduced flow in the portal vein, with intermittent flow reversal, which may be confined to a single branch of the portal vein [16]. In acute Budd Chiari syndrome the liver may be enlarged, with enlarged proximal hepatic veins, or visible narrowing. Altered flow is demonstrated in the veins on spectral Doppler, with either a flat trace or reversal (i.e. towards the liver). With chronic disease, collateral veins may be seen between the main hepatic veins, either intrahepatic or subcapsular in location. The caudate lobe will frequently enlarge and can compress the IVC [17].

12.10 Spleen

12.10.1 Anatomy

The spleen lies in the left upper quadrant of the abdomen, with its long axis orientated along the line of the 10th rib. It has a smooth curved wedge shape, with the upper lateral convex wall in contact with the left hemidiaphragm. The concave side of the spleen has potential contact with the stomach, left kidney and flexure (splenic) of the colon. Within its concave face the splenic hilum is the vascular pedicle of the spleen, containing the artery, veins, lymphatics and nerves, with the tail of the pancreas lying along the line of the main splenic vein.

At ultrasound the convex surface of the spleen is smooth, while the concave surface may be more lobular, with the splenic hilum clearly appreciated by the entry and exit of relatively anechoic vascular structures, which can be confirmed using colour Doppler. The echotexture of the spleen is quite homogeneous, the reflectivity being slightly higher than the liver and visibly higher than the adjacent left kidney. The central artery of the spleen is seen to branch out forming the main segmental arteries; again this is better appreciated using colour or power Doppler (Fig. 12.28).

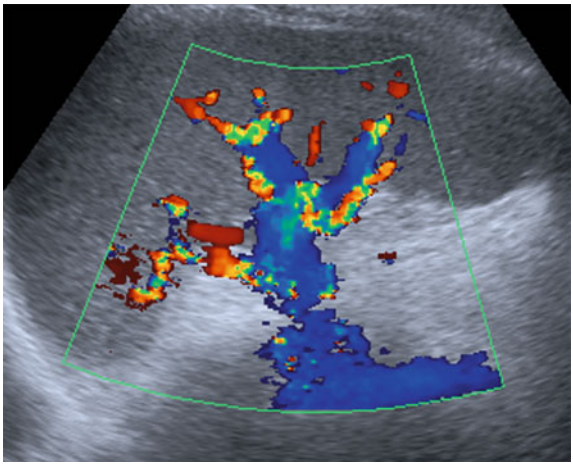

Fig. 12.28 Longitudinal view of the spleen showing normal arterial branching at the splenic hilum on colour Doppler (coded red)

10–30% of patients will have an accessory spleen (splenunculi), which failed to fuse with the main body of the spleen during its embryogenesis. At ultrasound these are seen as small (usually <2 cm) rounded or ovoid soft tissue masses, of similar echotexture to the main spleen. Most commonly these are closely related to the spleen or tail of the pancreas, but can lie elsewhere within the abdomen [18].

Rarely the spleen may lie in an unexpected location, including the pelvis. This wandering spleen is due to under development or elongation of its supporting ligaments and can result in misinterpretation of the spleen for an abdominal mass.

Another pitfall to be wary of is the adjacent stomach. In the presence of a gastric ileus or NG feed within the stomach, it can be misinterpreted at ultrasound for an air containing collection deep to or beyond the spleen (Fig. 12.29). Confirmation that

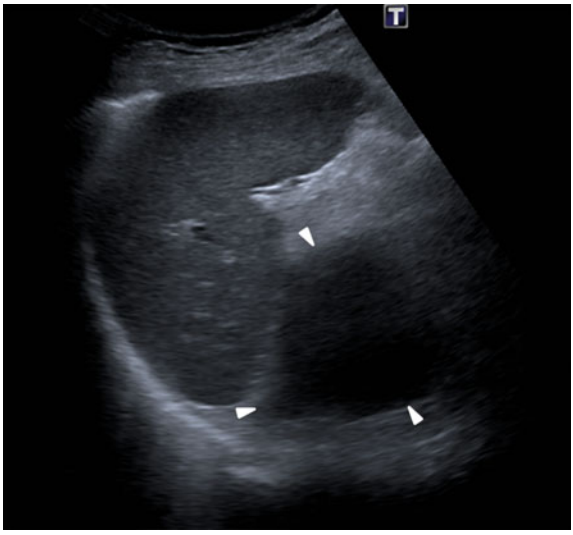

Fig. 12.29 Longitudinal oblique view through the spleen, with the stomach containing fluid and feed distal to this (arrowheads). This can be misinterpreted as a collection in the left upper quadrant

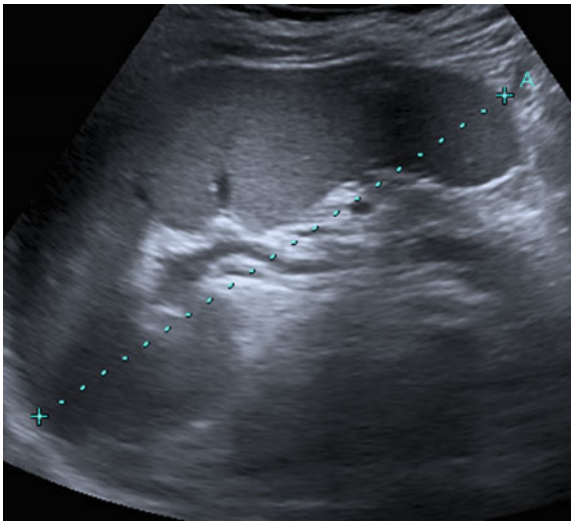

Fig. 12.30 Longitudinal view for measuring splenic length. The width can be measured by rotating the probe 90° clockwise for an anteroposterior measurement at the hilum

this is in fact the stomach can be made by scanning in the epigastric region, both in transverse and longitudinal plane.

12.10.2 Splenic Size

By placing the ultrasound probe within the 10th -11th intercostal space it should be possible to obtain a reasonable longitudinal image of the spleen, from which a splenic length and width measurement can be obtained (Fig. 12.30): sometimes this will require altering patient position as described above. Normal splenic length does vary according to patient age, sex, and body habitus, but a general rule of 12 cm as the upper limit of normal is usually accepted, with 12–13 cm seen as indeterminate and more than 13 cm (>5 cm antero-posterior width) enlarged. There are numerous causes of splenomegaly (Table 12.5) and it is usually not possible to identify the cause with ultrasound alone.

Splenic length <7 cm and width <3 cm is viewed as small, and may indicate functional hyposplenia [19].

12.10.3 Infarcts

Infarction of the spleen, may be either arterial or venous in origin, with haematological disorders a common cause in the younger patient and embolic events seen more in the older patient. Venous infarction may occur with portal or splenic vein

Table 12.5 Causes of splenomegaly

Pathological Process	Type	Example
Infection	***Viral***	Infectious mononucleosis, AIDS, CMV
	Bacterial	Tuberculosis, brucellosis, typhoid, Abscess
	Fungal	Histoplasmosis, candidiasis
	Protozoal	Malaria, Schistosomiasis, Leishmaniasis
Haemodynamic		Cirrhosis, Portal/Splenic vein obstruction, Budd Chiari, Right heart failure
Lymphohaematological	***Anaemias***	Sickle Cell, Thalassaemia, Spherocytosis, Pyruvate Kinase Deficiency,
	Myeloproliferative Lymphoma Leukaemia	Myelofibrosis, Polycythaemia Vera Hodgkin's Disease, Non-Hodgkins lyphoma Chronic Myeloid leukaemia, Chronic Lymphocytic leukaemia
Storage Diseases		Gaucher's disease, Niemann-Pick disease, Mucopolysaccharidoses
Connective Tissue		Rheumatoid arthritis, Systemic lupus Erythematosus
Neoplastic		Haemangioma, Lymphangioma, Angiosarcoma, Metastases
Trauma		Haematoma, Pseudocyst
Miscellaneous		Amyloid, sarcoid

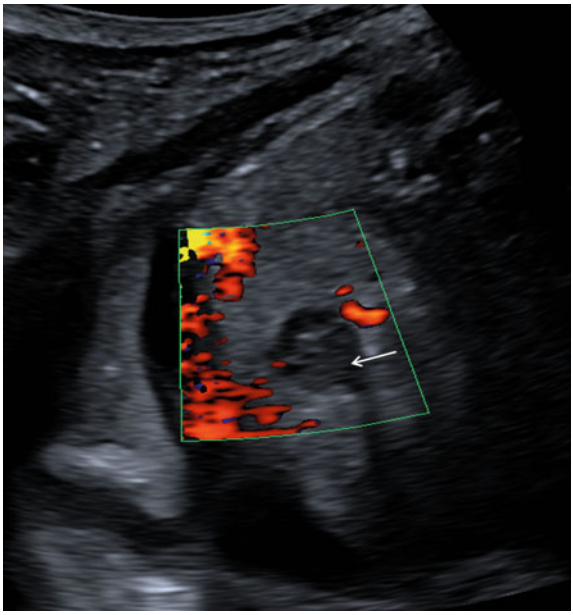

Fig. 12.31 Splenic infarct: Well circumscribed area of reduced reflectivity (arrow) in the spleen, with relatively straight margins and no associated power Doppler signal

thrombosis. It can be asymptomatic, present with left upper quadrant pain and sometimes fever, or other constitutional symptoms. Sonographically changes may not be apparent in the first 24 h. When visualised they are typically a peripherally based, wedge shaped region of reduced reflectivity, with the apex orientated towards the hilum of the spleen (Fig. 12.31). Colour Doppler can be helpful by confirming a segmental absence of blood flow in this region: although this is not always seen. Not all infarcts are wedge shaped however, with some taking on a rounded or oval contour, making it difficult to distinguish from other hypovascular splenic mass lesions. In these situations, the recognition of thin linear echogenic interfaces within the affected splenic tissue can increase operator confidence in diagnosing a focal infarct, rather than an alternative pathology [20]. As infarcts mature they tend to reduce in size, and become relatively echogenic with respect to the background spleen.

12.10.4 Abscess

Splenic abscesses are relatively rare and may be due to either bacterial, protozoal, or fungal agents. Bacterial infections are usually through haematogenous spread, but can also arise through direct spread of infection from adjacent organs (e.g. pancreas) or penetrating injury. The typical clinical presentation is with fever, left upper quadrant pain and a leucocytosis, but it can also be relatively asymptomatic, particularly in the immunocompromised patient. Sonographically abscesses can be single or multiple, with a variable appearance depending upon their aetiology. The typical appearance is of a rounded, but irregular thick-walled, low reflective, partially cystic lesion with some through transmission of sound seen in the splenic tissue beyond this. Rarely gas may be present within the abscess in which case there will be "dirty" acoustic shadowing beyond the strongly echogenic gas interface. Colour Doppler interrogation will typically show absence of any flow within the central component of the abscess.

In the immune compromised patient, involvement of the spleen by Mycobacterium tuberculosis or fungal infections such as Candida albicans can appear as multiple hypoechoic nodules [21, 22], which needs to be distinguished from lymphoma. Ultrasound findings in the rest of the abdomen can be helpful here, with the associated findings of ascites, intestinal wall thickening and lymphadenopathy suggestive of tuberculosis. Whereas Candida has a number of patterns in the spleen, most typically a 'wheel within a wheel' or 'bulls-eye' pattern, both of which demonstrate an echogenic centre to the hypoechoic nodule, the former with a further hypoechoic central nidus.

For both patterns of splenic abscess, diagnosis can be confirmed through ultrasound guided fine needle aspiration. For the larger focal abscess, percutaneous catheter drainage under ultrasound guidance is now the standard management approach rather than surgical intervention [23].

12.10.5 Cysts

Unlike the liver and kidneys splenic cysts are relatively uncommon and can be divided up into primary cysts, which include congenital cysts, parasitic cysts, cystic tumours, and secondary cysts or pseudocysts. True congenital cysts, also known as epidermoid cysts, are characterised by an inner endothelial lining and unless very large are usually an incidental finding. Typically, they are purely anechoic with a well-defined thin echogenic interface, best seen where the cyst wall is perpendicular to the ultrasound beam, and demonstrate posterior acoustic enhancement (Fig. 12.32). They can sometimes contain fine internal echoes from cholesterol crystals and thin echogenic septations have also been reported [24].

Parasitic cysts are usually due to hydatid disease, the majority due to infection by Echinococcus granulosusa which has a variety of appearances at ultrasound depending upon the stage of infection. The presence of multiple daughter cysts within the main cyst or a collection of central curvilinear echoes representing detached floating membranes are reported as pathognomonic for this condition [25].

Pseudocysts lack an epithelial lining and are either post-traumatic in aetiology, or are the sequela of previous infection or infarction. Usually they are sonographically indistinguishable from congenital cysts. The presence of wall calcification seen as echogenic foci, casting acoustic shadows, favours the diagnosis of a pseudocyst.

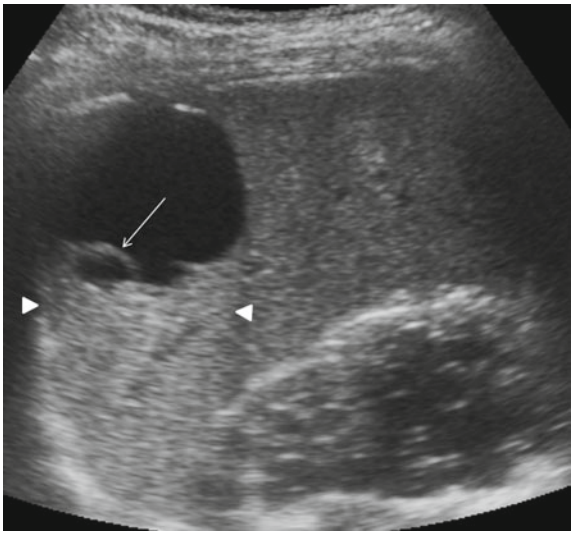

Fig. 12.32 Longitudinal view of the spleen, containing an anechoic, thin walled cyst, with a single echogenic septation (arrow). There is associated posterior acoustic enhancement (arrowheads), indicating likely fluid content

12.10.6 Focal Masses

Solid tumours of the spleen are rare, with benign lesions slightly more common. Uniformly echogenic solitary mass lesions <2 cm in size with mild posterior acoustic enhancement, can be assumed benign and are most likely cavernous or capillary haemangiomas [26, 27]. Atypical haemangiomas may be hypoechoic, partially cystic or contain shadowing echoes of calcification. These may require further characterisation with either contrast ultrasound [28] or MRI.

Lymphoma is the most common malignant tumour in the spleen and if detectable at ultrasound has a number of appearances including: multiple small or large hypoechoic nodules; infiltrating low reflective masses, or a more subtle diffuse alteration in splenic echotexture [29]. Multiple small echogenic nodules have also been rarely reported.

Metastases to the spleen are uncommon and primary non-lymphomatous malignancies of the spleen are exceptionally rare, both having variable appearances at ultrasound making accurate characterisation virtually impossible.

12.10.7 Rupture

Splenic rupture usually results from blunt abdominal trauma, but can occur through infection or haematological malignancy. In acute rupture of the spleen ultrasound can demonstrate fissures within the spleen as echogenic or low reflective clefts

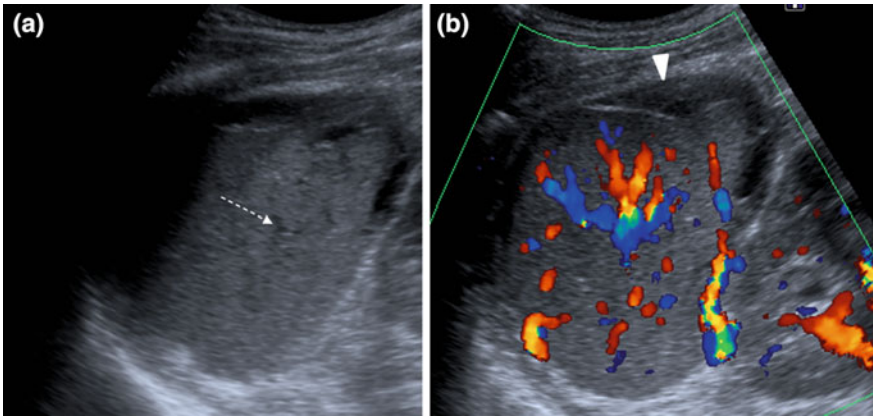

Fig. 12.33 Splenic trauma: **a** Longitudinal oblique view through traumatised spleen, with an irregular contour and low reflective lines within the parenchyma representing lacerations (dashed arrow). **b** Colour Doppler can help highlight perisplenic haematoma (arrowhead), through its lack of vascularity, as this can sometimes be isoechoic to the adjacent spleen

(Fig. 12.33) [30]. With increasing severity subcapsular haematomas of varying reflectivity are seen, which can be highlighted through colour Doppler, demonstrating the avascular rim of haematoma. Free fluid in the peritoneum is a non-specific finding indicating haemoperitoneum. Active haemorrhage is extremely difficult to demonstrate, even with colour Doppler, but post traumatic pseudoaneurysms can be seen as a rapidly alternating colour flow pattern, inside a cystic like space. The primary assessment of splenic trauma however remains contrast enhanced CT.

12.11 Gallbladder and Bile Ducts

Ultrasound is the first line imaging investigation for patients on ICU with jaundice, right upper quadrant pain or suspected sepsis/inflammation of the biliary tree. Careful systematic examination of the gallbladder, common bile duct and intrahepatic bile ducts may reveal gallbladder wall thickening, gallstones or sludge within the lumen, a peri-cholecystic collection suggesting perforation, or dilation of the common and or intra-hepatic ducts due to an intraluminal obstruction or from extrinsic compression.

12.11.1 Anatomy

The intrahepatic bile ducts run in the portal tracts of the liver, parallel to the portal vein radicals, and at the porta hepatis the right and left hepatic ducts join to form the common hepatic duct. This lies anterior to the main portal vein and continues inferiorly for about 3 cm before the cystic duct, from the gallbladder, joins it to form the common bile duct. The common bile duct then continues caudally, positioned anterior to the lateral margin of the portal vein, with the hepatic artery medial to it. It enters the head of the pancreas, where it turns laterally to drain into the second part of the duodenum, accompanied by the pancreatic duct.

The gallbladder is a pear-shaped reservoir, measuring 8–12 cm in length, with a thin wall (2 mm) made up of a mucosal lining, fibromuscular layer and serosal surface. It lies in a fossa on the under surface of the right lobe of the liver, with the distal fundus often projecting below the inferior margin of the liver. The proximal neck of the gallbladder curves back round on itself, heading caudally to become the cystic duct. This latter structure contains a number of mucosal folds—spiral valves—which can cast acoustic shadows at ultrasound, potentially mimicking calculi.

On ultrasound, the normal right and left hepatic ducts are visible as anechoic tubular structures, lying anterior to the right and left portal veins and measuring up to 2 mm in diameter. The more peripheral intrahepatic ducts are often too small to resolve. The common hepatic duct is usually seen on a right longitudinal oblique

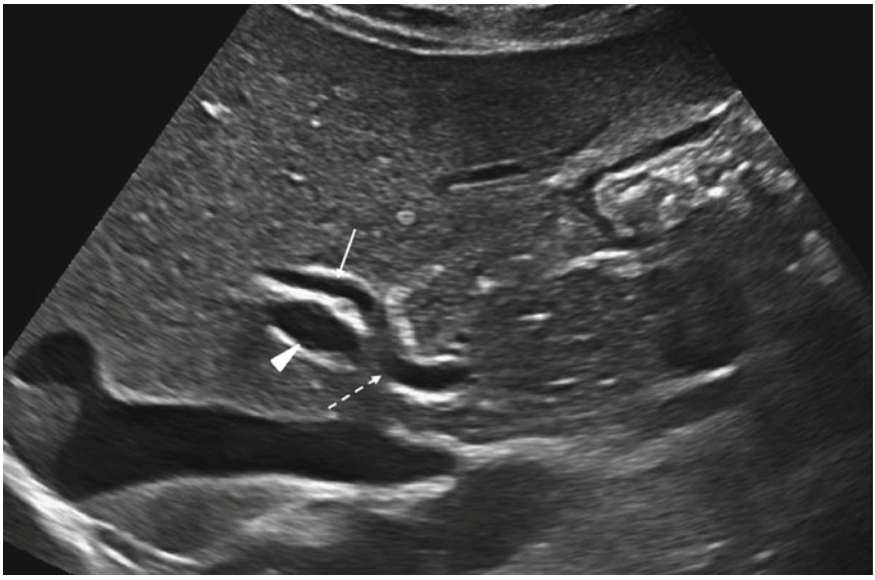

Fig. 12.34 Longitudinal oblique view of the porta, with the common hepatic duct (arrow) seen adjacent to the portal vein (arrowhead). Beyond the porta, where the duct tends to bend (dashed arrow), it is usually referred to as the common bile duct

view of the porta, measuring up to 5 mm (inner wall to inner wall) (Fig. 12.34). It is often difficult on ultrasound to determine the junction with the cystic duct, but beyond the porta the duct is generally assumed to represent the common bile duct; here it is allowed to measure up to 6 mm. In the elderly patient small increases in common duct diameter may be seen, although it should still remain below 6–7 mm

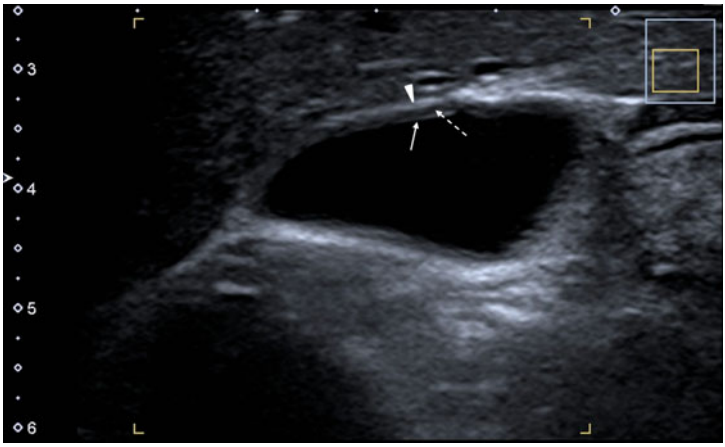

Fig. 12.35 Zoomed image of partially contracted gallbladder, with the mucosal interface (arrow), muscle wall (dashed arrow) and serosal interface (arrowhead) seen as three distinct layers

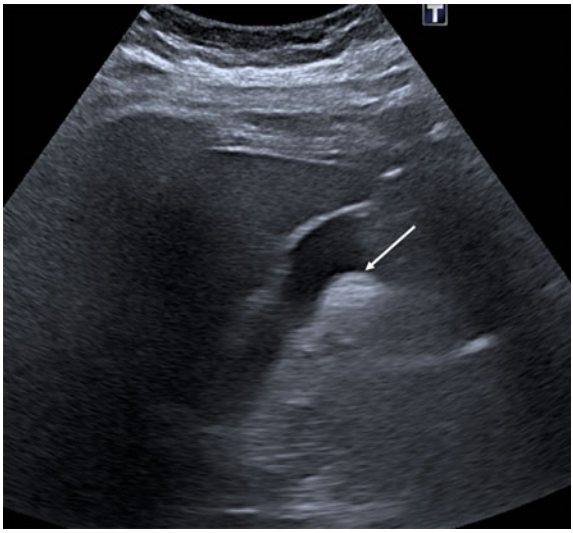

Fig. 12.36 Oblique longitudinal view through the gallbladder. In this rather limited view, gas within the duodenum (arrow) is seen as a rounded echogenic area that appears to lie within the gallbladder lumen and could be mistaken for a gallstone

[31]. Post cholecystectomy the common bile duct may increase in calibre, with acceptable limits up to 1 cm.

In the fasting state, the gallbladder lumen is anechoic and the wall is seen as a single echogenic interface, measuring <3 mm. This is best measured on a true longitudinal image of the gallbladder, from the anterior wall. Care should be taken to ensure the wall is truly perpendicular to the ultrasound beam to avoid artefactual thickening. There maybe be infolding of the wall of the gallbladder (mucosal folds), usually seen at the neck of the gallbladder or fundus, which can lead to interpretation errors. When contracted, the gallbladder wall has three visible layers, an outer and inner echogenic interface and a low reflective layer in between (Fig. 12.35).

In some patients the closely related duodenum can indent the posterior wall of the gallbladder, with echogenic gas in the duodenum giving the impression of gallbladder pathology (Fig. 12.36). Repositioning the patient, changing scanning approach or introducing some fluid into the duodenum can help clarify this, where there is uncertainty.

12.11.2 Gallbladder Thickening

A gallbladder wall thickness of >3 mm is considered abnormal in the normal fasting gallbladder: although measurements between 3 and 4 mm are viewed as indeterminate in their significance. Measuring the wall thickness in the transverse plane is not recommended, to avoid artefactual thickening of the anterior wall through scanning obliquely (Fig. 12.37). At the same time as measuring the wall thickness, assessment can be made for any evidence of gallbladder wall tenderness by gentle probe compression.

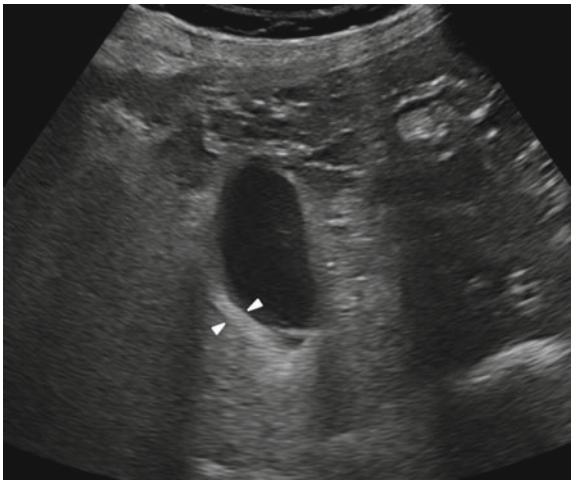

Fig. 12.37 An oblique transverse view through the gallbladder, demonstrating how the gallbladder wall can appear thickened (arrowheads). Subsequent longitudinal views confirmed normal wall thickness

Table 12.6 Causes of diffuse and focal gallbladder wall thickening

Diffuse	Focal
Physiological: Post Prandial **Cholecystitis**: Acute Chronic Gallbladder empyema Xanthogranulomatous Acalculous	**Polyps**: Cholesterol Adenomatous **Malignancy**: Gallbladder Carcinoma Metastases (rare) Focal Adenomyomatosis Focal Xanthogranulomatosis Adherent Gallbladder Sludge (pseudo-focal thickening)
Adjacent Inflammation: Hepatitis Pancreatitis Severe Pyelonephritis Colitis **Systemic**: Cardiac failure Renal failure Hypoalbuminaemia Sepsis **Hypertrophic:** Adenomyomatopsis **Malignancy**: Gallbladder Carcinoma Lymphoma	

The thickened gallbladder usually demonstrates a 3-stripe layer, with a central low reflective echo. Depending upon the underlying pathology, there may also be pericholecystic fluid or ascites present. In addition to acute or chronic inflammation, gallbladder wall thickening can be a result of non-biliary disease processes

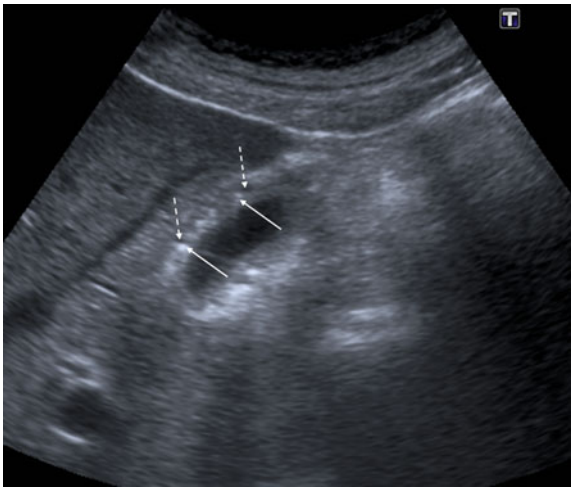

Fig. 12.38 Oblique longitudinal view of a partially contracted gallbladder, showing multiple echogenic foci in the anterior wall (arrows), some demonstrating comet tail artefact and associated cystic spaces (dashed arrows), typical for adenomyomatosis

including renal failure and AIDS [32]. There are a number of causes for gallbladder wall thickening which are listed in Table 12.6.

Focal thickening of the gallbladder wall can be seen in adenomyomatosis, where regional mucosal hyperplasia results in the development of intramural diverticular lined by mucosa: the Rokitansky-Aschoff sinus. Usually affecting the fundus of the gallbladder, these are seen on ultrasound as either tiny cystic spaces in the thickened wall, or if they contain cholesterol crystals/bile salts, tiny echogenic foci, with associated comet tail artefact (Fig. 12.38) [33].

12.11.3 Stones, Polyps and Sludge

At ultrasound the gallbladder lumen may contain: anechoic bile; echogenic bile salts; focal echogenic structures representing stones or polyps; or fine echoes from haemorrhage or biliary sludge.

Ultrasound is considered the gold standard test for gallstones, with sensitivity for their detection around 96%. Gallstones are typically seen as strongly echogenic, intra-luminal mobile structures that cast acoustic shadows (Fig. 12.39). The acoustic shadow seen with gallstones differs to that produced by bowel gas in the adjacent duodenum, having a much more defined edge and lacking internal echoes from reverberation. This is because the incident ultrasound beam is mainly absorbed by the stone rather than reflected, as it is at an air interface [34]. The acoustic shadowing artefact from gallstones can be enhanced by adjusting the focal zone to lie at the level of the stones, scanning using the highest frequency possible and altering the angle of insonation to a more perpendicular approach. Some small cholesterol stones (<3 mm) however may not cast acoustic shadows and in this situation, demonstrating their mobility is important to make the distinction between

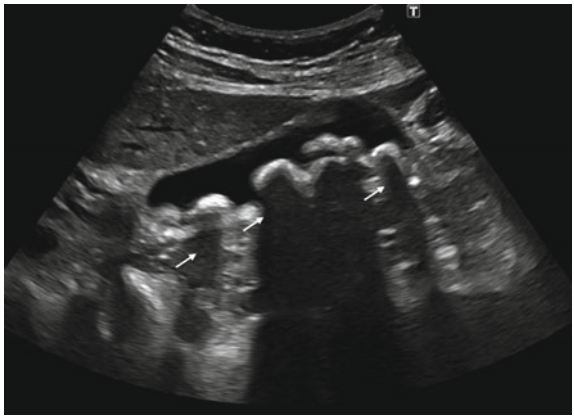

Fig. 12.39 Longitudinal oblique view through gallbladder, with normal wall thickness. Multiple gallstones are present casting several acoustic shadows (arrows)

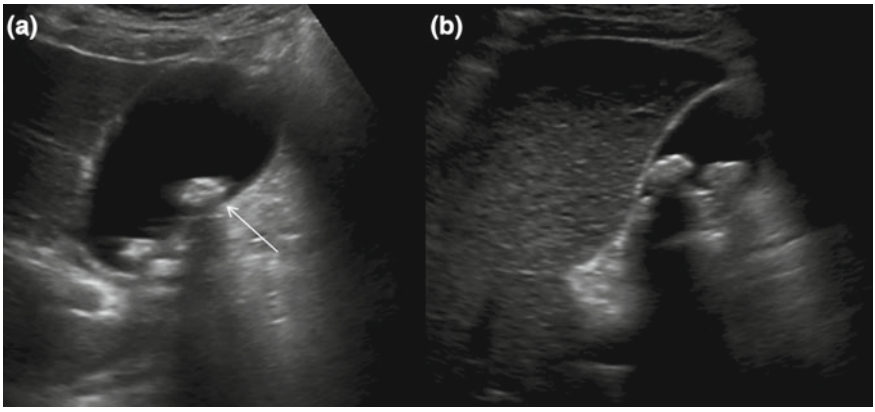

Fig. 12.40 **a** Supine position, dependent gallstones (arrow) along posterior GB body. **b** Left lateral decubitus position, gallstones have moved position, bunched up at GB neck

a stone and a gallbladder polyp. This often requires moving the patient, either onto their left side or even semi-prone and then repeating the scan to demonstrate a change in position of the stone (Fig. 12.40). Sometimes the gallbladder will be packed with stones and contracted, so that all that is appreciated at ultrasound within the gallbladder fossa is a double echogenic arc, representing the gallbladder wall and layer of stones, with an associated strong acoustic shadow. In this situation careful scanning of the gallbladder fossa from different planes is required to distinguish this from adjacent bowel (Fig. 12.41).

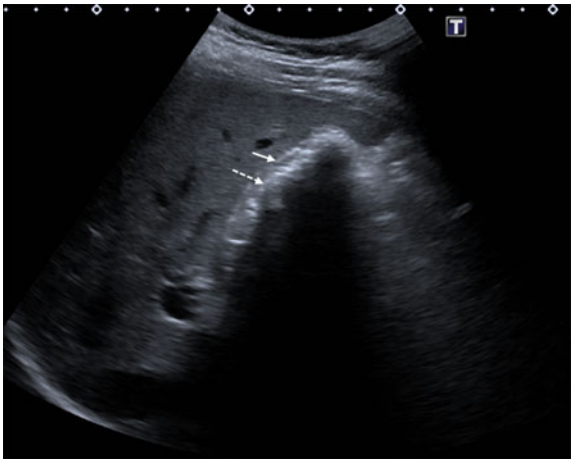

Fig. 12.41 Oblique longitudinal view of the gallbladder, which is packed with stones, giving a "double arc" echogenic interface. The outer arc (arrow) represents the gallbladder wall and the inner (dashed arrow) the gallstones. This is also known as the "wall-echo-shadow" sign, with the "shadow" referring to the acoustic shadow from the gallstones

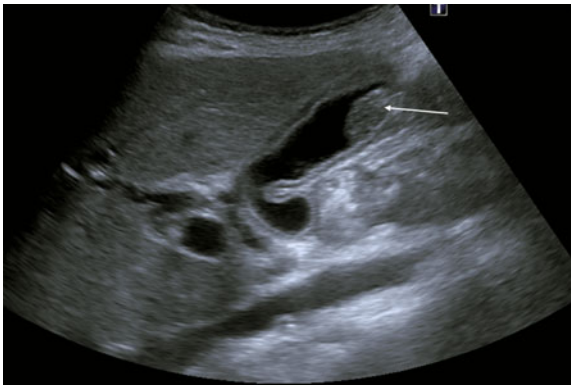

Fig. 12.42 Oblique longitudinal view of the gallbladder, with an apparent echogenic mass in the fundus (arrow), which was confirmed as sludge on MRI

Gallbladder polyps are the main differential at ultrasound for gallbladder stones and are relatively common, with a reported incidence of up to 6.9% [35]. These are mainly cholesterol polyps, which are typically multiple, <10 mm in size and can cast a faint acoustic shadow at ultrasound. Their lack of mobility or attachment to the anterior wall of the gallbladder is often their only distinguishing feature from a stone at ultrasound. True adenomatous polyps are much less common, are usually solitary and are either sessile or pedunculated in shape. While cholesterol polyps are truly benign, adenomatous polyps are viewed as having malignant potential and ultrasound follow-up of these may be required, depending upon polyp size, its contour and the patient's age.

Biliary sludge or echogenic bile is a common finding in the ICU patient, due to biliary stasis. This represents precipitates of calcium salts and cholesterol crystals, which usually form a dependent layer in the gallbladder lumen, but can on occasion

aggregate to form a sludge ball that can mimic a gallbladder wall mass (Fig. 12.42). Demonstrating flow or movement of the sludge to separate these possibilities is not always clear, as it can be extremely viscid: in which case repeating the ultrasound after the patient has left ITU should confirm resolution of this finding.

Echogenic bile may also be seen when there is blood or pus in the gallbladder lumen and the clinical presentation, history (any recent intervention or trauma), is key to making this distinction.

12.11.4 Acute Cholecystitis

Usually as a result of gallbladder obstruction from a gallstone, the sonographic findings in acute cholecystitis can be variable. The described "major" diagnostic findings are: the presence of gallstones in the gallbladder (a stone may be seen in the cystic duct), gallbladder wall oedema, gas in the gallbladder wall and visible patient discomfort, when the ultrasound probe directly overlies the gallbladder (sonographic Murphey's sign) [36]. Less specific—"minor"- findings include: pericholycystic fluid, wall thickening, increased distention and luminal changes (i.e. sludge, stranding across lumen). A combination of major and minor findings at ultrasound, can give a diagnostic sensitivity for cholecystitis of up to 90–98% and a specificity of 94–98% [37].

Gallbladder wall oedema is seen on ultrasound as a thickening of the low reflective central zone of the wall, which if marked can take on a stratified appearance (Fig. 12.43), or as an echo- poor halo around the gallbladder. Increased mural blood flow along the anterior wall may be seen on colour Doppler, although as a diagnostic finding for cholecystitis this is relatively non-specific: particularly with modern ultrasound systems which can demonstrate the cystic artery in normal gallbladders [38].

As well as confirming a suspected diagnosis of cholecystitis, ultrasound can detect the possible complications that can occur, including empyema, gangrenous cholecystitis, perforation, pericholecystic collections and emphysematous cholecystitis. Gallbladder empyema has a non-specific finding of echogenic "sludge like"

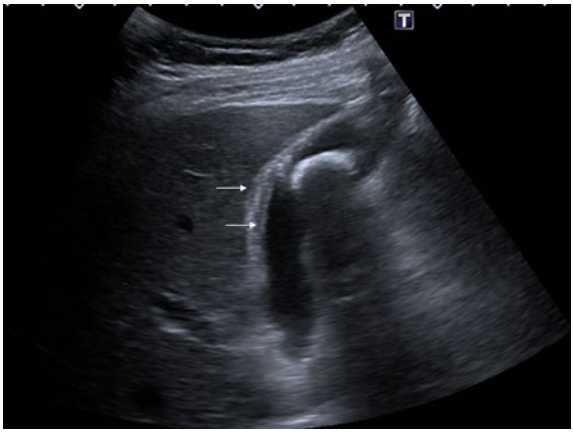

Fig. 12.43 Longitudinal oblique view of an inflamed gallbladder containing a gallstone. There is thickening and stratification of the gallbladder wall, with alternating hypoechoic (arrows) and echogenic lines, consistent with gallbladder wall oedema

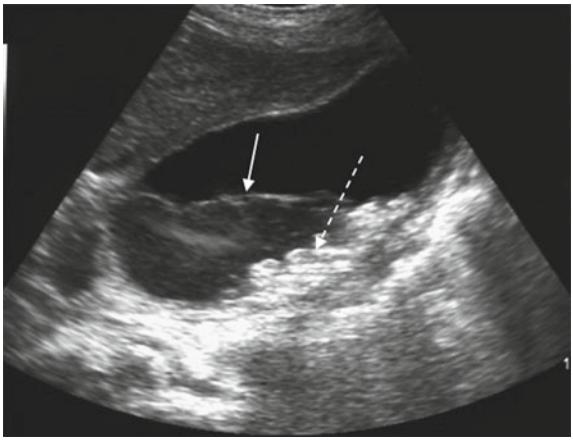

Fig. 12.44 Longitudinal oblique view of a thick-walled gallbladder with stones (dashed arrow) and layered material (arrow), which is suggestive of pus in keeping with empyema

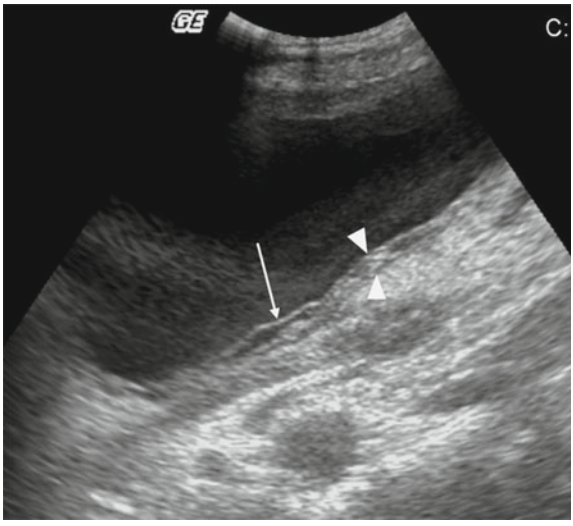

Fig. 12.45 Longitudinal view of an irregularly thickened (arrowheads) gallbladder wall, with a separated linear interface (arrow), very suggestive for mucosal separation, due to developing gangrenous cholecystitis

material, which is typically dependent in location (Fig. 12.44). With the onset of gangrenous change, irregular thickening of the gallbladder wall at ultrasound reflects the intramural haemorrhage, abscess formation and necrosis occurring. Intraluminal echogenic strands may be seen, representing fibrinous debris and mucosal sloughing (Fig. 12.45). With the onset of gangrene, the sonographic Murphy's sign will usually be negative, due to denervation of the gallbladder. Gallbladder perforation occurs in 5–10% of cases of cholecystitis and is a significant risk in gangrenous cholecystitis. It can be acute, sub-acute or chronic, with differing findings at ultrasound. Sub-acute perforation results in either pericholecystic fluid collections or frank abscess formation; which can be either predominantly echogenic, or a complex pattern of anechoic fluid with echogenic septations,

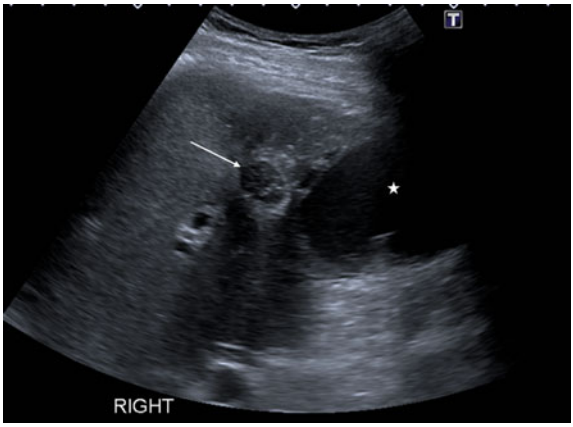

Fig. 12.46 Oblique view through the gallbladder fossa showing an inflamed gallbladder (star), with an adjacent oval shaped, intrahepatic collection/abscess (arrow)

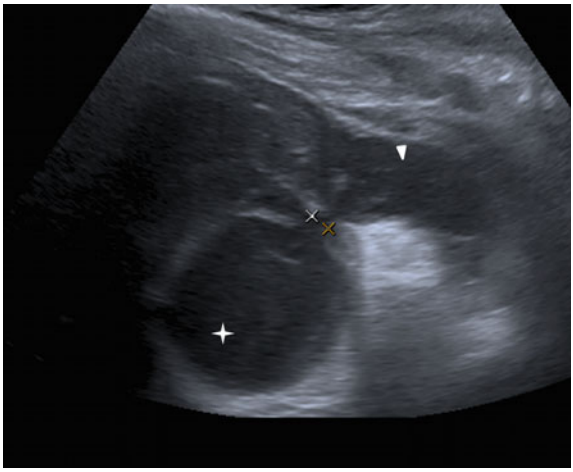

Fig. 12.47 Perforated gallbladder (star). Transverse view showing a focal defect of gallbladder wall (crosshairs) known as the "hole sign", with an adjacent collection (arrowhead)

although both will typically demonstrate through transmission of sound. Abscess formation may sometimes be seen within the adjacent liver (Fig. 12.46) rather than gallbladder fossa and pericholecystic fluid collections can also be seen secondary to pancreatitis, peritonitis or duodenal perforation. Careful interrogation of the gallbladder wall, in both transverse and longitudinal plane, may identify a perforation as a focal defect within the wall of the gallbladder: the hole sign (Fig. 12.47).

Gas in the gallbladder wall is the result of proliferating anaerobic infection (e.g. Clostridium) and is a potentially life threatening complication in cholecystitis, merited as a surgical emergency. More commonly seen in diabetic patients, approximately 30% of cases of emphysematous cholecystitis occur in the absence of gallstones. Mural gas formation is seen as focal, non-dependent echogenic areas in a thickened gallbladder wall, with comet-tail and ring down artefact within an acoustic shadow. If there is gas within the gallbladder lumen, it may be difficult to

discern the gallbladder as being separate to adjacent gas filled bowel, as it displays a diffuse linear echogenic interface and posterior acoustic shadowing containing internal reverberations. Changing patient position can help to confirm the gallbladder as separate from adjacent bowel and any gas within its wall may be seen to move with gravity [39]. If there is any doubt over the diagnosis, CT will confirm the presence of mural gas and distinguish this from calcification (i.e. porcelain gallbladder), which is the main differential for the appearances described.

Acalculous cholecystitis is gallbladder inflammation in the absence of gallstones, it accounts for about 10% of all cases of cholecystitis and typically occurs in hospitalised patients who are acutely ill or have undergone major surgery. Although the histological changes in the gallbladder are similar to gallstone cholecystitis, the pathogenesis is unclear, with a much higher incidence of gangrenous change and perforation. At ultrasound the lack of gallstones contributes to diagnostic difficulty, but gallbladder wall thickening, with hypoechoic regions and pericholecystic fluid are reported as the two most reliable findings [40]. The gallbladder may also contain echogenic sludge. In uncertain cases, a repeat ultrasound at 24 h may be helpful in demonstrating progression of changes. Ultrasound can also guide percutaneous aspiration of gallbladder contents for microbiology, although this has a recognised false negative rate [41].

12.12 Jaundice: Biliary Dilatation

In additional to the haematological and biochemical workup of the jaundiced patient, ultrasound has a key imaging role. It can sometimes detect a hepatocellular cause for the jaundice, such as underlying cirrhosis, malignant infiltration or an inflammatory process such as a liver abscess. However it is in the detection of biliary duct obstruction that ultrasound demonstrates a high level of accuracy; 80–85% in cases of proven obstruction, with a false positive rate of less than 5% [42–44].

Depending upon its aetiology, bile duct dilatation either affects the intrahepatic bile ducts, the extrahepatic ducts (common hepatic and common bile duct), or both. Levels of potential obstruction can be divided into hilar or porta hepatis, suprapancreatic and pancreatic; with ultrasound being able to correctly identify the level of obstruction in 92–95% of the time [45]. Obstruction at the hilar/porta hepatis is usually due to malignancy, most frequently cholangiocarcinoma and less commonly malignant lymphadenopathy.

Early or mild intrahepatic duct dilatation is best appreciated by scanning near the porta and assessing the diameter of the main right and left hepatic ducts. As already stated, these are normally <2 mm in diameter, while the more peripheral ducts should be <40% of the adjacent portal vein branch. With increasing duct dilatation the appearance in the liver has been described as the double channel or double-barrelled shot gun sign, depending upon the plane of scanning (when scanned along their length the dilated duct and adjacent portal vein appear as two

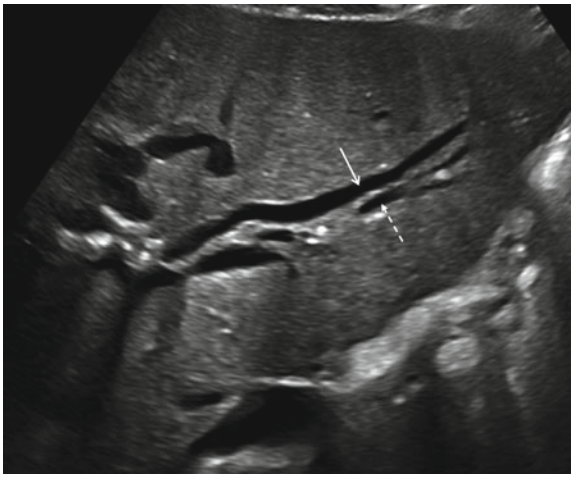

Fig. 12.48 Double barrelled shotgun sign: View through the left lobe of the liver, showing a portal vein branch (arrow) and adjacent dilated intrahepatic bile duct (dashed arrow)

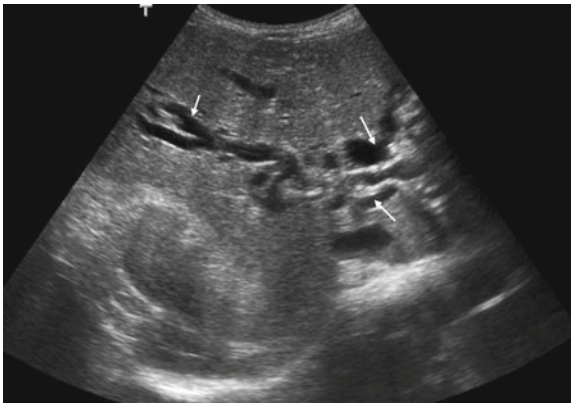

Fig. 12.49 Transverse view left lobe of liver with intrahepatic bile duct dilation (arrows), due to a cholangiocarcinoma of the common bile duct. Typical serpiginous branching pattern of tubular structures

channels, while in cross-section they are seen as if looking into a double-barrelled shot gun) (Fig. 12.48). At this degree of dilatation care must be taken not to mistake an enlarged segmental hepatic artery, associated with portal hypertension or portal vein occlusion, for bile duct dilatation and the use of colour Doppler to confirm absence of pulsatile flow can be useful. With established intrahepatic bile duct dilatation, the appearance seen at ultrasound is that of 'too many tubes' within the liver: the dilated ducts having an irregular/tortuous contour to them, and converge towards the porta to give a 'stellate pattern' (Fig. 12.49). As already stated, obstruction by an intrahepatic malignancy may appear as an abrupt cut-off of bile ducts, with the actual tumour difficult to discern on a non-contrast ultrasound. Obstruction at the porta due to periportal lymph nodes will usually show multiple oval or rounded hypoechoic masses in line with the portal vein.

Pitfalls can occur in early intrahepatic biliary obstruction, when they may have not been time for the ducts to dilate yet and in this situation repeat interval scanning is recommended, if there is strong clinical suspicion [46]. Segmental bile duct dilatation within the liver, due to a localised stricture or occluding mass, can be overlooked, without a careful segmental approach to assessing the liver parenchyma. Blood or debris within the bile ducts will make them relatively isoechoic to the liver parenchyma and may therefore mask dilatation. Non-obstructive bile duct dilatation can be seen in patients following biliary surgery, such as a biliary-enteric anastomosis.

Suprapancreatic obstruction is again most likely due to a primary neoplasm or metastatic disease, with gallstones or an inflammatory stricture much less likely. Rarely obstruction at this level can occur from a gallstone lodged in the cystic duct or neck of the gallbladder, leading to inflammatory swelling and extrinsic compression of the common bile duct or common hepatic duct, known as Mirizzi's syndrome. Ultrasound can confirm the presence of a stone within the cystic duct and demonstrate dilatation of the common hepatic duct proximal to this [47].

When bile duct dilatation is encountered on ultrasound, the gallbladder should be assessed for any degree of distention as this can sometimes aide in determining the level of obstruction. A distended gallbladder would suggest a low common duct obstruction, while a contracted gallbladder would tend to place the level of obstruction proximal to the cystic duct confluence within the common hepatic duct (Fig. 12.50). If the obstruction is due to gallstones however, this cannot be relied upon as previous episodes of gallstone cholecystits may have rendered the gallbladder fibrotic and unable to distend.

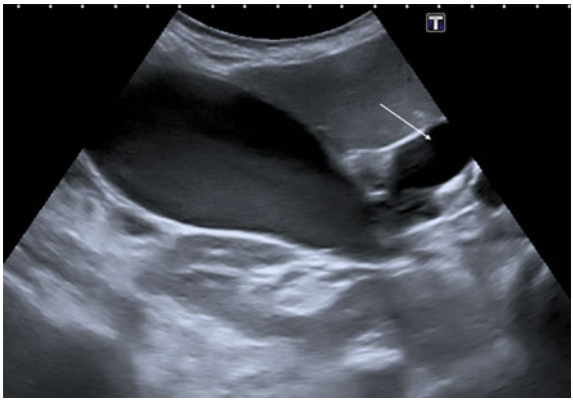

Fig. 12.50 Longitudinal view of a markedly distended gallbladder, in a patient presenting with jaundice. There is layering of echoes within the gallbladder lumen as a result of obstruction with a dilated common hepatic duct seen within the porta (arrow)

Obstruction at pancreatic level is the most common site of obstruction and can be due to gallstones, inflammatory strictures or masses and benign or malignant neoplasms. With careful technique and good equipment, the sensitivity of ultrasound for choledocholithiasis is between 75 and 82% [48]. This reduced sensitivity, compared to stones in the gallbladder, can be due to a number of factors: acoustic shadowing from gas in the adjacent duodenum can obscure the distal common duct; in early or intermittent obstruction the bile duct may not be significantly dilated, resulting in a lack of surrounding echo free bile, which normally helps highlight the relatively echogenic stone; around 10% of bile duct stones lack an acoustic shadow making these stones difficult to distinguish from other bile duct content such as sludge. Air within the common duct due previous sphincterotomy or gallstone complication (see below), may lead to a false positive diagnosis.

A tumour of the distal bile duct may be seen as a low reflective irregular mass, or as an abrupt, shouldered stricture of the distal duct, with a soft tissue tubular shaped structure distal to this. Malignant masses arising in the head of the pancreas will also lead to distal bile duct obstruction and are generally low reflective mass lesions with respect to the adjacent pancreatic tissue.

12.13 Pneumobilia

Gas/air in the bile ducts can be secondary to a surgical biliary—enteric anastomosis or fistula, biliary stent, incompetent sphincter of Oddi, erosion of a gallstone into the duodenum, or perforation of a duodenal ulcer into the common bile duct. At ultrasound, the intra hepatic or common bile duct lumen is obscured by either short echogenic segments, or longer branching linear echogenic foci, which may cast acoustic shadows, comet tail or ring down artefacts (Fig. 12.51). In the supine patient the air preferentially collects in the more anterior intrahepatic ducts within

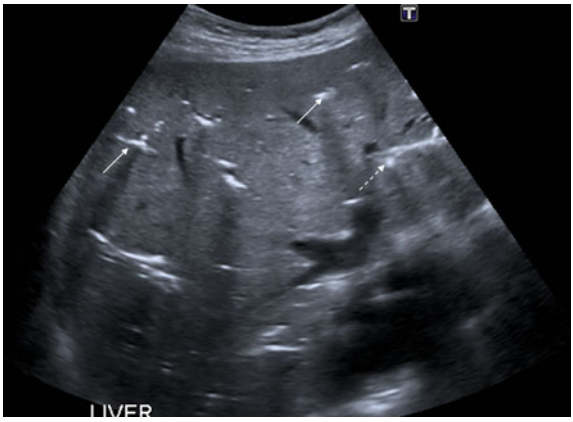

Fig. 12.51 Transverse scan through the right liver showing pneumobilia. There are numerous strongly reflective linear structures, representing bile ducts containing air/gas. Sone cast acoustic shadows (arrows), others generate comet tail or ring down artefact (dashed arrow)

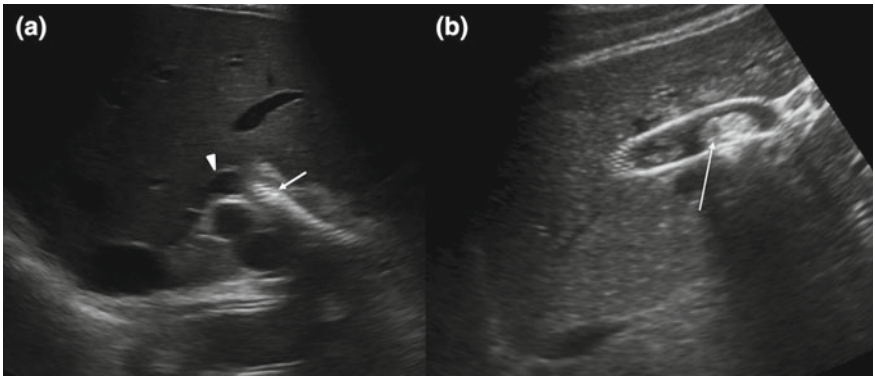

Fig. 12.52 Stent occlusion: **a** Hatched linear echogenicity at the porta hepatis indicates the position of a common bile duct stent (arrow). The common hepatic duct is dilated (arrowhead) and lacks pneumobilia indicating stent malfunction/occlusion. **b** Echogenic filling defects within the lumen of a malfunctioning intrahepatic stent (arrow) consistent with sludge. Again, the lack of pneumobilia indicates stent occlusion

the left lobe of the liver and in certain circumstances movement of the air can be appreciated as a flickering in the ring down/comet tail artefact. Small discrete foci of air can sometimes cast a 'clean' shadow mimicking a bile duct calculus.

In patients with a known biliary stents in situ, the absence or relative paucity of air with the intrahepatic bile ducts is strongly suggestive of stent malfunction (Fig. 12.52)

12.14 Cholangitis

Acute or ascending cholangitis has the reported triad of: fever, right upper quadrant pain and jaundice, although in reality this is seen in <40% of patients, with acute confusion and haemodynamic collapse another reported presentation. It is almost always associated with biliary obstruction, most commonly bile duct calculi, but also pre-existing bile duct strictures, malignant biliary obstruction or previous biliary surgery and interventional procedures. At ultrasound, biliary dilatation is a common finding and the level of obstruction can usually be determined with ultrasound. Purulent bile will produce echogenic debris within the bile ducts and there may be concordant intraductal calculi present. Thickening of the walls of the bile ducts tends to be seen with more chronic or recurrent episodes of cholangitis. Intrahepatic abscesses are not infrequently seen with acute cholangitis and ultrasound can be used to guide percutaneous aspiration of these and if there is obstruction percutaneous drainage of the biliary system.

References

1. Nicolaou S, Talsky A, Khashoggi K, Venu V. Ultrasound-guided interventional radiology in critical care. Crit Care Med. 2007;35(5 Suppl):S186–97.
2. Middleton WD, Melson GL. Diaphragmatic discontinuity associated with perihepatic ascites: a sonographic refractive artefact. Am J Roentgenol. 1988;151:709–11.
3. Le Couinaud C. foie: etudes anatomiques et chirurgicales. Paris: Masson; 1957.
4. Sidhu PS, Chong WK. Measurement in ultrasound: a practical handbook. London: Arnold; 2004.
5. Scatarige JC, Scott WW, Donovan PJ, Siegelman SS, Sanders RC. Fatty infiltration of the liver: ultrasonographic and computed tomographic correlation. J Ultrasound Med. 1984;3:9–14.
6. Jüttner HU, Ralls PW, Quinn MF, Jenney JM. Thickening of the gallbladder wall in acute hepatitis: ultrasound demonstration. Radiology. 1982;142:465–6.
7. Kuligowska E, Connors SK, Shapiro JH. Liver abscess: sonography in diagnosis and treatment. AJR Am J Roentgenol. 1982;138:253–7.
8. Hui JY, Yang MK, Cho DH, Li A, Loke TK, Chan JC, Woo PC. Pyogenic liver abscesses caused by Klebsiella pneumoniae: US appearance and aspiration findings. Radiology. 2007;242:769–76.
9. Vassiliades VG, Bree RL, Korobkin M. Focal and diffuse benign hepatic disease: correlative imaging. Semin Ultrasound CT MR. 1992;13:313–35.
10. Liu GJ, Lu MD, Xie XY, Xu HX, Xu ZF, Zheng YL, Liang JY, Wang W. Real-time contrast-enhanced ultrasound imaging of infected focal liver lesions. J Ultrasound Med. 2008;27:657–66.
11. Cai YL, Xiong XZ, Lu J, Cheng Y, Yang C, Lin YX, Zhang J, Cheng NS. Percutaneous needle aspiration versus catheter drainage in the management of liver abscess: a systematic review and meta-analysis. HPB (Oxford). 2015;17:195–201.
12. Gandolfi L, Leo P, Solmi L, Vitelli E, Verros G, Colecchia A. Natural history of hepatic haemangiomas: clinical and ultrasound study. Gut. 1991;32:677–80.
13. Ebara M, Ohto M, Shinagawa T, Sugiura N, Kimura K, Matsutani S, Morita M, Saisho H, Tsuchiya Y, Okuda K. Natural history of minute hepatocellular carcinoma smaller than three centimeters complicating cirrhosis. A study in 22 patients. Gastroenterology. 1986;90:289–98.
14. Huang C-Y, Sun J-T, Tsai K-C, Wang H-P, Lien W-C. Hepatic portal venous gas: review of the literature and sonographic implications. J Med Ultrasound. 2014;22:66–70.
15. Hokama A, Arakaki S, Shibata D, Maeshiro T, Kinjo F, Fujita J. "Playboy Bunny" sign of congestive heart failure. West J Emerg Med. 2011;12:433–4.
16. Yoshimoto K, Ono N, Okamura T, Sata M. Recent progress in the diagnosis and therapy for veno-occlusive disease of the liver. Leuk Lymphoma. 2003;44:229–34.
17. Ralls PW, Johnson MB, Radin DR, Boswell WD, Lee KP, Halls JM. Budd-Chiari syndrome: detection with color Doppler sonography. AJR Am J Roentgenol. 1992;159:113–6.
18. Mortelé KJ, Mortelé B, Silverman SG. CT features of the accessory spleen. AJR Am J Roentgenol. 2004;183:1653–7.
19. Görg C1, Eichkorn M, Zugmaier G. The small spleen: sonographic patterns of functional hyposplenia or asplenia. J Clin Ultrasound. 2003; 31(3):152–5.
20. Llewellyn ME, Brooke Jeffrey R, DiMaio MA, Olcott EW. The sonographic "Bright Band Sign" of splenic infarction. J Ultrasound Med. 2014;33:929–38.
21. Sharma SK, Smith-Rohrberg D, Tahir M, Mohan A, Seith A. Radiological manifestations of splenic tuberculosis: a 23-patient case series from India. Indian J Med Res. 2007;125:669–78.
22. Pastakia B, Shawker TH, Thaler M, O'Leary T, Pizzo PA. Hepatosplenic candidiasis: wheels within wheels. Radiology. 1988;166:417–21.

23. Chou YH, Tiu CM, Chiou HJ, Hsu CC, Chiang JH, Yu C. Ultrasound-guided interventional procedures in splenic abscesses. Eur J Radiol. 1998;28:167–70.
24. Warshauer DM, Hall HL. Solitary splenic lesions. Semin Ultrasound CT MR. 2006;27:370–88.
25. WHO Informal Working Group. International classification of ultrasound images in cystic echinococcosis for application in clinical and field epidemiological settings. Acta Trop. 2003;85:253–61.
26. Goerg C, Schwerk WB, Goerg K. Sonography of focal lesions of the spleen. AJR Am J Roentgenol. 1991;156:949–53.
27. Goerg C, Schwerk WB, Goerg K. Splenic lesions: sonographic patterns, follow-up, differential diagnosis. Eur J Radiol. 1991;13:59–66.
28. Chiavaroli R, Grima P, Tundo P. Characterization of non-traumatic focal splenic lesions using contrast enhanced sonography. JCU. 2011;39; 310–315.
29. Gorg C, Weide R, Schwerk WB. Malignant splenic lymphoma: sonographic patterns, diagnosis and follow-up. Clin Radiol. 1997;52:535–40.
30. McKenney KL, Nuñez DB Jr, McKenney MG, Asher J, Zelnick K, Shipshak D. Sonography as the primary screening technique for blunt abdominal trauma: experience with 899 patients. AJR Am J Roentgenol. 1998;170:979–85.
31. Perret RS, Sloop GD, Borne JA. Common bile duct measurements in an elderly population. J Ultrasound Med. 2000;19:727–30.
32. Romano AJ, vanSonnenberg E, Casola G, Gosink BB, Withers CE, McCutchan JA, Leopold GR. Gallbladder and bile duct abnormalities in AIDS: sonographic findings in eight patients. AJR Am J Roentgenol. 1988;150:123–7.
33. Raghavendra BN, Subramanyam BR, Balthazer EJ, et al. Sonography of adenomyomatosis of the gallbladder: radiologic pathologic correlation. Radiology. 1983;146:747.
34. Sommer FG, Taylor KJ. Differentiation of acoustic shadowing due to calculi and gas collections. Radiology. 1980;135:399–403.
35. Andrén-Sandberg A. Diagnosis and management of gallbladder polyps. N Am J Med Sci. 2012;4:203–11.
36. Ralls PW, Halls J, Lapin SA, Quinn MF, Morris UL, Boswell W. Prospective evaluation of the sonographic Murphy sign in suspected acute cholecystitis. J Clin Ultrasound. 1982;10:113–5.
37. Marton KI, Doubilet P. How to image the gallbladder in suspected cholecystitis. Ann Intern Med. 1988;109:722–9.
38. Jeffrey RB Jr, Nino-Murcia M, Ralls PW, Jain KA, Davidson HC. Color Doppler sonography of the cystic artery: comparison of normal controls and patients with acute cholecystitis. J Ultrasound Med. 1995;14:33–6.
39. Bloom RA, Fisher A, Pode D, Asaf Y. Shifting intramural gas—a new ultrasound sign of emphysematous cholecystitis. J Clin Ultrasound. 1984;12:40–2.
40. Cornwell EE III, Rodriquez A, Mirvis SE, et al. Acute acalculous cholecystitis in critically injured patients. Preoperative diagnostic imaging. Ann Surg. 1989;210:52.
41. McGahan JP, Lindfors KK. Acute cholecystitis: diagnostic accuracy of percutaneous aspiration of the gallbladder. Radiology. 1988;167:669–71.
42. Haubek A, Pedersen JH, Burcharth F, Gammelgaard J, Hancke S, Willumsen L. Dynamic sonography in the evaluation of jaundice. AJR Am J Roentgenol. 1981;136:1071–4.
43. Dewbury KC, Joseph AE, Hayes S, Murray C. Ultrasound in the evaluation and diagnosis of jaundice. Br J Radiol. 1979;52:276–80.
44. Vallon AG, Lees WR, Cotton PB. Grey-scale ultrasonography in cholestatic jaundice. Gut. 1979;20:51–4.
45. Laing FC, Jeffrey RB Jr, Wing VW. Biliary dilatation: defining the level and cause by real-time ultrasound. Radiology. 1986;160:39.

46. Muhletaler CA, Gerlock AJ Jr, Fleischer AC, James AE Jr. Diagnosis of obstructive jaundice with nondilated bile ducts. AJR Am J Roentgenol. 1980;134:1149–52.
47. Freeman ME, Rose JL, Forsmark CE, Vauthey J. Mirizzi syndrome: a rare cause of obstructive jaundice. Dig Dis. 1999;17:44–8.

Chapter 13
Abdominal Ultrasound—Bowel and Peritoneum

James M. Pilcher and Pawan Patel

Keywords Abdominal ultrasound · Scanning technique · Bowel wall thickening · Intraperitoneal fluid

13.1 Introduction

Ultrasound is increasingly used to assess small and large bowel pathology. The technique is often targeted to a specific clinical question and frequently employs a combination of ultrasound transducers to optimize visualisation of the bowel wall layers. The real time aspect of ultrasound is invaluable in assessing small bowel peristalsis, while colour or power Doppler can help in determining whether the bowel is perfused and potentially highlight areas of inflammation. Extensive gaseous distention of the bowel can potentially counter diagnostic studies, although techniques such as graded compression and use of oral contrast agents can significantly improve visualisation of the area of interest.

13.1.1 Anatomy

Within the abdomen the gastrointestinal tract consists of the stomach, duodenum, jejunum, ileum, appendix, colon and rectum. The intraperitoneal stomach lies in the left upper quadrant, bordered by the left hemidiaphragm superiorly, the spleen postero-lateraly and the pancreas posteroinferiorly. The lessor omentum connects its lesser curve to the inferior border of the liver, while the greater omentum hangs

J. M. Pilcher (✉) · P. Patel
Consultant Radiologist, St George's University Hospitals NHS Foundation Trust, Blackshaw Road, Tooting, London SW170QT, UK
e-mail: James.Pilcher@stgeorges.nhs.uk

P. Patel
e-mail: pavpatel87@gmail.com

A. Walden et al. (eds.), *Ultrasound in the Critically Ill*,
https://doi.org/10.1007/978-3-030-71742-1_13

down from its greater curve. Internally the mucosal folds or rugae increase its surface area significantly. The duodenum is a C-shaped tube connecting the stomach at the duodenal bulb, to the jejunum at the ligament of Trieitz. Apart from the duodenal bulb it is retroperitoneal in location, with the second part attached to the pancreatic head and the third part crossing between the aorta and the superior mesenteric vessels. The jejunum and ileum are intraperitoneal, hanging off the small bowel mesentery, with the jejunum demonstrating an extensive mucosal fold pattern, valvulae conniventes, which diminishes in the ileum up to the junction of the terminal ileum with the caecum. The caecum and appendix usually lie in the right iliac fossa and are intraperitoneal structures, along with the transverse colon which hangs from its mesentery between the hepatic and splenic flexures of the colon, and the rectosigmoid colon. The ascending colon, descending colon and mid rectum are retroperitoneal, while the distal rectum is extraperitoneal terminating at the anus. The wall of the colon forms sacculations—haustra—which are due to the contraction of three bands of muscle, the tinea coli, that run along the length of the colon, just deep to the serosa. The superior mesenteric artery and vein supply and drain the whole of the jejunum, ileum and colon up to the splenic flexure, while the inferior mesenteric artery and vein provide the same for the descending colon and rectum.

On ultrasound the curvilinear array is used to survey the bowel and identify its gross anatomy within the abdomen, while the higher frequency linear array is used to target specific areas of bowel and demonstrate the detail of the bowel wall layers. With the curvilinear array positioned in a slightly oblique longitudinal orientation in the left upper quadrant the gastro-oesophageal junction can be demonstrated and it diameter measured at the oesophageal hiatus (Fig. 13.1). The fundus of the stomach is often difficult to appreciate scanning from an anterior approach, but may be seen through the spleen when scanning laterally in the left upper quadrant. The gastric rugae are seen as low reflective bands with bright echoes of air between them. Scanning transversely in the midline the gastric antrum, pylorus and duodenal cap can be seen and if fluid filled the layers of the bowel wall are easily appreciated. The third part of the duodenum is more challenging to identify, particularly if collapsed, but careful scrutiny of the space between the proximal superior mesenteric artery and aorta should reveal a tubular shaped, low reflective structure that peristalses. The small bowel is generally assessed with a higher frequency array, either small faced curvilinear, or linear. The operator should apply graded compression with the probe to displace bowel gas and spread bowel loops, bringing them closer to the probe, to allow inspection of the bowel wall layers (Fig. 13.2). The increased mucosal folds in the jejunum are seen to fill the lumen of the bowel and are described as a “herring bone” pattern, while the ileum has a flatter mucosal fold pattern (Fig. 13.3). The normal calibre of small bowel is <3 cm and the normal wall thickness is between 2 and 3 mm [1]. Rather than trying to trace the length of the small bowel with ultrasound, systematic sweeps of the ultrasound probe, up and down across the abdomen, allows for interrogation of the whole of the small bowel. Being relatively fixed in location, most of the large bowel can be scanned using anatomical landmarks, with the ascending and descending colon viewed by

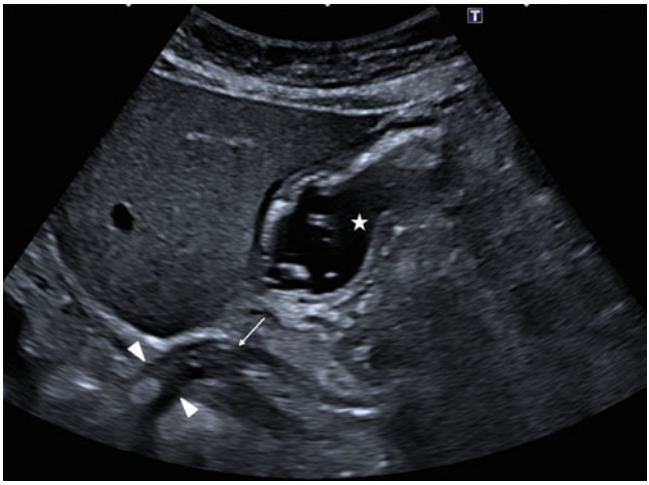

Fig. 13.1 Longitudinal oblique view through the left upper quadrant showing the gastro-oesophageal junction (arrow) just beyond the oesophageal hiatus of the diaphragm (arrowheads). The fluid filled body of the stomach is also seen (star)

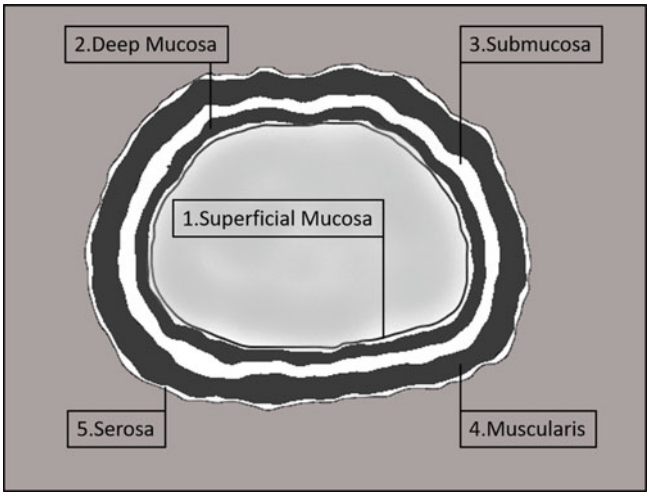

Fig. 13.2 Labelled schematic of the five small bowel wall layers seen at ultrasound

scanning the flanks in longitudinal and transverse section. They are typically the most lateral and posteriorly placed segments of bowel, often gas filled and showing a haustral fold pattern, seen as indentations in the contour of the bowel wall, with no peristalsis. The caecum is identified by careful graded compression, tracing the ascending colon down into the right iliac fossa, where the ileo-caecal junction is

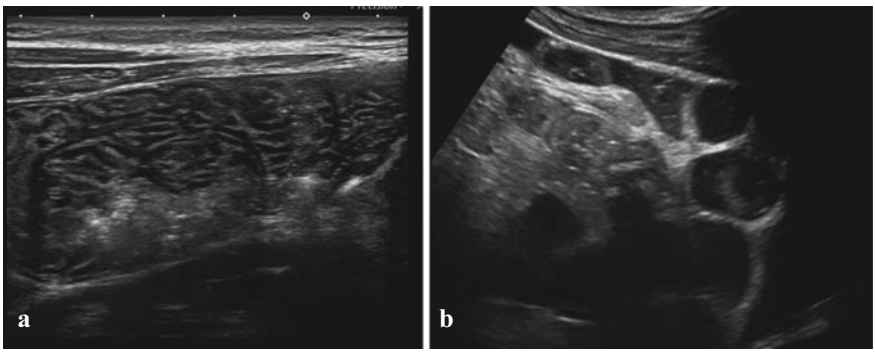

Fig. 13.3 **a** Typical sonographic appearance of jejunum, with multiple mucosal folds filling the collapsed lumen, giving a "fish bone" pattern. **b** Fluid filled loops of ileum, showing minimal mucosal folds

usually seen. Adopting a longitudinal orientation, the caecal pole should then be identified (Fig. 13.4) as a blind end to the colon; its calibre should be <9 cm. From there, careful graded compression in a lateral to medial direction may demonstrate both the terminal ileum and the appendix (normal calibre < 6 mm), although this is very dependent upon the variable location of these structures. The transverse colon is best traced in cross-section, the ultrasound probe being in longitudinal section, from the hepatic flexure to the splenic flexure, its calibre should < 6 cm. Likewise, the sigmoid colon can be traced down in its short axis from the descending colon to the rectum.

13.2 The Gut Wall Signature

With optimal imaging of the bowel at high frequency, five distinct bowel wall layers can be appreciated as concentric circles of alternating hyper- and hypoechogenicity. These approximate to the histological layers of the bowel (Fig. 13.5), which starting from the luminal surface are: 1. Superficial mucosal interface (thin echogenic line); 2. The deep mucosa and lamina propria (mid grey); 3. The submucosa (echogenic band); 4. The muscularis propria (dark band); 5. Serosal interface (fine echogenic line). Often the inner and outer interfaces are difficult to appreciate, very much dependent upon whether the bowel is distended or not, the echogenicity of the bowel lumen content and any adjacent structures. The submucosal and muscularis propria are the two most visible layers, due to their relative thickness and high contrast; although with the lower frequency curvilinear array only the echogenic layer may be appreciated. Pathology of the bowel may affect one or more layers of the bowel wall and with careful scanning this can often be determined on high resolution ultrasound, however with progressive involvement

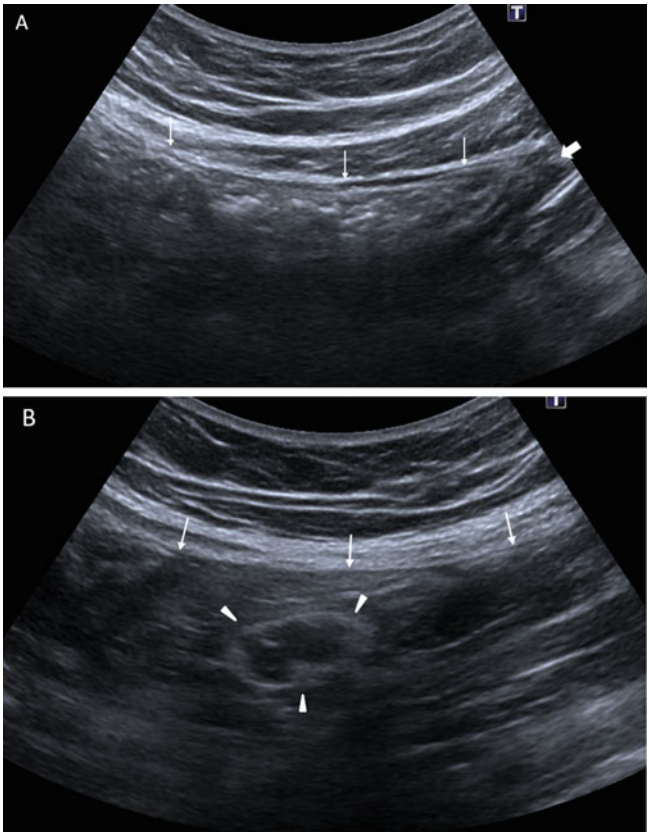

Fig. 13.4 **a** Longitudinal section image in the right lower quadrant shows the anterior wall of the caecum (arrows) and the tip of the caecal pole (fat arrow). **b** Sliding the probe slightly medially reveals the ileal-caecal junction (arrowheads)

of the bowel wall there is loss of these layers, with the bowel wall becoming uniformly hypoechoic.

13.3 Nasogastric Tube Positioning

The incorrect positioning or subsequent displacement of a nasogastric tube (NGT) can result in serious consequences for the intensive care patient, with the risk of aspiration of gastric contents or parenteral feed. Methods to confirm correct siting of NGTs include auscultation over the stomach, aspiration of stomach contents and chest radiographs. Ultrasound can also be used as a quick assessment of NGT position. Using the longitudinal view described above, the NGT can be

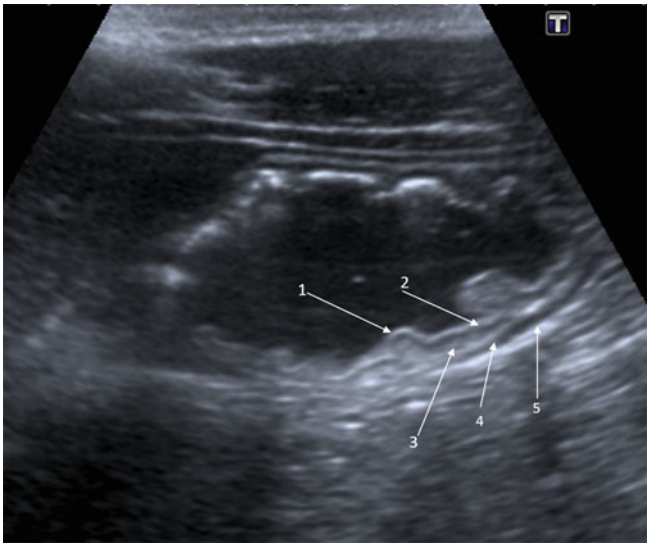

Fig. 13.5 High resolution ultrasound of normal terminal ileum, following oral fluid load, showing the five bowel wall layers outlined in Fig. 13.2. 1. Superficial mucosa; 2. Deep mucosa; 3. Submucosa; 4. Muscularis; 5. Serosa

identified as it crosses the gastro-oespohageal junction as a linear strong echo, with posterior acoustic shadowing. Location within the stomach can be confirmed, by injecting a combination of saline and air down the NGT and observing its arrival in the gastric antrum. A limited number of studies have reported both good sensitivity and positive predictive values for this technique [2, 3].

If the NGT cannot be confidently visualised, the cervical oesophagus should be scanned with a high frequency linear array to ensure that there has been an oesophageal intubation: although a chest radiograph will be required to confirm its distal location.

13.4 Small Bowel Ileus/Obstruction

In patients with apparent gut failure, increased nasal aspirates and dilated bowel loops on a plain abdominal radiograph, ultrasound can offer further information regarding the length of bowel involvement, evidence of peristalsis, potential site of an obstruction and indicate if there is developing ischaemic change. Ultrasound has been shown to have a sensitivity of 89% compared with 71% for conventional abdominal radiography in diagnosing small-bowel obstruction [4]. The real-time aspect of ultrasound lends itself well when assessing bowel peristalsis so that in a mechanical small bowel obstruction the proximal small bowel will be dilated

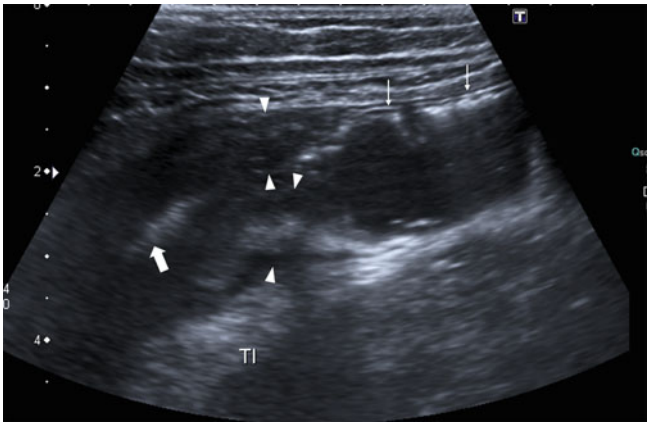

Fig. 13.6 Inflammatory stricture of the terminal ileum, in a patient with Crohn's disease. High resolution ultrasound along the length of the terminal ileum shows fluid distended normal terminal ileum (white arrows), with an acute transition to markedly thick-walled distal terminal ileum (arrow heads outline anterior and posterior walls), with a little gas in the almost effaced lumen (fat arrow)

(> 3 cm) and as it becomes fluid filled increased peristalsis will be seen, combined with a to and fro movement of the luminal content. The level of mechanical obstruction may be determined by distinguishing the mucosal fold pattern of the jejunum from the ileum [5]. The cause of obstruction may also be identified with ultrasound such as a hernia, inflammatory mass, intussusception or tumour (Fig. 13.6): however CT is recognised as having superior accuracy for this. Ultrasound can be used to monitor ongoing obstruction; with increasing small bowel wall thickness (>4 mm), reducing peristalsis and the development of free fluid between bowel loops indicators for urgent surgical intervention [6]. Colour Doppler can also be used to assess for any changes in mural blood flow in the obstructed bowel.

With an adynamic ileus the bowel loops are dilated and my show mild thickening, with no peristalsis seen (assessed over 5 min). There should be no transition point.

13.5 Bowel Ischaemia

Acute intestinal ischaemia accounts for 2% of gastrointestinal conditions and is an abdominal emergency. The underlying pathophysiology is variable and includes acute arterial mesenteric ischemia, acute venous mesenteric ischemia, non occlusive mesenteric ischemia, ischemia/reperfusion injury and ischemic colitis. Mortality rate is up to 90%, depending upon aetiology, length of involved bowel and time to

diagnosis. Acute severe abdominal pain, vomiting and diarrhoea are followed by abdominal distention with signs of peritonitis, fever and hypotension.

Contrast enhanced CT is the investigation of choice for all forms of mesenteric ischaemia, with high sensitivity and specificity, however ultrasound is frequently used as the first line investigation in an acute abdomen. In acute arterial ischaemia the bowel wall tends to remain thin [7], gradually filling with fluid and showing loss of peristalsis. Occlusions or a tight stenosis in the proximal caeliac axis, superior or inferior mesenteric arteries may be detectable on colour and spectral Doppler. In venous ischaemia, mural thickening is an early feature, with reduced reflectivity of mucosal layers due to oedema, while colour Doppler may reveal occlusion of the superior mesenteric vein. Increasing fluid content is seen in the bowel, with loss of peristalsis and in the late stage, intramural gas may be appreciated as strong echoes with shadowing or ring down artefact. Ischaemia/reperfusion injury can be seen after periods of hypovolaemia of various aetiologies, with the small bowel and right side of the colon more sensitive to states of shock [8]. With the recovery of mesenteric blood flow, reperfusion injury can occur, with ultrasound showing thickened bowel loops containing increased fluid and reduced peristalsis. If there is prolonged ischaemia frank necrosis develops, with intramural gas and perforations. Ischaemic colitis (IC) is the commonest form of mesenteric ischaemia, presenting with abdominal pain and rectal bleeding; it is associated with underlying cardiovascular disease, diabetes, hyperlipidaemia and renal failure [9]. It predominantly involves the left colon and ultrasound has a high degree of sensitivity for detecting the mural changes of IC. Segmental or circumferential wall thickening is seen, initially with preservation of wall stratification and there may be thickening and increased reflectivity of the pericolic fat. Findings on colour/power Doppler are variable, with a significant percentage of patients showing reduced or absent mural blood flow, but in cases of transient ischaemia there may be paradoxical increased mural flow seen [10]. If there is good visualisation of the colon, ultrasound may be employed to monitor ischaemic changes and help guide management. With advancing ischaemia there is loss of mural stratification, with the development of discrete echogenic foci in the bowel wall representing pneumatosis coli. Pericolic fat changes are also more frequently seen with transmural necrosis: these findings indicating the need for surgical intervention.

13.6 Pseudomembranous Colitis

There are a number of inflammatory and infective conditions that can also cause thickening of the wall of the colon on ultrasound (Fig. 13.7) and some of these, along with their main features are summarised in Table 13.1. Clostridium difficile colitis or pseudomembranous colitis has become an increasingly common cause of acute severe diarrhoea in the hospitalised patient receiving broad spectrum antibiotics. In a patient with this history ultrasound appearances of the colon can be strongly suggestive for this diagnosis. There is diffuse thickening of the wall of the

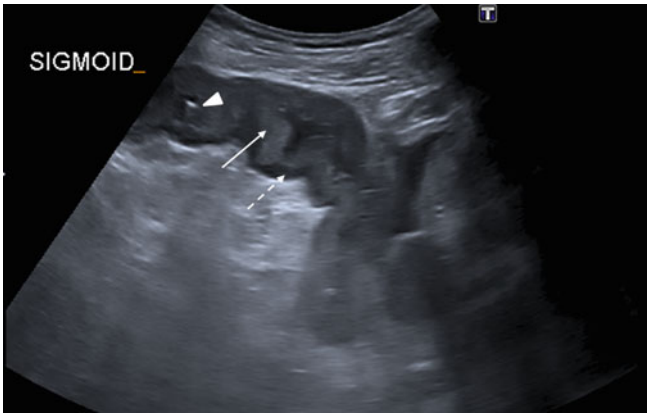

Fig. 13.7 Long axis view of sigmoid colon, in a patient with hospital acquired infective diarrhoea. The mucosal and submucosal layers are thickened and identical in their reflectivity (arrow). The outer muscle wall is also thickened (dashed arrow). Linear strong echo of luminal gas is seen proximally (arrowhead)

colon; tending to be much more marked than in other inflammatory colitides. The haustral pattern is preserved, with thickening of the interhaustral folds to give a polypoid appearance to the bowel known as the accordion sign or gyral fold pattern [11]. Stratification of the bowel wall layers is preserved in mid cases, but with increasing severity there is loss of the bowel wall layers and almost complete effacement of the lumen. Infiltration of the peri-colic fat is seen in a significant number of cases, along with abdominal ascites and on colour Doppler the mural blood flow tends to be reduced or absent. On high resolution ultrasound linear hyperechoic structures have been described parallel to the mucosal interface, which are thought to represent the pseudomembranes seen at colonoscopy [12].

Table 13.1 Causes of colonic wall thickening

Pathology
Diverticular disease
Carcinoma Inflammatory Bowel Disease: Ulcerative colitis, Crohn's
Colitis: Pseudomembranous, Ischaemic, Tuberculous, Typhlitis
Post-Operative Oedema
Intussusception
Lymphoma
Amyloidosis Endometriosis

13.7 The Peritoneal Cavity

A good understanding of peritoneal cavity anatomy is important for the intensivist interpreting free and focal fluid collections within the abdomen using ultrasound. Pneumoperitoneum is an important diagnosis not to miss on any patient, but can be difficult to call when using ultrasound: understanding the anatomy of the peritoneum can increase the confidence of the operator in identifying this appearance.

13.7.1 Anatomy

The peritoneal cavity is the potential space between the parietal peritoneum, which lines the abdominal cavity and the visceral peritoneum that covers the solid and hollow viscera; it normally contains a few millilitres of fluid to lubricate the bowel loops. The peritoneal cavity is divided into the greater sac and the lesser sac that communicates with the former via the epiploic foramen. The lesser sac is part of the supramesocolic compartment which lies cranial to the origin of the transverse colon mesentery and also includes the left and right subphrenic spaces, right subhepatic space and left perihepatic space. The inframesocolic compartment is divided into the right and left inframesenteric spaces, paracolic gutters and pelvic cavity (Fig. 13.8).

The small bowel mesentery is a fan shaped double layer of peritoneum that arises obliquely off the posterior wall of the abdomen, crossing L2 and extending down into the right iliac fossa. It covers the jejunum and ileum and contains mesenteric vessels, nerves, lymph nodes and varying degrees of fat.

The transverse mesocolon runs transversely across the abdomen in front of the pancreas, duodenum and right kidney.

The omenta are also specialised multi-layered folds, again containing blood vessels, lymphatics, and fat. The lessor omentum connects the lesser curve of the stomach and proximal duodenum to the liver and contains the common bile duct, hepatic vessels and portal vein. The greater omentum hangs down from the greater curve of the stomach and then folds back upon itself to form a four layered structure with a central space potentially communicating with the lesser sac. This folded back layer, then splits to cover the transverse colon.

At ultrasound the normal peritoneal cavity with its defined spaces, mesentery and omenta are difficult to appreciate. The parietal peritoneum can be seen anteriorly, using a high frequency linear array, in the midline as an echogenic interface deep to the extraperitoneal fat layer (Fig. 13.9). Moving bowel loops will lie directly deep to this and will glide past the interface with respiration. The small bowel mesentery can also be partly appreciated as an echogenic structure centrally (becoming more obvious in patients with increased intraabdominal fat), containing small anechoic blood vessels and occasionally visible lymph nodes. This is better appreciated if the operator has access to a higher frequency curvilinear array. In the

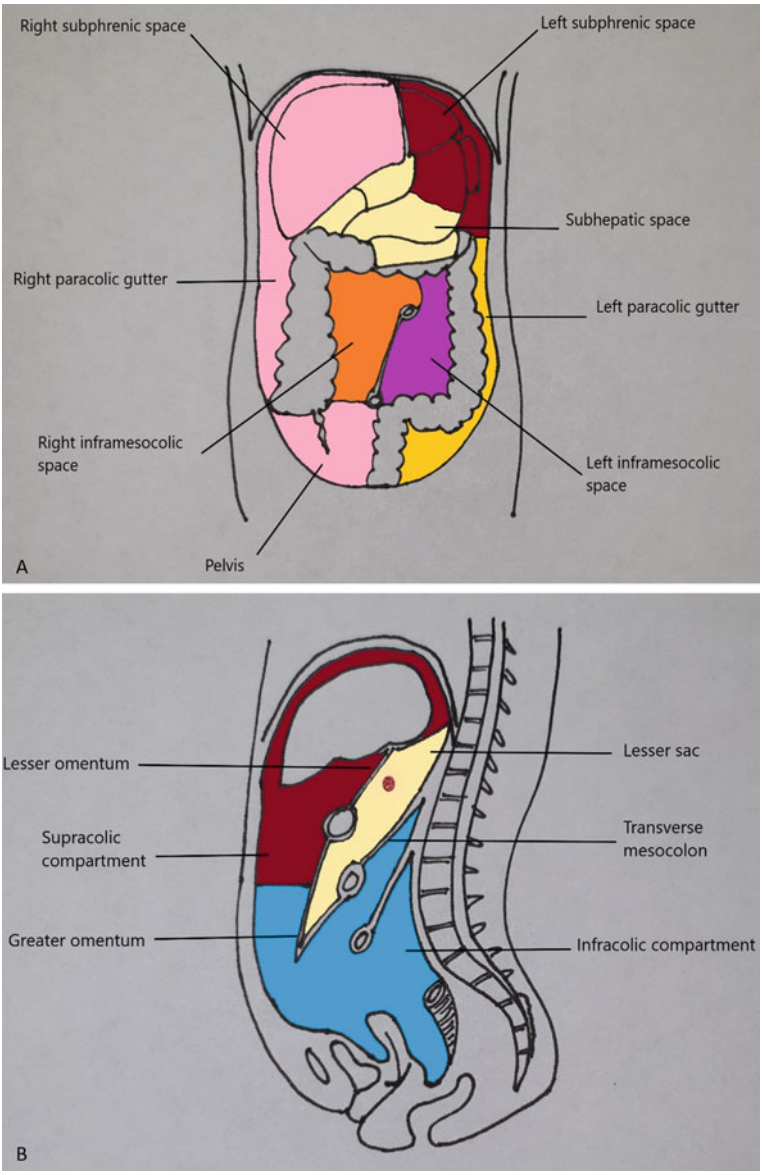

Fig. 13.8 Diagrams of the peritoneal cavity. **a** The peritoneal compartments are the greater and lesser sacs, with the greater sac divided into two by the transverse colon mesentery. **b** The perintoneal spaces are separated by a number of peritoneal ligaments. This influences the spread of peritoneal disease processes, location of ascites and fluid collections

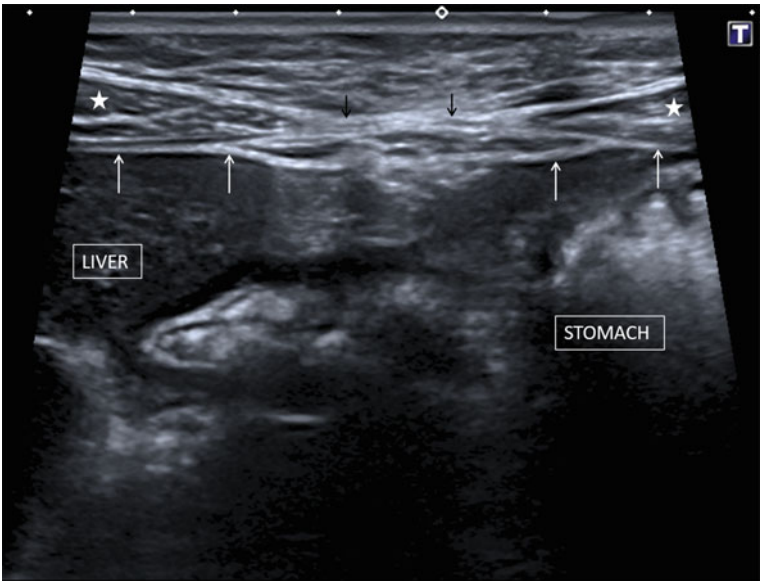

Fig. 13.9 High frequency transverse image through the epigastrium. The underlying liver and stomach are labelled. The peritoneal interface is seen as a continuous echogenic line (white arrows), deep to the rectus muscles (stars) and the extraperitoneal fat, that lies deep to the linea alba (black arrows)

presence of free fluid however, all of the peritoneal folds and spaces become more readily appreciable and any disease process causing thickening to the mesentery or omentum will make these structures more visible at ultrasound. Infiltration of the greater omentum can be appreciated using a higher frequency curvilinear or linear array; being appreciated as a predominantly echogenic structure, which may contain lower reflective nodular areas, interspaced between the thin peritoneal echo and the moving bowel loops.

13.8 Ascites

Increased accumulation of fluid, within the peritoneal cavity can be readily detected with ultrasound, with as little as 10 ml detectable in the pouch of Douglas or Morrison's pouch. On the intensive care unit, patients with cirrhosis, congestive cardiac failure, renal failure, abdominal malignancy and infections such as tuberculous peritonitis, will account for most of those with ascites. The initial approach to diagnosing free fluid in the abdomen with ultrasound, is the same as that used in the trauma patient using the FAST protocol (focused abdominal sonography for trauma). The four positions described are the right and left upper quadrants,

subxiphoid and pelvic view (Fig. 13.10). The first two points are located by taking a horizontal line from the xiphisternum around to the mid-axillary line and placing the curvilinear abdominal ultrasound probe in a longitudinal position at this point to obtain a coronal view across the abdomen. On the right this will include the liver, right kidney and part of the right hemi-diaphragm (Fig. 13.11), while on the left the spleen, left kidney and left hemi-diaphragm will be seen. The ideal views are optimised be tilting the probe in a more posterior direction and rotating the probe slightly so that it lies between the ribs. The pelvic view is obtained with the probe placed in a longitudinal orientation in the midline, directly above the pubic symphysis and angled slightly caudal to view the peritoneal recess behind the bladder (Fig. 13.12). The time gain compensation may need to be adjusted if the bladder is full, to reduce the stronger reflections deep to the bladder, which may mask the presence of free fluid. The operator should fan the probe from right to left to include the bowel loops in the iliac fossae. A transverse orientation should then be adopted to further assess the peritoneal recesses either side of the bladder. The final position is the subxiphoid view, with the probe placed in a transverse midline position below the xiphisternum. Although the main intention of this position is to assess for a pericardial effusion, it will also reveal free intraperitoneal fluid around the superior aspect of the liver.

Free intraperitoneal fluid may sometimes be confused with fluid containing structures such as bowel; the angulated borders seen with collections of free fluid can help make the distinction. Uncomplicated ascites can be either a transudate or exudate and will typically appear anechoic; with increasing volumes the small bowel loops will be seen to be free floating and become pushed to the midline, obscuring visualisation of retroperitoneal structures. Complicated ascites is always exudative and is due to infection or malignancy. The appearance is variable, but often contains free floating echoes, echogenic septations across the fluid and evidence of matted or adherent bowel loops, showing diminished or absent peristalsis [13]. Associated features may also be appreciated, such as thickening of the mesentery or omentum due to malignant infiltration. Haemoperitoneum can occur as a result of trauma, surgery or occasionally anticoagulation. Although acute intraperitoneal haemorrhage can appear anechoic, it more typically has fine, swirling echoes within it. If a patient is static in position, then these will start to layer out, producing fluid debris levels within the ascites. With significant haemoperitoneum a haematoma can form within the peritoneal cavity, which appears as an echogenic mass, with no blood flow demonstrated within it on colour Doppler. Over time clot lysis will result in the development of cystic like areas within the haematoma, some containing septations and debris.

Another, relatively uncommon, source of ascites producing free floating echoes or a layered effect on ultrasound is chylous, arising due to the disruption of the lymphatic system as a result of trauma, surgery, malignant infiltration of the lymphatics or lymphadenitis [14].

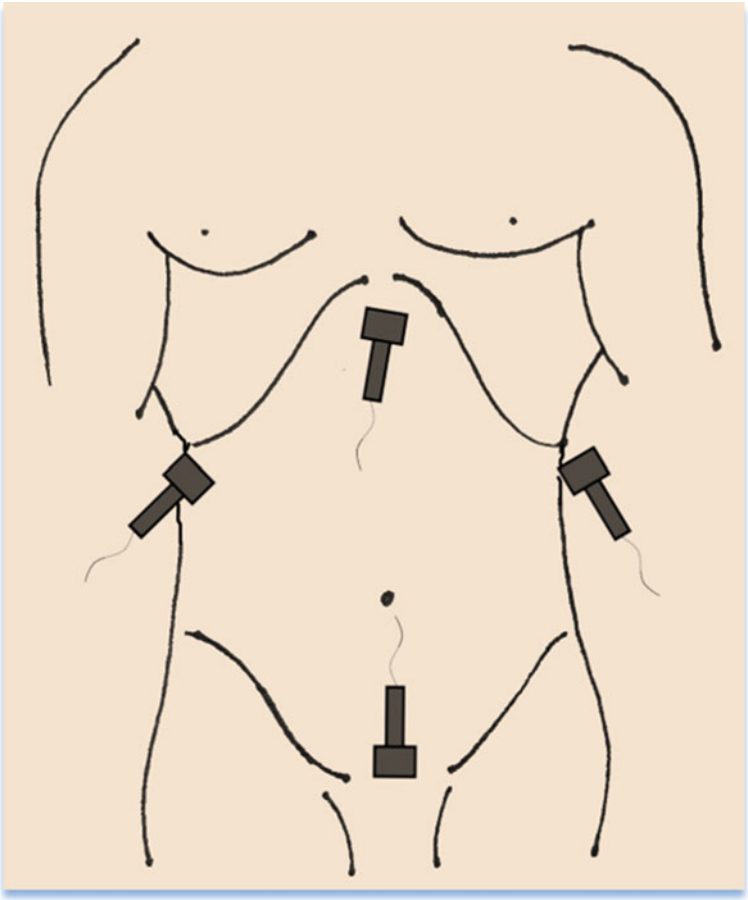

Fig. 13.10 FAST scan approach for free fluid. Probe positions include right and left flanks examining the upper quadrants, subxiphoid and pelvic view

13.9 Peritonitis

Defined as diffuse inflammation of the parietal and visceral peritoneum, there are infective: bacterial, viral, fungal, parasitic, and non-infective causes: chemical, granulomatous and sclerosing. Infective causes tend to be secondary to a disease process originating in one of the abdominal organs, although spontaneous bacterial peritonitis can occur in patients with underlying cirrhosis or nephrotic syndrome. Appearances of infected peritonitis include: increased peritoneal fluid containing debris, septations or gas locules. Thickening of the peritoneal stripe can be appreciated with high resolution ultrasound, while the curvilinear array can be used to identify thickening of the mesentery and omentum.

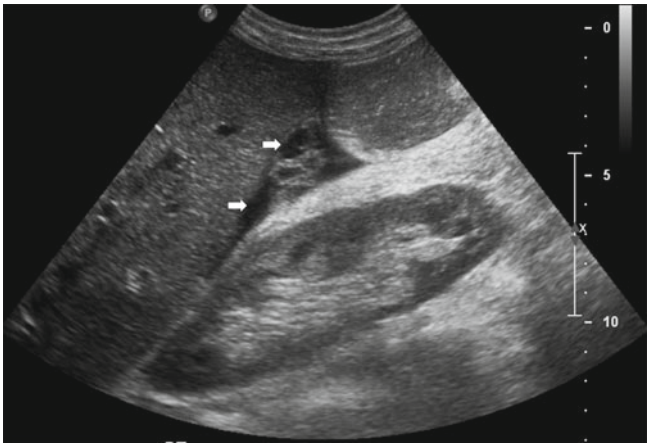

Fig. 13.11 FAST view 1, is an oblique longitudinal view through the liver, right kidney and right hemidiaphragm (not seen here). There is a septate fluid collection seen in the hepato-renal space (arrows)

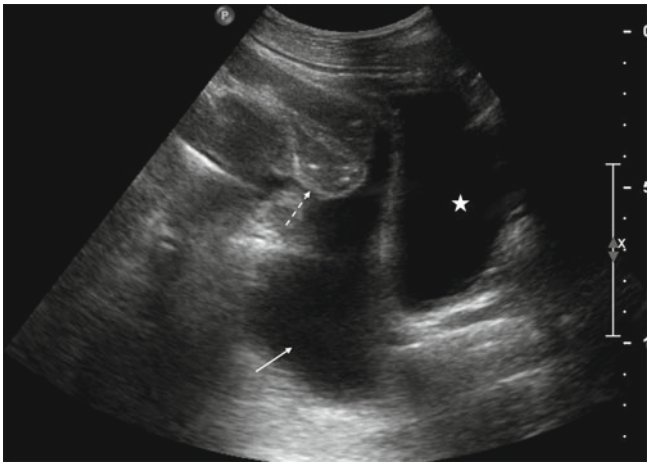

Fig. 13.12 FAST view pelvis in same patient shows free fluid (arrow) behind the bladder (star). Small bowel loops are seen within the free fluid (dashed arrow)

Tuberculous peritonitis is one of the more common extrapulmonary manifestations of this infection and its incidence is increased in patients with advanced HIV infection [15]. It can mimic a number of other disease processes, including malignancy and ultrasound can be used to guide diagnostic aspiration of ascites, or enlarged intra-abdominal lymph nodes. Three types of tuberculous peritonitis have been described: wet, dry and fibrotic; with the latter forming a mass of omentum, loops of bowel and mesentery [16]. Although in themselves non-specific, in the

correct clinical context, the following findings on ultrasound can suggest this as a diagnosis: ascites that is either anechoic or contains particulate material; or fine fibrotic septations producing a lattice-like pattern [17].

Sclerosing peritonitis is uncommon, but is one of the major complications of patients on CAPD and is characterised by total, or partial encasement of the small bowel within a thick fibrocollagenous membrane. Patients experience symptoms of small bowel obstruction and loss of ultrafiltration. In the early stages, echogenic strands in ascitic fluid are typically seen around the liver, followed by matting of bowel loops which show wall thickening. Finally the small bowel is encased by an echogenic membrane measuring 1–4 mm, which is seen to lie anterior to the bowel [18].

13.10 Abscess

Ultrasound may not have the sensitivity and specificity of CT for identifying focal intraperitoneal abscess formation (Fig. 13.13), but in the immobilized intensive care patient, it is an important first line imaging modality when a focal intra-abdominal collection is suspected. A methodical approach is required, with dependent areas in the peritoneal cavity the most likely locations for a collection, although they can form between bowel loops (Table 13.2). A similar scanning technique to that used for free fluid will cover most of the likely areas, although this should be extended to include both flank areas for paracolic and psoas collections (Fig. 13.14). Sonographic appearance of abscesses varies considerably, from a relatively well defined anechoic collection, indistinguishable from loculated ascites, to one with irregular margins containing fee floating echoes or clumps of solid material. The presence of gas within a focal collection is virtually diagnostic of an abscess and causes bright focal echoes, some of which may produce reverberation artifact or acoustic shadowing [19]. If this is located between bowel loops however, it may be difficult to confidently distinguish this as an abscess separate to bowel.

13.11 Percutaneous Aspiration and Drainage

Ultrasound is now routinely used to guide percutaneous aspiration and drainage procedures within the peritoneal cavity. Although there can be some limitations for ultrasound guidance, such as when bowel loops are closely related to a gas filled collection, it is still possible to approach the majority of fluid collections/abscesses using ultrasound guidance. There is a measurable increase in successful paracentesis performed using ultrasound [20], while critical structures, namely the inferior epigastric artery, are avoided. Techniques for this are covered in another chapter.

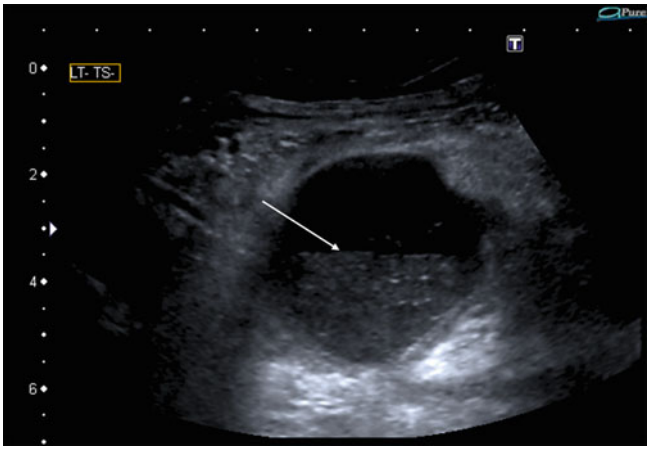

Fig. 13.13 Transverse image showing a focal pelvic collection in a patient following a perforated appendix. There is layering of echoes within the fluid collection (arrow), in keeping with high protein content/pus

Table 13.2 Locations of intraabdominal collections

Intraabdominal location
Subphrenic Spaces
Subhepatic Space
Hepatorenal Fossa
Lessor Sac
Paracolic gutters
Pelvis (cul de sac)
Surgical Sites

13.12 Pneumoperitoneum

The presence of free air within the peritoneal cavity is usually due to either recent abdominal surgery or the perforation of a hollow viscus. Traditionally the diagnosis had been made using erect chest radiographs, or in the supine patient abdominal radiographs, with lateral decubitus views to try and identify air outlining the liver. The reference imaging standard is now CT, which gives information on volume and location of free intraperitoneal air, but obviously this requires the patient to be transported off the intensive care unit.

Ultrasound can diagnose pneumoperitoneum, with a positive predictive value of up to 97% and overall accuracy of 90% [21]. The approach is similar to that when diagnosing a pneumothorax in the chest. A curvilinear or high frequency linear array are placed upon the epigastric region in longitudinal section and then moved laterally across the liver. The patient is then turned onto their left side (lateral

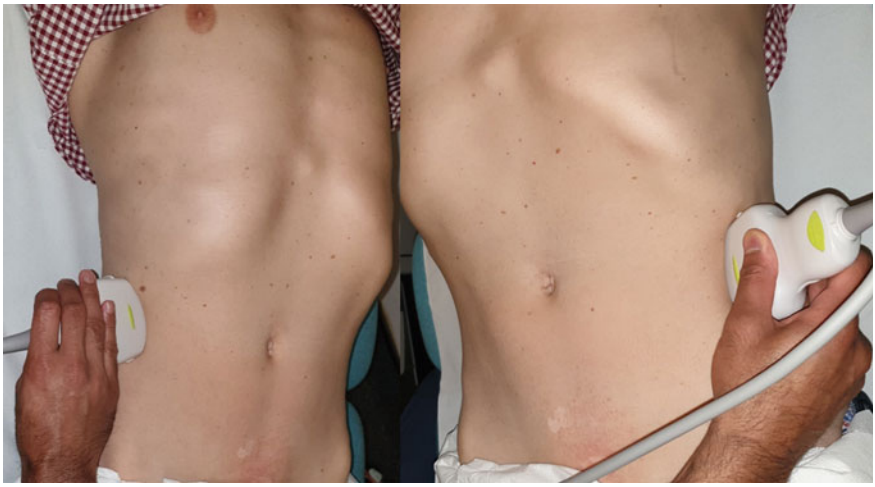

Fig. 13.14 Probe position for obtaining view of the right and left paracolic gutters, when looking for free fluid/collections

decubitus) and the scan repeated over the lateral aspect (i.e. highest) point of the liver. The operator is looking for the artefacts of a free air interface, namely ring-down or comet tail, which are generally better appreciated with the linear array. With the movement of free air the right lobe of the liver will be lost, as the air interface moves to the highest point (Fig. 13.15). If there is free peritoneal gas against the diaphragm the reverberation artefact may appear continuous with the chest. Careful scrutiny at the level of the diaphragm however will reveal that the air interface in the costophrenic recess from lung (assuming there is no pleural effusion), will overlap the air interface generated at the liver surface from a pneumoperitoneum as the patient breaths in, and then these two interfaces will separate during expiration (Fig. 13.16) [22].

In the presence of gas filled loops of bowel, distinguishing between free air against the anterior peritoneum and a loop of bowel containing gas can be challenging. With a high frequency linear array, the peritoneal stripe should be clearly identified as a thin echogenic interface. Free air will be seen as a strongly echogenic interface within this stripe, usually with reverberation or comet tail artefact. Gas in the bowel will also produce a strong echogenic interface, but there will be a small gap between this and the peritoneal stripe due to the wall of the bowel (Fig. 13.17) [23].

Depending upon the source of a pneumoperitoneum, free air may also be seen along the under surface of the liver, gallbladder fossa, or near the porta. If there is associated peritoneal free fluid or a localised collection, locules of gas will be seen within the fluid as highly reflective floating or fixed (depending upon how complex the fluid is) particles.

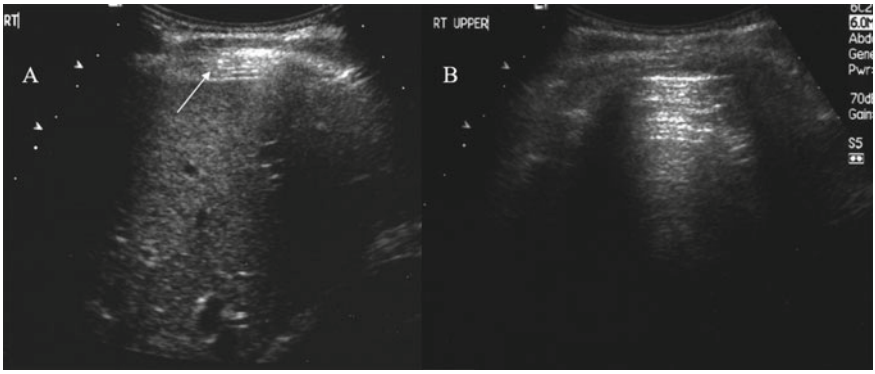

Fig. 13.15 **a** Transverse view through the liver, with some reverberation artefact over the liver surface, suspicious for free intraperitoneal air. **b** Repeat ultrasound with the patient now in left lateral decubitus position. The liver is no longer seen due to extensive reverberation artefact from free intraperitoneal air

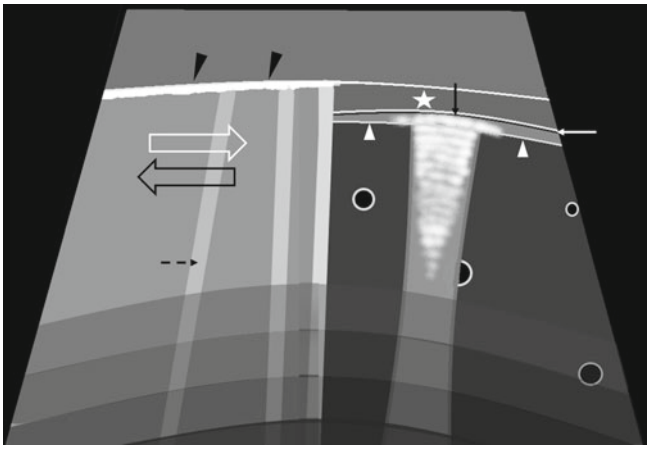

Fig. 13.16 Diagram of right costophrenic recess (star) ultrasound, showing free intraperitoneal air (black arrow) producing a comet tail artefact, over the liver edge (white arrowheads), deep to the parietal peritoneum (white arrow). The strongly reflective pleural interface, with its own ring down artefact (dashed arrow), is seen to move in an out of the recess (clear arrows) with respiration, passing over the top of the liver surface

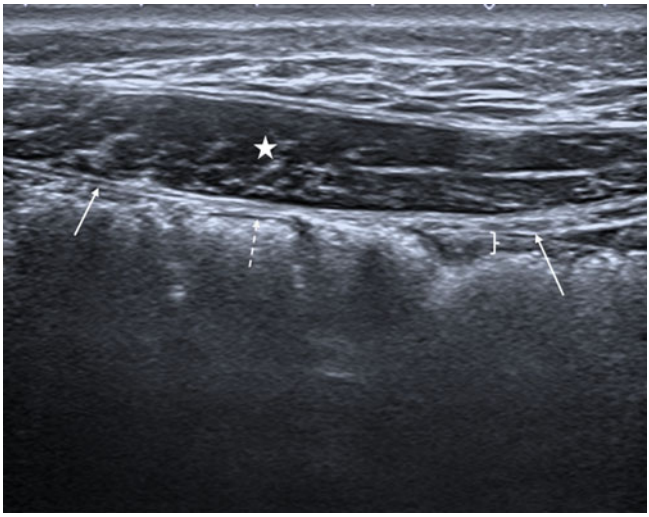

Fig. 13.17 High resolution image of gas filled bowel against the rectus sheath of the anterior abdominal wall (star), with visible bowel wall layers (bracket). The parietal peritoneum (arrow) is seen superficial to this and the air-mucosal interface is appreciated as a separate layer (dashed arrow)

13.13 Conclusion

Although traditionally the bowel has not been felt to be ideal for ultrasound imaging, it has good diagnostic accuracy and is especially useful in sick patients who may be unsafe to transfer round for CT scanning. It is essential in ensuring safe interventional procedures such as paracentesis.

See also:

Chapter 10 FAST scanning..

Chapter 11 Renal tract ultrasound

Chapter 12 Liver, Spleen and Biliary Tree.

Chapter 24 The Patient with Acute Abdominal Pain.

References

1. Fleischer AC, Muhletaler CA, James AE Jr. Sonographic assessment of the bowel wall. AJR Am J Roentgenol. 1981;136:887–91.
2. Kim HM, So BH, Jeong WJ, Choi SM, Park KN. The effectiveness of ultrasonography in verifying the placement of a nasogastric tube in patients with low consciousness at an

emergency center. Scand J Trauma Resusc Emerg Med. 2012;20:38. https://doi.org/10.1186/1757-7241-20-38.
3. Vigneau C, Baudel JL, Guidet B, Offenstadt G, Maury E. Sonography as an alternative to radiography for nasogastric feeding tube location. Intensive Care Med. 2005;31:1570–2.
4. Schmutz GR, Benko A, Fournier L, et al. Small bowel obstruction: role and contribution of sonography. Eur Radiol. 1997;7:1054–8.
5. Hefny AF, Corr P, Abu-Zidan FM. The role of ultrasound in the management of intestinal obstruction. J Emerg Trauma Shock. 2012;5:84–6.
6. Grassi R, Romano S, D'Amario F, Giorgio Rossi A, Romano L, Pinto F, Di Mizio R. The relevance of free fluid between intestinal loops detected by sonography in the clinical assessment of small bowel obstruction in adults. Eur J Radiol. 2004;50:5–14.
7. Danse EM, Kartheuser A, Paterson HM, Laterre PF. Color Doppler sonography of small bowel wall changes in 21 consecutive cases of acute mesenteric ischemia. JBR-BTR. 2009;92:202–6.
8. Tarrant AM, Ryan MF, Hamilton PA, Benjaminov O. A pictorial review of hypovolaemic shock in adults. British J Radiol. 2008;81:252–7.
9. Theodoropoulou A, Koutroubakis IE. Ischemic colitis: clinical practice in diagnosis and treatment. World J Gastroenterol. 2008;14:7302–8.
10. Ripollés T, Simó L, Martínez-Pérez MJ, Pastor MR, Igual A, López A. Sonographic findings in ischemic colitis in 58 patients. AJR Am J Roentgenol. 2005;184:777–85.
11. O'Malley ME, Wilson SR. US of gastrointestinal tract abnormalities with CT correlation. Radiographics. 2003;23:59–72.
12. Ramachandran I, Sinha R, Rodgers P. Pseudomembranous colitis revisited: spectrum of imaging findings. Clin Radiol. 2006;61:535–44.
13. Edell SL, Gefter WB. Ultrasonic differentiation of types of ascitic fluid. AJR Am J Roentgenol. 1979;133:111–4.
14. Franklin JT, Azose AA. Sonographic appearance of chylous ascites. J Clin Ultrasound. 1984;12:239–40.
15. Marshall JB. Tuberculosis of the gastrointestinal tract and peritoneum. Am J Gastroenterol. 1993;88:989–99.
16. Ozkan K, Gurses N, Gurses N. Ultrasonic appearances of tuberculous peritonitis. J Clin Ultrasound. 1987;15:350–2.
17. Denton T, Hossain J. A radiological study of abdominal tuberculosis in a Saudi population, with special reference to ultrasound and computed tomography. Clin Radiol. 1993;47:409–14.
18. Hollman AS, McMillan MA, Briggs JD, Junor BJ, Morley P. Ultrasound changes in sclerosing peritonitis following continuous ambulatory peritoneal dialysis. Clin Radiol. 1991;43:176–9.
19. Doust BD, Quiroz F, Stewart JM. Ultrasonic distinction of abscesses from other intra-abdominal fluid collections. Radiology. 1977;125:213–8.
20. Nazeer SR, Dewbre H, Miller AH. Ultrasound-assisted paracentesis performed by emergency physicians vs the traditional technique: a prospective, randomized study. Am J Emerg Med. 2005;23:363–7.
21. Chen S-C, Wang H-P, Chen W-J, Lin F-Y, Hsu C-Y, Chang K-J, Chen W-J. Selective Use of Ultrasonography for the Detection of Pneumoperitoneum. Acad Emerg Med. 2002;9:643–5.
22. Lee DH, Lim JH, Ko YT, Yoon Y. Sonographic detection of pneumoperitoneum in patients with acute abdomen. AJR Am J Roentgenol. 1990;154:107–9.
23. Kuzmich S, Harvey CJ, Fascia DTM, Kuzmich T, Neriman D, Basit R, Tan KL. Clinical perspective. Perforated pyloroduodenal peptic ulcer and sonography. Am J Roentgenol. 2012;199:W587–W594. https://doi.org/10.2214/ajr.11.8292.

Chapter 14
Vascular Access

Manik Chandra and Andrew Bodenham

Keywords Ultrasound · Central venous catheterisation · Jugular vein · Subclavian vein · Axillary vein · Femoral vein · PICC line catheterisation

14.1 Introduction

Vascular access is essential for fluid therapy, invasive monitoring, drug administration, parenteral nutrition, renal replacement therapy, extracorporeal circuits and transvenous cardiac pacing. This chapter provides an overview of the use of ultrasound guided vascular access.

Ultrasound can be used directly or indirectly. Direct use allows visualisation of the needle entering the vein in real time whilst indirect use allows confirmation of the position of a patent vein prior to cannulation. Direct guidance is now recommended for internal jugular vein access but is likely to be beneficial for other sites of access [1–3].

Vessels can be imaged in short and long axis views and accessed using either in plane or out of plane needle techniques.

14.2 Equipment

High-frequency (5–15 MHz), high-resolution linear array probes are typically used. Small foot-print or hockey-stick style transducers are suitable for confined areas and children. Doppler imaging can supplement 2D ultrasound to demonstrate blood flow to help differentiate veins (mono-phasic flow) and arteries (bi-phasic flow).

M. Chandra (✉) · A. Bodenham
Department of Anaesthesia, Leeds Teaching Hospitals NHS Trust, Great George Street, Leeds LS1 3EX, West Yorkshire, UK
e-mail: manikchandra@nhs.net

A. Bodenham
e-mail: andy.bodenham@nhs.net

A. Walden et al. (eds.), *Ultrasound in the Critically Ill*,
https://doi.org/10.1007/978-3-030-71742-1_14

Prior to imaging review the settings to ensure optimum pictures. Select "vascular" settings to help enhance vascular images or nerve if looking for nerves to avoid (e.g. median nerve during PICC placement). Ensure an adequate depth setting to allow visualisation of the entire vessel and structures lying posterior to the target.

14.3 Sonographic Anatomy

Generally veins are accompanied by a corresponding artery. Veins are compressible and non-pulsatile whilst arteries demonstrate opposite characteristics. Prior to cannulation imaging of the vessel is essential to ensure full vessel patency and to identify at risk structures such as other vessels, pleura and nerves. Echogenic structures within vessels include thrombus, valves, calcification and atheroma.

14.4 Performing Venous Access

Once a site has been selected and a sterile field created, the operator should stand with the ultrasound image directly in front of them with the patient in between. Using real time scanning the vein is accessed. A short axis out of plane technique in commonly used because it allows easier visualisation of surrounding structures. Whilst providing negative pressure via a syringe the introducer needle is advanced towards the target vessel. Tenting of the anterior vessel wall is seen followed by a "give" with a corresponding flow of blood into the syringe as the needle enters the vessel. Whilst holding the needle the attached syringe is removed. Often a steady flow of blood is seen at the needle hub or it may vary with respiration. Arterial puncture is indicated if the flow of blood is pulsatile and cannulation should be abandoned if arterial access is not required.

The guidewire can now be introduced ensuring the proximal end is always visible. The position of the guidewire in the vessel should be confirmed with ultrasound prior to dilatation and subsequent catheter insertion. The guidewire should then be removed to avoid complications relating to guidewire retention. Once successful cannulation of the vein has been achieved, in the case of internal jugular and subclavian veins, a post-procedural chest radiograph or ECG guidance should be performed to confirm catheter tip position, the former can also exclude complications such as a pneumothorax.

14.5 Sites of Access

Common sites for central venous access include internal jugular veins, subclavian veins, axillary veins, upper arm and femoral veins. Factors influencing site choice include:

Vessel features—such as patency, size, depth and course.

Clinical factors—e.g.: subclavian/axillary access is often preferred in head injured patients.

Patient factors—the femoral route for patients who cannot tolerate head down positioning. Blocked or thrombosed veins from previous cannulation.

Surrounding pathology—such as overlying cellulitis.

Operator skills and experience.

14.5.1 Internal Jugular Vein

The most common site for central venous access is the internal jugular vein due to its easily accessible location but also less thrombotic and mechanical complications. The right side is preferred due to its straighter course to the SVC.

If tolerated, the patient, should lay supine in a slight head down position to allow filling of the jugular vein and also reduce the risk of air embolus. The probe is placed on the side of the neck. A field depth of 3–4 cm is usually adequate for imaging the internal jugular vein. A short axis out of plane technique is commonly used.

The main challenge with this route is avoiding the carotid artery which lies in close proximity to the vein (see Fig. 14.1).

Prior scanning of the vein's course allows identification of a suitable position for needle entry that avoids arterial puncture and valve damage. Other arterial vessels, such as the subclavian artery and its branches, can often be seen posterior to the vein and these are at risk if the posterior vein wall is punctured [4].

14.5.2 Subclavian/Axillary Vein

Subclavian and axillary vein access is associated with lower infective complications, increased patient comfort, easier dressing and securement. Visualisation of the subclavian vein can be impeded by the clavicle. However, the subclavian vein continues laterally as the axillary vein and this can be visualised in a short axis view below the lateral half of the clavicle (see Fig. 14.2) [5]. The pleura, which lies deep to the subclavian/axillary veins, should be identified to minimise the risk of pneumothorax. Supraclavicular approaches are an alternative.

The patient should lie supine with slight head down if possible. A field depth of 4–5 cm is usually required. Arm abduction can help central passage of guidewires and catheters.

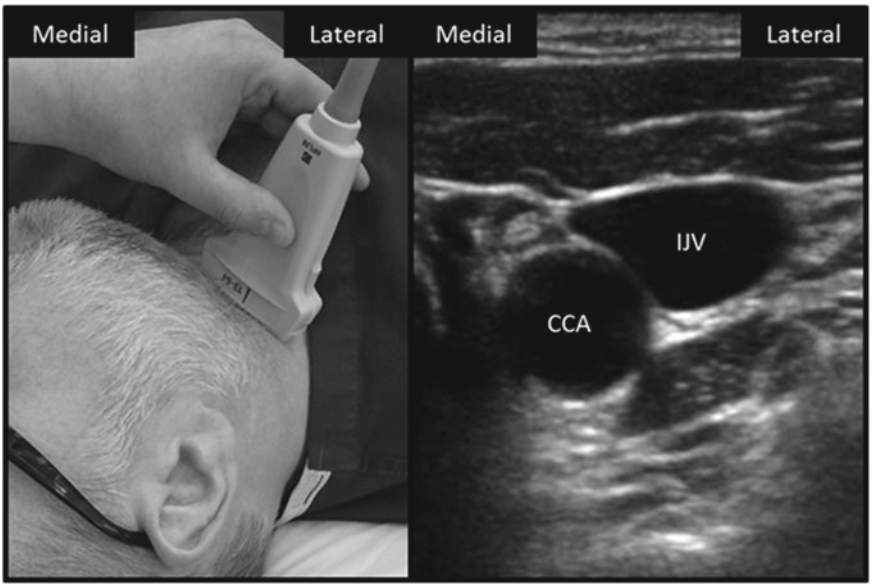

Fig. 14.1 Right internal jugular vein (IJV) at the level of the cricoid showing close proximity of common carotid artery (CCA)

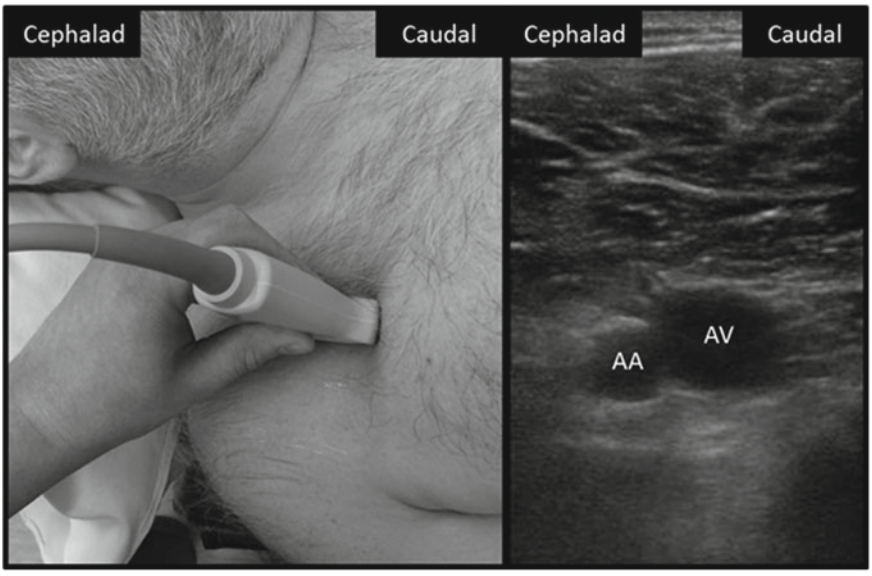

Fig. 14.2 Short axis view of right axillary vein (AV) lying in close proximity to axillary artery (AA)

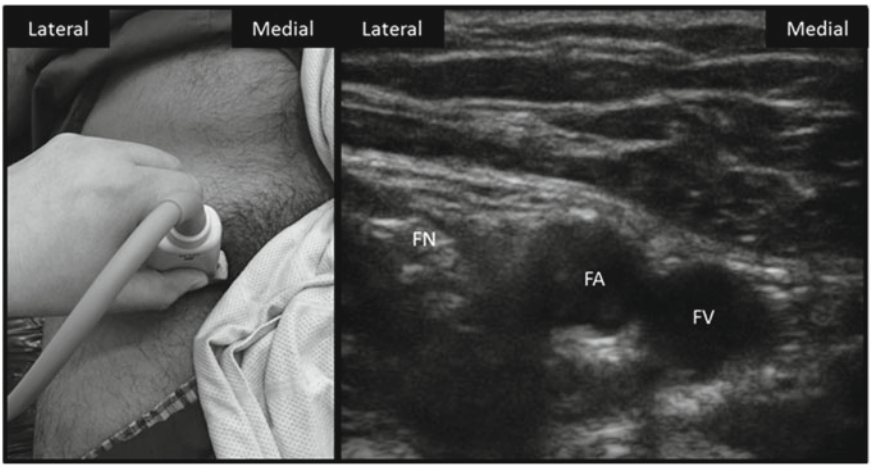

Fig. 14.3 Short axis view of right groin showing femoral vein (FV) and highlighting relationship with femoral artery (FA) and femoral nerve (FN) laterally

14.5.3 Femoral Vein

Whilst the femoral route is associated with higher risk of infection, it is preferred when other sites are not available or for specific therapies such as veno-venous and/or veno-arterial extracorporeal circuits.

With the patient supine the ultrasound probe is placed below the inguinal ligament. The femoral vein usually lies medial to the femoral artery (see Fig. 14.3). A short axis out of plane technique is commonly used. A field depth of 4 cm is usually adequate.

14.6 Complications

Inadvertent arterial puncture can occur at any site. Once recognised the next steps depend on the stage of cannulation. Whilst a small calibre guidewire can be removed and pressure applied, a larger dilator or catheter should be left in situ and help sought from a vascular surgeon or radiologist. Inadvertent vessel puncture can lead to haematoma and arteriovenous fistula formation.

Pneumothorax or haemothorax is a particular risk of subclavian vein cannulation but can occur with internal jugular and axillary vein access. The post procedural X-ray should be reviewed to rule out such complications.

Other complications include infection, thrombosis, cardiac tamponade, air embolism and nerve damage.

14.7 Arterial Access

As with venous cannulation ultrasound can be used to assess arterial vessel anatomy and patency. Ultrasound should be used early if there is difficulty using other techniques or a less commonly used artery such as the ulnar or dorsalis paedis is targeted. A short axis out of plane technique is commonly used.

14.8 Peripheral Access (PICCs/Cannulae)

Ultrasound can be used to aid peripheral cannulation in difficult cases such as intravenous drug abusers. Ultrasound use is essential for peripherally inserted central catheters (PICCs) in the upper arm, as the veins used tend to be deeper and close to at risk structures such as the median nerve (see Fig. 14.4).

14.9 Useful Adjuncts

Needles with echogenic tips can be used to improve tip visualisation. Needle guides can help with needle trajectory. Self-aspirating bulbs can allow the operator better control by handling the needle directly. There is insufficient evidence to support the routine use of these devices.

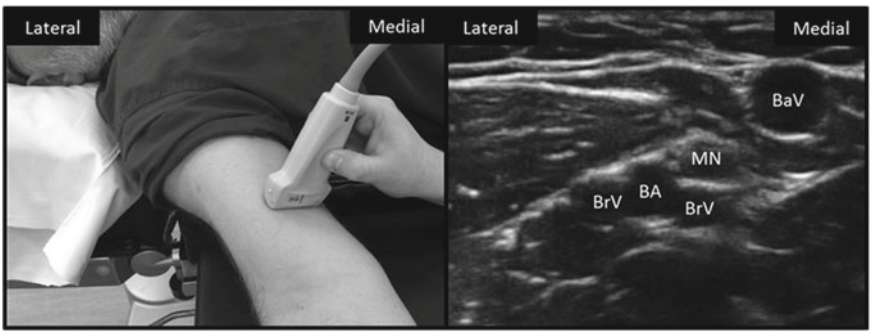

Fig. 14.4 Short axis view of right mid humeral arm veins (brachial vein (BrV) and basilic vein (BaV)) demonstrating at risk structures such as brachial artery (BA) and median nerve (MN)

14.10 Conclusion

Ultrasound has become the standard of care for central venous access and can be used for direct visualisation of all the major proximal veins. It is also useful when peripheral arterial or venous access is problematic.

See also:

Chapter 15 Venous Sonography.

References

1. Association of Anaesthetists of Great Britain and Ireland (AAGBI). Safe vascular access 2016. Anaesthesia. 2016;71:573–85.
2. Lamperti M, Bodenham AR, Pittiruti M, et al. International evidence-based recommendations on ultrasound-guided vascular access. Intensive Care Med. 2012;38:1105–17.
3. National Institute for Health and Clinical Excellence (NICE). Technology Appraisal No 49: guidance on the use of ultrasound locating devices for placing central venous catheters. 2002;1–24, https://www.nice.org.uk/guidance/TA49/chapter/1-guidance (2002, Accessed 30th April 2016).
4. Chandra M, Start S, Roberts D, et al. Arterial vessels behind the right internal jugular vein with relevance to central venous catheterisation. JICS. 2015;16:202–7.
5. O'Leary R, Ahmed SM, McLure H, et al. Ultrasound-guided infraclavicular axillary vein cannulation: a useful alternative to the internal jugular vein. Br J Anaesth. 2012;109:762–8.

Chapter 15
Venous Sonography

Eugene Tabiowo

Keywords Venous sonography · DVT · Common femoral vein

15.1 Introduction

Venous thromboembolisim (VTE) accounts for a sizable workload in health care [1]. Apart from its significant mortality impact, its non-fatal events still impose great pressure on the health service.

The NICE (2012) guidance on VTE recommends proximal leg vein ultrasound scanning as the diagnostic endpoint in DVT investigations [2]. This requires a formal, complete proximal vein assessment with ultrasound. In other words, a rule-out scan.

As part of the assessment of the sick or suspected VTE patient, early indication of a significant clot burden is important for the tailoring of management and overall care of the patient. There is now mounting evidence, that is supportive of rule-in scans to address this critical question [3–5].

This chapter aims to explain the process of a systematic rule-in scanning protocol. This management aid identifies significant clot load, if present, at that critical time point in the patients care. This however is not a rule-out departmental scan.

15.2 Equipment

For the assessment of DVT, a Brightness (B) mode ultrasound machine that is regularly safety checked and serviced is needed.

The probes needed for good vascular assessment need to be high in frequency. High frequency probes however have lower penetration. Hence, a linear transducer

E. Tabiowo (✉)
Royal Glamorgan Hospital, Ynysmaerdy, Llantrisant CF728XR, Wales, UK
e-mail: eugenetabiowo@hotmail.com

A. Walden et al. (eds.), *Ultrasound in the Critically Ill*,
https://doi.org/10.1007/978-3-030-71742-1_15

vascular probe has high frequency and is useful for high-resolution assessment of small legs were low depths are anticipated. For legs requiring higher depths, the curvilinear transducer which has lower frequency is more appropriate.

15.3 Anatomy

The anatomy of interest is the area from the common femoral vein (CFV) down to the distal popliteal vein (tri-fication).

During the scanning process, the common femoral vein, femoral vein, profunda vein and the popliteal vein are visualised.

15.4 Scanning Process

As with other medical processes, this should begin with an introduction by the person scanning, where possible. The machine should be set up with the patient's details and explanation of the process to the patient, where possible, is also a recommended starting point.

Verbal consent and patient cooperation is necessary before exposure of the exam area (groin to below knee). Patient positioning is a critical step to ensure comfort for the patient and the person scanning as well as helping to optimise image acquisition. Positioning is best supine with head tilt, hip externally rotated and with the knee slightly flexed (Fig. 15.1).

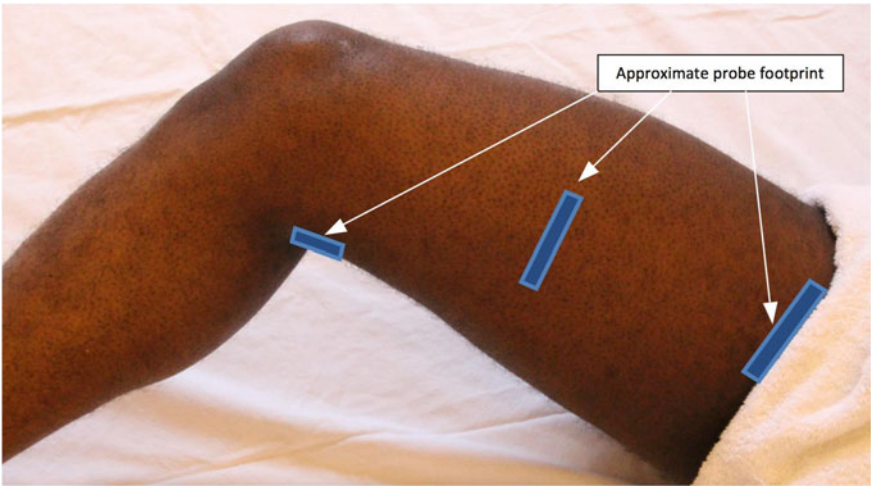

Fig. 15.1 Ideal scanning leg position and probe footprint. The 3 points of interest

Once the above is set, prepare the probe with gel and find the 'Mickey Mouse Sign' [6, 7].

The Mickey Mouse sign represents the level (in transverse plane) at which the femoral vein (common femoral vein) and the sapheno-femoral junction are visible. The face of Mickey Mouse represents the common femoral vein (CFV), while the ears represent the common femoral artery (CFA) and the long saphenous vein (LSV). The orientation of the 'ear' vessels depends on which leg is being scanned. The sapheno-femoral junction (SFJ) is therefore the attachment point of the corresponding ear, to the face of Mickey Mouse (Fig. 15.2).

After identifying the Mickey Mouse sign, identify the CFV. Visually inspect the lumen of the vein (thrombus may be seen as a mixed echogenic material within the lumen of the vessel which normally has an anechoic/black appearance) before applying a little downward pressure on the probe to ensure that the common femoral vein (CFV) compresses (Fig. 15.3). Complete wall-to-wall compression signifies a patent vessel. Partial compression signifies non-occlusive thrombus and no compression signifies an occlusive thrombus (Refer to Table 15.1—ultrasonic differentiation of veins and arteries).

This represents the first point in the 3-point scan. After gentle compression, the probe should then be moved medially down the thigh, while keeping focus of the femoral vein in the middle of the screen. Visualising the lumen and compressing down the length of the femoral vein will increase the sensitivity of the scanning process. Once at the mid thigh region, visualise the lumen and then gently compress the femoral vein. This represents the second point in the 3-point scan.

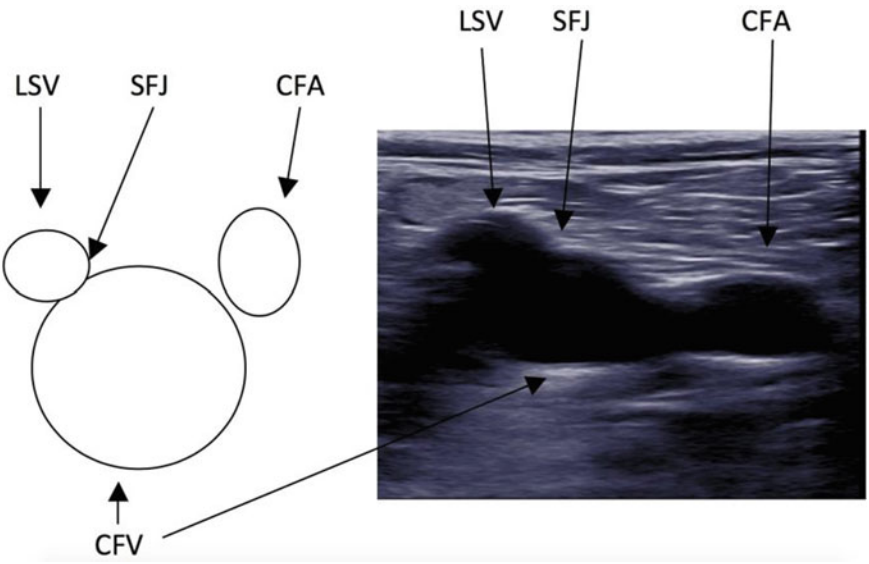

Fig. 15.2 Schematic of the Mickey Mouse sign—Left Leg. This shows the locations of the common femoral vein (CFV), Sapheno-femorel junction (SFJ), Long Saphenous Vein (LSV), and Common Femoral Artery (CFA)

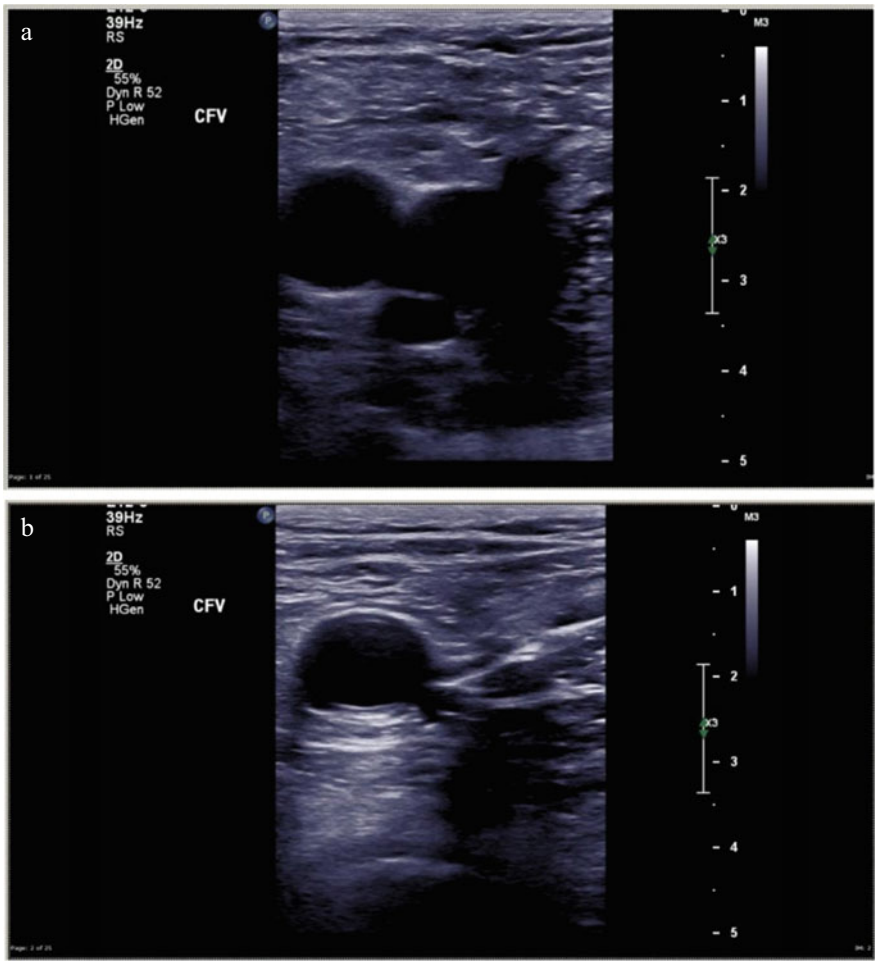

Fig. 15.3 Transverse view of the Common femoral vein before (**a**) and after (**b**) compression

Table 15.1 Ultrasonic differentiation of veins and arteries

	Vein	Artery
Wall	Thin	Thicker (Brighter)
Pulse	Non-pulsatile	Pulsatile
Compression with minimal pressure	Compressible	Much less compressible
Spectral Doppler	Low velocity	Higher velocity

After completion of above, continue to scan distally. Visualise and gently compress as you go along, until the femoral vein becomes difficult to visualise medially, as it continues on its course behind the knee. Lift the probe and place it in the popliteal fossa to visualise the popliteal vein. After attaining an acceptable image, visualise the lumen and gently compress. Assess for wall to wall vein compression, which signifies patency. This is the third point on the 3-point scan.

15.5 Use of Colour Doppler

Incorporating colour Doppler in the assessment process described above provides additional analysis of that vessel segment being interrogated.

To use colour Doppler, the machine would have to be equipped with this modality.

As with the above process, the only changes would be to use colour in between the visualisation and gentle compression steps; and the use of a longitudinal view of the vessel segment as opposed to the transverse view used above (Fig. 15.4).

For instance, once the CFV is identified in transverse section (Mickey Mouse), visually inspect the lumen, and then rotate the probe 90 degrees (with probe marker or light directed towards the head). Once in longitudinal view, apply colour and ensure that there is wall to wall filling of the colour signal within the lumen. Wall to wall filling equates to a patent vessel. The scale of the colour Doppler may have to be altered on the machine (understanding of knobology would be of use) to ensure adequate power scale. Partial filling with colour signifies partial obstruction and no filling suggests a totally occluded vessel.

15.6 What's 'Normal' or Not

A 'normal' scan in this context does not mean the exclusion of a DVT, as this is a rule-in process alone.

Clear identification of the common femoral vein, down to the distal femoral vein and popliteal vein, with complete wall-to-wall compression is 'normal' in this context.

A positive scan in this context identifies the presence of thrombotic material within the examined vessel. This identification occurs visually, or in the absence of complete wall-to-wall compression or filling (in colour Doppler mode). The vessel could be identified as completely occluded (with obvious thrombus seen within ± no compression or colour filling) or partially occluded (with obvious thrombus seen within part of the lumen ± partial compression or colour filling) (Fig. 15.5).

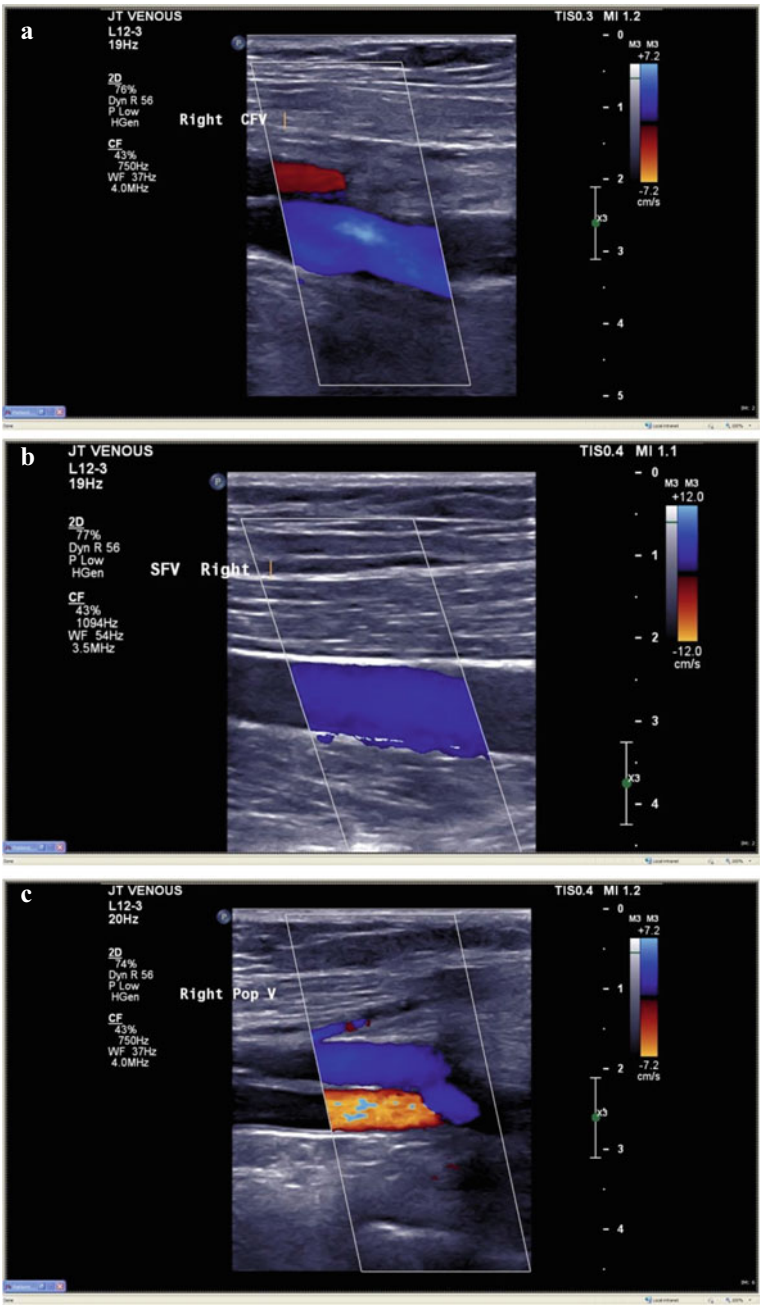

Fig. 15.4 Longitudinal view of CFV (**a**), FV (**b**), and PV (**c**) with wall to wall filling on colour Doppler reflecting patent vessels

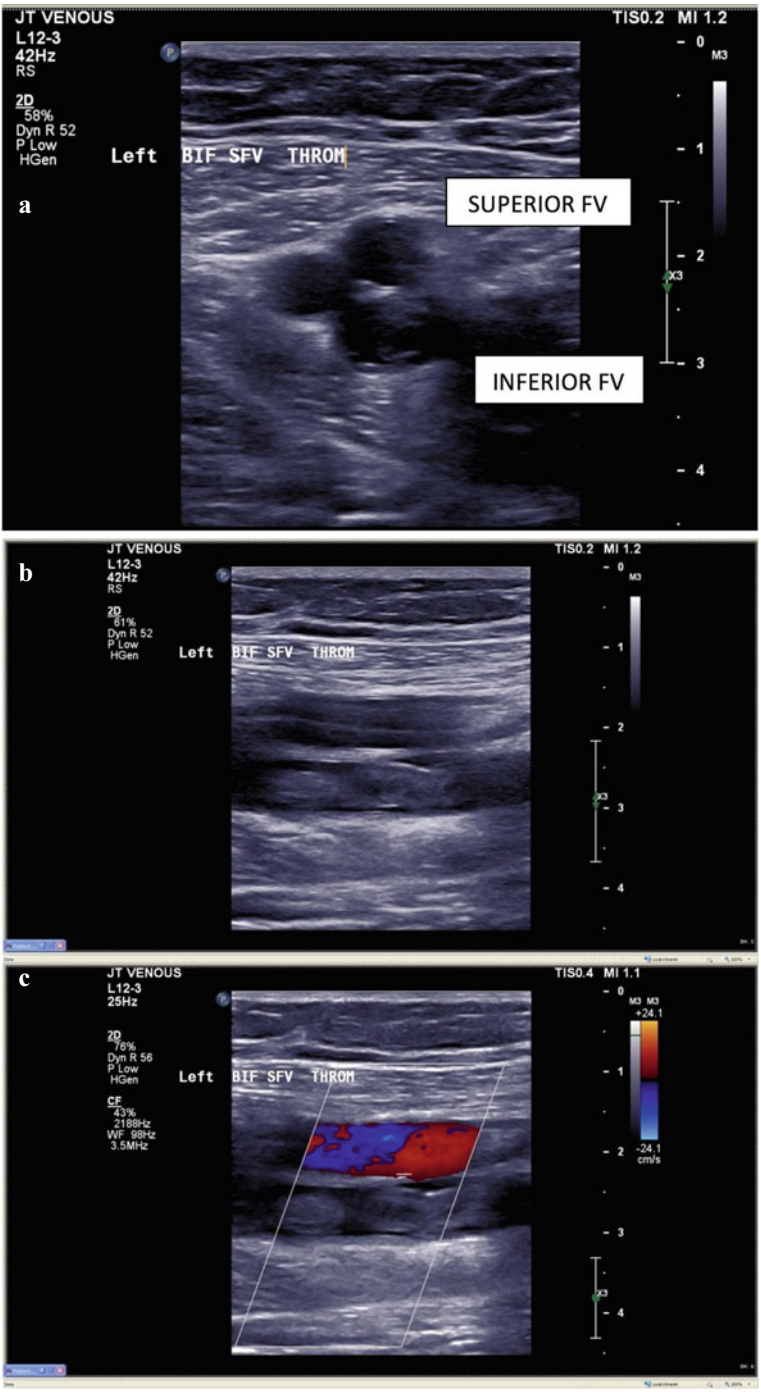
JT VENOUS
L12-3
42Hz
RS
2D
58%
Dyn R 52
P Low
HGen
Left
BIF SFV THROM
TIS0.2 MI 1.2
M3
SUPERIOR FV
INFERIOR FV
a
b
JT VENOUS
L12-3
42Hz
RS
2D
61%
Dyn R 52
P Low
HGen
Left
BIF SFV THROM
TIS0.2 MI 1.2
M3
c
JT VENOUS
L12-3
25Hz
2D
76%
Dyn R 56
P Low
HGen
CF
43%
2188Hz
WF 98Hz
3.5MHz
Left
BIF SFV THROM
TIS0.4 MI 1.1
M3 M3
+24.1
-24.1
cm/s

◂**Fig. 15.5** **a** Transverse view of Proximal CFV showing bifid CFV with thrombus in the inferior FV; **b** Longitudinal view of the same; **c** Longitudinal view of the same with no colour filling. This is consistent with complete lumen obstruction by the clot material visually, on compression and with colour flow

Studying the physics of ultrasound allows for a greater understanding of how images are acquired and artefacts generated. A basic primer in physics is essential in any ultrasound based training program and this chapter sets out to give an overview as well as common artefacts and imaging modes.

References

1. NICE: Venous thromboembolism: reducing the risk for patients in hospital. https://www.nice.org.uk/guidance/cg92/resources/venous-thromboembolism-reducing-the-risk-for-patients-in-hospital-975745995973 (2010).
2. NICE: Venous thromboembolic diseases: diagnosis, management and thrombophilia testing. https://www.nice.org.uk/guidance/cg144/resources/venous-thromboembolic-diseases-diagnosis-management-and-thrombophilia-testing-35109570835141 (2012). Accessed 29 Jan 2017.
3. Blaivas M, et al. Lower-extremity doppler for deep venous thrombosis—can emergency physicians be accurate and fast? Acad Emerg Med. 2000;7:120–6.
4. Bernardi E, Camporses G, Büller HR. Serial 2-Point ultrasonography plus D-dimer vs. whole-leg colour-coded doppler ultrasonography for diagnosing suspected symptomatic deep vein thrombosis. A randomised controlled trail. JAMA. 2008;300(14):1653–59.
5. Adhikari S, et al. Isolated deep venous thrombosis: implications for 2-point compression ultrasonography of the lower extremity. Ann Emerg Med. 2014;1-5.
6. Igari K, et al. Anatomical variation at the Sapheno-Femoral junction. Ann Vasc Dis. 2013;6(4):702–5.
7. Coleridge-Smith P, et al. Duplex ultrasound investigation of the veins in chronic venous disease of the lower limnbs—UIP consensus document. Part 1. Basic principles. Eur J Vasc Endovasc Surg. 2006;31:83–92.

Chapter 16
Neuro-ophthalmic Ultrasound

Claire Shevlin

Keywords Ocular ultrasound · Optic nerve sheath diameter · Point of care ultrasound

16.1 Introduction

The bedside use of ultrasound for both neuromonitoring, and as an aid to diagnosis on the intensive care has not had the same surge in popularity as other modes of ultrasound. Reasons for this include an absence of familiarity, lack of equipment or a perception of difficulty in comparison to more standard measures of intracranial pressure (ICP) and pathology. However, neuro-ultrasound is much less invasive than standard ICP monitors, cost-effective and portable.

Supporting evidence and the basic techniques in practical ultrasound of the optic nerve and pupil are described. This chapter should be read in conjunction with Chap. 17 on trans-cranial doppler.

16.2 Ophthalmic Ultrasound

The eye is a particularly rewarding organ to scan—the amount of fluid contained within the globe permits excellent conduction of sound waves and the consequent production of clear images and well-visualised structures.

First performed in 1956 by Fledelius [1], the quality of ophthalmic ultrasound has evolved dramatically in recent decades. B-scan (brightness scans) of the eye produce accurate and fairly detailed images of intraocular pathophysiology.

C. Shevlin (✉)
Intensive Care Unit, Craigavon Area Hospital, Portadown, Northern Ireland, UK
e-mail: claireshevlin@gmail.com

A. Walden et al. (eds.), *Ultrasound in the Critically Ill*,
https://doi.org/10.1007/978-3-030-71742-1_16

16.2.1 Anatomy of the Optic Nerve Sheath and Pupillary Aperture

The intraorbital section of the optic nerve extends from the globe, where it inserts medially, to the optic canal located in the lesser wing of the sphenoid bone. It is encased by a meningeal sheath consisting of dura mater, arachnoid mater and pia mater. Cerebrospinal fluid is contained in the trabeculated subarachnoid space and is continuously and slowly filtered. As a result the optic nerve sheath is in direct communication with the intracranial subarachnoid space. It is this relationship that forms the physiological basis for using the optic nerve sheath as a surrogate for intracranial pressure measurement.

After light passes through the transparent cornea in the anterior portion of the eye, a fraction enters the pupillary aperture before entering the crystalline lens. The size of this opening is adjusted by the constriction and dilatation of the iris. The iris is a complicated structure of four layers—a superficial anterior layer, the stroma and sphincter muscle, the anterior epithelium, and a posterior pigmented epithelium which lends colour to the iris. The complexity of this structure and the difference in its density in comparison to surrounding structures means that it is well delineated on ultrasound in most views.

When an ultrasound transducer is placed on the closed eyelid, the globe is seen as a round, dark, fluid filled structure. It is commonly visualized in the antero-posterior plane. The cornea appears as a smoothly arched hyperechoic line (Fig. 16.1).

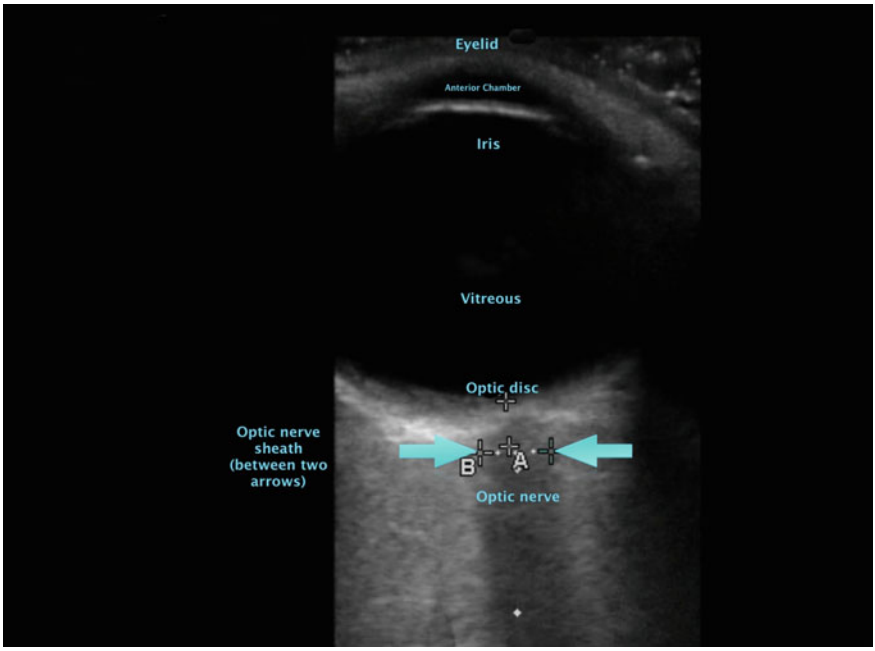

Fig. 16.1 Ophthalmic ultrasound anatomy on transverse imaging

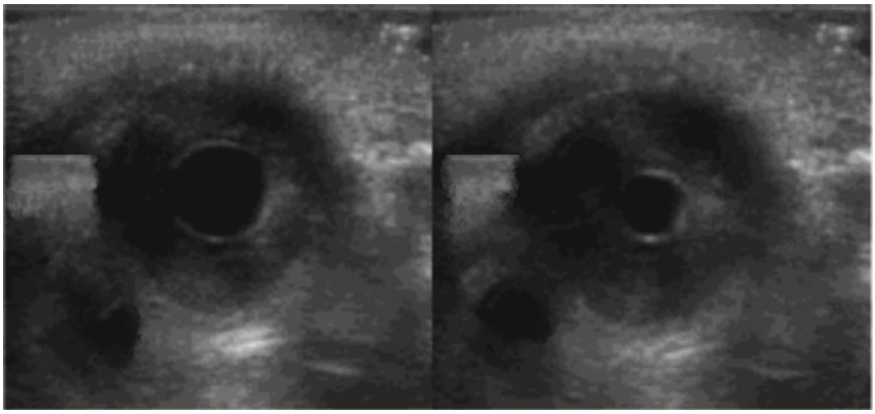

Fig. 16.2 Coronal image of the iris and pupillary aperture before and after consensual response

The anterior chamber—and generally speaking, the lens, if normal—are anechoic. The iris appears bright and echogenic. The choroid and retina may be seen as a thin grey layer at the posterior aspect of the globe. The optic nerve is the 'black stripe' running away from the posterior aspect of the globe and optic disc, and should ideally be positioned in the centre of the ultrasound screen. The nerve sheath, as seen on ultrasound examination, has a high reflectivity compared to the homeogenous appearance of the nerve, and should be relatively easy to distinguish.

Assessment of the pupil and pupillary response is made possible by the fact that as well as the antero-posterior planes utilized for visualization of the globe and optic nerve, the eye can also be examined in coronal or near coronal section. This view allows the iris and aperture representing the pupil to be seen clearly and distinctly from the strongly reflective lens, and allows assessment of the consensual pupillary response (Fig. 16.2).

16.3 Evidence for Ultrasound of the Optic Nerve Sheath

The diameter of the optic nerve sheath (ONS) on ultrasound has been found to be a strong predictor of raised intracranial pressure, with a high sensitivity and specificity in multiple studies and in a systematic review [2]. It also performed well in comparison to computed tomography for both the exclusion and inclusion of raised ICP [3].

Ultrasound measurement of the optic nerve sheath diameter (ONSD) permits repeated noninvasive assessments of intracranial pressure and allows evaluation of the response to treatment. As invasive intracranial pressure monitoring is typically restricted to neurosurgical centres, this mode of investigation is particularly suited to patients suspected of raised intracranial pressure prior to transfer for definitive

treatment, as well as patients who continue to be cared for in non-neurosurgical critical care units. In addition to its diagnostic goal, there is some, albeit limited, evidence to suggest that ONSD can also be used for prognostication [4, 5].

The majority of articles on ONSD measurement are in the setting of raised intracranial pressure secondary to traumatic brain injury. However, a few studies have used this measurement to diagnose or assess the severity of other pathologies, including meningitis, stroke, hepatic encephalopathy, epilepsy, and acute mountain sickness [6–9].

The potential value of this technique is reflected in the significant number of studies performed to date. Unfortunately, most have small patient numbers and hence low power, and could be criticised for potential observer bias. Efforts are ongoing to define the ONSD indicating 'true' raised intracranial pressure, the best sonographic approach to visualise the optic nerve sheath, the optimum axis to assess the optic nerve sheath, and the impact of operator experience on measurement variability.

16.3.1 Advantages and Disadvantages of Optic Nerve Ultrasound

Advantages of optic nerve ultrasound include:

1. Reproducibility of measurements
2. Non-invasive nature of the technique
3. Ready availability of equipment
4. Portability of equipment
5. Rapid performance
6. Relatively low costs
7. Avoidance of ionising radiation
8. Avoidance of patient transport for imaging.

Practical disadvantages are few and relate primarily to the need to acquire competence in the scanning technique to optimise accuracy, the potential risk of pressure injury to the globe if technique is poor, and the potential for injury resulting from thermal and non-thermal effects of ultrasound.

The primary clinical disadvantage, given the relative novelty of the technique, lies in the ongoing lack of a uniform cut-off value for the diagnosis of raised intracranial pressure. In the earlier studies conducted on ONSD, a tentative association emerged between an ONSD of 5.0 mm and the presence of raised intracranial pressure. In a study of 59 emergency department patients, [10] Tayal (2007) found an ONSD of 5.0 mm had a 100% sensitivity to detect patients with raised intracranial pressure. Another emergency department study by [11] Qayyum (2013), found a sensitivity and specificity of 100% and 75%, respectively, for a cutoff of 5.0 mm, with positive and negative predictive values of 94.5 and 100%.

However, other studies have found evidence for different optimal cut-offs, using 5.2 [12] or even 5.7 mm [13, 14]. Generally speaking, 5.0 mm is taken to be the cut-off but the higher the figure, the more positive the association.

Of note, ethnic differences may need to be taken into account when measuring ONSD as a surrogate measure of ICP. Asian populations in particular have shown widely varying results—a study in Chinese patients correlated an elevated opening pressure on lumbar puncture with a significantly lower ONSD than in Caucasian populations [15]. In contrast, a confounding article in a similar population showed a median sonographic measurement of 5.1 in a group of 519 healthy Chinese adults [16].

ONSD measurement has not been widely examined in paediatric patients and no strong evidence to diagnose raised intracranial pressure exists. One study, in 64 paediatric patients, reported a very low specificity of ONSD for raised intracranial pressure [17].

16.4 Technique of Optic Nerve Ultrasound

- Select the high frequency linear array probe on the ultrasound machine as this provides the best compromise between footprint and resolution of superficial structures (Fig. 16.3).
- Apply ultrasound gel liberally to the closed eyelid. If desired, a clear thin dressing (e.g. IV cannula dressing) can be used as a barrier between the closed eyelid and the gel medium although this is not strictly necessary.
- Resting the probe hand on a bony structure such as the forehead or brow ridge stabilises the image and lowers the risk of inadvertent pressure on the globe.
- Place the ultrasound probe lightly over the gel in a transverse orientation initially. There should neither be any direct contact of the probe with the eyelid nor pressure exerted on the globe. The probe marker should be orientated laterally (Fig. 16.4a).

Fig. 16.3 High frequency linear array probe

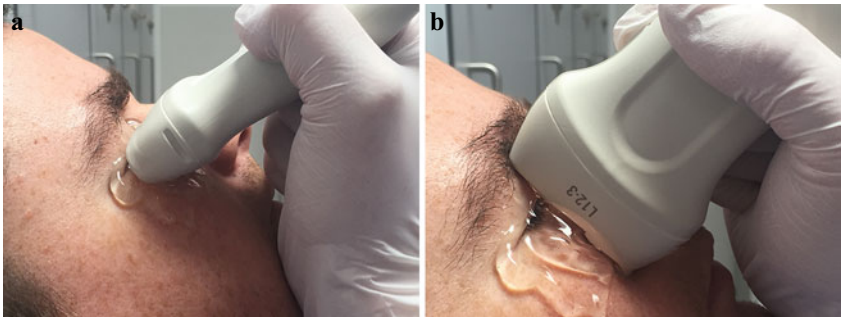

Fig. 16.4 **a** Transverse imaging. **b** Parasagittal imaging

- With small, subtle movements scan from side to side (i.e. temporal to nasal), slowly angling the probe superiorly or inferiorly to bring the optic nerve into view. The nerve will appear as a 'black stripe' running posteriorly from the rear of the globe. The goal is to centre this on the monitor. If the lens or iris is not seen in your image, the imaging plane is likely off-axis and may result in an underestimation of ONSD.
- The globe should also be scanned in the parasagittal plane, with the probe marker superiorly, towards the patient's forehead (Fig. 16.4b).
- Both eyes should be scanned, in case of unilateral papilloedema.
- The time spent in active scanning should be minimised. Once the optimum view has been obtained, store the image either as a frame or a video loop and remove the probe from the eye. Measurements can then be performed without unnecessary exposure of the eye to ultrasound energy.
- Use the caliper function on the ultrasound to enable precise measurement. First locate a point 3 mm posterior to the optic disk. At this point place the calipers at 90° to the axis of the optic nerve to measure the diameter of optic nerve and optic nerve sheath (Fig. 16.5).

If the optic nerve sheath is markedly dilated, it may be possible to diagnose this from visual estimation alone. In general, however, the software calipers should be used to ensure accurate measurement and recording. In severely raised intracranial pressure, it may be possible to visualise a 'crescent sign' [18], an echolucent circular artefact within the sheath separating the sheath from the nerve due to increased subarachnoid fluid.

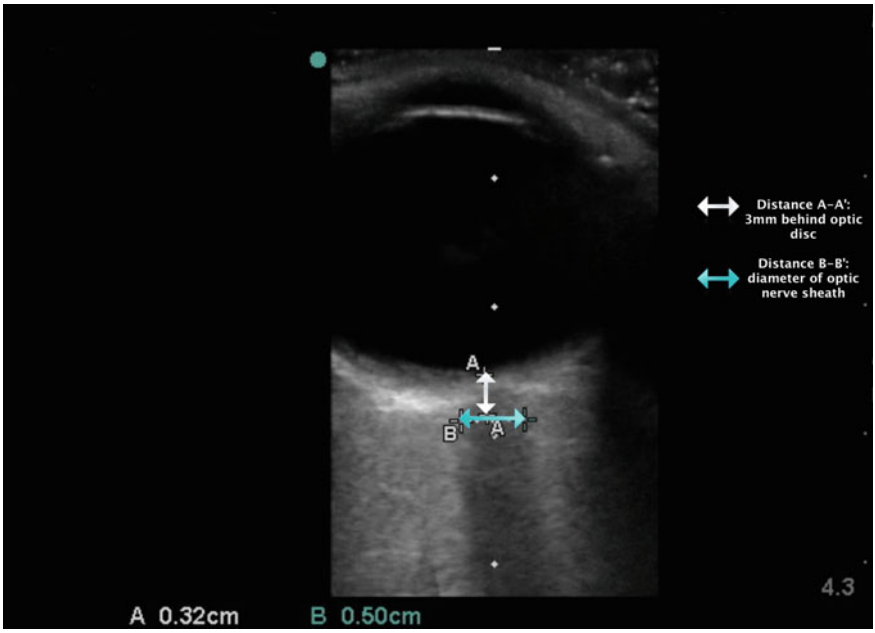

Fig. 16.5 Caliper positions for ONSD measurement

16.5 Ultrasonic Examination of the Pupillary Reflex

Assessment of the pupillary light reflex is a common component of clinical examination in the intensive care unit. The iris and its response to light and darkness stimuli offers useful information in a variety of conditions [19].

Designed to control how much light enters through the pupillary aperture, the pathway leading to pupil constriction has an afferent limb within the second cranial nerve, and an efferent limb in the oculomotor nerve (the third cranial nerve). The reflex is consensual—stimuli to one eye results in reaction in both. The pupillary 'dark response'—dilatation of the pupil when light is removed—involves the relaxation of the iris sphincter and contraction of the iris dilator, the latter is controlled by the sympathetic nervous system.

The common method of examination of the pupillary light reflex is the shining of a focused light into one eye and observing the response in both pupils. In some patient groups—for example, those with substantial orbital trauma and associated oedema, or hyphaema, this can be a challenging examination. However it has prognostic significance and is important to perform—absence of the pupillary light reflex (PLR) is directly associated with increased mortality in head trauma [20]. It is useful to have an alternative to direct clinical examination, and ophthalmic ultrasound readily fills this niche. In patients with severe head injuries, serial ultrasound

examinations could be used to monitor for non-reactive pupils [21]. The technique described below is assessment of the consensual PLR which is similar to direct PLR in terms of the degree of constriction of the pupil [22].

Antero-posterior planes of the eye, coronal or near coronal sections of the eye are obtainable with ultrasound. It is a relatively simple procedure—in one study, imaging of the iris was achieved in all subjects in less than 2 min with an average time of 1 min 10 s [23].

16.5.1 Technique of Ultrasonic Examination of Consensual Pupillary Light Reflex

- The patient should be supine. Similar to optic nerve sheath ultrasound, a high resolution linear array ultrasound transducer should be employed. The iris is ideal to scan as it has a complex structure, irregular surface due to its multiple layers, and returns many echoes back to probe allowing visualisation.
- Place a large amount of ultrasound gel over the closed eyelid. As with the optic nerve sheath diameter ultrasound, a clear plastic occlusive dressing may be employed to protect the eye from inadvertent intrusion of the gel.
- The transducer is placed transversely across and below the orbit. The globe is visualised and identification of the anterior chamber is performed as in the first example.

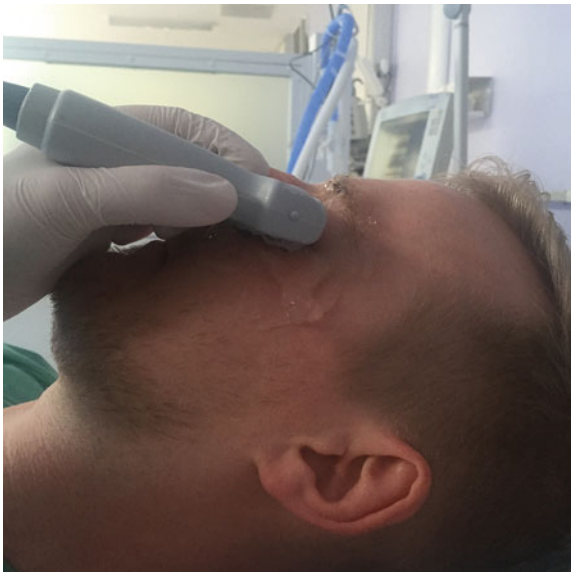

Fig. 16.6 Transverse imaging of the iris and pupillary aperture

- The transducer is then redirected caudally. The probe should be resting on the zygomatic bone. The probe is tilted 45°.
- The probe is manipulated until the iris and pupil are seen in cross section as in Fig. 16.6. It is important that a coronal or near coronal section of the eye is attained so that the pupil may be visualised separately from the strongly reflective lens.
- A light is shone in the other eye in order to perform a sonographic consensual pupillary reflex. The globe axis may change with the patient looking to right or left.
- The diameter of the pupil can be measured with calipers before and after light stimulation in the contralateral eye. This is best performed in a darkened area.
- M-mode may be utilized to better visualize the constriction and dilatation of the pupil over time.

Constriction of the pupil on the screen confirms function of the second and third cranial nerves. It also assesses the integrity of the retina, optic nerve and a portion of the midbrain.

16.6 Conclusion

There is scope to advance our practice with regard to neuro-ultrasound—the diagnosis and monitoring of response to treatment in raised intracranial pressure, for example. ONSD ultrasound is promising in this regard, and transcranial Doppler which is non-invasive, does not involve allergenic contrast mediums or exposure to ionizing radiation, or transport outwith the intensive care unit, could also add some valuable data to our day to day assessment of selected patient groups. The assessment of the iris and pupil, as well as the direct and indirect pupillary responses to light, is a useful adjunct to clinical examination in cases of ocular trauma.

With all ultrasound modalities, the pitfall lies principally in the operator's potential lack of familiarity with the technique and the inability to interpret findings in light of existing comorbidities and factors affecting scanning conditions.

See also:

Chapter 17 Transcranial Doppler.

References

1. Fledelius HC. Ultrasound in ophthalmology. Ultrasound Med Biol. 1997;23(3):365–75.
2. Dubourg J, Javouhey E, Geeraerts T, Messerer M, Kassai B. Ultrasonography of optic nerve sheath diameter for detection of raised intracranial pressure: a systematic review and meta-analysis. Intensive Care Med. 2011;37(7):1059–68. http://dx.doi.org/10.1007/s00134-011-2224-2.
3. Ohle R, McIsaac SM, Woo MY, Perry JJ. Sonography of the Optic nerve sheath diameter for detection of raised intracranial pressure compared to computed tomography: a systematic review and meta-analysis. J Ultrasound Med. 2015;34(7):1285–94.
4. Hwan Kim Y, Ho Lee J, Kun Hong C, Won Cho K, Hoon Yeo J, Ju Kang M, et al. Feasibility of optic nerve sheath diameter measured on initial brain computed tomography as an early neurologic outcome predictor after cardiac arrest. Acad Emerg Med. 2014;21(10):1121–8. http://dx.doi.org/10.1111/acem.12477.
5. Legrand A, Jeanjean P, Delanghe F, Peltier J, Lecat B, Dupont H. Estimation of optic nerve sheath diameter on an initial brain computed tomography scan can contribute prognostic information in traumatic brain injury patients. Crit Care. 2013;17(2):R61. https://doi.org/10.1186/cc12589.
6. Nabeta HW, Bahr NC, Rhein J, Fossland N, Kiragga AN, Meya DB, Dunlop SJ, Boulware DR. Accuracy of noninvasive intraocular pressure or optic nerve sheath diameter measurements for predicting elevated intracranial pressure in cryptococcal meningitis. Open Forum Infect Dis. 2014 Oct 11;1(3):ofu093
7. Shirodkar CG, Rao SM, Mutkule DP, Harde YR, Venkategowda PM, Mahesh MU. Optic nerve sheath diameter as a marker for evaluation and prognostication of intracranial pressure in Indian patients: An observational study. Indian J Crit Care Med. 2014 Nov;18(11):728–34
8. Fonseca P, Manno RL, Miller NR. Bilateral sequential trochleitis as the presenting feature of systemic lupus erythematosus. J Neuroophthalmol. 2013 Mar;33(1):74–6
9. Fagenholz PJ, Gutman JA, Murray AF, Noble VE, Camargo CA Jr, Harris NS. Optic nerve sheath diametercorrelates with the presence and severity of acute mountain sickness: evidence for increasedintracranial pressure. J Appl Physiol (1985). 2009 Apr;106(4):1207–11
10. Tayal VS, Neulander M, Norton HJ, Foster T, Saunders T, Blaivas M. Emergency department sonographic measurement of optic nerve sheath diameter to detect findings of increased intracranial pressure in adult head injury patients. Ann Emerg Med. 2007;49(4):508–14. http://dx.doi.org/10.1016/j.annemergmed.2006.06.040.
11. Qayyum H, Ramlakhan S. Can ocular ultrasound predict intracranial hypertension? A pilot diagnostic accuracy evaluation in a UK emergency department. Eur J Emerg Med. 2013;20(2):91–7. http://dx.doi.org/10.1097/MEJ.0b013e32835105c8.
12. Rajajee V, Vanaman M, Fletcher JJ, Jacobs TL. Optic nerve ultrasound for the detection of raised intracranial pressure. Neurocrit Care. 2011;15(3):506–15. http://dx.doi.org/10.1007/s12028-011-9606-8.
13. Soldatos T, Karakitsos D, Chatzimichail K, Papathanasiou M, Gouliamos A, Karabinis A. Optic nerve sonography in the diagnostic evaluation of adult brain injury. Crit Care. 2008;12(3):R67. http://dx.doi.org/10.1186/cc6897.
14. Bäuerle J, Nedelmann M. Sonographic assessment of the optic nerve sheath in idiopathic intracranial hypertension. J Neurol. 2011;258(11):2014–9. https://doi.org/10.1007/s00415-011-6059-0.
15. Wang L, Feng L, Yao Y, Wang Y, Chen Y, Feng J, et al. Optimal optic nerve sheath diameter threshold for the identification of elevated opening pressure on lumbar puncture in a Chinese population. PLoS One. 2015;10(2):e0117939. http://dx.doi.org/10.1371/journal.pone.0117939.
16. Chen H, Ding G, Zhao Y, Rong-Guo Y, Zhou J. Ultrasound measurement of optic nerve diameter and optic nerve sheath diameter in healthy Chinese adults. BMC Neurology 2015;15(106).

17. Le A, Hoehn ME, Smith ME, Spentzas T, Schlappy D, Pershad J. Bedside sonographic measurement of optic nerve sheath diameter as a predictor of increased intracranial pressure in children. Ann Emerg Med. 2009;53(6):785–91. http://dx.doi.org/10.1016/j.annemergmed.2008.11.025.
18. Marchese RF, Mistry RD, Scarfone RJ, Chen AE. Identification of optic disc elevation and the crescent sign using point-of-care ocular ultrasound in children. Pediatr Emerg Care. 2015;31(4):304–7. http://dx.doi.org/10.1097/PEC.0000000000000408.
19. Kardon R. Pupillary light reflex. Curr Opin Ophthalmol. 1995;6:20–6.
20. Schreiber MA, Aoki N, Scott BG, Beck JR. Determinants of mortality in patients with severe blunt head injury. Arch Surg. 2002;137(3):285–90.
21. Harries A, Shah S, Teismann N, Price D, Nagdev A. Ultrasound assessment of extraocular movements and pupillary light reflex in ocular trauma. Am J Emerg Med. 2010;28(8):966–9.
22. Smith SA, Ellis CJ, Smith SE. Inequality of the direct and consensual light reflexes in normal subjects. Br J Ophthalmol. 1979;63:523–7.
23. Sargsyan AE, Hamilton DR, Melton SL, Amponsah D, et al. Ultrasonic evaluation of pupillary light reflex. Crit Ultrasound J. 2009;1(2):53–7.

Chapter 17
Cranial Doppler

Claire Shevlin

Keywords Transcranial Doppler ultrasound · Point of care ultrasound

17.1 Introduction

The bedside use of ultrasound for both neuromonitoring, and as an aid to diagnosis on the intensive care has not had the same surge in popularity as other modes of ultrasound. Reasons for this include an absence of familiarity, lack of equipment or a perception of difficulty in comparison to more standard measures of intracranial pressure (ICP) and pathology. However, neuro-ultrasound is much less invasive than standard ICP monitors, cost-effective and portable.

Supporting evidence and the basic techniques in transcranial Doppler are described. This chapter should be read in conjunction with chapter 16 on neuro-ophthalmic ultrasound.

17.2 Transcranial Doppler

Transcranial Cerebral Doppler (TCD) has been used in clinical practice since the 1980s—Aaslid [1] showed cerebral arterial flow velocities could be measured using pulsed Doppler through the skull. It has grown in use in recent decades as a monitoring and diagnostic tool. Currently it is the only mode that can provide real-time data with regard to cerebral haemodynamics.

It has several applications within an intensive care unit—the assessment of severity of vasospasm following a subarachnoid haemorrhage, an additional aid in the assessment of increased intracranial pressure and as an adjunct to diagnose cerebral circulatory arrest and support the clinical diagnosis of brainstem death. It

C. Shevlin (✉)
Intensive Care Unit, Craigavon Area Hospital, Portadown, Northern Ireland
e-mail: claireshevlin@gmail.com

A. Walden et al. (eds.), *Ultrasound in the Critically Ill*,
https://doi.org/10.1007/978-3-030-71742-1_17

has also been used to diagnose non-convulsive status epilepticus on the intensive care unit [2].

Outside of ICU, it has been used to monitor cerebral circulation during vascular surgery (e.g. carotid artery stenting, endarterectomies) or cardiopulmonary bypass.

17.2.1 The Transcranial Doppler Transducer

TCD uses a hand-held Doppler transducer to assess the velocity and pulsatility of cerebral blood flow within the major branches of the Circle of Willis—the communication between the anterior (internal carotid artery and its branches) and posterior (vertebral and basilar arteries) circulatory systems. There is a specific Doppler transducer that can be utilized—however, the use of the low-frequency cardiac probe is more common in day to day use in the intensive care unit. This allows visualisation of intracranial structures as well as blood flow profiles (transcranial colour-coded duplex sonography, TCCD). Bone will attenuate around 90% of sound waves so a low frequency probe is employed as attenuation is lower at the frequency range of 2 MHz.

17.2.2 Acoustic Windows

The transducer is applied over suitable acoustic windows in an intact skull where the bones are relatively thinner and allow greater penetration of ultrasound.

Possible windows that have been described are temporal, occipital, orbital and submandibular. Of these, the temporal, occipital and orbital are the most commonly employed. Submandibular and transforaminal approaches have also been described [3].

The transtemporal window is used to assess the middle cerebral artery (MCA), the anterior cerebral artery (ACA), the posterior cerebral artery (PCA) and the terminal portion of the internal carotid artery (TICA) before its bifurcation. The temporal approach provides the most useful insonation window for the brain and its vessels but unfortunately is inadequate in many subjects.

The orbital window looks at the ophthalmic artery and the internal carotid artery at the distal level.

The transforaminal (or occipital) window allows sonography of the distal vertebral arteries and the basilar artery.

17.3 Principles of TCD Scanning

A B-mode scan is performed firstly to identify the components of the circle of Willis, and the relevant anatomy. Following this, the depth and direction of the blood flow are identified relative to the placement of transducer and ultrasound beam. Flow moving towards the transducer is displayed as a positive waveform, whereas flow moving away as a negative waveform. The brightness of colour indicates the strength of the signal. From the waveform, peak systolic velocity (PSV) and end diastolic velocity can be measured.

From the probe position on the skull, the ultrasound beam is reflected back from the erythrocytes moving at speed within the blood vessels—the consequent Doppler shift signal obtained is spectrally analysed to produce two-dimensional data. Transcranial Doppler ultrasound is a pulsed technique—a pulse of ultrasound is emitted and then there is a period of 'listening' for the signal to be returned. The time from emission to reception will determine the depth from which any Doppler frequency shift is found.

The two principal indices examined are the flow velocities within the arteries (FV) and the pulsatility index (PI).

The pulsatility index or PI is indicated by

$$\mathrm{FVs} - \mathrm{FVd}/\mathrm{FVm}$$

where

FVs = flow velocity during systole).

FVd = flow velocity during diastole.

FVm = mean flow velocity.

The earliest sign of increased intracranial pressure is increased pulsatility as a measure of increased downstream resistance. A strong correlation has been suggested between pulsatility index and increased intracranial pressure [4, 5], and between the cerebral perfusion pressure and pulsatility index [6].

Another value sometimes calculated is the Pourcelot's resistance index (RI) that is a surrogate measurement of peripheral flow resistance.

This is represented by:

$$\mathrm{RI} = (\text{Peak systolic flow velocity} - \text{end diastolic flow velocity})/\text{Peak diastolic FV}$$

High vascular resistance is indicated by low diastolic flow velocities and a high RI (>0.8) and vice versa.

17.4 Pitfalls of TCD Ultrasound

Transcranial Doppler has the potential to be a valuable bedside tool in the ICU—it is non-invasive, inexpensive, reliable and relatively easily taught.

However images can be difficult to obtain through the acoustic windows. Several factors can affect the acquisition of visual information and data—increased blood viscosity, hypotension, inexperience of operator, very low flow within the vessels can all affect the results of the scan. Also, miscellaneous factors and conditions may affect flow velocity.

17.4.1 Factors Increasing FV

1. Vasopasm/hyperaemia
2. Loss of autoregulation
3. Narrowed cerebral arterial circulation
4. Sickle cell anaemia
5. AV malformation
6. Meningitis
7. Pre-eclampsia
8. Sepsis
9. Extremes of age.

17.4.2 Factors Decreasing FV

1. Increased intracranial pressure
2. Cerebral circulatory arrest or brainstem death
3. Reduced cardiac output or hypotension
4. Pregnancy
5. Most anaesthetic agents
6. Hypothermia.

17.5 The Use of Transcranial Doppler as Ancillary Test in Brainstem Death

Brain death in the ICU is principally a clinical diagnosis, based on clinical examination. Ancillary testing has been utilised in complicated cases e.g. EEG, radionuclide scans, cerebral angiography. TCD can also be used to help confirm the diagnosis.

Increased intracranial pressure will usually lead to an increased PI.

Following this, the flow velocities within the arteries will gradually fall.

When the ICP is severely elevated, the diastolic blood flow in the cerebral arteries appears negligible. Retrograde diastolic flow, small systolic spikes, and finally absence of flow may occur. When these are present in over a prolonged period of time, this is valuable supplemental evidence in the diagnosis of brain death [7, 8].

17.6 Technique of Transcranial Doppler

Ideally, sit at the head of the patient. Identify which of the acoustic windows you are able to access/obtain images. Apply plenty of acoustic gel to area to be insonated.

For the transtemporal approach, the transducer is placed on temporal bone either anterior to external auditory canal, or posterior above the earlobe. Orient the probe slightly upwards, anteriorly. This allows the best visualisation of the circle of Willis. The MCA is commonly examined as it carries 50–60% of the carotid artery flow and usually produces a good signal quality. It should be identifiable in 90% of subjects.

The temporal window is bounded by a line drawn from the tragus to the lateral canthus of the eye and the area 2–3 cm above.

Move the probe slowly over this area, performing slight and slow adjustments if a faint signal is found. Use colour signals—depth of 50 mm initially, and repeat if no signal is found using depths from 45 to 70 mm.

Once the middle cerebral artery has been located, attempt to follow the vessel toward the bifurcation of the internal carotid into the MCA and anterior cerebral artery. It ca be difficult to distinguish the signal from the anterior and posterior arteries from the middle cerebral artery (Fig. 17.1).

In the orbital view, the transducer is placed so it rests lightly on the closed eyelid to look at ophthalmic artery and internal carotid artery. The transducer is angled slightly medial and upwards. Flow signals at a depth of approximately 60 mm or less towards the probe reflect flow from the ophthalmic artery. In order to examine the internal carotid distally, the sample volume has to be increased beyond a 60 mm depth. The ICA is a curved artery at this point and so flow signals may be towards or away from the probe (Fig. 17.2).

Fig. 17.1 Transtemporal approach to transcranial Doppler ultrasound

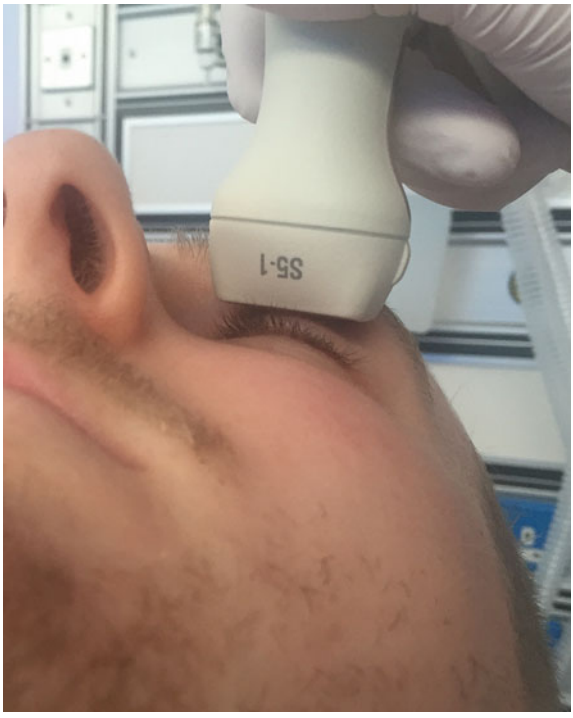

Fig. 17.2 Orbital approach

In order to view the distal vertebral and basilar arteries, the occipital approach is used. For the ICU patient, if possible, the patient should be turned to one side. The transducer is placed in the midline below the occiput and angled cephalad to allow visualisation of the posterior circulation. The probe is directed slightly medially. Depths of 50–75 mm will obtain flow signals from the vertebral artery. Following this signal, and orientating the transducer upwards and medially from depths of 75–220 mm may obtain basilar artery flow signals. The signals from both of these probes are away from the probe (Fig. 17.3).

Vessels are identified with greyscale and colour Doppler flow imaging. Utilise a pulsed Doppler system with a low frequency 1–2 MHz ultrasonic signal. A continuous wave Doppler in this situation will not be able to localize to the depth required.

A spectral Doppler waveform is produced in a visual display of blood flow areas within a specific area of the blood vessel. From the waveform, peak systolic velocity (PSV) and (EDV) can be measured and used to calculate the mean flow velocity.

Obtain spectral waveforms bilaterally from proximal, mid and distal MCA, and single measurements bilaterally in visualized ACA, PCA and terminal portion of the internal carotid artery. Flow velocity in the distal ICA is also measured if possible (Fig. 17.4).

Fig. 17.3 Occipital approach

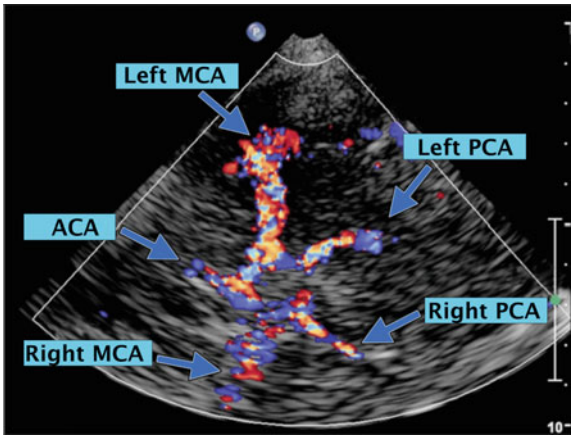

Fig. 17.4 Colour flow in Circle of Willis via transtemporal approach

17.7 Safety Concerns with Ophthalmic and Transcranial Ultrasound

Ultrasound is generally acknowledged to be a safe technique. The largely hypothetical risks of ultrasound centre on the potential biological consequences of interaction between the scanned tissues and the ultrasound wave. These consequences may be thermal or non-thermal, and are measured by the safety indices Thermal Index (TI) and Mechanical Index (MI), which are displayed in real-time on the screen of most modern ultrasound machines. Ultrasound is presumed to be safe when the values of the TI and MI are less than 1.0. The TI is the ratio of the power used to the power required to produce a temperature rise of 1 °C.

Ultrasound energy from the probe passes into scanned tissues and is reflected from tissue interfaces; some energy is absorbed and converted to thermal energy, elevating the temperature of local tissues. Scanning time should be minimised to prevent possible thermal injury. It is advised that tissue temperature increase should be kept below 1.5 °C.

The MI gives an approximate figure of the risk of the non-thermal effects. These include cavitation, which is the expansion and contraction of tissue gas bubbles during the cycle, and streaming, referring to the movement of complex fluids brought about by the ultrasound energy.

Optic nerve sheath ultrasound should not be used in the presence of evident or suspected rupture of the globe, or when there is significant periorbital injury. The technique is likely to be of limited incremental value in patients with chronically raised intracranial pressure or long-standing papilloedema.

Energy transfer from the beam could result in mechanical injury or increased temperature of the scanned tissues. A good principle is to use the lowest output power and shortest scanning time possible to achieve the necessary information. The eye is also susceptible to thermal injury because of its reduced ability to thermoregulate given decreased perfusion.

17.8 Conclusion

There is scope to advance our practice with regard to neuro-ultrasound—the diagnosis and monitoring of response to treatment in raised intracranial pressure, for example. ONSD ultrasound is promising in this regard, and transcranial Doppler which is non-invasive, does not involve allergenic contrast mediums or exposure to ionizing radiation, or transport outwith the intensive care unit, could also add some valuable data to our day to day assessment of selected patient groups. The assessment of the iris and pupil, as well as the direct and indirect pupillary responses to light, is a useful adjunct to clinical examination in cases of ocular trauma.

With all ultrasound modalities, the pitfall lies principally in the operator's potential lack of familiarity with the technique and the inability to interpret findings in light of existing comorbidities and factors affecting scanning conditions.

See also:

Chapter 16 Neuro-ophthalmic Ultrasound.

Chapter 20 The Unconscious Polytrauma Patient.

References

1. Aaslid R, Markwalder TM, Nornes H. Non-invasive transcranial Doppler ultrasound recording of flow velocity in basal cerebral arteries. J Neurosurg. 1982;57:769–74.
2. Merceron S, Geeraerts T, Montlahuc C, Bedos JP, et al. Assessment of cerebral blood flow changes in nonconvulsive status epilepticus in comatose patients: a pathophysiological transcranial Doppler study. Seizure. 2014;23(4):284–9.
3. Alexandrov AA. Intracranial cerebrovascular ultrasound examination techniques in Cerebrovascular Ultrasound in Stroke Prevention and Treatment. 2nd ed. USA: Blackwell Publishing; 2011. p. 13–25.
4. Bellner J, Romner B, Reinstrup P, et al. Transcranial Doppler sonography pulsatility index (PI) reflects intracranial pressure (ICP). Surg Neurol. 2004;62(1):45–51.
5. Ursino M, Giulioni M, Lodi CA. Relationships among cerebral perfusion pressure, autoregulation, and transcranial Doppler waveform: a modeling study. J Neurosurg. 1998;89(2):255–66.
6. Zweifel C, Czosnyka M, Carrera E, et al. Reliability of the blood flow velocity pulsatility index for assessment of intracranial and cerebral perfusion pressures in head-injured patients. Neurosurgery. 2012;71(4):853–61.
7. Petty GW, Mohr JP, Pedley TA. The role of transcranial Doppler in confirming brain death: sensitivity, specificity, and suggestions for performance and interpretation. Neurology. 1990;40(2):300–3.
8. Babikian VL, Feldmann E, Wechsler LR, et al. Transcranial Doppler ultrasonography: year 2000 update. J Neuroimaging. 2000;10(2):101–15.

Chapter 18
Musculoskeletal Ultrasound

Kausik Mukherjee

Keywords Ultrasound · Fracture · Infection · Foreign body · Joint effusion

18.1 Introduction

Modern Emergency Medicine has seen an exponential increase in the use of ultrasound both for diagnosis and for management. Patients presenting with musculoskeletal problems are also benefitting from the use of ultrasound. Undisplaced fractures, missed on plain films, can be detected with the help of ultrasound as can non-radio-opaque foreign bodies or infection in soft tissue. It is also highly sensitive in picking up joint effusion. Linear array, high frequency probe (5–12 MHz) is used for musculoskeletal imaging.

18.2 Fractures

Plain film is the primary investigative tool in the management of fractures.

The easy accessibility, widespread availability and relative accuracy of X-ray ensure that it remains the first line of investigation in the acute setting. Usually, the next line of investigation for fracture is a CT scan. Bi-planar and 3-D reformatting in CT helps to delineate complex fractures for pre-operative planning.

However, ultrasound may be useful in cases of undetected fractures. Patients with persistent symptoms, referred for ultrasound for soft tissue injury, may have co-incidental fractures (Fig. 18.1). Lack of ionising radiation and relative low cost, when compared with other cross-sectional imaging modalities, are further advantages [1].

K. Mukherjee (✉)
Department of Radiology, University Hospital of Wales, Heath Park, Cardiff, Wales CF14 4XW, UK
e-mail: kausik.mukherjee@wales.nhs.uk

A. Walden et al. (eds.), *Ultrasound in the Critically Ill*,
https://doi.org/10.1007/978-3-030-71742-1_18

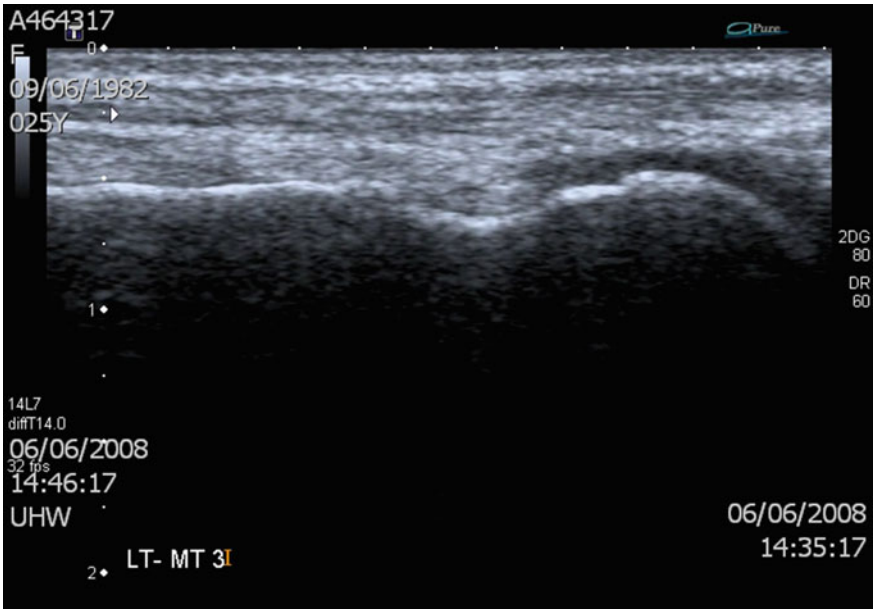

Fig. 18.1 Stress fracture of the 3rd metatarsal bone. There is a clear interruption of the sharp white line of the bone periosteum

There have been several reports highlighting the usefulness of ultrasound in detecting undisplaced fractures. Identification of undisplaced fractures of greater tuberosity [2] (Fig. 18.2), scaphoid [3], lateral talar process [4], anterior process of calcaneus and cuboid can be notoriously difficult on plain films. Similarly, fracture of the rib may not be detected on plain films. Further imaging in the form of CT or ultrasound [5] may be useful.

The primary finding on ultrasound is the disruption of the hyperechoic cortical line. Focal haematoma and/or periosteal thickening may help to confirm the diagnosis [6]. The pitfall is the focal cortical breach at the site of the nutrient vessel. Doppler examination may help to identify the vessel.

Ultrasound in an acute confirmed fracture may also be useful in establishing any neurovascular complication. The radial nerve in the spiral groove of the humerus or the common peroneal nerve next to the neck of fibula, are typical examples [7].

18.3 Foreign Body

Radio-opaque foreign bodies can be identified on plain films. However, majority of the soft tissue foreign bodies are radiolucent plant fragments that are unlikely to be detected on X-rays. Ultrasound is an extremely useful tool in this scenario [8, 9].

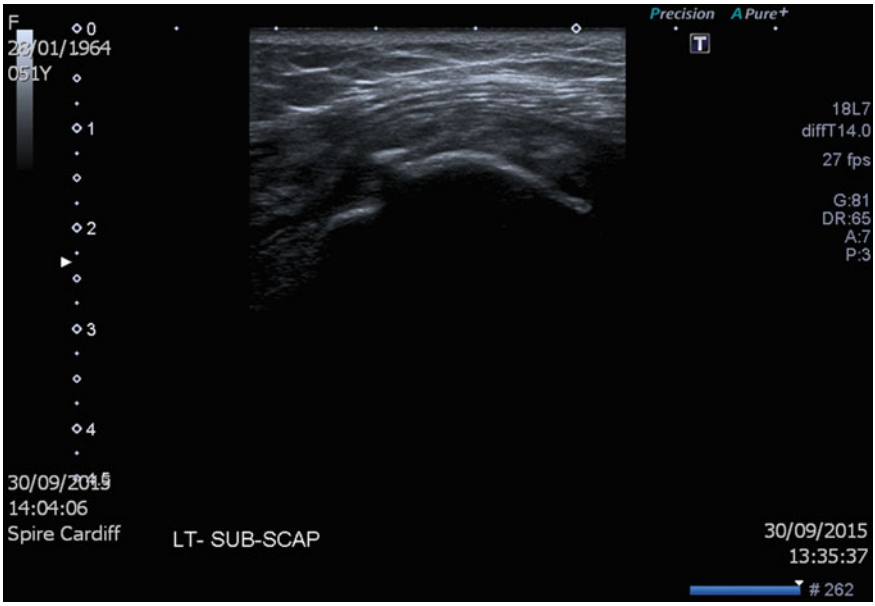

Fig. 18.2 Fracture of the left proximal humerus with a step seen in the bright white periosteal line

Foreign bodies in the soft tissue are usually post-traumatic. A fragment of the foreign body may remain undetected and lead to complications depending on the site. Subcutaneous abscess, tenosynovitis or septic arthritis may ensue. Formation of a granuloma is also not uncommon.

Routinely a plain radiograph is performed. Although this may demonstrate the foreign body, the associated complications may go undetected.

A high frequency, small field of view, linear array probe is quite useful. The aim is to identify the foreign body, its location, depth, orientation and relation to surrounding structures.

The foreign bodies are known to migrate from the site of initial entry point due to repeated muscle contractions. This has to be appreciated if the initial scan is negative [10].

The foreign body appears on ultrasound as a reflective structure with posterior acoustic shadowing. Quite often there is a hypoechoic halo around the retained foreign body, which corresponds to granulation tissue/fibrin. Doppler examination may also demonstrate increased vascularity due to neovascularisation [11]. The position of the foreign body in relation to its surrounding structures can also be assessed (Fig. 18.3). As already described, several complications may ensue. Ultrasound will help to identify these.

Finally, using ultrasound, the site and orientation of the foreign body can be marked on the skin, to facilitate its removal.

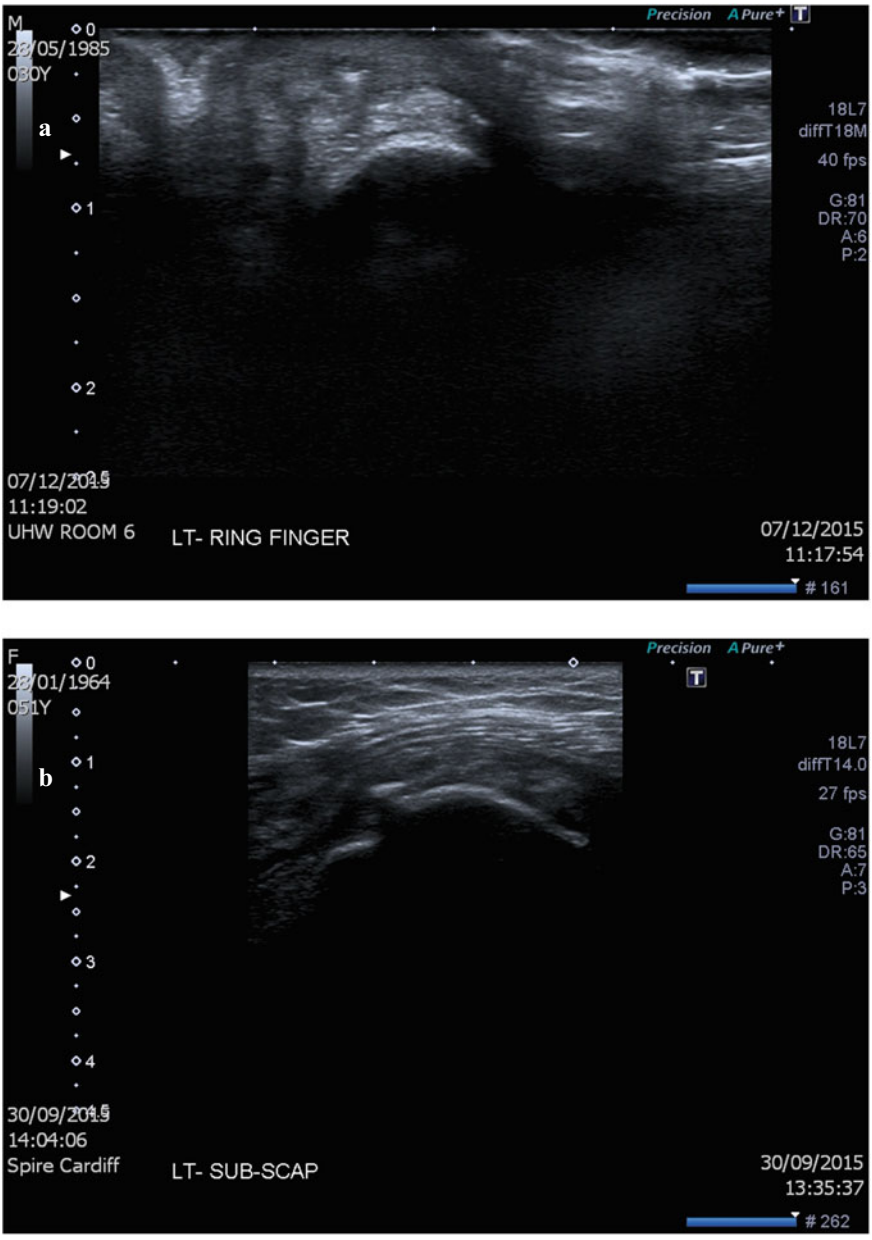

Fig. 18.3 **a** and **b** Foreign body in soft tissues of left ring finger

Although not routinely practised, ultrasound following removal of foreign body may be useful.

18.4 Soft Tissue Infection

Soft tissue infection can arise from a variety of causes. This may be post-traumatic, blood borne or as a complication in diabetes. The infection itself can present as simple cellulitis, skin and soft tissue infection (SSTI), infective bursitis, infective tenosynovitis or an abscess.

Cellulitis is the commonest form of musculoskeletal infection and may be associated with superficial thrombophlebitis. It may progress to an abscess formation. Ultrasound examination demonstrates a cobblestone appearance of the subcutaneous fat along with hyperaemia.

SSTI or necrotising fasciitis is a severe form of cellulitis, where there is severe inflammation and necrosis of the subcutaneous tissues and the underlying deep fascia. Ultrasound examination demonstrates perifascial fluid collection along with swelling of the subcutaneous tissues and muscle [12].

Superficial bursa, for example olecranon and pre-patellar bursa are commonly infected. S. aureus is the usual organism involved. Ultrasound demonstrates bursal fluid with mixed echogenicity, hyperaemia of the wall and oedema of the surrounding soft tissue (Fig. 18.4).

Infective tenosynovitis is usually the result of penetrating injury and the flexor tendons of the hand and wrist are more commonly involved. Ultrasound is useful in the diagnosis, identifying the presence of inflammation or effusion in the tendon sheath. Needle aspiration can be performed under ultrasound guidance (Fig. 18.5).

An abscess can be seen in the subcutaneous tissue or in the muscle. Clinical examination may raise the suspicion of a soft tissue collection in the right clinical setting. However the true extent of the collection is difficult to assess and ultrasound can be a valuable tool [13].

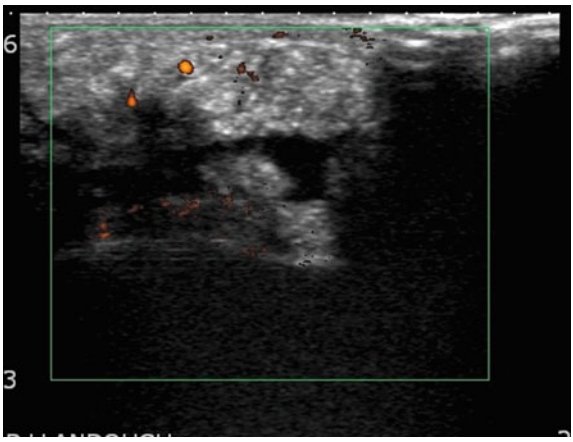

Fig. 18.4 Olecranon bursa with thickened, inflamed wall and bursal fluid

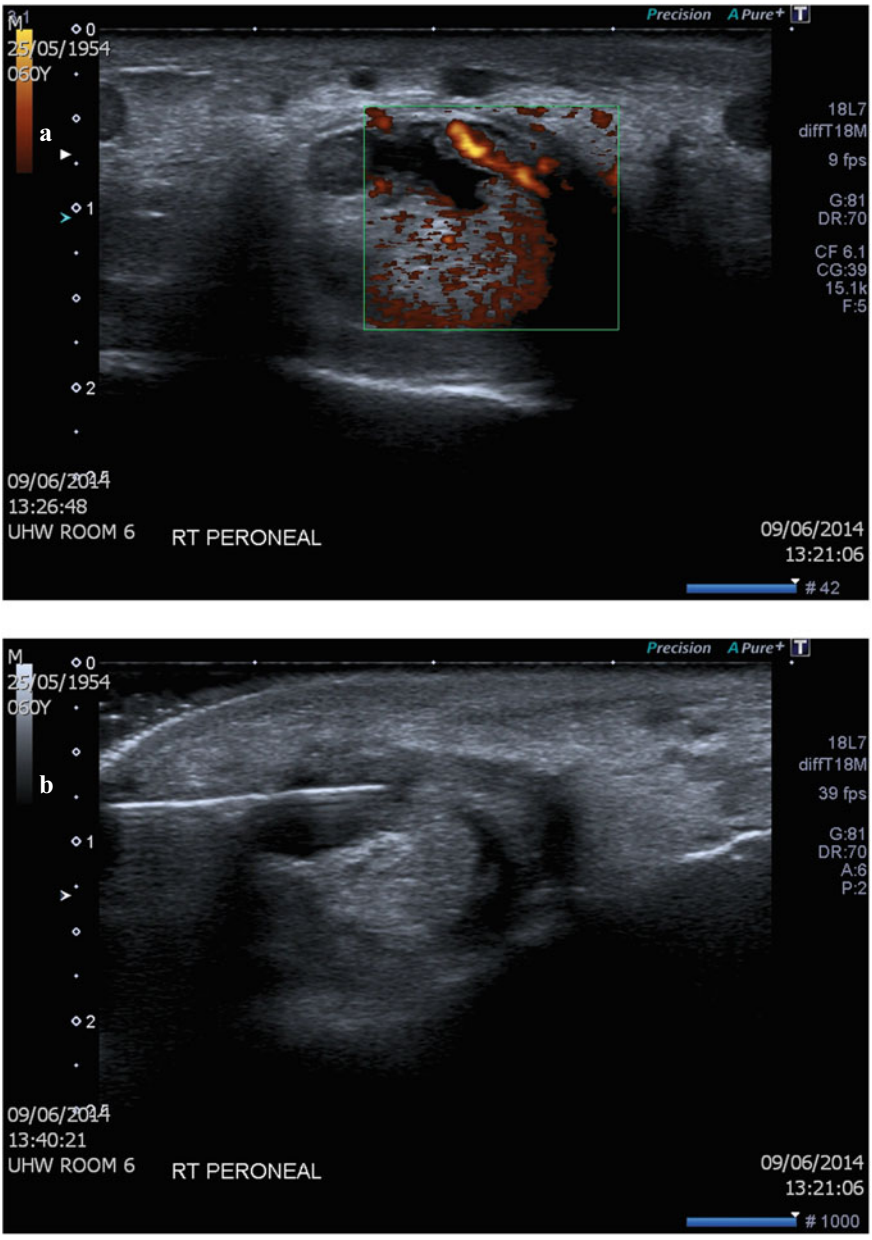

Fig. 18.5 **a** Identification of collection surrounding the right peroneal tendon with doppler indicating localised increased vascularity. **b** Aspiration of infected collection surrounding the right peroneal tendon

An abscess typically has a heterogeneous appearance due to the presence of debris in the collection. A seroma may be anechoic. Doppler examination demonstrates peripheral increased vascularity due to inflammation of the wall of the collection [14, 15].

18.5 Joint Effusion/Haemarthrosis

Swelling of a joint can be secondary to effusion/haemarthrosis or synovitis. Differentiation between the two or even confirming either of these can be difficult clinically.

Detection of moderate effusion in superficial joints, as in knee or elbow, is feasible. Deep joints like hip or shoulder can pose a clinical challenge.

Plain films are useful in detecting effusion in the knee, elbow and ankle joints provided there is a significant volume.

Ultrasound on the other hand is extremely sensitive in detecting even small volumes of fluid (Fig. 18.6). A simple joint effusion will be anechoic without significant neovascularisation. In case of infective effusion (septic arthritis), there may be scattered echogenicity due to proteinaceous fluid or cellular debris. Echogenicity may also be demonstrated in haemarthrosis. In general, ultrasound is not sensitive in detecting the type of effusion [16].

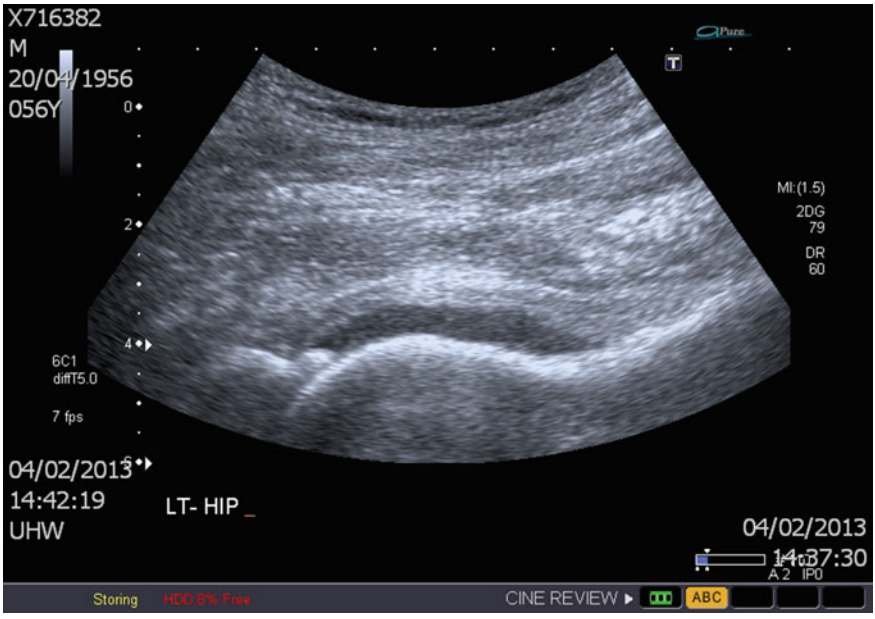

Fig. 18.6 Effusion around the left femoral head

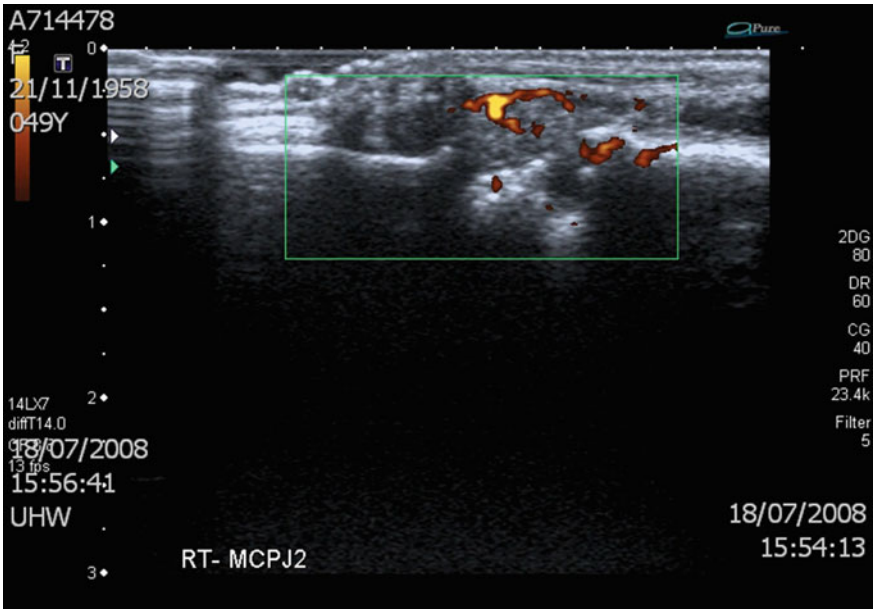

Fig. 18.7 Acute synovitis of the right 2nd metacarpophlangeal joint with doppler indicating increased flow in the synovium

Swelling of a joint can also be due to synovitis. This is particularly prominent in the small joints of the hands or feet. Ultrasound again is useful in confirming this finding. Thickening of the synovial lining of the joints are seen with or without effusion. Doppler examination demonstrates increased flow within the synovium [17] (Fig. 18.7).

Synovitis of the knee and elbow will present clinically as joint swelling. This may not be that obvious in hip, shoulder or ankle and pain with decreased range of movement may be the primary symptom.

Ultrasound is useful in further management, as needle for aspiration or biopsy may be inserted under its guidance.

18.6 Conclusion

Musculoskeletal ultrasound is a robust, evidence based tool in the management of fractures, foreign bodies, swollen joints and soft tissue infections.

See also:

Chapter 20 The Unconscious Polytrauma Patient.

References

1. Hubner U, et al. Ultrasound in the diagnosis of fractures in children. J Bone Joint Surg Br. 2000;82(8):1170–3.
2. Patten RM, et al. Nondisplaced fractures of the greater tuberosity of the humerus: sonographic detection. Radiology. 1992;182(1):201–4.
3. Senall JA, et al. Ultrasound for the early diagnosis of clinically suspected scaphoid fracture. J Hand Surg Am. 2004;29(3):400–5.
4. Copercini M, et al. Sonographic diagnosis of talar lateral process fracture. J Ultrasound Med. 2003;22(6):635–40.
5. Chan SS. Emergency bedside ultrasound for the diagnosis of rib fractures. Am J Emerg Med. 2009;27(5):617–20.
6. Hoffman DF, Adams E, Bianchi S. Ultrasonography of fractures in sports medicine. Br J Sports Med. 2015;49(3):152–60.
7. Choi SJ, et al. Ultrasonography for nerve compression syndromes of the upper extremity. Ultrasonography. 2015;34(4):275–91.
8. Graham DD Jr. Ultrasound in the emergency department: detection of wooden foreign bodies in the soft tissues. J Emerg Med. 2002;22(1):75–9.
9. Mohammadi A, Ghasemi-Rad M, Khodabakhsh M. Non-opaque soft tissue foreign body: sonographic findings. BMC Med Imaging. 2011;11:9.
10. Choudhari KA, Muthu T, Tan MH. Progressive ulnar neuropathy caused by delayed migration of a foreign body. Br J Neurosurg. 2001;15(3):263–5.
11. Davae KC, et al. Value of power Doppler imaging and the hypoechoic halo in the sonographic detection of foreign bodies: correlation with histopathologic findings. J Ultrasound Med. 2003;22(12):1309–13; quiz 1314–6.
12. Parenti GC, et al. Necrotizing fasciitis of soft tissues: role of diagnostic imaging and review of the literature. Radiol Med. 2000;99(5):334–9.
13. O'Rourke K, Kibbee N, Stubbs A. Ultrasound for the evaluation of skin and soft tissue infections. Mo Med. 2015;112(3):202–5.
14. Breidahl WH, et al. Power Doppler sonography in the assessment of musculoskeletal fluid collections. AJR Am J Roentgenol. 1996;166(6):1443–6.
15. Arslan H, et al. The role of power Doppler sonography in the evaluation of superficial soft tissue abscesses. Eur J Ultrasound. 1998;8(2):101–6.
16. Zamzam MM. The role of ultrasound in differentiating septic arthritis from transient synovitis of the hip in children. J Pediatr Orthop B. 2006;15(6):418–22.
17. Rees JD, et al. A comparison of clinical vs ultrasound determined synovitis in rheumatoid arthritis utilizing gray-scale, power Doppler and the intravenous microbubble contrast agent 'Sono-Vue' . Rheumatology (Oxford). 2007;46(3):454–9.

Chapter 19
The Haemodynamically Unstable Patient

Ashley Miller

Keywords Shock · Organ blood flow · Echocardiography · Sepsis · Cardiomyopathy · Lung ultrasound · Fluid responsiveness

19.1 Introduction

Management of haemodynamic instability, along with respiratory failure, is the mainstay of the job of the Intensivist. A recent, and perhaps the most useful, definition of circulatory shock is 'a potentially life threatening reduction in organ blood flow' [1]. Treating this condition relies on 3 key steps. (1) The ability to identify its presence, (2) the ability to identify the cause and (3) being guided in its optimal management. There are a plethora of monitoring devices and investigations that all seek to provide some of the answers to these 3 steps whether it be blood pressure, preload, afterload, contractility, cardiac output, stroke volume, systemic vascular resistance, indices of fluid responsiveness, lactate levels, the microcirculation etc. This chapter will outline the role ultrasonography has in guiding us through these steps. In particular it will show how integrating different ultrasound modalities makes its use a powerful, and arguably mandatory, tool for the intensivist.

19.2 Organ Blood Flow

It is relatively simple to measure cardiac output with echocardiography. Tracing the spectral doppler envelope of flow through the left ventricular outflow tract yields the velocity time integral (VTI) which represents the stroke distance. Measurement

A. Miller (✉)
Department of Anaesthetics, Shrewsbury and Telford Hospitals NHS Trust, Mytton Oak Rd., Shrewsbury SY3 8XQ, UK
e-mail: ashleymiller@nhs.net

A. Walden et al. (eds.), *Ultrasound in the Critically Ill*,
https://doi.org/10.1007/978-3-030-71742-1_19

of the LVOT diameter, at the same point the VTI is measured, is simply converted into the cross sectional area (CSA) and then stroke volume is calculated by multiplying the VTI by the CSA. It is also possible to measure the blood flow of specific organs or organ systems using the same principles. If shock is common, and is caused by reduced organ blood flow, it is remarkable that a systematic review found that renal blood flow measurement in critically ill patients has only been reported in 5 studies which included a total of only 46 patients [2]. Renal blood flow can be measured and estimated in a variety of ways. Doppler ultrasound of the renal artery, combined with measurement of its diameter, is a relatively simple concept akin to measuring SV with echocardiography (described below). The commonest measure is the resistive index (RI) calculated with the formula:

$$\text{RI} = \text{Peak systolic velocity} - \text{lowest diastolic velocity}/\text{peak systolic velocity}$$

This method has a number of limitations but has been shown to predict acute kidney injury (AKI) in critically ill patients [3].

It is also possible to measure blood flow in all the abdominal and pelvic organs with doppler ultrasonography by subtracting the bilateral proximal femoral arterial blood flow from the upper abdominal aorta blood flow above the coeliac trunk [4]. The splanchnic circulation, via the sympathetic nervous system, plays the major role in determining venous return to the heart but this method has not been studied in critically ill patients.

It is clear then, at present, ultrasonography is confined to a role in the research setting for the assessment of organ perfusion. Fortunately, signs of reduced organ perfusion are readily detectable by other methods using simple clinical assessment and investigations. Ultrasound comes into its own in addressing the 2nd and 3rd components. When we identify a shocked patient, we then reach for the ultrasound machine.

19.3 The Cause of Shock

The causes of shock can be divided into hypovolaemic, cardiogenic, obstructive and distributive.

19.3.1 Hypovolaemic Shock

Echocardiography is a useful method of identifying hypovolaemia as the cause of shock and has a number of characteristic features as outlined in Fig. 19.1.

If these features are not present then other signs of fluid responsiveness can be elicited. Changes of over 12% in either the LVOT VTI, LVOT peak velocity or the IVC diameter with respiration (in fully ventilated patients with sinus rhythm) are

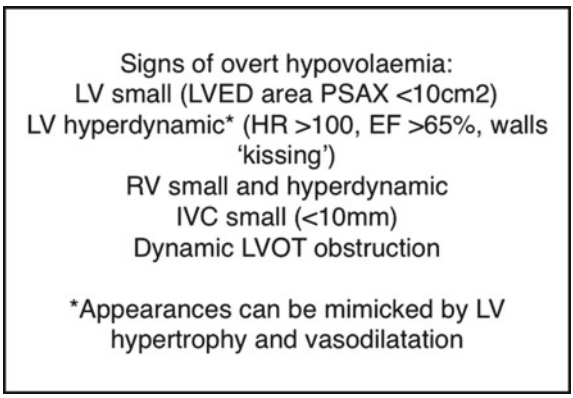

Fig. 19.1 LVED left ventricular end diastolic area, PSAX parasternal short axis, HR heart rate, EF ejection fraction, RV right ventricle, IVC inferior vena cava, LVOT left ventricular outflow tract

relatively sensitive and specific. Increased VTI after a fluid challenge or passive leg raise is also indicative. It is worth noting, however, that it is normal for our hearts to operate on the ascending limb of the Frank Starling curve and so fluid responsiveness does not necessarily signify hypovolaemia. There is no good evidence that increasing SV in a normovolaemic patient will be beneficial while there are many reasons to believe it may be harmful [5].

Patients who are hypovolaemic are either bleeding or severely dyhydrated or have lost large volumes of fluid into their abdomen due to an intra-abdominal catastrophe. In a trauma situation, if blood loss is not obvious then ultrasonography will quickly reveal whether there is free fluid within the abdomen, pelvis or even chest (see relevant chapters).

19.3.2 Cardiogenic Shock

This is where echocardiography is the gold standard. Other methods can reliably estimate or measure cardiac output but the ability to actually see the heart contracting and valves moving is unmatched by practical alternatives. The cause of the cardiogenic shock will be readily apparent whether it be cardiac ischaemia (with regional wall motion abnormalities), cardiomyopathy, acute valve disease or aortic root pathology. Ejection fraction, stroke volume, cardiac output and left heart pressures can all be measured or estimated.

Sepsis causes myocardial dysfunction in around 60% of affected patients and shock can result from this or from vasodilatation with reduced venous return or both. Distinguishing between these two clinically or with other forms of monitoring is extremely challenging and prone to error and so echocardiography should be mandatory in the shocked septic patient. Causes of cardiomyopathy are listed in Table 19.1.

Table 19.1 Classification of cardiomyopathies. HOCM hypertrophic cardiomyopathy, RV right ventriclT

Cardiomyopathies		
General	(Heart may be dilated but not classified as such)	Sepsis, ischaemia, valve disease, hypertension
Dilated		Myocarditis, alcohol, pregnancy, prolonged tachycardia
Hypertrophic	Obstructive	Genetic (HOCM), athlete's heart
	Restrictive	Infiltration or deposition – amyloid, haemochromatosis, fibrosis, sarcoid, glycogen storage disease
Arrhythmogenic RV cardiomyopathy		

19.3.3 Obstructive Shock

19.3.3.1 Tamponade

Pericardial effusions are usually easy to see with echocardiography. Effusions are usually circumferential but may be localised so it is important to interrogate all views. Pleural effusions and ascites may both be mistaken for pericardial fluid so it is important for the critical care physician, who is not an expert in echocardiography, to have a basic knowledge of lung and abdominal ultrasound.

Tamponade occurs when pressure in the pericardial space exceeds pressure in the cardiac chambers enough to impair cardiac filling. This can be caused by a small volume of fluid if it accumulates quickly (such as with ventricular perforation). Chronic effusions, on the other hand, can be very large without necessarily causing tamponade.

Pressure effects will become apparent in the lowest pressure chambers of the heart first, progressing from the RA to RVOT to the whole of the RV and then to the LA and LV. Compression of the RA will be seen in ventricular systole when the RA is filling. Inversion of the RA free wall for more than 1/3 of systole is a strong indication of tamponade. Pulsus paradoxus will also be present and can be measured with echo by using doppler to assess flow velocity changes through the tricuspid and mitral valves with respiration (Fig. 19.2).

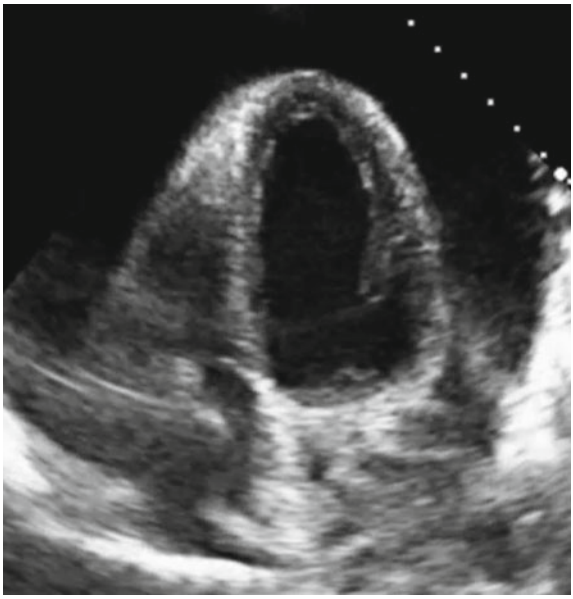

Fig. 19.2 Inversion of the RA free wall in systole

19.3.3.2 Pulmonary Embolism

Thrombus may be visualised in the right heart or proximal pulmonary arteries although it is relatively rare to see this as the clot will often have propagated further into the pulmonary arterial tree.

If large enough to cause shock then there will be acute cor pulmonale with a dilated right heart. This can most simply be assessed by the RV to LV ratio which if >1 demonstrates severe dilatation. In acute PE, PA pressures will not usually exceed 50 mmHg as the RV has not had time to hypertrophy to generate higher pressures. Two other signs (which have a relatively low sensitivity) are:

McConnell's sign—hypokinesis of the RV free wall with apical sparing.

60/60 sign—RVOT acceleration time <60 ms with a PASP <60.

The hallmark of lung ultrasound in PE, similarly to chest radiography, is a normal scan. Peripheral wedge shaped infarcts from small emboli may be seen but are unusual. A patient presenting with acute respiratory failure and a normal lung ultrasound has a PE until proven otherwise.

Echo features combined with severe shock are an indication for thrombolysis. Repeated studies are of course useful to monitor the response.

A 2 point compression test of the femoral and popliteal veins is a very simple way to identify the presence or absence of a DVT. A clot may of course have completely embolised but it provides useful additional information. The combination of lung ultrasound and leg vein ultrasound (without echo) has been shown to have a very high diagnostic accuracy for identifying PE in acute respiratory failure (BLUE protocol).

19.3.3.3 Pneumothorax

A pneumothorax large enough to cause circulatory failure will also cause respiratory failure. Lung ultrasound can rule a pneumothorax in or out in less than 1 minute. The presence of pleural sliding in the most non-dependent region of the lung immediately rules one out. With absent sliding, the absence of a lung pulse and presence of a lung point rules one in with certainty.

19.3.3.4 Pleural Effusion

Very large pleural effusions have been reported to produce tamponade like effects on the heart. These are simple to see with lung ultrasound and echocardiography.

19.3.4 Distributive

Venous return to the heart is determined by the pressure gradient between the mean circulatory filling pressure (MCFP) and the right atrial pressure. A key determinant of the MCFP is the venous tone of the splanchnic venous system which is usually tightly regulated by the sympathetic nervous system. Compromise of this venous tone from sepsis, liver disease or spinal cord injury can result in reduced venous return and shock.

Echocardiographic features of vasodilatation are similar to those of hypovolaemia with tachycardia, small, hyperdynamic ventricles and a high ejection fraction. The clinical picture should help the physician to distinguish between the two. It is important to remember that sepsis does not cause hypovolaemia directly (although if the patient has been ill for a few days they may be dehydrated and therefore somewhat hypovolaemic).

Liver ultrasound may reveal features of portal hypertension such as cirrhosis, ascites and abnormalities in portal vein flow which my be reduced, biphasic or even reversed. Such patients are usually vasodilated.

19.4 Guiding Management

Step 2 took us through how ultrasound can diagnose the causes of shock. But how should we actually use it at the bedside to make the diagnosis promptly and guide our management and how can ultrasound be used to monitor this?

Of course all patients are different and any standardised approach may have to be modified depending on the circumstances. It should be remembered that any investigation should be performed only having thought about the pre-test probability.

We would advocate the following approach when faced with a patient with acute circulatory failure.

Does the patient also have respiratory failure?

Yes:

Lung ultrasound should be the 1st step (followed by a focused echo)

Respiratory failure may of course be cardiac in origin. B lines are the sonographic appearance of pulmonary oedema. This may be cardiogenic or non cardiogenic. Either way, the lungs are wet. Fibrosis and interstitial pneumonitis also cause B lines but are much rarer conditions which should be apparent from the history.

Pneumothorax, pneumonia (as the cause of septic shock) and massive pleural effusions can all lead to circulatory failure. These can be ruled in or out in less than 5 min with lung ultrasound as seen in earlier chapters. Appropriate management can then be instituted.

If the scan is normal, *in the context of respiratory failure,* then a PE should be strongly suspected. If there is pneumonia then septic shock may be the cause. If there are bilateral B lines then there are characteristic features that distinguish whether pulmonary oedema is cardiac in origin. In all of these instances it would then be appropriate to perform echocardiography.

No:

Focussed echocardiography should be the 1st step

Exclude tamponade

Tamponade should first be excluded and treated as a matter of urgency if present. Echo guided pericardiocentesis is safe with a low complication rate as long as the operator is proficient. The site of needle entry is at the location where the effusion is largest (rather than the traditional blind subcostal approach). This can be anterior, lateral or subcostal. A perpendicular angle is easiest to duplicate for needle insertion which favours an anterior or lateral approach. Often the best approach is by the A4C view. As with all US guided needle insertion, careful note should be taken of the depth and angle of insertion. Real time insertion is not necessary but catheter and wire position should be confirmed with US. A few mls of agitated saline can be useful to confirm the presence of the catheter in the pericardium. Follow up studies will be needed to ensure tamponade does not reoccur.

What do the ventricles look like

LV

A hyperdynamic heart will be seen in hypovolaemic and distributive shock. Assessment of whether the patient is fluid responsive or not is outlined below. If the LV is failing then we need to decide the likely cause as is outlined in step 2 above. Wall motion abnormalities and a history consistent with myocardial ischaemia should prompt referral to a cardiologist for possible urgent coronary artery

intervention. Any signs of left ventricular outflow tract obstruction, which is more likely in states of reduced venous return, should result in urgent expert referral. This is an important cause of shock but relatively rare and beyond the scope of this chapter. Similarly, dilated or hypertrophic cardiomyopathies should prompt referral to a cardiologist. These are unusual to see in critically ill patients however. By far the most common cardiomyopathies encountered in critically ill patients are those with either decompensated chronic heart failure (ischaemia, hypertension, valve disease) or acute heart failure due to sepsis. Sepsis causes systolic heart failure in at least 50% of patients and diastolic failure in two thirds. A reduced cardiac output from heart failure *may* mean that inotropes should be considered instead of, or alongside, vasopressors (although they increase myocardial oxygen demand so should be used with care) and should prompt extreme caution in fluid administration.

Septic cardiomyopathies change from day to day. It may not be present on day 1 of sepsis, then intervene for a few days and then the heart may return to normal over the next few days. It should be intuitive that frequent reevaluation is therefore appropriate to tailor the correct treatment.

RV

The RV may be dilated with either preserved function or with impaired function. If RV pressures are high there will be septal flattening and dyskinesia. In either case the cause should be addressed. If PA pressures are low then RV infarction should be considered. If they are high, it could be due to fluid overload, ARDS, PE, chronic cor pulmonale or chronic biventricular failure. It should be noted that a severely failing RV may not be able to generate high pressures so these may be low in these conditions too. Appropriate measures include fluid removal with diuretics or RRT, lowering ventilation pressures, taking other steps to reduce pulmonary vascular pressures and using vasopressors to increase RV coronary perfusion. It is important to remember that RV failure will produce false positives for signs of fluid responsiveness related to respiratory variation. A dilated RV should make the physician extremely cautious about giving fluid (Fig. 19.3).

Will the patient be fluid responsive?

Correction of hypovolaemia should result in a rapid improvement to the patient's condition. It will usually be obvious without echocardiography if a patient is profoundly hypovolaemic. Many times however it may not be clear if the patient will respond to fluid or at what point to stop administering it. Both echocardiography and lung ultrasound can be invaluable tools in this circumstance.

Echo

It is now firmly established that static markers such as CVP, PAOP and ventricular size do not predict fluid responsiveness. Dynamic indices derived from assessing the response of the circulation to heart lung interactions or passive leg raising are, in contrast, excellent predictors of fluid responsiveness. Figure 19.4 outlines how echocardiography can be used to assess fluid responsiveness. It is of course possible

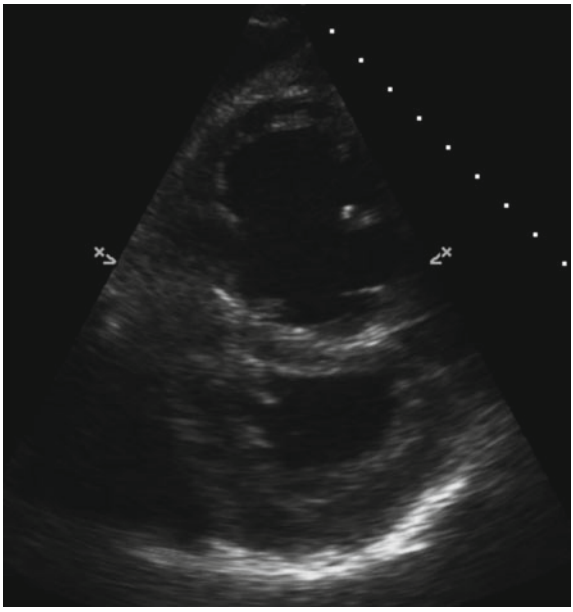

Fig. 19.3 A pressure overloaded RV compressing the ventricular septum

to perform a number of dynamic assessments without echocardiography but these give little information on ventricular performance (Fig. 19.5).

A dilated RV should raise the possibility of fluid overload and should prompt extreme caution in fluid administration. As both ventricles occupy a fixed space constrained by the pericardium, RV dilatation can compromise LV filling, not to mention all the other negative consequences of fluid overload (such as high venous pressures compromising organ perfusion).

Lung Ultrasound

The absence of B-lines can reassure you that administering a fluid bolus will not result in significant pulmonary oedema as B-lines are reported to occur before alveolar flooding from swelling of the interlobular alveolar septae. Similarly the presence of B lines makes it highly likely (as they are usually caused by pulmonary oedema) that administering fluid will worsen respiratory failure.

It has been proposed that administering fluid until B lines appear ensures the patient has reached the top of their starling curve and is therefore 'well filled' without having crossed over into overt pulmonary oedema (FALLS protocol). Lichtenstein [6] we would not advocate this approach however, as the cause of hypotension in critically ill patients is usually not hypovolaemia and an increasing amount of evidence is emerging showing a strong association with fluid overload and worse outcomes.

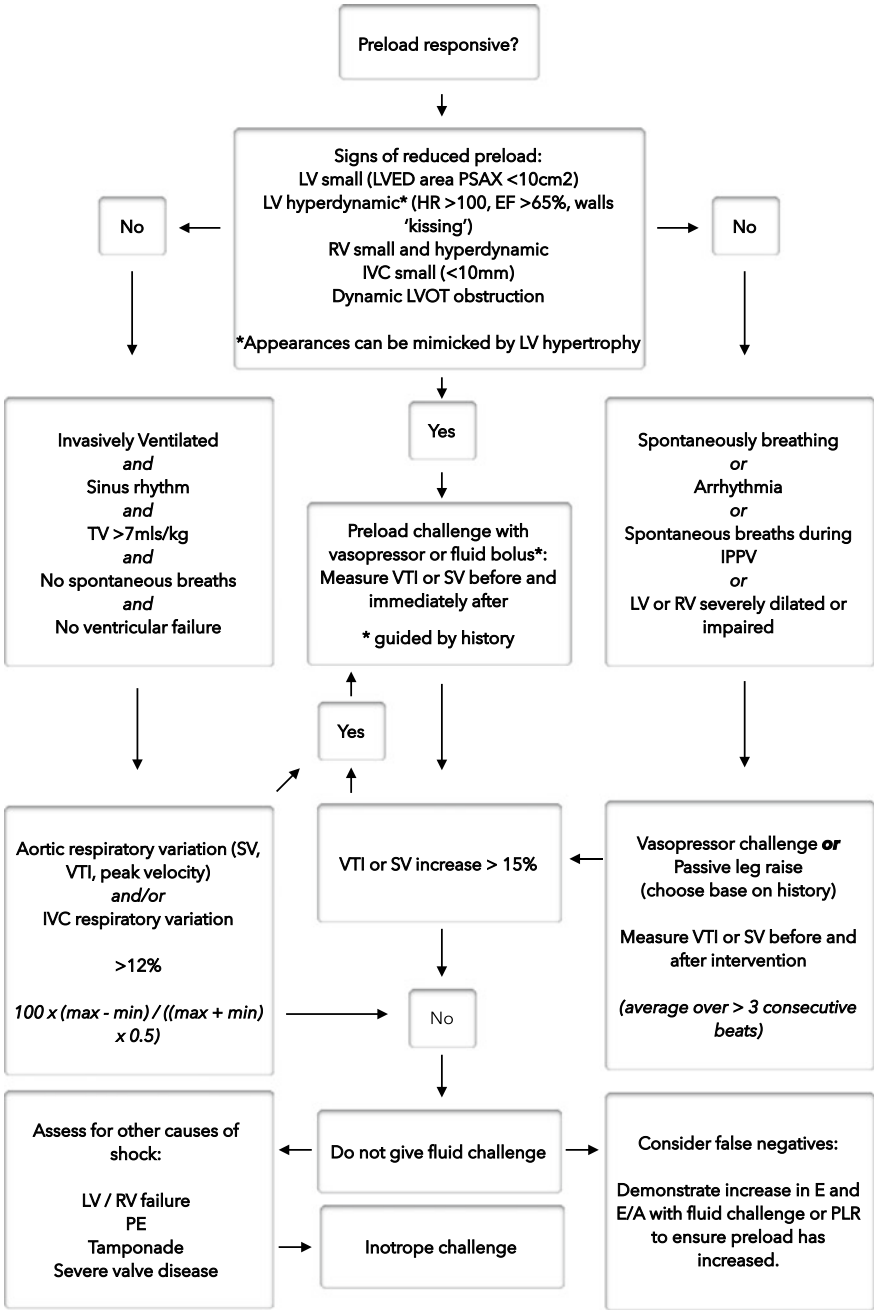

Fig. 19.4 Flowchart showing the use of echocardiography to guide resuscitation

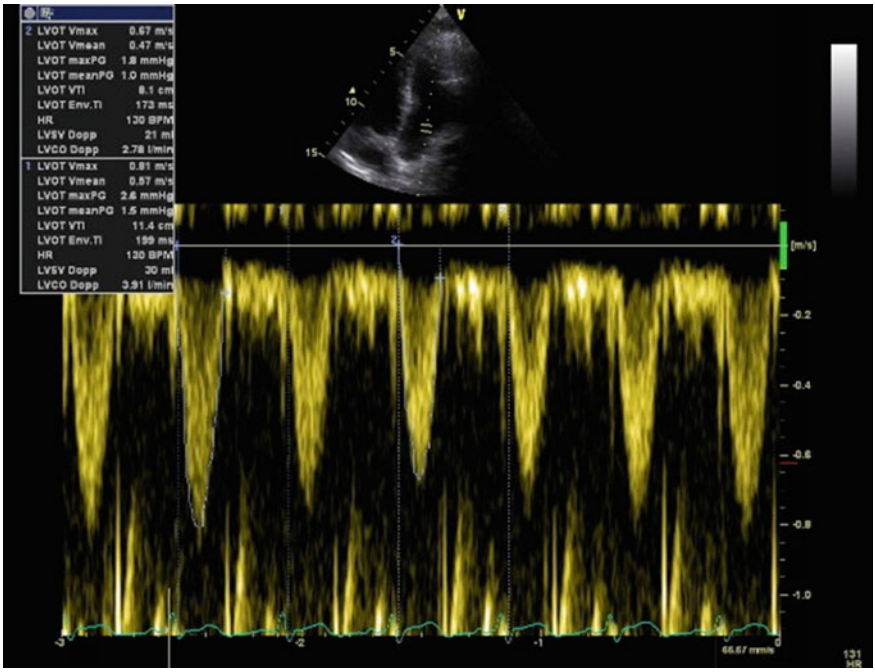

Fig. 19.5 Doppler trace of the left ventricular outflow tract (LVOT) demonstrating the change in blood flow with respiration in a ventilated fluid responsive patient

Other Cardiac Pathology

Aortic dissection and severe valvular regurgitation (for example from papillary muscle rupture) are among other causes of shock which can be detected with echocardiography. While more expertise is required to detect these than with focussed echocardiography, rapid access to these diagnostic skills should be readily available, either from bedside clinicians or on-call services.

Other Modalities

Abdominal Ultrasound

Abdominal ultrasound should be performed if there is suspicion of hypovolaemia either in trauma or postoperatively (to look for blood). A FAST scan interrogating the RUQ, LUQ and pelvis will reveal if there is any free fluid. FAST scanning in trauma is highly specific for bleeding but less sensitive and so should not replace a CT scan (Fig. 19.6).

In sepsis, if the source is unclear, then sub-diaphragmatic collections, biliary sepsis and solid organ abscesses are relatively easy to identify. Ultrasound can be used to guide drain placement.

Lack of peristalsis may be a sign of an abdominal catastrophe.

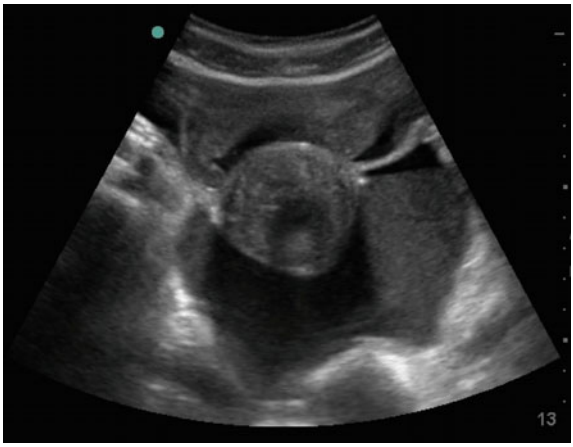

Fig. 19.6 Pelvic blood around the uterus of a stabbing victim with a liver laceration

Vascular Ultrasound

If a PE is suspected from the lung and heart ultrasound then scanning for a DVT is useful to provide more information (though not essential for treatment).

19.5 Conclusion

Ultrasound is able to rapidly identify the cause of haemodynamic instability at the bedside whether it be distributive, hypovolaemic, cardiogenic or obstructive. An integrated approach with focused scanning of the heart and lungs (and sometimes the abdomen) is unrivalled by other scanning and monitoring devices in terms of speed, diagnostic accuracy, safety and simplicity to name but a few. The argument that ultrasound should be mandatory in shock is compelling and difficult to contradict. The only obstacle to its use is the presence of a trained, competent practitioner and the availability of an ultrasound machine. It is likely that ultrasound will universally become integral for the assessment and management of the haemodynamically unstable patient.

References

1. Marik P. The physiology of volume resuscitation. Current Anesthesiol Rep. 2014;4(4):353.
2. Prowle JR, Ishikawa K, May CN, Bellomo R. Renal blood flow during acute renal failure in man. Blood Purif. 2009;28(3):216–25.
3. Lerolle N, Guérot E, Faisy C, Bornstain C et al. Renal failure in septic shock: predictive value of Doppler-based renal arterial resistive index. Intensive Care Med. 2006;32(10):1553–9.

4. Osada T, Murase N, Kime R, Shiroishi K et al. Arterial blood flow of all abdominal-pelvic organs using Doppler ultrasound: range, variability and physiological impact. Physiol Meas. 2007;28(10):1303–16.
5. Marik P, Bellomo R. A rational approach to fluid therapy in sepsis. BJA: Br J Anaesth. 2016;116(3):339–49.
6. Lichtenstein D. FALLS-protocol: lung ultrasound in hemodynamic assessment of shock. Heart Lung Vessel. 2013;5(3):142–7.

Chapter 20
The Polytrauma Patient

Liza Keating

Keywords Ultrasound · Polytrauma · Extended FAST · Fluid status · Raised intra-cranial pressure

20.1 Introduction

In a patient who has undergone polytrauma there are a number of potentially useful applications for ultrasound scanning in the resuscitation room. Focused assessment with sonography in trauma (FAST) scanning has become an essential initial screening tool, which is part of the ABCDE assessment of the polytrauma patient However in the context of polytrauma there are a number of other uses of ultrasound to be considered.

20.2 FAST Scanning

FAST is a well-established standardised set of ultrasound views for the evaluation of the injured patient. There are robust recommendations for FAST examination in the haemodynamically unstable adult patient with suspected haemorrhage in whom there is no or limited response to volume replacement [1, 2]. Be aware that a negative FAST does not exclude intraperitoneal or retroperitoneal haemorrhage and whilst the FAST may identify free fluid it will not identify the source of the bleed or more specifically the aetiology. By convention, a low frequency (2.5–5 MHz) curvilinear or phased array probe is used to allow for appropriate viewing depth when performing the standard FAST scan.

Ultrasound has a number of advantages over other techniques: it is cheap, does not expose the patient to ionizing radiation, and the ability to repeat the examination

L. Keating (✉)
Intensive Care Unit, Royal Berkshire Hospital, London Road, Reading, RG1 5AN, UK
e-mail: Liza.keating@royalberkshire.nhs.uk

A. Walden et al. (eds.), *Ultrasound in the Critically Ill*,
https://doi.org/10.1007/978-3-030-71742-1_20

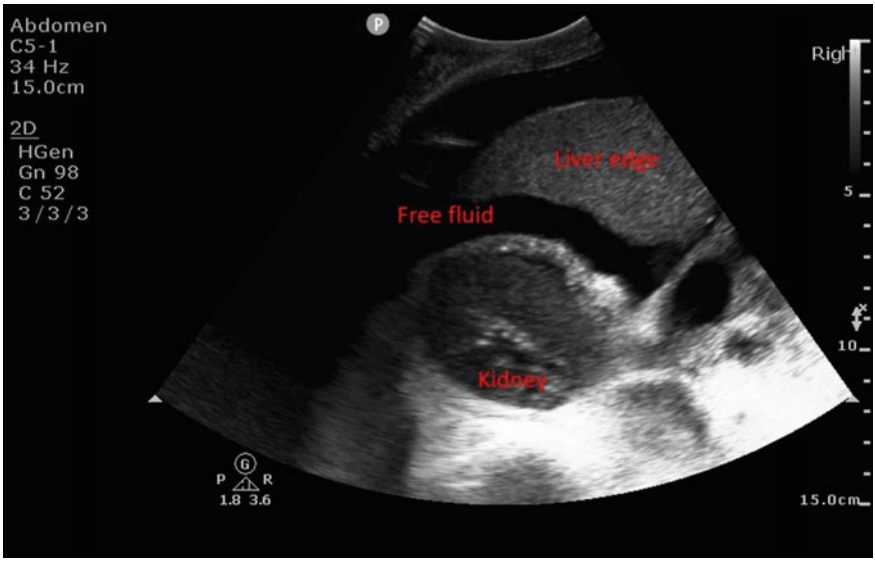

Fig. 20.1 Free peritoneal fluid in Morrison's pouch

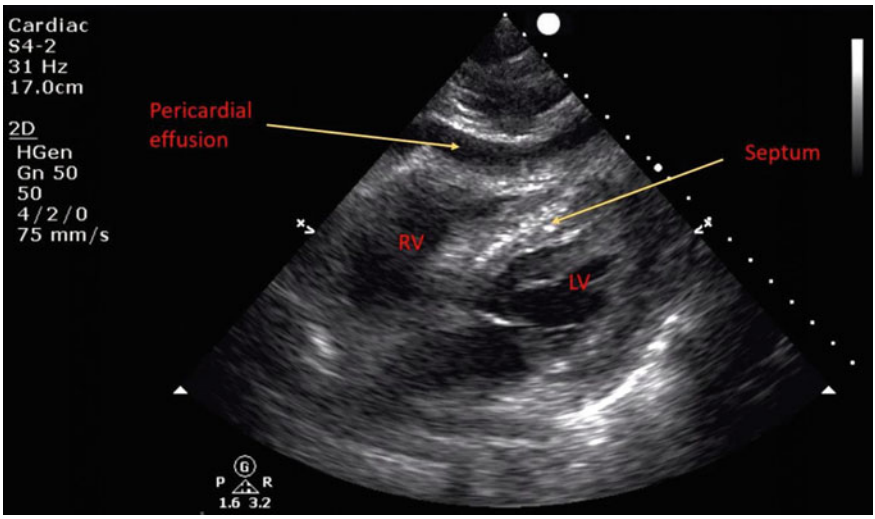

Fig. 20.2 Pericardial fluid

improves its diagnostic accuracy. The purpose of ultrasound in the context of trauma is to rule in free fluid either in the intraperitoneal (Fig. 20.1) or pericardial space (Fig. 20.2), which appears as a hypoechoic or anechoic (i.e., dark grey or black) collection. It has a clear role in the evaluation of thoracic and abdominal trauma since the presence of pericardial fluid or intraperitoneal fluid is likely to

change management priorities. The need for immediate surgery is a contra-indication to FAST scanning.

In the context of the polytrauma patient ultrasound is not seen as a replacement for more detailed sensitive examinations. A stable polytrauma patient may go straight to computed tomography (CT). In patients who are responding to resuscitation or if their haemodynamic status is stable immediate computerised tomography (CT) should be considered for polytrauma patients to rule out haemorrhage [1]. CT is highly sensitive for both intraperitoneal haemorrhage and solid organ injury and is the imaging study of choice in stable patients with suspected intra-abdominal or intra-thoracic injury.

There are limitations to FAST scanning since a number of intra-abdominal and thoracic injuries are not detectable by ultrasound. These include: diaphragmatic tears, solid organ injuries including pancreatic lesions and bowel perforations, mesenteric trauma, and abdominal injuries that do not produce free fluid in amounts detectable by ultrasound (generally >200 mL) [3].

In addition the use of ultrasound in the context of pelvic fractures has a number of limitations. Firstly retroperitoneal bleeding will not be visible on ultrasound scan, injuries to the kidneys are hard to detect and in addition ultrasound is not able to differentiate between blood and urine. In addition to this ultrasound is limited by patient factors. For example: in patients with obesity accurate cardiac or abdominal images may be difficult to obtain. In patients with chronic pulmonary disease, and consequently hyper-inflated lungs, it may also be difficult to obtain accurate cardiac images. Less commonly patients with subcutaneous emphysema are likely to be difficult to obtain good imaging. Finally, abdominal ultrasound has also been shown to have only modest sensitivity in detecting haemoperitoneum in children and is not recommended [4].

The standard FAST has been extended to the focused assessment with sonography for trauma (extended FAST or eFAST) to include the pleural spaces. Ultrasound has a role in the evaluation of pneumothorax, haemothorax and lung contusion. The NICE guidance recommends that in adults (16 or over) with chest trauma consideration should be given to chest X-ray and/or eFAST as part of the primary survey with severe respiratory compromise [1]. The detection of such pathology may change management priorities in the context of trauma. The current recommendation is that in adults, with suspected chest trauma without severe respiratory compromise, responding to resuscitation or whose haemodynamic status is normal consideration should be given to immediate CT thorax. Whilst in children (under 16 s) who have undergone chest trauma the emphasis is on the use of plain radiography and lung ultrasound as first line imaging even in stable patients [1].

Instead of the standard (2.5–5 MHz) curvilinear or phased array transducer probe used for the basic FAST examination, a high frequency (5–10 MHz) linear transducer probe can be used to improve the views of the interface between the visceral and parietal pleura of the lung. The field depth needs to be adjusted to a shallow setting (approximately 4 cm). The diagnosis of pneumothorax is made by the direct visualisation of both a lack of sliding motion of the visceral pleura against the parietal pleura and the absence of B-lines, which are also known as comet tails.

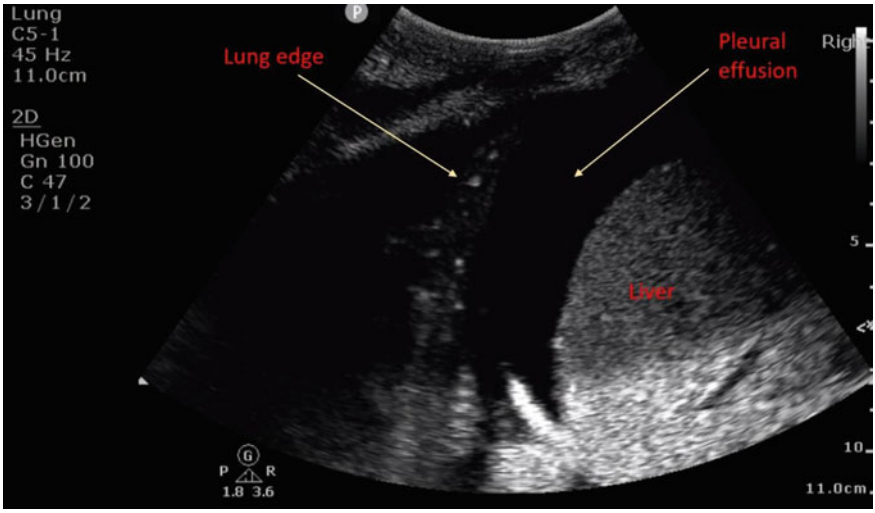

Fig. 20.3 Pleural effusion

A pleural effusion can be seen as a black (hypoechoic) stripe between the diaphragm and the lungs (Fig. 20.3). The differentiation between pleural fluid and blood on ultrasound can be difficult. In the context of trauma it is possible to use lung ultrasound to add a diagnosis of lung contusion. The presence of B-lines, although suggestive of alveolar or interstitial oedema and not specific, isolated to one area can be suggestive of lung contusion and the comparison between the two lungs fields can be helpful.

In the context of the polytrauma patient there maybe a place for the use of ultrasound in the assessment of volume status. The addition of the ultrasound assessment of the inferior vena cava to the standard eFAST views is currently under evaluation. This can be done with either the cardiac or the low frequency probe. Whilst it is technically relatively easy to perform, research is ongoing to establish its usefulness. The limitations with the current evidence are that the studies are small and the populations under review are heterogenous. The measurements obtained or both the diameter and the degree to which it collapses on inspiration must be used on the context of other information obtained from the clinical examination [5].

Less routine is the use of ultrasound in the context of trauma for the detection of raised intracranial pressure through the measurement of optic nerve sheath diameter (ONSD). Invasive measurement of intracranial pressure is the gold standard and is carried out routinely by neurosurgical teams in tertiary centres. There is some evidence that ultrasonography of the ONSD has diagnostic accuracy for the presence of raised intra-cranial pressure [6]. The optic nerve is surrounded by cerebral-spinal fluid and is the point of the central nervous system that can be visualised. Changes in intracranial pressure are transmitted through the sub-arachnoid fluid and onto the optic nerve. Given that the equipment required is readily available, the costs are low and there is now widespread use of

ultrasonography in the resuscitation room there is some argument to support its development as a technique. Authors have commented that technically it can be more difficult than other uses of ultrasound in trauma. Whilst studies are promising there is currently insufficient evidence to support its widespread uptake [5].

20.3 Conclusion

The role of ultrasound in the patient who has undergone polytrauma is well established. Ultrasound has a place within the initial assessment and stabilisation of the patient and is an accepted adjunct to clinical examination. Extended FAST scanning allows a rapid evaluation of the abdomen, pericardium and the chest to exclude a pneumothorax. Its limitations are widely acknowledged. The use of ultrasound in the assessment of fluid responsiveness in the context of trauma has been less widely adopted although continues to generate some interest whilst the measurement by ultrasound of raised intracranial pressure is still largely confined to specialist centres.

See also:
Chapter 10 FAST scanning
Chapter 16 Neuro-opthalmic Ultrasound
Chapter 18 Musculoskeletal Ultrasound
Chapter 19 The Haemodynamically Unstable Patient
Chapter 21 The Patient with Acute Breathlessness.

References

1. National Institute for Health and Care Excellence. CG 39 Major trauma: assessment and initial management. London: NICE, 2016 www.nice.org.uk/guidance/ng39.
2. Diercks, Deborah B, et al. Clinical policy: critical issues in the evaluation of adult patients presenting to the emergency department with acute blunt abdominal trauma. Ann Emerg Med. 2011;57:387–404.
3. Frankel HL, Kirkpatrick AW, Elbarbary M, Blaivas M, Desai H, Evans D, Summerfield DT, Slonim A, Breitkreutz R, Price S, et al. Guidelines for the appropriate use of bedside general and cardiac ultrasonography in the evaluation of critically Ill patients-part I: general ultrasonography. Crit Care Med. 2015;43(11):2479–502.
4. Holmes JF, Gladman A, Chang CH. Performance of abdominal ultrasonography in pediatric blunt trauma patients: a meta-analysis. J Pediatr Surg. 2007;42(9):1588–94.
5. Sofia S. Bedside US imaging in multiple trauma patients. Part 1: US findings and techniques. J Ultrasound. 2013;16(4):147–59.
6. Dubourg J, Messerer M, Karakitsos D, et al. Individual patient data systematic review and meta-analysis of optic nerve sheath diameter ultrasonography for detecting raised intracranial pressure: protocol of the ONSD research group. Syst Rev. 2013;2:62. https://doi.org/10.1186/2046-4053-2-62.

Chapter 21
The Patient with Acute Breathlessness

Thomas Clark

Keywords Echocardiography · Lung Ultrasound · Dyspnoea · Breathlessness

21.1 Introduction

Focused ultrasound is a powerful tool for diagnosing the cause of acute breathlessness. It can (1) improve both the accuracy and speed of your diagnosis, and (2) help direct your management plan.

21.2 Making that Diagnosis

When faced with dyspnoea a list of diagnoses will automatically crystallise in your mind, the details of which partly depend on the clinical circumstances. The differentials will predominantly centre around cardiac or respiratory disorders, although hyperventilation secondary to metabolic acidosis or patient anxiety remain common possibilities. Focused ultrasound assessment of heart, lungs and vasculature acts as a rapid 'rule-in' or 'rule-out' diagnostic technique. In certain circumstances its accuracy rivals that of CT, and certainly outstrips CXR and clinical examination. Binary 'yes/no' algorithms are used to convert ultrasound signs into clinically useful information. The predominant algorithm currently in publication and used by the Intensive Care Society FUSIC accreditation pathway is the modified BLUE (Bedside Ultrasound in Emergency) protocol (1). This algorithm can be nicely complemented with focused cardiac protocols (e.g. Focused Intensive Care Echocardiography (FICE) (2)) that allow a basic visual assessment of cardiac function to produce a well rounded understanding of your patient's cardio-respiratory function.

T. Clark (✉)
Department of Critical Care, Torbay and South Devon NHS Foundation Trust, Torquay, UK
e-mail: thomasclark1@nhs.net

A. Walden et al. (eds.), *Ultrasound in the Critically Ill*,
https://doi.org/10.1007/978-3-030-71742-1_21

In this chapter I will briefly outline the steps I take when using focused ultrasound in my clinical practice. I will also briefly focus on specific ICU benefits of this technology.

21.3 Step 1—the BLUE Protocol/Focused Lung Ultrasound

This is a focused ultrasound assessment of the lung and is the starting point when faced with a breathless patient. It must be emphasised that the evidence for this protocol is in spontaneously ventilating patients who have one of five diagnoses—pneumonia, 'alveolar interstitial syndrome' (pulmonary oedema—either cardiogenic or non-cardiogenic), pneumothorax, pulmonary embolism (PE) or an acute exacerbation of asthma/COPD. To make the diagnosis of PE requires further cardiac and vascular assessment. There is no option for 'normal', pleural effusion or hyperventilation from other causes, and this must be kept in mind. The claimed diagnostic accuracy approximates 90% and its use speeds time to correct diagnosis when implemented into Emergency Department practice. As for all investigations you must interpret lung ultrasound findings in the context of the clinical picture—this author appreciates the concept of having a 'pre-test probability' i.e. what you think the diagnosis is, that is then modified by your lung US findings (using the likelihood ratio) to give you 'the most likely diagnosis'. It is outside the remit of this chapter to discuss the BLUE algorithm in detail, however below are the important key features.

1. It's a six-point examination using six pre-defined locations that approximate to the left and right upper, middle/lingular and lower lobes. It mimics the step-wise auscultation examination used by most clinicians. Four of these points are on the front of the chest whilst two are postero-lateral.
2. You progress through the protocol answering 'yes/no' to a series of questions until you have a diagnosis. Once you do, you stop.
3. Pulmonary oedema manifests as a very clear picture of bilateral, anterior, multiple 'B-lines'. These 'B-lines' are probably caused by fluid accumulation in the lobular septa. Pulmonary oedema can either be cardiogenic or non-cardiogenic. Clarification between these two diagnosis will be discussed below.
4. Pulmonary embolism as a diagnosis requiring ultrasound evidence of a deep vein thrombosis. A focused echocardiogram is a useful 'follow-up' scan in this case, again this will be discussed below.
5. Pneumonia can be diagnosed in a number of ways. One of these is a positive Postero-Lateral Alveolar Pleural Syndrome (PLAPS) sign. This sign includes evidence of a pleural effusion. Clearly, if you see a large pleural effusion then this can be a cause of dyspnoea not detailed by the protocol itself.

6. Pneumothaoraces can only be 'ruled-in' by finding a 'lung-point'—this sign having 100% specificity. However, in certain populations where pneumothoraces are a common finding e.g. in polytrauma patients, other signs may nearly 'prove' a pneumothorax as long as certain other complications are excluded e.g. absent 'lung-sliding' with prominent 'A-lines' once endobronchial intubation with a endo-tracheal tube is excluded.
7. This protocol is not valid in patients with chronic lung disease.

Whether you use the BLUE protocol or not, lung ultrasound makes the diagnosis of pneumonia, pulmonary oedema, pneumothoraces and large pleural effusions rapid, accurate and simple.

21.4 Step 2—Focused Cardiac Ultrasound

This is an important second step after lung ultrasound. This is for a number of reasons.

1. It allows you to diagnose the cause of pulmonary oedema and to differentiate between cardiogenic and non-cardiogenic (ARDS) that may look very similar on CXR. There are obvious important ramifications of discriminating between these two pathologies.
2. It aids in the diagnosis and treatment of PEs. Evidence of impaired right ventricular function and normal blood pressure MAY make you consider thrombolysis but SHOULD make you optimise diastolic blood pressure and be cautious over your fluid administration.
3. Knowing cardiac function is ALWAYS useful—it helps with admission decisions and helps to moderate your fluid and inotropic therapy.

As for lung ultrasound echocardiography at its most simple depends on binary 'yes/no' answers to a series of focused questions. These questions vary depending on which training package you have completed, but the FICE accreditation pathway requires you to assess cardiac activity, left ventricular size and function, right ventricular size and function, evidence of pericardial effusion and evidence of reduced venous return. It is beyond the scope of this chapter to delve any deeper into this process but it is very simple to discriminate between the poorly contracting, severely impaired ventricle and the ventricle that is not, and here lies the power of focused echocardiography. It is quick and simple to diagnose likely cardiac shock and cardiogenic pulmonary oedema (in conjunction with step 1). More advanced abilities will allow you to investigate for causes of flash pulmonary oedema such as acute mitral regurgitation secondary to ruptured papillary muscles and infective endocarditis or interrogate chronic pericardial effusions for evidence of cardiac limitation that may be causing dyspnoea.

21.5 ICU-Specific Problems

21.5.1 Diagnosing The 'Acute Respiratory Failure' Referral

Lung ultrasound is very useful in the more complex patients who have been admitted to hospital for a period of time and who have multiple co-morbidites. These patients will often have co-existing ischaemic heart disease and chronic lung disease, coupled with a long period of immobility and immunosuppression due to one reason or another. Pulmonary oedema and hospital acquired pneumonia are two common diagnoses and it can be difficult to discriminate the main pathology causing dyspnoea on clinical grounds alone, particularly if both co-exist. Lung ultrasound not only allows you to rapidly identify the key offender but also measure the adequacy of treatment e.g. the response to diuretic therapy and the need for further doses.

21.5.2 Is that a Pleural Effusion?

We have all been faced with the CXR that could be basal consolidation or could be an effusion, or possibly both. Lung ultrasound will allow you to discriminate between these and if a pleural effusion is seen, will allow you to estimate its size and look for evidence of empyema. It will also bring a measure of increased safety to any procedure e.g. insertion of chest drain, both by allowing you to make a more informed decision on whether to undertake your intervention and in helping to avoid surrounding structures e.g. a raised hemi-diaphragm (always higher than you would expect in the ventilated patient), aerated lung, the liver or spleen.

21.5.3 The Patient 'Stuck' on a Ventilator and Not Weaning

In patients ventilated for multiple-organ failure, lung ultrasound can be used to assess 'extra-vascular lung water'. This appears as multiple 'B-lines', areas of atelectasis and effusions. When seen this can direct the physician to alter fluid removal or ventilator settings. Similar signs are also seen in patients who are struggling with their ventilator wean or who remain hypoxic. It can be used during a spontaneous breathing trial to better predict those who are likely to fail (in comparison to clinical scoring systems). If seen, then extubation may be re-considered and deferred until more appropriate. It can also be used to optimise PEEP and mean airway pressure to better recruit lung.

In summary, focused ultrasound is an excellent tool. It allows you to diagnose the cause of dyspnoea, determine the correct treatment and monitor the effect of treatment.

21.6 Conclusion

Lung ultrasound and focused echocardiography give rapid and accurate assessment of the cause of acute breathlessness. These tools are especially useful in those patients presenting through the Emergency Department or on Acute Medical Units but also are of value in the diagnosis and management of Intensive Care patients.

See also:

Chapter 5 Basic Lung Ultrasound.

Chapter 6 Advanced Lung Ultrasound.

Chapter 7 Focused Transthoracic Echocardiography.

Chapter 8 Advanced Transthoracic Echocardiography.

Chapter 22 The Patient Difficult to Wean from Mechanical Ventilation.

Chapter 22
The Patient Difficult to Wean from Mechanical Ventilation

Andrew Walden and Karim Fouad Alber

Keywords Mechanical Ventilation · Weaning failure · Spontaneous Breathing Trial · Lung Aeration · Diastolic heart failure · Neuromuscular Weakness · Lung Ultrasound · Echocardiography · Diaphragm Ultrasound

22.1 Introduction

Weaning and discontinuation of mechanical ventilation are pivotal in the recovery from critical illness. If a patient is unable to complete a spontaneous breathing trial or requires re-intubation within 48 h of extubation then they are considered to have failed to wean. Between 20 and 30% of critically ill patients fall into this group and the morbidity, mortality and health costs are high. The problems are often multifactorial involving neuromuscular, cardiac and respiratory problems. It is therefore important to take a systematic approach to failure to wean from mechanical ventilation. Point of care ultrasound is invaluable in this assessment.

22.2 Respiratory Assessment

The ultrasound assessment of the lungs can be split into three main areas: Lung aeration, pleural effusion and diaphragmatic function.

A. Walden (✉) · K. Fouad Alber
Royal Berkshire Hospital, Reading RG1 5AN, UK
e-mail: andrew.walden@nhs.net

A. Walden et al. (eds.), *Ultrasound in the Critically Ill*,
https://doi.org/10.1007/978-3-030-71742-1_22

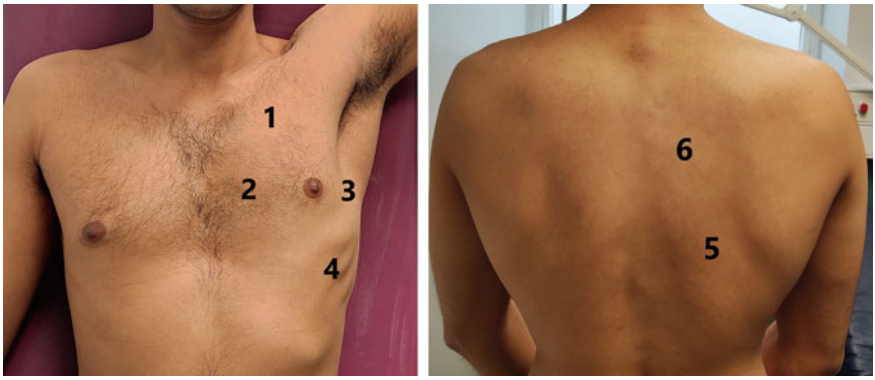

Fig. 22.1 12-zone approach for lung ultrasound

22.2.1 Lung Aeration

Direct ultrasound of the lung can characterise different patterns of lung aeration. The dynamic change in this pattern during a spontaneous breathing trial (SBT) can predict the likely success of subsequent extubation with some certainty [1]. Using a 12 zone approach as shown in Fig. 22.1 and characterising the degree of lung aeration in each zone as shown in Fig. 22.2, it is possible to create a score for each area.

During an SBT, a dynamic aeration score is calculated. This is by examining the change in aeration in each lung zone. A score of one is given if there is a mild worsening of lung aeration, three if it is a moderate loss and five if it is a severe loss. Conversely, if there is an improvement in aeration this is then subtracted from the final score.

In the aforementioned study, a score of <13, predicted a very low likelihood of extubation failure and a score of >17 predicted an 85% chance of extubation failure.

In practice this score can be cumbersome to calculate and specific lung ultrasound findings may point to the need for increased PEEP or physiotherapy in the presence of frank atelectasis and measures to reduce the total lung water such as diuretics and fluid restriction.

22.2.2 Pleural Effusions

Pleural effusions are common in intensive care patients occurring in up to 50% within 48 h of admission [2]. There are multiple adverse effects on breathing: (1) Uncoupling of lung from the chest wall results in an increase in the area of tidal ventilation and potential atelectotrauma (2) Compression of the underlying lung

No. points	Aeration	Description	Appearance
0	Normal	A-line pattern with maximum of 2 B-lines per sector	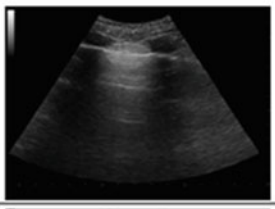
1	Moderate loss	Multiple B-lines regularly spaced or coalescent but within a limited portion of sector	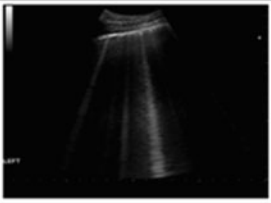
2	Severe loss	Coalescent B-lines throughout a sector	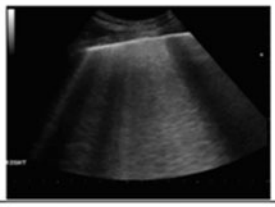
3	Total loss	Lung consolidation	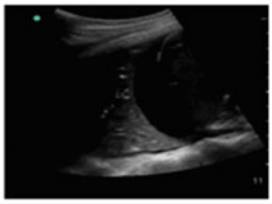

Fig. 22.2 Lung aeration. Evaluating lung aeration using ultrasound findings in each zone, producing a cumulative score based on objective findings

with atelectasis leads to ventilation perfusion mismatch with shunt (3) As pressure builds up in an effusion it can result in downward pressure on the hemidiaphragm affecting respiratory mechanics and the ability to ventilate the underlying lung (4) Outward pressure on the chest wall leads to stimulation of stretch receptors and rapid, shallow breathing [3].

There have been no large scale clinical trials of thoracocentesis in this situation however meta-analysis of the available data shows that it appears to be a safe thing to do and results in improvements of surrogate physiological measures such as oxygenation and P:F ratios [4].

Pleural effusions in critically ill patients are easily visualised on ultrasound (see Fig. 22.3). It is possible to quantify the amount of fluid by ultrasound however it is often qualitative aspects which determine the likelihood of thoracocentesis being beneficial to weaning.

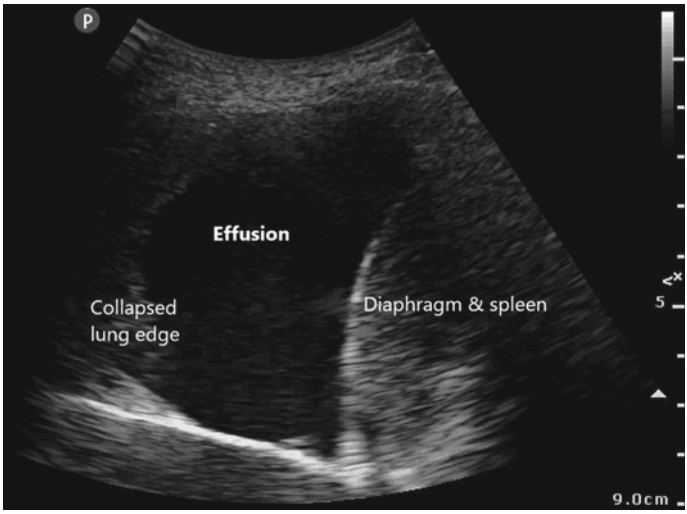

Fig. 22.3 Pleural effusion. The fluid appears hypoechoic (dark) compared to the adjacent viscera

Evidence of septation or fibrin deposition within the pleural effusion may suggest it is more likely to be an exudated and raises the possibility of pleural infection or empyema. The plankton sign is also suggestive of an exudative effusion and is a whorling, particulate pattern seen within the effusion (see Figs. 22.4 and 22.5). These findings should prompt a diagnostic tap to rule out pleural infection or malignancy and consideration of CT scanning of the chest to characterise the extent of the pleural collection. Drainage in this situation is important both for source control of infection but also to reduce the risk of lung trapping and to improve respiratory mechanics.

The presence of flattening or inversion of the hemidiaphragm (see Fig. 22.6) is another sign that the patient is likely to benefit from pleural drainage. In the presence of this sign the diaphragm is likely to be on an adverse portion of its length/tension curve. In addition, the increased outward pressure on the chest wall will further affect respiratory mechanics and stimulation of stretch receptors will worsen subjective feelings of dyspnoea which drive a rapid, shallow breathing pattern. It is likely in this situation that drainage with lead to improvements in respiratory mechanics and subjective feelings of dyspnoea aiding the process of weaning from mechanical ventilation.

Quantifying pleural effusion volume is possible from several unidimensional measurements on from B mode scanning:

The intra-pleural distance at the base of the lung (see Fig. 22.7) has been shown to correlate with volume of pleural fluid in two studies. With patients supine, an intra-pleural distance at the base of the lung of 45 mm on the left or 50 mm on the right reliably predicts a pleural fluid volume of greater than 800 mL [5].

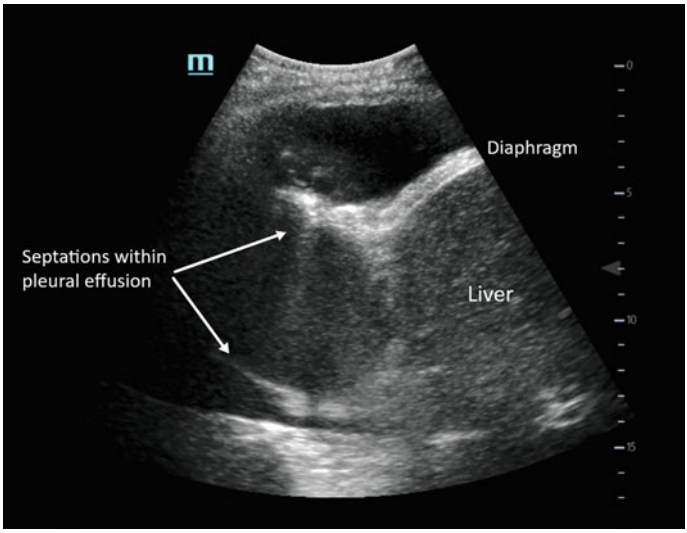

Fig. 22.4 Septated pleural effusion. The presence of septations suggests a complex/loculated pleural effusion

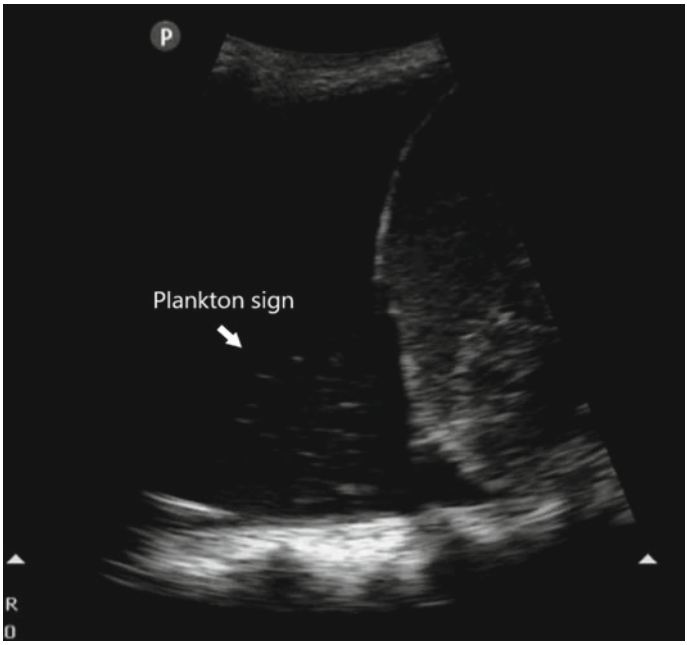

Fig. 22.5 Plankton Sign. Hyperechoic particles observed within the effusion are suggestive of an exudate

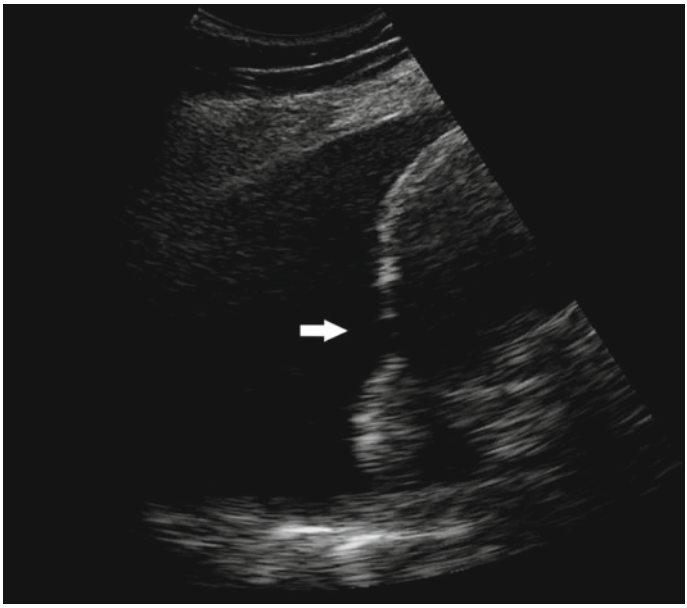

Fig. 22.6 Inverted Diaphragm. Depression or inversion of the hemi-diaphragm due to increased pressure from a large volume pleural effusion

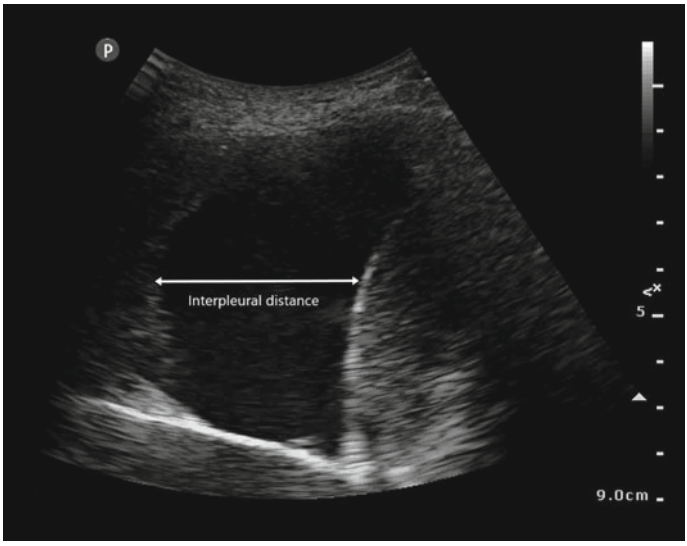

Fig. 22.7 Intrapleural distance. This measurement can be used to estimate the volume of the effusion

In another study, supine patients with a 15° elevation had their maximum intrapleural distance measured and following drainage they demonstrated that the fluid volume in millilitres is the separation distance in millimetres multiplied by 20 [6].

Whilst there is no clear cut off volume at which drainage is indicated, the larger the volume, the higher the likelihood of benefits in terms of gas exchange and respiratory mechanics. There appears to be a dose response in terms of amount of fluid drained and improvements in oxygenation [7].

22.2.3 Diaphragmatic Function

The diaphragm is essential for normal spontaneous breathing and its function is often impaired in critically ill patients and thus can lead to delayed weaning from mechanical ventilation. There are many ways of investigating diaphragmatic function including fluoroscopy, transdiaphragmatic pressure measurements and electromyography however in critically ill patients these are either impractical or unnecessarily invasive. Visualisation of the diaphragm with ultrasound can help to identify problems such as post- operative or traumatic diaphragmatic dysfunction and can also help in determining the likelihood of liberation from mechanical ventilation.

22.3 Diaphragmatic Paralysis or Weakness

Phrenic nerve damage secondary to trauma, cardiothoracic or upper gastrointestinal surgery can lead to unilateral or bilateral diaphragmatic paralysis. In health, it is easy to demonstrate good diaphragmatic excursion on deep inspiration by scanning up throught the dome of the diaphragm in the mid-clavicular line (see Fig. 22.8), this excursion is absent in patients with diaphragmatic paralysis. High cord injuries in trauma can also result in bilateral diaphragmatic paralysis. Neuromuscular diaphragmatic failure can also occur from medical causes such as acute polyneuropathy chronic degenerative conditions such as motor neurone disease or as symptoms of primary myopathic problems such as myasthenia gravis.

The hallmark of complete paralysis of a hemidiaphragm is paradoxical movement in inspiration from M-mode in the subcostal view. Where there is weakness rather than paralysis, the features may be more subtle. A reduction in the diaphragmatic thickness at the zone of apposition is a feature of atrophy.

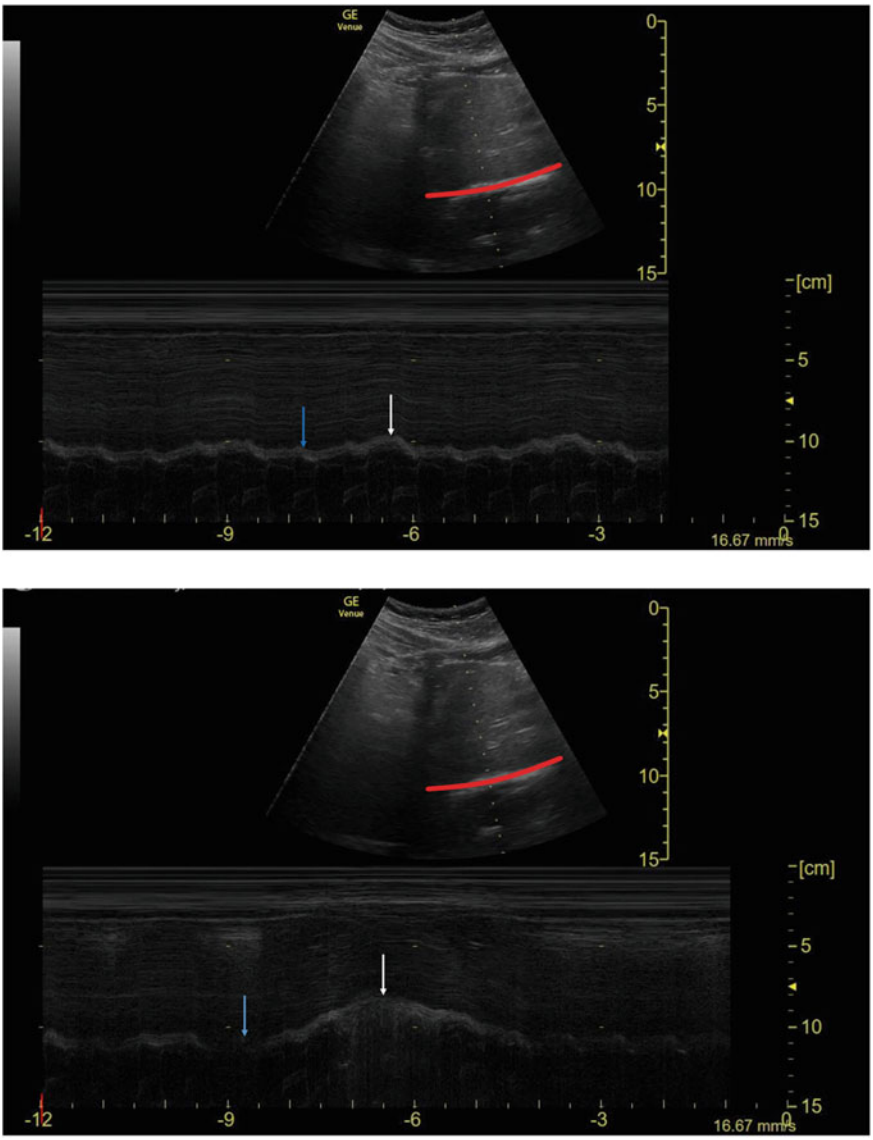

Fig. 22.8 **a** M mode ultrasound through dome of hemidiphragm (HD) during normal respiration; The dome of the hemi-diaphragm is demarcated with the red curve; the blue arrow demonstrates the position of the HD on expiration and the white line on inspirtion. **b** M mode ultrasound through dome of HD during deep inspiration; the blue arrow demonstrates the position of the HD on expiration and the white line on deep inspirtation.

22.3.1 Cardiac Function

Discontinuation of mechanical ventilation has a number of adverse effects on cardiac function: (1) Removing positive intrathoracic pressure leads to increased venous return and therefore preload; (2) Loss of PEEP results in increased left ventricular wall stress and thus an increase in left ventricular afterload; (3) An increased work of breathing will mean that cardiac output will need to increase to drive respiratory muscles; (4) Stopping sedation will result often results in rebound hypertension further increasing left ventricular afterload. Indeed patients who fail a spontaneous breathing trial have been shown to have lower mixed venous oxygen saturations than those that do not. A cardiac aetiology for weaning failure is implicated in 40% of cases.

Useful measures of systolic and diastolic function can be made using transthoracic echocardiography both of which may be implicated and may lead to new treatments like the use of diuretics, beta-blockers and angiotensin-converting enzyme inhibitors as a means of optimising cardiac function prior to weaning and discontinuing mechanical ventilation. Assessment of LV and RV systolic function have been covered extensively in previous chapters. Assessment of diastolic dysfunction is a more advanced echocardiographic skill. Pulsed wave Doppler of the Mitral inflow in diastole provides information on the E wave during early diastole and the A wave due to atrial systole in late ventricular diastole. Tissue Doppler analysis of mitral valve annulus allows determination of the e′ wave of LV relaxation and the E/e′ ratio which correlates to the LV filling pressure.

Several studies have examined these measurements prior to extubation and their relationship to failure of a SBT. An Ejection fraction of <40%; An E/A ratio of >2 in the presence of impaired LV function; An E/e′ ratio of >12 in the presence of preserved LV function are all associated with a higher likelihood of failure of a SBT.

Towards the end of a failing SBT Echocardiography may also help to demonstrate a cardiac cause for the failed trial. Increases in E/A ratio and E/e′ ratio are correlated with measurement of increased pulmonary artery occlusion pressure with a reasonable sensitivity and specificity where E/A ratio >0.95 and the E/e′ ratio >8.5.

References

1. Soummer A, et al. The Lung Ultrasound Study Group (2012) Ultrasound assessment of lung aeration loss during a successful weaning trial predicts postextubation distress. Crit Care Med. 2012;40:2064–72.
2. Mattison LE, Coppage L, Alderman DF, Herlong JO, Sahn SA. Pleural effusions in the medical ICU: prevalence, causes, and clinical implications. Chest. 1997;111(4):1018–23.
3. Walden AP, Jones QJ, Matsa R, Wise MP. Pleural effusions on the Intensive Care Unit, hidden morbidity, therapeutic potential. Respirology. 2013;18(2):246–54.

4. Goligher E, Leis J, Fowler R, Pinto R, Adhikari N, Ferguson N. Utility and safety of draining pleural effusions in mechanically ventilated patients: a systematic review and meta-analysis. Crit Care. 2011;15(1):R46.
5. Vignon P, Chastagner C, Berkane V, Chardac E, François B, Normand S, Bonnivard M, Clavel M, Pichon N, Preux PM, Maubon A, Gastinne H. Quantitative assessment of pleural effusion in critically ill patients by means of ultrasonography. Crit Care Med. 2005;33 (8):1757–63.
6. Balik M, Plasil P, Waldauf P, Pazout J, Fric M, Otahal M, Pachl J. Ultrasound estimation of volume of pleural fluid in mechanically ventilated patients. Intensive Care Med. 2006;32 (2):318.
7. Walden AP, Garrard CS, Salmon J. Sustained effects of thoracocentesis on oxygenation in mechanically ventilated patients. Respirology. 2010;15(6):986–92.

Chapter 23
The Patient with Acute Kidney Injury

James H. Briggs

Keywords Acute kidney injury · Renal tract Ultrasound · Kidney Ultrasound · Obstruction · Hydronephrosis · Urosepsis

23.1 Introduction

Acute kidney injury is a well-known clinical syndrome, but not a definitive diagnosis. It is extremely common, being encountered in 13–18% of all hospital admissions. AKI can be a primary cause of admission, or a consequence of other pathology. It can affect individuals with normal kidney function, but is most common in patients with pre-existing renal impairment or risk factors.

The definition of AKI in adults is variable. Some commonly used are given here:

A rise in serum creatinine of ≥ 26 μmol/L within 48 h.

A 50% or greater rise in serum creatinine within 7 days.

A fall in urine output to less than 0.5 mL/kg/h for more than 6 h in adults.

Delays in recognition and treatment of AKI lead to worse clinical outcomes, including increased mortality. Outcomes for patients with AKI can be reduced with risk assessment, early recognition and treatment. The extensive list of potential causes of AKI means that a wide range of tests and diagnostic tools can be required. As well as biochemical and clinical assessment, imaging plays a critical role in diagnosing the underlying process leading to acute renal impairment. Ultrasound is a powerful tool for investigation AKI which can be used at the point of care.

J. H. Briggs (✉)
Royal Berkshire Hospital, Reading, Berkshire RG1 5AN, UK
e-mail: james.briggs@royalberkshire.nhs.uk

A. Walden et al. (eds.), *Ultrasound in the Critically Ill*,
https://doi.org/10.1007/978-3-030-71742-1_23

23.2 Normal Sonographic Appearances of the Kidney

Ultrasound assessment of the kidney is usually performed with the patient in the supine position. The probe is positioned longitudinally, along the flank, just posterior to the mid-axillary line. The kidney should be imaged in the longitudinally and axial plane. Key features of the normal renal anatomy are shown below (Fig. 23.1).

23.3 Causes of AKI

If and where ultrasound is used in the evaluation of renal disease depends upon the likely underlying cause. As with all diagnostic tests, ultrasound is most helpful when there is understanding of the likely and important outcomes, and specific questions to answer. This allows interpretation of findings within the clinical context.

The causes of AKI are numerous. They are commonly considered within the following groups; pre-renal, Intrinsic and post-renal. The list here is not exhaustive, but contains some common and important conditions.

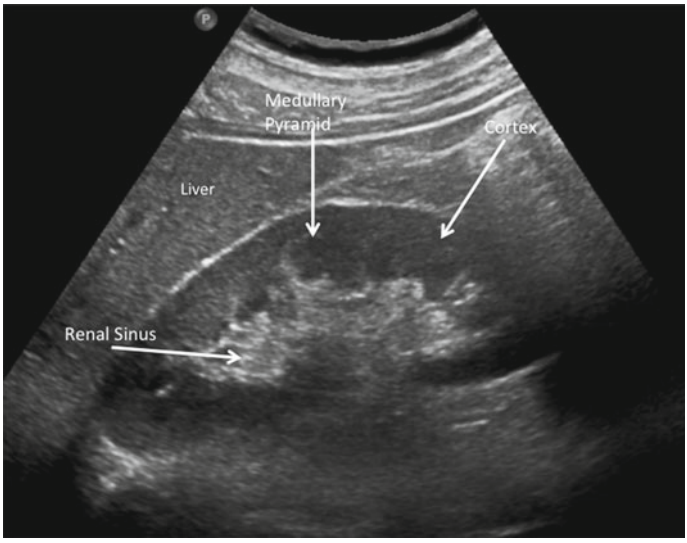

Fig. 23.1 Normal sonographic appearances of the right kidney with major structure labelled

23.3.1 Pre Renal

Pre-renal causes are those relating to hypoperfusion of the kidney. The commonest causes are hypovolaemia, sepsis, congestive heart failure, cirrhosis, and drugs which alter renal perfusion, including ACE inhibitors and NSAIDs. Renal ultrasound is normal in most cases of pre-renal failure (and therefore most cases of AKI overall). Vascular causes for renal failure are the main exception; these include renal artery stenosis (RAS) and renal vein thrombosis (RVT).

Renal Artery Stenosis (RAS): This uncommon condition is due to atherosclerosis in over 75% of cases (Fig. 23.2), but in younger patients fibromuscular dysplasia should be considered. Rarer causes include vasculitis or dissection. Definitive diagnosis of RAS is difficult with ultrasound, but significant difference in kidney size (>10%) can be a clue. Diagnostic criteria using peak systolic flow and resistive indices within the renal arteries, as well as a parvus and tardus waveform have been described.

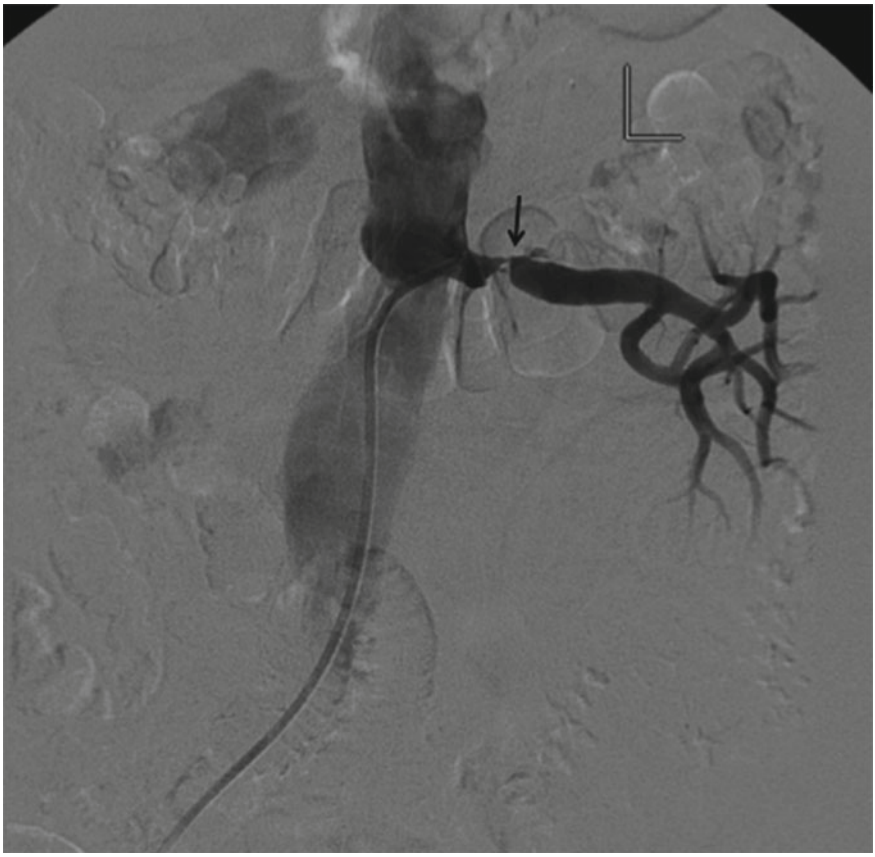

Fig. 23.2 Subtraction angiogram showing stenosis in the left renal artery (arrow)

Renal Vein Thrombosis: Also uncommon with a variety of causes, including nephrotic syndrome, trauma, tumour invasion, and any hypercoagulable state. It is more common in the left than right renal vein. Ultrasound in the acute phase may show enlargement of the affected kidney, with hyperechoic cortex relecting oedmea. Dopper analysis may show diastolic flow reversal, absent venous flow or thrombus within the vein. Later findings include decreased size and echogenicity of the kidney.

23.3.2 Intrinsic

Acute tubular necrosis (ATN) is the commonest final pathway causing intrinsic AKI. Common causes include nephrotoxic drugs, hypotension, trauma and iodinated contrast media. Many causes of glomerular, interstitial and vascular renal disease are also included here. Ultrasound is usually normal in cases of AKI of intrinsic aetiology.

23.3.3 Post Renal

Post renal or obstructive causes account for a relatively small proportion of cases of AKI, but are important as early recognition and treatment can significantly improve outcomes. Hydronephrosis, meaning dilation of the collecting system within the kidney, is the key feature of obstructive uropathy. Depending on the site of obstruction, there may also be dilation of the ureter or bladder, with involvement of one or both systems. In a mildly dilated kidney, only the calyces may be dilated, with normal infundibula and renal pelvis. As the degree and duration of obstruction increases, the extent of dilation becomes more apparent (Fig. 23.3).

KEY POINT: Hydronephrosis does not necessarily indicate kidney obstruction. It can also be a feature of reflux, e.g. in patients with ileal conduit, ectopic ureteric implantation or in certain clinical conditions e.g. pregnancy or transplanted kidney.

Common causes of obstructive uropathy include renal calculi, urothelial tumours, pelvic or retroperitoneal malignancy, iatrogenic and traumatic injury, and bladder outflow obstruction. CT can be a useful tool to determine the underlying cause of obstruction (Fig. 23.4).

23.4 Urosepsis

Pyelonephritis Infection within the kidney is a common clinical presentation, often without significant renal impairment. Simple pyelonephritis does not routinely require imaging and usually responds to conservative management. Ultrasound may

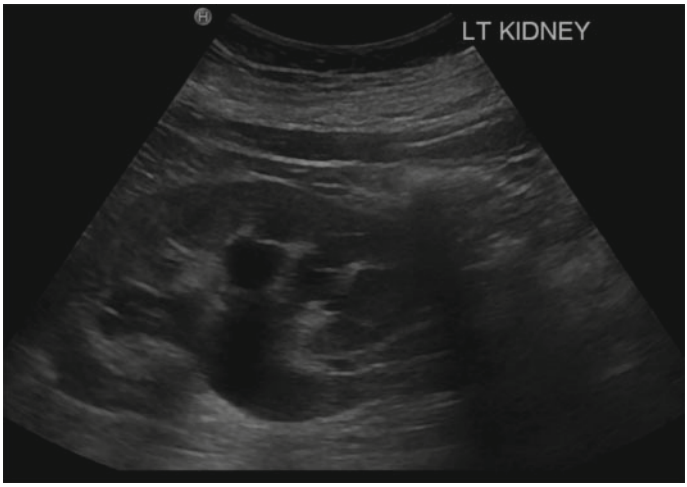

Fig. 23.3 Hydronephrosis, with dilation of the calyces and renal pelvis

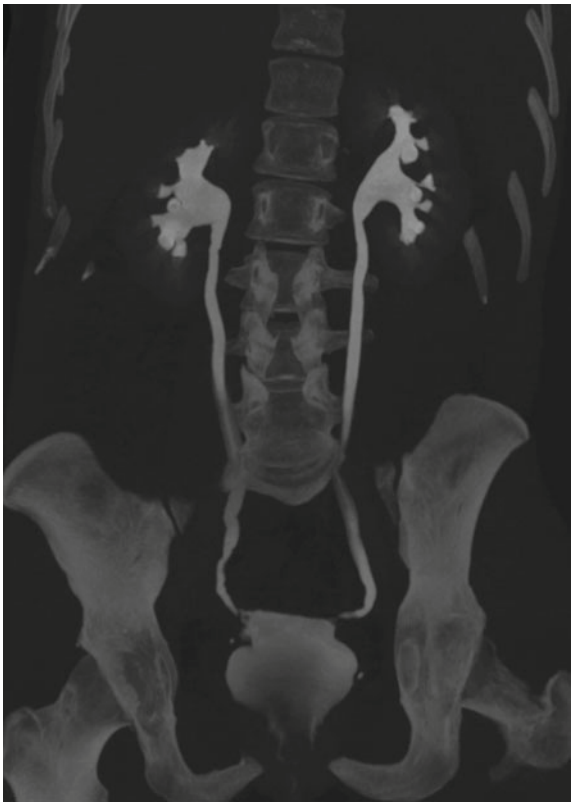

Fig. 23.4 Maximum intensity projection image from a CT urogram showing bilateral hydroureter and hydronephrosis due to ureteric injury

show increased doppler signal, or hyperechoic renal parenchyma, but is normal in around 75% of cases. However, ultrasound does have a role where there is concern of complications of pyelonephritis, including hydronephrosis, abscess or infarction. Gas may be detected in emphysematous pyelonephritis.

Infected obstructed kidney where there is infection within an obstructed kidney, intervention to drain the kidney either percutaneously or surgically is often required to prevent or treat sepsis. Ultrasound is highly sensitive in detection of hydronephrosis, with ancillary signs such as hyperechoic renal parenchyma or perinephric fat suggesting inflammation. Renal calculi may also be visible. Assessment of ureteric dilation may also assist in determining the level and cause of obstruction.

23.5 Exclusions

This chapter is not intended as a guide for assessment of AKI in children, pregnant patients or transplant kidneys. This should be undertaken by an operator experienced in these specialist areas of imaging.

23.6 Conclusion

Pre-renal and intrinsic causes of AKI are the most common, accounting for >80% of cases. Ultrasound is most often normal in these patients. However, ultrasound does offer a highly sensitive, widely available and safe tool in the detection or exclusion of obstructive uropathy, which can be performed at the bedside or in the community. It should be undertaken early in the diagnostic pathway where obstruction is considered likely.

See also:

Chapter 11 Renal Tract Ultrasound.

Chapters 12 and 13 Abdominal Ultrasound.

Chapter 24
The Patient with Acute Abdominal Pain

Andrew Campbell and Poonam Mohan Shenoy

Keywords Aortic aneurysm · Liver failure · Acute cholecystitis · Portal vein thrombus · Pyonephrosis · Ruptured ectopic pregnancy · Strangulated hernia · Appendicitis

24.1 Introduction

An acute abdomen represents a surgical emergency and carries with it significant morbidity and mortality. Time to diagnosis and operative intervention is often key to a positive outcome [1].

The use of focused ultrasound to diagnose intra-abdominal haemorrhage in trauma has been widely accepted by resuscitationists world-wide. In the United Kingdom, FAST (Focused Assessment with Sonography in Trauma) scanning finds its place on Advanced Trauma Life Support courses and is taught to a wide range of health care professionals as part of their required competencies [2].

The use of ultrasound in the acute non-traumatic abdomen has not enjoyed the same acceptance from health care professionals. This is in part due to advancement in computer tomography (CT) technology allowing fast and accurate three dimensional imaging in an increasing number of clinical situations. The literature however still supports the diagnostic capabilities of ultrasound in patients presenting to the Emergency Department with an acute abdomen and remains one of the most frequently requested radiological investigations for generalised abdominal pain [3].

Ultrasound has some key advantages over CT in the critically ill patient with abdominal pain. Being a point of care investigation, it has the potential to be

A. Campbell (✉)
Department of Critical Care Medicine, Wrexham Maelor Hospital, Wrexham LL13 7TD, UK
e-mail: andy.campbell@wales.nhs.uk; andy.campbell@nwcriticalcare.com

P. M. Shenoy
Department of Radiology, Wrexham Maelor Hospital, Wrexham LL13 7TD, UK
e-mail: Poonam.shenoy@wales.nhs.uk

A. Walden et al. (eds.), *Ultrasound in the Critically Ill*,
https://doi.org/10.1007/978-3-030-71742-1_24

immediately available and used to supplement the emergency physician's physical examination. It can be performed in parallel with other interventions or concurrent resuscitative management. It can be abandoned quickly if surgery is required and the patient transfered to the operating theatre, equally if conservative management is decided apon, ultrasound can easily be repeated to observe any interval changes in findings. Immediate patient feedback during the scan can help focus in on pathology during the scan. A classic example is the ultrasound Murphy's sign, helping to confirm a diagnosis of cholecystitis when scanning the gallbladder [4]. Ultrasound exposes the patient to no ionizing radiation or risk of contrast induced nephropathy (CIN) and will have cost saving benefits over CT imaging [5].

24.2 Indications

One of the paramount benefits of Point of Care Ultrasound (POCUS) is that it has very few contraindications to its use. The operator must be mindful though, application of the probe repeatedly against an acute painful abdomen may be uncomfortable for the patient and a challenge for the operator in acquiring images. This finding is usually due to acute peritoneal inflammation (peritonitis) and may indicate the patient that requires immediate surgery rather than the need for further diagnostic imaging. It is of key importance when performing an intervention to assess the capabilities of both the operator and the ultrasound exam as to not delay time to a definitive diagnosis or intervention. Where there is a clear need for surgical intervention, this should not be delayed by trying to gain ultrasound images. Ultrasound is often a rule in intervention, a "negative" scan in the face of a convincing clinical history, needs strong consideration of imaging through CT or MRI [3].

24.3 Equipment

At this point it would be suggested that you refresh yourself with the chapters on the physics of ultrasound and the various intra-abdominal ultrasound chapters in order to set up the ultrasound machine and decide on which probe to use. Images of the abdomen can be acquired with many of the multi frequency probes, however for imaging beyond the peritoneum, the curve-linear probe (3.5–5 MHz) is the most frequently used.

Recognition of ultrasound appearances of the following structures:
- Liver spleen and kidneys
- Bowel

Detection of free intraperitoneal fluid
- Assessment of ascites
- Distinguishing abdominal and pleural fluid

Performance of ultrasound guided diagnostic tap and paracentesis
Bladder assessment
- Recognition of full bladder
- Differentiate full bladder from pelvic fluid and ascites

Fig. 24.1 CUSIC syllabus

24.4 Protocols

There is a relative paucity of nationally agreed protocols for the use of ultrasound in the emergency patient presenting with an acute abdomen. The Intensive Care Society has developed what it considers are the essential skills required for abdominal ultrasound in intensive care. (Core Ultrasound Intensive Care accreditation—CUSIC) (Fig. 24.1) [6].

It is however imperative that a structured approach is followed and the scan is not terminated after one abnormality is identified. It is also important to be sensible in the approach to a time-critical focused scan, as it's name suggests it is focused to pathologies likely to cause immediate harm. Renal cysts, biliary polyps and anatomical variations while interesting, require expert evaluation and may require further investigation at a later stage, it is important to document their existence, but attention should not be drawn away from the intentions of the emergency scan.

24.5 A Proposed Approach

See Fig. 24.2.

24.6 Right Upper Quadrant

Placing the probe in the right upper quadrant will reveal images of the liver and gall bladder, the depth and contrast maybe adjusted to optimise these images. Our main focus in this area will be looking for perihepatic fluid (blood or ascites) or focusing on gall bladder pathology and biliary tree anatomy (Fig. 24.3). The liver texture

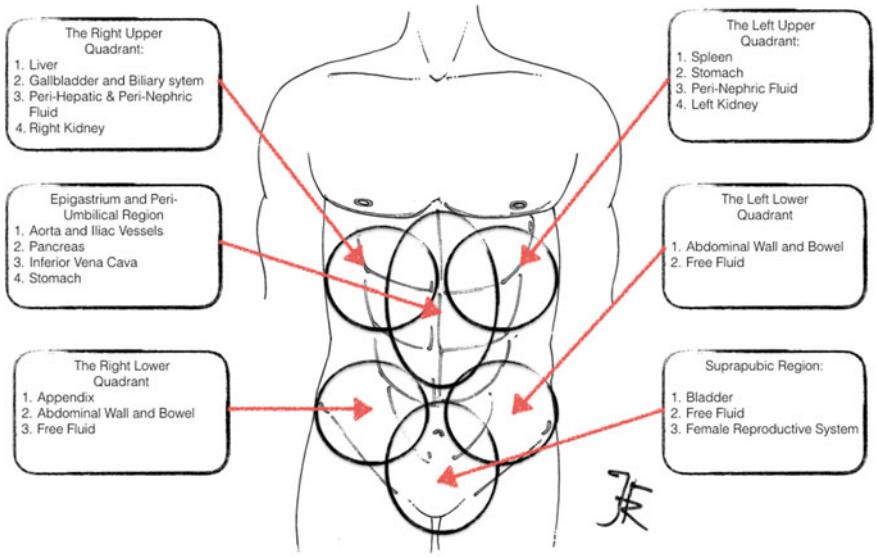

Fig. 24.2 Acute ultrasound protocol. Illustrator Dr. Harsha Reddy

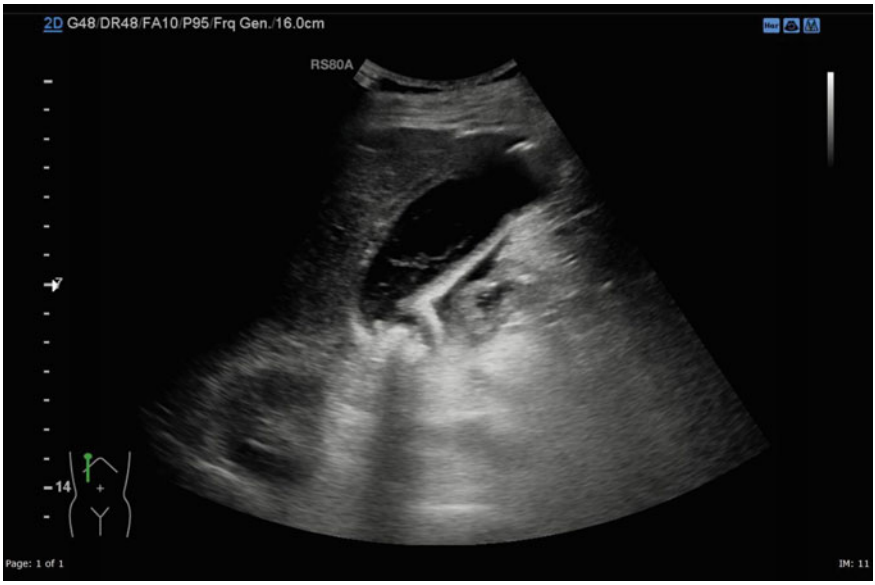

Fig. 24.3 Acute cholecystitis. Irregular wall thickening, multiple calculi and presence of pericholecystic fluid

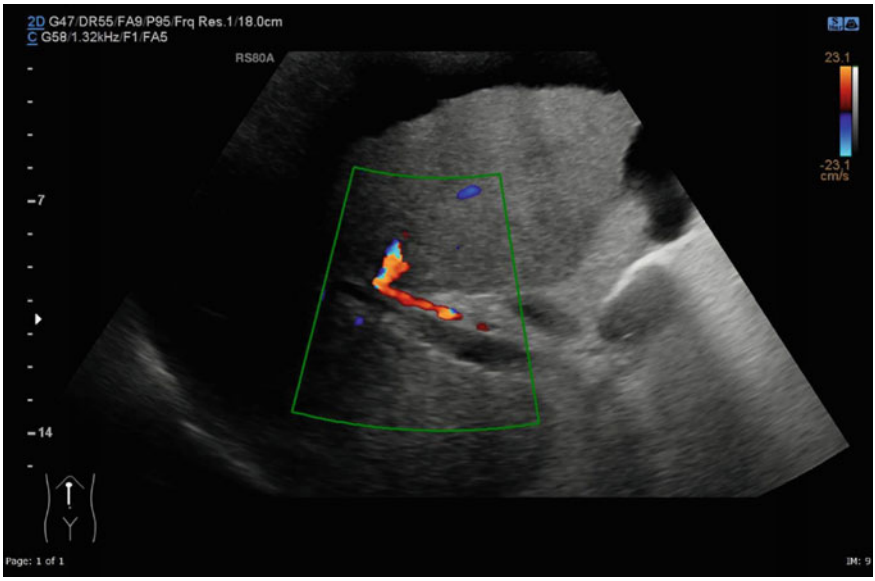

Fig. 24.4 Portal vein thrombosis. Cirrhotic liver with no colour flow identified in the portal vein and presence of ascites

itself may also be of interest, a small liver with a nodular and coarse echotexture may indicate hepatic cirrhosis. The extent of the focused exam in this area may depend on the clinical context, for example if the patient is jaundiced or the bloods suggest hepatic derangement, more attention will be placed on biliary dilatation and the patency of the portal and hepatic vessels (Fig. 24.4).

From a lateral and still relatively anterior window, images of the kidney can be acquired. The focus for these images should visualise the hepatorenal recess or Morison's Pouch to identify the presence of free fluid separating the organ borders. Visualising the kidney in its entirety is important to identify collections that could represent a perinephric abscess. As the kidney is imaged it is essential to scan throw in both a longitudinal and transverse plane, the main pathological findings to exclude would be dilation of the renal pelvis and calyces suggesting hydronephrosis or pyonephrosis, depending on the clinical context (Fig. 24.5).

24.7 Epigastrium and Peri-umbilical Region

Longitudinal and transverse images should be acquired of the abdominal aortic artery. Imaging should be performed along the path of the abdominal aorta, as a minimum, from superior to the origin of the superior mesenteric artery to the bifurcation of the iliac vessels. The findings are considered abnormal if the

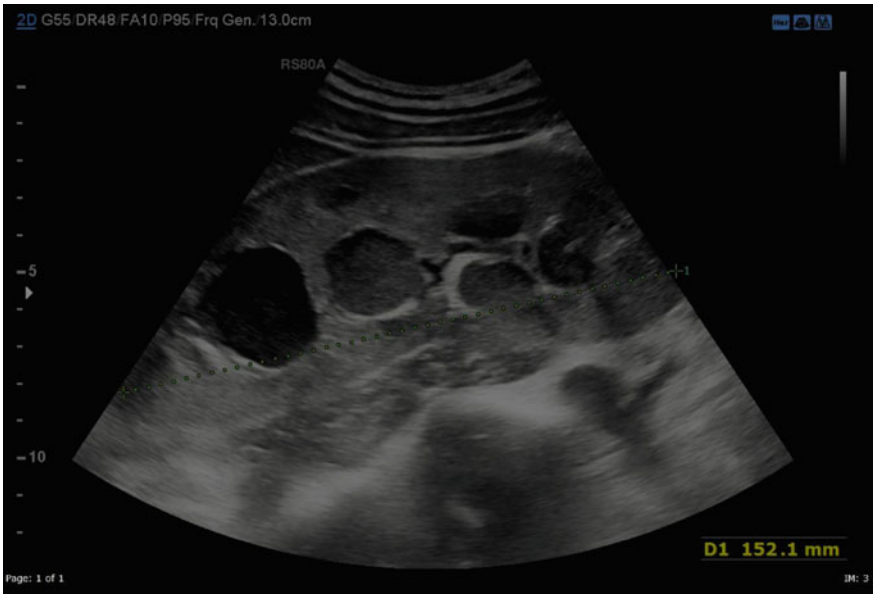

Fig. 24.5 Pyonephrosis. Enlarged kidney shows gross dilatation of the calyces and renal pelvis with non-dilatation of the ureter, suggestive of PUJ obstruction

transverse aortic diameter exceeds 3 cm. The larger the aneurysm, the higher the likelihood of an associated rupture. Abdominal aortic aneurysms greater than 5 cm have a 5-year rupture risk of 25–40% whereas those less than 5 cm have a risk of just 1–7% [7]. If it is deemed that an aneurysm is an incidental finding it is important to ensure appropriate follow up is put into place. The supplementation of colour flow doppler is useful to appreciate flow within the aorta itself and helps to rule out thrombus formation or any intimal dissection (Fig. 24.6).

With the probe placed transversely in the epigastric region, a couple of inches below the xyphoid process, the pancreatic head can be visualised nestled between the vena cava and the liver. It is found at the level of the splenic vein which can often be seen outlining the inferior border of the pancreatic body. It is frequently extremely hard to image and will often necessitate further imaging with a CT pancreas. Overlying bowel gas will often obliterate the view in over 30% of cases, especially in the presence of an acute abdomen [8]. If the pancreas is visualised, an increase in diameter, the presence of echogenic fat or surrounding hypoechogenic fluid will help complement a working diagnosis of severe acute pancreatitis [9].

On the right side of the epigastrium and lying lateral to the aorta is the inferior vena cava (IVC), this is distinguishable from the aorta due to its anatomical position but also due to its thin walled and compressible structure. If doubt still persists use the colour doppler setting to determine the direction of flow. Viewing the IVC in the epigastrium as it passes trans-diaphragmatically can give an indication of preload to the right side of the heart. A collapsed IVC or one that demonstrates collapse of

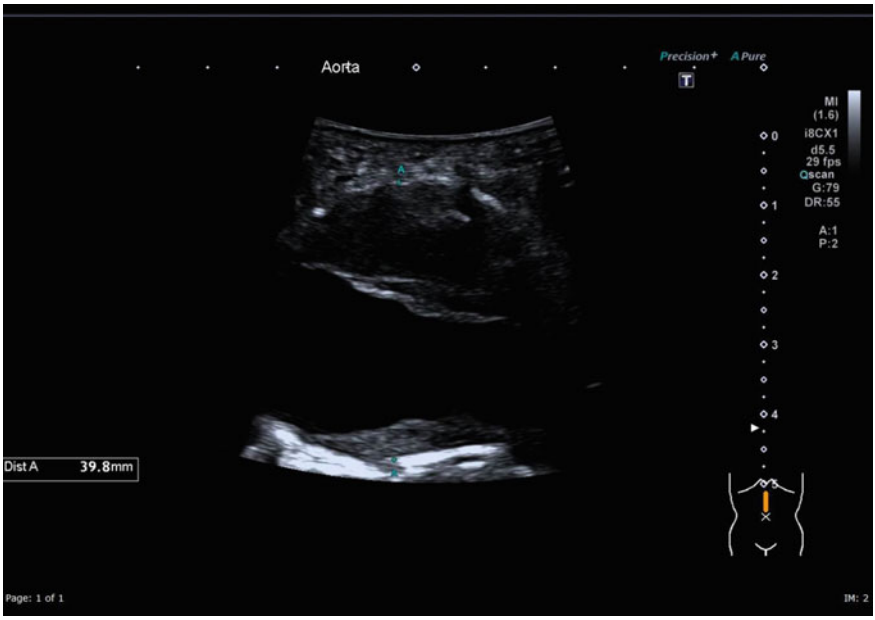

Fig. 24.6 Abdominal aortic aneurysm. Longitudinal view of an infrarenal abdominal aortic aneurysm containing thrombus has a maximum inner to inner AP diameter of 40 mm

greater than 50% during respiration can corelates with hypovolaemia from haemorrhage for example or may suggest the shocked patient who is likely to be fluid responsive (see Chap. 19—The Haemodynamically Unstable Patient).

In the epigastrium, but sometimes best seen in the left upper quadrant, the stomach can be visualised. Gastric stasis is frequently seen in an acute abdomen. The stomach can be identified as a loculated collection of fluid between the spleen and the liver, with echogenic matter moving indiscriminately within it. With gastric stasis it is often possible to identify a fluid gas interface.

24.8 The Left Upper Quadrant

This window is used to visualise the spleen, to look for injury or splenomegaly. The spleno-renal fossa is imaged to identify the presence of free fluid in the left upper quadrant, which may indicate the presence of intraabdominal blood. Imaging of the left kidney is always more challenging then that of the right, this is due in part to the liver which act as a convenient ultrasound window on the right side. As a result, the probe needs to be placed much more posteriorly, often placed obliquely at the posterior axillary line to obtain the sharpest view.

24.9 The Left Lower Quadrant

As we move to the lower half of the abdomen, our focus changes on to the bowel, peritoneum, abdominal wall and bladder (in females of [5] childbearing age, aim to identify the uterus, fallopian tubes and ovaries).

The left lower quadrant and up towards the peri umbilical area is a useful window to look for free fluid, and subsequently a good site for ascitic drainage. View of both the descending large bowel and small bowel can be appreciated, using a combination of the higher and lower frequency probes to help identify abnormal bowel pathology. For example, ultrasound boasts high sensitivity and specificity for diagnosing diverticulitis in patients with left iliac fossa pain (see Chap. 13—Abdomen 2).

Defects in the soft tissue surrounding the peritoneal cavity can be found anywhere along the abdominal wall. It is important to use the higher frequency probe over specific sites of pain to make sure a strangulated or incarcerated hernia is not missed (Fig. 24.7).

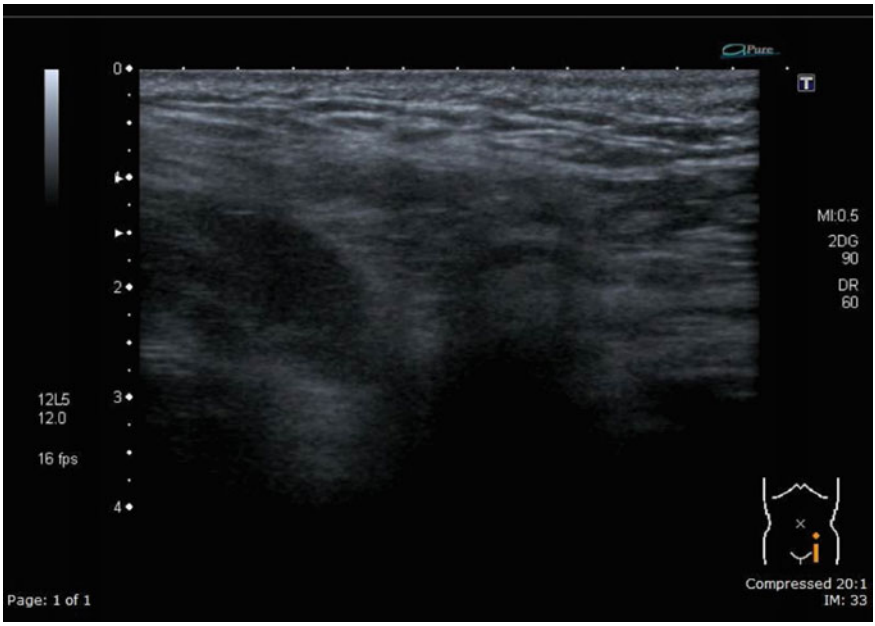

Fig. 24.7 Left inguinal hernia. Seen during Valsalva

24.10 Supra Pubic Region

By placing the transducer above the pelvic symphysis and angling it inferiorly, the pelvic organs can be identified. The bladder is often easily seen if full, but if the patient is catheterised, it may only be seen collapsed around the catheter balloon.

The full bladder acts as a good window to view the uterus and the recto-uterine pouch (pouch of Douglas) lying posteriorly to the bladder in female patients. If a pregnancy test returns positive, or those who know they are pregnant, imaging the uterus to ensure the pregnancy is actually in the uterus (IUP) is obviously an important finding. A female with a positive pregnancy test, empty uterus and free fluid within the abdomen is highly suspicious of a complicated ectopic pregnancy, and requires an urgent gynaecological consultation, whilst preparations are made for surgery with the potential for major blood loss.

The identification of an adnexal mass, gestational sac, a pseudo gestational sac or a yolk sac with or without an embryo can often be appreciated with ultrasound by angling the probe laterally from the central sagittal plane. However, this is considered a specialist skill, and the presence of an empty uterus and hemoperitoneum in a pregnant female is sufficient to strongly suspect a ruptured ectopic pregnancy (Fig. 24.8a, b).

Free fluid such as blood or ascites is often identified in the pelvis due to it pooling under gravity. It is visualised in the peritoneal reflections behind, lateral and even in front of the bladder. Pelvic free fluid can often be mistaken as fluid within the bladder, in such cases it is very important to identify the margins of the bladder wall to correctly identify the location of the fluid (see Chap. 10—The FAST Scan).

24.11 Right Lower Quadrant

Examination of the right lower quadrant is similar to that of the left, focus is on the bowel and the presence of free fluid in the paracolic gutter and pelvis. One of the most important diagnoses to make in acute right iliac fossa pain, is acute appendicitis. Point of care ultrasound is good at ruling in the diagnosis of acute appendicitis but may often give false negatives, so continued high index of suspicion is required. The position of the appendix can vary significantly between individuals, it is normally identified anterior and between the iliac artery and psoas muscle as a blind-ended tubular pouch (Fig. 24.9a). It is sometimes useful to ask the patient to point to the most painful area and place the probe at this position gradually increasing probe compression (the pain is often due to the appendix irritating the peritoneum) [10]. An inflamed appendix is identified by its oedematous wall, adjacent free fluid or increased echogenicity of surrounding fat. Increased vascularity may be seen on doppler (Fig. 24.9b) and direct feedback from the patient of increasing discomfort on direct graduated compression is also suggestive or acute appendicitis.

(a)

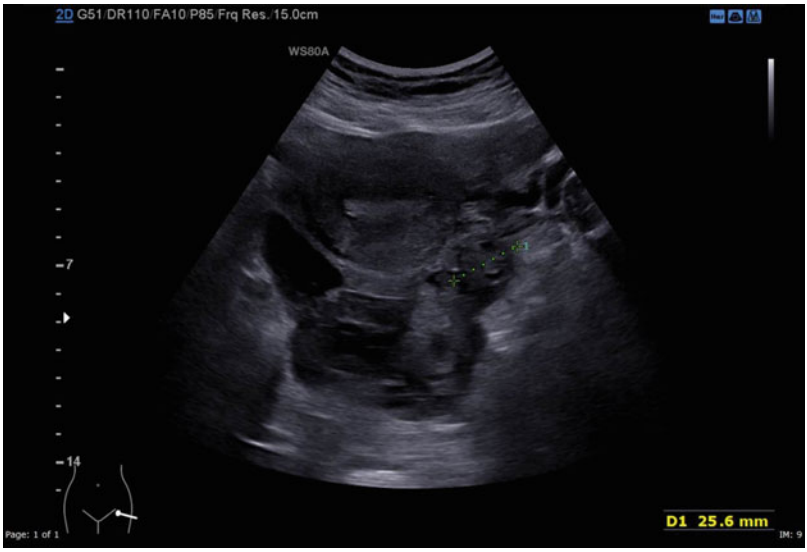

(b)

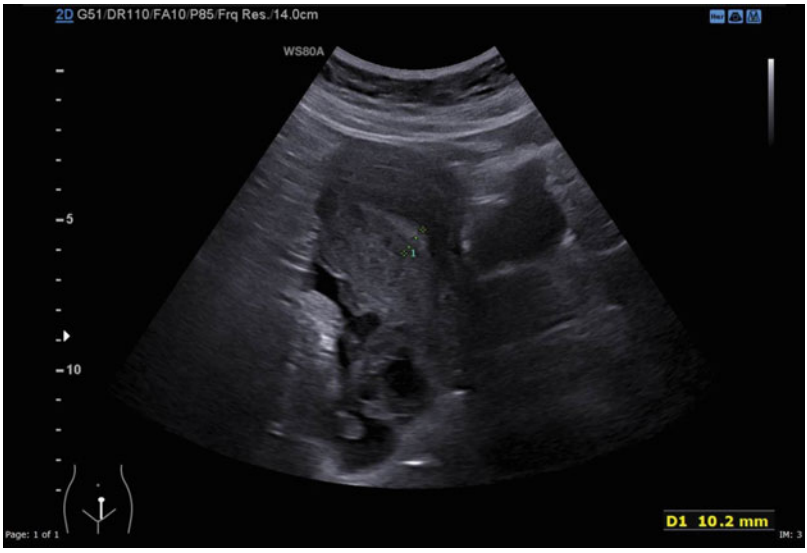

Fig. 24.8 **a**, **b** Ruptured ectopic pregnancy. Bulky uterus with no evidence of an intrauterine pregnancy. There is an echogenic mass situated in the pouch of Douglas (POD) towards the left adnexa which contains a central cystic component. Normal left ovary is seen adjacent to this mass. There is free fluid with internal echoes in the POD, suggestive of haemorrhage within

(a)

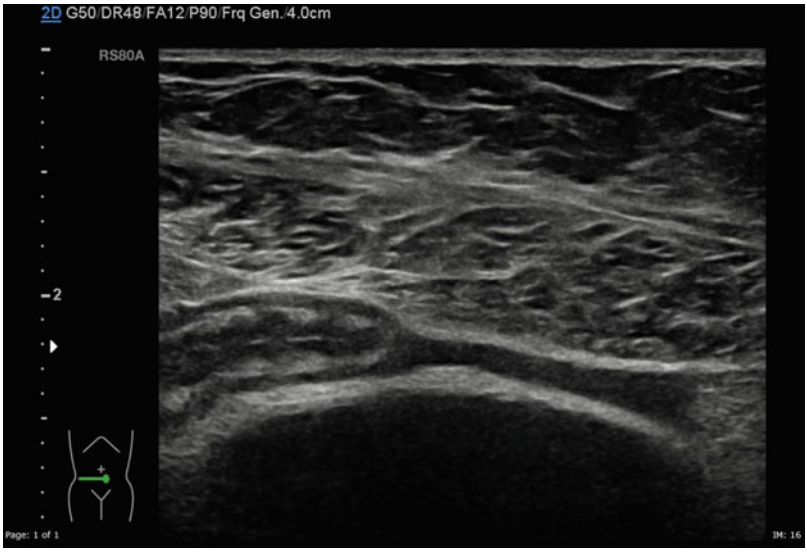

(b)

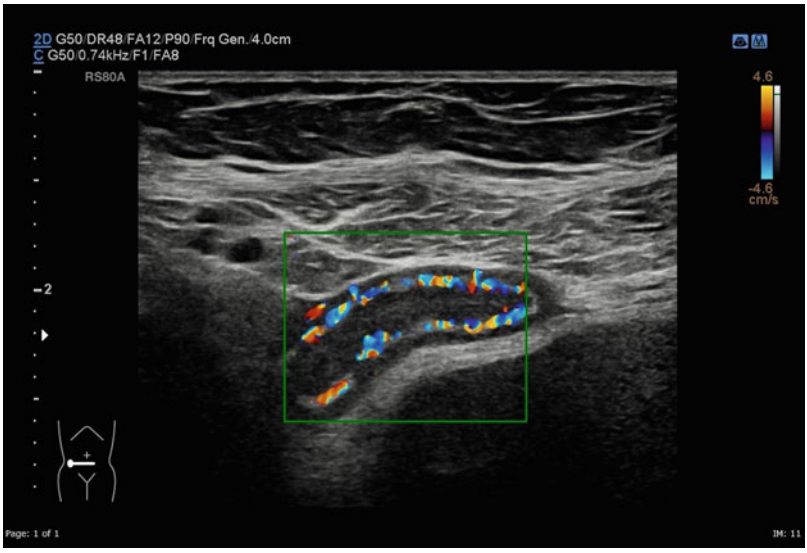

Fig. 24.9 **a**, **b** Acute appendicitis. Dilated, blind ending aperistaltic tubular structure in the RIF which is tender on palpation. Hypervascularity along the wall on Doppler. Periappendiceal fluid present

24.12 Conclusion

When approaching the patient with an acute abdomen, it is obviously important to concentrate your focus on the area of the abdomen causing maximal concern. As there can often be associated information found in other areas of the abdomen, a methodical approach to scanning the abdomen is required. This chapter gives an example of a sequential scan, but it will need tailoring to your particular skill set and experience. Point of care scanning can add a great deal to the clinical picture but should not be used in isolation. Even in the most experienced hands; CT, MRI and radiologist delivered ultrasound should always be considered.

References

1. Saunders DI, et al. Variations in mortality after emergency laparotomy: the first report of the UK emergency laparotomy network. Br J Anaesth. 2012;109(3):368–75.
2. McGahan JP, Richards JR. Focused assessment with sonography in trauma (FAST) in 2017: what radiologists can learn? Radiology. 2017;283(1):30–48.
3. Laméris W, et al. Imaging strategies for detection of urgent conditions in patients with acute abdominal pain: diagnostic accuracy study. 2009;338.
4. Ralls P, Colletti P, Lapin S, Chandrasoma P, Boswell WD Jr, Ngo C, Radin D, Halls J. Real-time sonography in suspected acute cholecystitis. Prospective evaluation of primary and secondary signs. Radiology. 1985;155(3):767–71
5. Brenner DJ, Hall EJ. Computed tomography: an increasing source of radiation exposure. N Engl J Med. 2007;357:2277–84.
6. CUSIC Accreditation. https://www.ics.ac.uk/ICS/Pdfs/CUSIC-accreditation.aspx.
7. Aggarwal S, et al. Abdominal aortic aneurysm: a comprehensive review. Exp Clin Cardiol. 2011;16(1):11–5.
8. Minniti S, et al. Sonography versus helical CT in identification and staging of pancreatic ductal adenocarcinoma. J Clin Ultrasound. 2003;31:175–82.
9. Costanza B, Salvatore M, Giacomo S. The role of ultrasound in acute pancreatitis. In: Imaging of the Pancreas. Springer;2009, p. 33–47.
10. Puylaert JB. Acute appendicitis: US evaluation using graded compression. Radiology. 1986;158:355–60.